Statistical Modelling of Extreme Rainfall in Madeira Island

DOCTORAL THESIS

Délia Canha Gouveia Reis
DOCTORATE IN MATHEMATICS
SPECIALTY: PROBABILITY AND STATISTICS

UNIVERSIDADE da MADEIRA
A Nossa Universidade
www.uma.pt

August | 2014

FCT Fundação para a Ciência e a Tecnologia
MINISTÉRIO DA EDUCAÇÃO E CIÊNCIA

Statistical Modelling of Extreme Rainfall in Madeira Island

DOCTORAL THESIS

Délia Canha Gouveia Reis
DOCTORATE IN MATHEMATICS
SPECIALTY: PROBABILITY AND STATISTICS

SUPERVISORS
Luiz Carlos Guerreiro Lopes
Sandra Maria Freitas Mendonça

UNIVERSIDADE da MADEIRA

Statistical Modelling of Extreme Rainfall in Madeira Island

Thesis presented by

Délia Canha Gouveia Reis

and **unanimously approved on 12 December 2014**,
in public session to obtain the PhD Degree in Mathematics

Jury

Chairman:

Doctor Maria Teresa Alves Homem de Gouveia
(by delegation of authority of the Rector of the Universidade da Madeira)

Members of the Committee (in alphabetical order)**:**

Doctor Dinis Duarte Ferreira Pestana
Full Professor, Universidade de Lisboa

Doctor João Alexandre Medina Corte-Real
Full Professor, Universidade de Évora

Doctor Luiz Carlos Guerreiro Lopes
Assistant Professor, Universidade da Madeira

Doctor Rita Cabral Pereira de Castro Guimarães
Assistant Professor, Universidade de Évora

Doctor Sandra Maria Freitas Mendonça
Assistant Professor, Universidade da Madeira

Doctor Sílvio Filipe Velosa
Assistant Professor, Universidade da Madeira

Abstract

Statistical Modelling of Extreme Rainfall in Madeira Island

Extreme rainfall events have triggered a significant number of flash floods in Madeira Island along its past and recent history. Madeira is a volcanic island where the spatial rainfall distribution is strongly affected by its rugged topography. In this thesis, annual maximum of daily rainfall data from 25 rain gauge stations located in Madeira Island were modelled by the generalised extreme value distribution. Also, the hypothesis of a Gumbel distribution was tested by two methods and the existence of a linear trend in both distributions parameters was analysed. Estimates for the 50– and 100–year return levels were also obtained. Still in an univariate context, the assumption that a distribution function belongs to the domain of attraction of an extreme value distribution for monthly maximum rainfall data was tested for the rainy season. The available data was then analysed in order to find the most suitable domain of attraction for the sampled distribution. In a different approach, a search for thresholds was also performed for daily rainfall values through a graphical analysis. In a multivariate context, a study was made on the dependence between extreme rainfall values from the considered stations based on Kendall's τ measure. This study suggests the influence of factors such as altitude, slope orientation, distance between stations and their proximity of the sea on the spatial distribution of extreme rainfall. Groups of three pairwise associated stations were also obtained and an adjustment was made to a family of extreme value copulas involving the Marshall–Olkin family, whose parameters can be written as a function of Kendall's τ association measures of the obtained pairs.

Keywords: statistics of extremes, annual maxima method, extreme domain of attraction, threshold choice, copula functions, extreme rainfall.

Resumo

Modelação Estatística da Precipitação Extrema na Ilha da Madeira

Os extremos de precipitação constituem um factor importante na ocorrência de cheias rápidas como algumas que marcaram significativamente a história da Ilha da Madeira. Esta ilha de origem vulcânica apresenta diferentes regiões relativamente aos extremos de precipitação condicionadas pela sua complexa orografia. Nesta tese, a função distribuição generalizada de valores extremos foi utilizada para modelar os máximos anuais dos valores diários de precipitação de 25 estações situadas na Ilha da Madeira. Além disso, a hipótese de escolha estatística da distribuição Gumbel foi testada por meio de dois métodos, tendo sido também analisada a existência de tendência linear nos parâmetros das duas distribuições. Foram também obtidas estimativas para níveis de retorno de 50 e 100 anos. Ainda num contexto univariado, a suposição de que a função de distribuição pertence ao domínio de atração de uma distribuição de valores extremos foi testada considerando os valores máximos mensais de precipitação diária da época das chuvas. Foram depois aplicados procedimentos para a escolha de domínios de atração para máximos considerando os valores disponíveis. Numa perspectiva distinta, foi também efectuada uma procura de valores para o limiar de séries de valores diários de precipitação por meio de uma metodologia assente numa análise gráfica. Num contexto multivariado, foi realizado um estudo sobre a dependência entre extremos de precipitação na Ilha da Madeira assente na medida de associação tau de Kendall, tendo sido formados grupos de três estações associadas duas a duas com os pares de estações obtidos. Este estudo sugere a influência da altitude, da orientação das vertentes, da distância entre estações e da sua proximidade ao mar na distribuição espacial dos extremos de precipitação. Foi também realizado um ajuste a uma família de cópulas de extremos envolvendo a família de Marshall–Olkin, cujos parâmetros podem ser escritos em função do tau de Kendall.

Palavras-chave: Estatística de extremos, modelo dos máximos anuais, domínios de atração, escolha do limiar, funções cópula, precipitação intensa.

Acknowledgements

To Professors Luiz Lopes and Sandra Mendonça, my supervisors, for encouraging me to work in the area of extreme value analysis and for suggesting the topic of the present thesis. The generosity with which they offered their time and ideas to this work is also appreciated. I would also like to acknowledge their support and encouragement to participate in scientific meetings and their confidence in my work.

To the Portuguese Foundation for Science and Technology (FCT), for the financial support through the PhD grant SFRH/BD/39226/2007, financed by national funds of the Ministry of Science, Technology and Higher Education (MCTES). I am also grateful to the Centre of Statistics and Applications of the University of Lisbon (CEAUL) for the bibliographical and financial support through FCT projects PEst-OE/MAT/UI0006/2011 and PEst-OE/MAT/UI0006/2014. To the University of Madeira for providing the appropriate conditions for the realisation of this thesis and for the logistic support.

To the Portuguese Institute for Sea and Atmosphere (IPMA), namely to Doctor Victor Prior, for providing the monthly maximum rainfall data used in this thesis. Thanks are also due to the Department of Hydraulics and Energy Technologies of the Madeira Regional Laboratory of Civil Engineering (LREC), in particular to Doctor Carlos Magro, for making available the daily rainfall data from 25 rain gauge stations maintained in the past by the General Council of the Autonomous District of Funchal.

I would also like to express my gratitude and appreciation to all those I have had the opportunity and the pleasure to learn and work with directly in courses of Statistics and Probability: Professor Ana Abreu, Professor Paulo Freitas, Professor Rita Vasconcelos, Professor Sandra Mendonça and Professor Sílvio Velosa. A special acknowledgement to Professor Rita Vasconcelos for her guidance when I first needed to use a statistical software, for all the concise and fruitful meetings about the courses I taught as her assistant, and for all the encouragement throughout the elaboration of

this thesis. I would also like to thank Professors Rita Vasconcelos and Paulo Freitas for sparing me from the grading task in the last weeks of the second semester of the academic year 2013/2014, so that I could dedicate some more time to the conclusion of the writing of this thesis. I am also grateful to Professors Ana Abreu and Sílvio Velosa for all their efforts to offer me precious time to dedicate to the elaboration of this thesis throughout the later five years. A special acknowledgement to Professor Ana Abreu for introducing me the R software and language, which was essential for the work developed and described here. I would also like to thank Professor Ana Abreu for the classes about the R software functionalities and also for the tips about R packages concerning maps, which were used in this thesis.

To all other colleagues at the Centre for Exact Sciences and Engineering for all their contributions to my education as a student and as a teacher. I am also grateful for their friendship and their support. A special acknowledgement to Professor Custódia Drumond for the encouragement, the care and also for the tea breaks which brightened many afternoons. A special acknowledgement to Professor José Carmo for having always assured me the best possible working conditions and for the constant encouragement throughout the elaboration of this thesis.

I would also like to express my appreciation to the participants of the scientific meetings organised by the Portuguese Society of Statistics (SPE) from whom I had the opportunity to learn. In particular, I would like to thank Professor Ivette Gomes for the encouraging comments and guidance about a work I presented in one of those meetings. A special acknowledgement to Professor Dinis Pestana for the guidance and bibliographical support.

To all my (present and former) students for the motivation that comes from the pleasure of lecturing to them.

To Maurício's family (now also mine) for receiving me with open arms and also for their friendship, support and care.

To Analuce, my sister, for personifying the persistence in the pursuit of aims and dreams. To Lúcia and António, my parents, for personifying the strength and joy of living. Thanks for all the support, care and love. I am blessed to have you three in my life.

To Maurício, for listening, cheering and caring.

Contents

List of Acronyms and Symbols

ASI	Advanced Statistical Institute
EVC	extreme value copula
GEV	generalised extreme value
GPD	generalised Pareto distribution
IPMA	Portuguese Institute for the Sea and Atmosphere
LREC	Regional Laboratory of Civil Engineering
ML	maximum likelihood
POT	peaks over threshold
PORT	peaks over random threshold
PWM	probability weighted moments

$\xrightarrow{d}$	converges in distribution to
$d_{X,Y}$	distance in meters between stations X and Y
$\widehat{q}_p$	$1/p$–year return level estimate
$\widehat{q}_\alpha^M$	$1/\alpha$–year return level estimate calculated by the method M ($\alpha \in (0,1)$)
χ^2_k	chi–square distribution with k degrees of freedom
r_α	return period of $E_\alpha = P(X_i > x_{i,\alpha})$ for $i \in \{1,2,3\}$ and $\alpha \in (0,1)$
X_i	observation at the i–th rain gauge station
$x_{i,q}$	$(1-q)$–quantile of X_i for $q \in (0,1)$ and $i \in \{1,2,3\}$
$x_{1:n}, ..., x_{n:n}$	ascending order statistics of the sample $(x_1, \ldots, x_n)$
$x_{(1)}, ..., x_{(k)}$	exceedances
$\tau_n^{X,Y}$	estimates based on a sample of size n of Kendall's τ association measure between stations X and Y

List of Figures

List of Tables

Chapter 1

Introduction

In the past and nowadays, hydrology is one of the most natural fields of application of the extreme value theory. In the first book on statistics of extremes, Emil Gumbel [107] wrote that the oldest problems connected with extreme values arise from the study of floods. Madeira Island is a volcanic island located in the Atlantic Ocean off the Northwest African coast, between latitudes 32°30'N-33°30'N and longitudes 16°30'W-17°30'W, that presents a significant number of rainfall-induced flash floods along its history. There are reports from the 17th century mentioning the occurrence of flash floods [192], but the one known to have caused the largest number of casualties, with more than 800 deaths, occurred on the 9th of October 1803 [70]. After that major occurrence, other extreme precipitation events have triggered at least thirty significant flash floods. More precisely, eight intense flash floods occured in the 19th century and twenty two in the last century [177]. Since 2001, at least ten events of this nature, with different intensities, have occurred in the island. More recently, the most significant one was the one that happened on the 20th of February 2010, which caused 45 casualties, six missing people and extensive damage to properties and infrastructures, being Funchal and Ribeira Brava the most affected areas [70, 162]. In the words of the authors Fragoso et al. [70], this event resulted from the record rainy season observed and the great amounts of precipitation observed on a daily and hourly scale during the event, particularly in the mid and upper slopes of the mountains. Therefore, Madeira Island, like other regions where the rainfall spatial distribution is strongly affected by the rugged orography, e.g., the Hawaian Islands [24] and Tuscany [34], is a natural laboratory for the analysis of extreme value rainfall events.

Extreme value theory has its origins in the beginnings of the twenties, although there were previous related works. A landmark in this theory was achieved in 1928

by Fisher and Tippet [66], who showed that extreme limit distributions can only be one of three types, namely the Gumbel (type I), Fréchet (type II) and Weibull (type III) distributions. The sufficient conditions under which each one of those three asymptotic distributions is valid were presented by von Mises [219] in 1936, while the necessary and sufficient conditions were provided by Gnedenko [83] in 1943. The Gumbel, Fréchet and Weibull distributions correspond to specific values of the shape parameter of the generalised extreme value (GEV) distribution, whose parametrization is usually attributed to the work from von Mises [220] in 1954 and also to the work of Jenkinson [121] in 1955. The importance of the Fisher–Tippet theorem, also known as Fisher–Tippet–Gnedenko theorem, is comparable to the one presented by the central limit theorem in the theory of sums of random variables. Furthermore, according to some authors, extreme value theory started to gain a coherence and attractiveness comparable to the one presented by the theory of sums of random variables with the doctoral dissertation by L. de Haan [39] in 1970. Also in the seventies the theoretical foundation of a branch of this theory, namely the peaks over threshold (POT) methodology, was set up by Pickands [171] and developed later by other authors, like, for example, Smith [196] in 1989 and Leadbetter [135] in 1991. More branches appeared in this rich and productive theory, which grew and broadened its applicability domain to areas such as insurance, finance and sports in addition to the classical application areas such as the strength of the materials and the environmental sciences.

1.1 Aims and contributions

The main goal of this study is to contribute to the knowledge about rainfall extreme value events in Madeira Island. More explicitly, the objective is to analyse rainfall values collected in Madeira over different periods of time within the extreme value theory. Diverse definitions of extreme values led to relevant methodologies under this quite general framework, providing a great source of application methods to the study of extremes whether they are univariate or multivariate. Therefore, an important aim of this study was to perform, in both of these contexts, an analysis about the behaviour of distributional models and also of various statistical techniques for extremes values in the modelling extreme rainfall events. In particular, a specific objective was to compare the fits produced by the Gumbel and the GEV distributions in the statistical modelling of extreme rainfall in Madeira Island, since this is a classical but still a relevant topic at the present time. Madeira's annual maximum and daily rainfall data is here analysed in a context

of univariate extremes under the Gumbel's and the POT approaches, respectively. The monthly rainfall data was studied through a more recent approach than the two previous ones, namely the PORT approach. Due to Madeira Island's topographic characteristics, an analysis of the spatial distribution of the extreme rainfall values was also a purpose for this study. So, in a context of multivariate extremes, a study with annual rainfall maxima data under an extreme value copula (EVC) approach was carried out. One dataset studied in this work consists of monthly maximum rainfall data from seven rain gauge stations, provided by the Portuguese Institute of the Sea and Atmosphere (IPMA). Also, Madeira Civil Engineering Laboratory's Department of Hydraulics and Energy Technologies supplied daily rainfall data from 25 rain gauge stations maintained in the past by the General Council of the Autonomous District of Funchal. In the following paragraphs, more detailed descriptions of the study, of the data and of the approaches followed are provided.

The GEV is widely used for modelling extremes of natural phenomena [119, e.g.], being this distribution also used in this study to model the available data. Under a Gumbel's approach, with the annual maxima obtained from the data provided by IPMA, the GEV distribution parameter estimates were determined by the methods of maximum likelihood (ML) and probability weighted moments (PWM). The hypothesis of a Gumbel distribution was tested by two methods present in the literature [26, 118, e.g.] and the existence of a linear trend in the distribution parameters was analysed. The estimates and confidence intervals for return levels of 50 and 100 years were obtained from the ML method. From the data provided by the Regional Laboratory of Civil Engineering (LREC), the parameter estimates of the function of the GEV distribution were also determined by the two mentioned methods. Additionally, the referred tests were applied to test the hypothesis of a Gumbel distribution and the existence of linear trend in the parameters of distribution was analysed. However, as the number of years for these datasets is shorter than the previous ones, a comparison of return levels of 50 and 100 years was performed using the estimates obtained by the ML method, and those obtained by the PWM method. The results of this study were presented in Gouveia–Reis et al. [93].

One of the alternative approaches to Gumbel's approach is the PORT approach, which only assumes that the common distribution function from n independent random variables belongs to the domain of attraction of an extreme value distribution. The method for testing a extreme value condition investigated by Dietrich et al. [54] was applied to the monthly maximum precipitation data for

the rainy season from the seven rain gauge stations maintained by IPMA. More explicitly, the hypothesis that the model F underlying the data was in the domain of the GEV was tested, which is the only assumption that has to be made in a semi-parametric framework. The statistical procedures for the problem of statistical choice of extreme domains of attraction analysed by Neves and Fraga Alves [159] were also applied to each station data set. The results of this analysis, presented in Gouveia et al. [92], indicate the possible number of upper extremes (k) to be used for each local sample and the sign of each extreme value index γ. On the other hand, the more classical POT approach to the study of extremes requires the analysis of observations that exceed a certain threshold, being the choice of this value of critical importance. With the purpose of evaluating possible threshold choices for each rain gauge station location, a graphical analysis was made to the daily values of rainfall recorded in Madeira provided by the LREC. The analysis for the period ranging from 1950 to 1980, which corresponds to 12 rain gauge stations, yielded a manuscript entitled *Aplicação do método dos excessos de nível a valores extremos de precipitação na Ilha da Madeira*, submitted for publication in the proceedings of the XXI *Congresso da Sociedade Portuguesa de Estatística*.

The dependence between variables plays a central role in multivariate extremes. The advantage of a copula function approach to this topic is the ability to describe and model the dependence between variables, regardless of their marginal distribution functions. Thus, in order to quantify the dependence of maximum annual rainfall in Madeira Island, a study was carried out within a copula approach using the data provided by LREC. This data was chosen in detriment to the one provided by IPMA because it comes from a higher number of rain gauge stations, allowing a better coverage of Madeira in spatial terms. Due to the existence of annual maximum values covering three different measurement periods, the dependence study was divided in three parts. In each one of these parts, a test of independence based on the empirical version of the Kendall's τ association measure was applied, given the significance level $\alpha = 0.01$ and the data from all pairs of stations were analysed within each of those three parts. In a second stage, the pairs formed by the considered stations, for which the independence was rejected, were used to form groups of three pairwise associated stations with the purpose of fitting a family of extreme value copulas involving the Marshall–Olkin family, whose parameters can be written as a function of Kendall's τ association measures of the considered pairs. For each of the obtained groups within each measurement period, two return periods were estimated. The work by Gouveia–Reis et al. [95]

presents the results obtained with a significance level of 0.05 for the period ranging from 1959 to 1980, considering only the group of stations belonging either to the northern or the southern Madeira's slope. From the obtained pairs, 16 groups of three pairwise associated stations on the southern slope of Madeira Island were obtained, while in the northern slope only four groups were obtained. These 20 groups and two corresponding return periods are presented in Gouveia–Reis et al. [94].

1.2 Organization of the thesis

Extreme value theory involves a wide range of concepts and methodologies. Moreover, its applicability to matters as important as the duration of human life or natural hazards such as floods, droughts, storms and landslides, considerably increases the research literature in this theory already prolific by itself. In Chapter 2, there is a brief description of the origins and recent past of this theory and its applications. In Subsection 2.1, special attention is given to the literature which deals with the methodologies that were applied in this thesis, while Subsection 2.2 is exclusively dedicated to the literature devoted to the application of the extreme value theory to the study of rainfall extremes.

A brief historical overview is also presented in Chapter 3, but with the focus on Madeira's flash flood history. Also in this chapter, characteristics of Madeira Island's topography and climate are described. Details about the rain gauge stations such as its origins, geographical location and altitude are also presented. The source, the type and the period range of the data available for this study are also described. For a better perception of the spatial distribution of the rain gauge stations considered, a map of Madeira Island is provided, which shows the location of each station.

Chapter 4 presents the concepts and methods of extreme value theory applied in this study. The generalised and also the standard extreme value distributions are recalled in Section 4.1, which also presents the estimation methods and the tests applied in this study through the application of the block maxima model or, in other words, the Gumbel's approach. The reasoning that supports the exploratory graphics used to model checking is also described in Section 4.1. Still in a univariate context, Section 4.2 presents the statistical tests for testing extreme value conditions and for choosing extreme domains of attraction that were applied in this study through a PORT approach. In Section 4.2, now in a POT context, a description of two graphical methods for threshold selection is presented. In the context of

multivariate extremes, the concepts and methodologies necessary to the application of the extreme copula approach considered in this thesis are presented in Section 4.3.

The application to Madeira rainfall data of the methodologies described in Chapter 4 led to the results compiled and discussed in Chapter 5, corresponding the Sections 5.1, 5.2 and 5.3 to the Sections 4.1, 4.2 and 4.3, respectively. Section 5.1 is subdivided in the Subsections 5.1.1, 5.1.2 and 5.1.3, one for each of the three different datasets analysed. In Subsection 5.1.1 the annual maximum precipitation data from the seven rain gauge stations maintained by the IPMA is analysed, while the analysis of the annual data extracted from the dataset provided by the LREC is made in Subsection 5.1.2. The dataset which results of joining all data concerning those stations that are common to the two previously mentioned sources was analysed in Subsection 5.1.3. The results obtained from the application of the PORT approach are presented in Subsection 5.2.1, while the ones resulting from the application made of the POT approach are presented in Subsection 5.2.2. The three analyses based on an EVC approach made to the annual LREC data form the three subsections of Section 5.3. In Subsection 5.3.1 the dataset corresponds to the highest values of annual daily precipitation on the island of Madeira from 12 rain gauge stations with measurement period from 1950 to 1980, while in Subsection 5.3.2 the measurement period ranges from 1950 to 1972 coming from 19 rain gauge stations. In Subsection 5.3.3 the same analysis is made, but now to a group of 18 rain gauge stations with the shorter measurement period considered in this study, which ranges from 1959 to 1980.

Chapter 6 summarises, examines and discusses the obtained results in a more detailed way. For completeness, an appendix is included in the final part of the thesis. This appendix is divided in chapters including diagnostic plots for annual maxima, threshold choice plots, tables with p–values of likelihood ratio tests, tables with exceedances distributions (in percentage) by month, and also the code of some functions implemented in R.

Chapter 2

State of the art (and a taste of the history of extreme value theory)

One of the first results of the theory that is nowadays called Extreme Value Theory (EVT) [107] was presented in the dissertation of Nicolaus Bernoulli, *De Usu Artis Conjectandi in Jure* (The Use of the Art of Conjecturing in Law) [14] [1], in 1709, where Bernoulli deduces the value of the expected duration of life of the last survivor in a group of n men of equal age that die within t years. However, it was only in 1922, in a paper by von Bortkiewicz [218], that the notion of distribution of the largest value was clearly defined for the first time. That paper dealt with the distribution of the range in random samples from a normal distribution and marked the beginning of a period of theoretical developments in the area of extreme value analysis [128].

The first systematic study [211, 212] about the behaviour of maxima and minima of samples of independent and identically distributed random variables seems to be from Dodd [57], that studied the limit behaviour of the maximum value of a random sample for six general classes of parent distributions that include the seven Pearson distribution types, among others. In this work Dodd also gave an expression for the median value of the maximum of a sample, and compares the median and the asymptotic values of the variation interval, computed with his formulas for the normal distribution, with the values obtained before by von Bortkiewicz [218]. In 1927, Fréchet [71] identified one possible limit distribution for the largest order statistic, known today as the Fréchet distribution, and, one year later, Fisher and Tippet [66] showed that extreme limit distributions could

[1] A translation of this work by Richard J. Pulskamp could be found online in the web address http://www.cs.edu/math/Sources/NBernoulli/de_usu_artis.pdf (last visited on October 26, 2013)

only be one of three types, named today after the names of Gumbel (type I), Fréchet (type II) and Weibull (type III). Later, in 1936, von Mises [219] presented sufficient conditions under which those three asymptotic distributions were valid. In 1943, Gnedenko [83] went a step foward by providing necessary and sufficient conditions for the convergence to these limit distributions. Gnedenko results were refined by some other authors (e.g. [39, 40, 140, 147]) and extended by others to the case of non identically distributed or non independent random variables (e.g. [123, 151, 152]). Among these works, the doctoral dissertation by L. de Haan [39] has been referred as the starting point of the extreme value theory as a coherent and attractive theory, comparable to the theory of sums of random variables [10].

From the application point of view, the astronomers were the first to study extreme values due to the need of a criterion for using or rejecting outlying observations when dealing with repeated observations of the same object [107, 128]. For example, Peirce in 1852 [167], and using the words of the author, by the application of the "fundamental principles of the Calculus or Probabilities", produced "an exact rule for the rejection of observations" of a series, when these differed considerably from others, "as to indicate some abnormal source or error not contemplated in the theoretical discussions". According to Kotz and Nadarajah [128], extreme values were also studied in other contexts outside the field of astronomy, such as flood flows and strength of materials (see, e.g., Fuller's paper from 1914 [73], Griffith's paper from 1920 [100] and Peirce's paper from 1926 [168]). An application in the actuarial sciences also appeared in the already mentioned work of Dodd from 1923 [57]. In 1939, Weibull [221, 222] addressed the topic of the strength of the materials and advocated the use of the statistical distributions that came to be called Weibull distributions. In the following years, flood analysis returned to be a topic of interest in the application of extreme value theory mainly by work of Gumbel [102, 104, 105] and other distinct topics emerged, such as, for example, seismic analysis by Nordquist in 1945 [164] and microorganism survival times by Velz in 1947 [217]. Gumbel was the first author to call the attention of statisticians and engineers to the applications of the extreme value theory in problems previously treated empirically, such as, for example, annual flood flows and precipitation maxima [128]. The books by Gumbel published in 1954 [106] and 1958 [107] gave a first global view of the applications of extreme value theory, being the latter one a mark in the references of this area.

Returning back to the highlights of the development of the extreme value theory, 1958 is the perfect year to mention the study of multivariate distributions. According to Galambos [76], the leap to higher dimensions was given in that year by Tiago de Oliveira in a paper on extremal distributions [202]. Nevertheless, some results in this topic had been already obtained by Finkelstein in 1953 [65]. The papers by Geffroy [78, 79] and Sibuya [191] presented some results related to bivariate extreme values and had some followers [13, 165], but it was Tiago de Oliveira that had a more relevant work in this subject [203, 204]. In 1964, Gumbel and Goldstein [110] illustrated for the first time the use of bivariate extremal distributions with two examples: to study the distribution of the oldest ages at death for the two genders and the distribution of the floods of the same river recorded at two stations located upstream and downstream [201]. In the following decade, necessary and sufficient conditions for the asymptotic independence of arbitrary extremes in any dimension were obtained by Mikhailov [153] and Galambos [74]. Also in the seventies, equivalent representations of multivariate asymptotic distributions of the maxima were given by Pickands [172], de Haan and Resnick [43], and Deheuvels [47]. The paper from de Haan and Resnick [43] used the concept of max-infinite divisibility introduced by Balkema and Resnick [8]. In 1980 and 1984, Deheuvels [49] worked on the existence and uniqueness of dependence functions and de Haan [41] obtained a spectral representation for max-stable processes, respectively. In these three decades there were also papers by Arnold [3], Tiago de Oliveira [205, 206, 207] and Pickands [173] that treated the statistical aspects of multivariate extremes.

Tiago de Oliveira wrote in the Preface of the NATO Advanced Statistical Institute (ASI) on Statistical Extremes and Applications held in Vimeiro in 1983 [209] that extreme value theory was at that time already a prolific area with numerous applications. Tiago de Oliveira continued writing that “the narrow and shallow stream [of extremes] gained momentum and is now a huge river, enlarging at every moment and flooding the margins”, providing a witty and acute description of the state of the art at that time and giving a timeless prediction of the future state of the art in extreme value theory. Facing this mighty river and given the above brief overview of its birth and growth, only some highlights of its past and recent waters and margins are mentioned in the next sections.

2.1 Univariate and multivariate extreme value approaches

A fundamental paper in the EVT framework, and particularly on univariate extremes, is the one due to Gnedenko [83], which establishes necessary and sufficient conditions for the convergence of the maximum of a series of independent and identically distributed random variables to one of the three extreme value distribution types, namely Gumbel, Fréchet or Weibull. These three distributions correspond to different signs of the shape parameter of the GEV distribution, whose parametrization is attributed in the literature to von Mises [220] and Jenkinson [121]. The Gumbel distribution corresponds to a null shape parameter, while Fréchet and Weibull distributions correspond respectively to a positive and a negative value of the shape parameter. So, this parameter, also called extreme value index or tail index was, and still is, of primary interest in extreme value analysis.

The class of GEV distributions [160] is used to model the maximum of a random sample obtained by equally spaced observation periods. This method, called Gumbel method, is also referred to as annual maxima method because of the typical choice of a one–year interval. In this approach, testing the Gumbel hypothesis versus the Fréchet or Weibull distribution has been treated extensively in the literature [160]. In the eighties, besides the revelant contribution of Tiago de Oliveira [208, 210, 213] on this topic, that the author called the "trilemma", there are also relevant contributions of his co–worker, Ivette Gomes [84, 85, 86]. Ivette Gomes also worked on this topic with van Montfort [90], who had done some work on the subject in the seventies [214, 215]. In this area, there were also, for example, the papers by Bardsley [9] and by Otten and Van Montfort [166] in the seventies, the paper by Hosking [118] in the eighties, and the papers by Marohn [141, 142] in the nineties.

In these two last decades, different ways to define extreme events have lead to different approaches to the study of statistics of extremes. One of the approaches considers, alternatively to the Gumbel method which considers only one value per block, the observations that exceed a certain high threshold u, called the exceedances. The values obtained by the difference between the exceedances and the threshold are denominated excesses over u [179]. An adequate model to these values is the Paretian excesses or the POT model [88]. The statistical development of this approach has relevant contributions by Smith [195] and by Davison [36], both published in the already mentioned Proceedings of the NATO ASI on Statistical

Extremes and Applications [209]. These two authors further synthesised their works in a paper [38], which also presents a survey about the POT methodology [88]. The deduction of the probability distribution of excesses — the generalised Pareto distribution (GPD) — is considered by some authors [7, 171] a very important result in EVT, as fundamental as Gnedenko's results in [83]. Analogously, the problem to testing the exponentiality of the upper tail of a distribution against other GPD was also a topic that attracted attention of many researchers. Besides the already mentioned work of Davison and Smith [38], there were, for example, the papers [160] by van Montfort and Witter [216], Gomes and van Montfort [90], Falk [63], Brilhante [15], and Marohn [143, 144].

Another approach to statistics of extremes is the PORT methodology, named in this way by Araújo Santos and collaborators [2]. This semi-parametric approach relies on the sample of excesses over a random threshold in the sense that, if the k largest values are selected, then the $n-k$ order observation can be regarded as a random threshold [179]. In this case, the test of the exponentiality of the upper tail versus other GPD is based on the $k+1$ largest order statistics instead of the exceedances over a threshold u. Unlike the parametric methodology above, the only assumption in this semi-parametric approach is that the distribution function F is in the domain of attraction of an extreme value distribution. To test this hypothesis, Dietrich et al. [54] introduced, in 2002, a test statistic which includes the moment estimator due to Dekkers et al. [51]. In 2006, Drees et al. [59] established a test statistic using a tail approximation to the empirical distribution function [160]. Also in 2006, tables of the critical points corresponding to these two tests were given by Hüsler and Li [120], who analysed the two above mentioned statistical tests through a simulation study. When the hypothesis that F belongs to the domain of attraction of an extreme value distribution is not rejected, it may be useful for applications to know what is the most suitable domain of attraction for the sampled distribution. In this topic, and according to Neves et al. [159], the test by Hasofer and Wang [113], from 1992, may be pointed out as one of the most commonly used. Earlier in the eighties, Galambos [75] and Castillo et al. [20] had already worked on the problem of finding the domain of attraction that included the sampled distribution [160]. In 1996, Fraga Alves and Gomes [69] presented a comparison between the Hasofer and Wang [113] test procedure and other different tests of other authors for the statistical choice of extremal models. Since then, other procedures appeared in the literature, such as in the papers from 1999 by Fraga Alves [68], from 2000 by Segers and Teugels [188], from 2006 by Neves et al. [161], and from 2007 by Neves and

Fraga Alves [159]. In 2008, Neves and Fraga Alves [160] gave a brief overview of the topic of the statistical choice of extreme value domains and also of the above mentioned approaches.

Problems such as the ones that include, for example, a number of different physical processes analysed at one site or a spatial process observed at a finite number of sites, require a multivariate rather than an univariate approach [201]. Indeed, data recorded at multiple locations, such as rainfall or temperature, constitute spatial datasets that are necessarily multivariate [31]. A review of spatial extremes methods based on latent variables, copulas and spatial max-stable processes is presented by Davison et al. [37], which refer that appropriately chosen copula or max-stable models seem to be essential for the spatial modelling of extremes. The importance of max-stable and copula approaches for modelling spatial dependence is also emphasised by other authors such as Cooley et al. [31]. Max–stable processes can be viewed as infinite-dimensional generalizations of extreme value distributions [10]. A spectral representation for such processes due to de Haan [41] in 1984, already mentioned above, was used by Smith [197] to develop a construction method for multivariate extreme value distributions in 1990 [10], being this method applied to rainfall by Smith [197] and also by Coles and Tawn [29] in 1996. This application and others appeared in the nineties in consequence of the advances achieved in the eighties in multivariate extreme value theory. Some of those applications [128] are, for example, in the study of extreme concentrations of a pollutant by Joe [122], of extremely cold temperatures by Coles et al. [30], and of extreme sea levels by Dixon and Tawn [55].

The dependence structure of a multivariate distribution can be described through a copula function, as mentioned above, being the term copula used for the first time in 1959 by Sklar [194]. The copula function had appeared earlier under different names in the works of Fréchet, Dall'Aglio, Féron and other authors, being results about such functions traceable to the early work of Hoeffding, who called them "standardised distributions" [156]. In 1959, and unaware of the existence of two papers written in German in the beginning of the forties by Hoeffding [116, 117], Fréchet [72] obtained some of the results established earlier by Hoeffing, leading to expressions such as "Fréchet–Hoeffding bounds". In the seventies, the copula functions were rediscovered by other authors, including Kimeldorf and Sampson [126], who called them "uniform representations", and Galambos [76] and Deheuvels [47], who termed them as "dependence functions" [156]. In 1975, Galambos [74] worked with a copula

function that became to be known as the negative logistic model or Galambos copula. According to Gudendorf and Segers [101], the notion of the definition of extreme value copulas can be traced back at least to the first edition of the book by Galambos [76] published in 1978, being also present in the paper by Deheuvels [50] included in the already mentioned Proceedings of the NATO ASI on Statistical Extremes and Applications [209]. Earlier in 1979, Deheuvels [48] estimated the copula function and constructed nonparametric tests of independence by means of the empirical copula's application, being one of the many authors that applied copula functions to the study of dependence. More recently, in 2010, Gudendorf and Segers [101] advocated that extreme value copulas can be considered proper models for the dependence structure between rare events, presenting also a state of the art review in dependence modelling through extreme value copulas. Already in the sixties, Gumbel [108, 109] had worked with an EVC considered today as one of the oldest multivariate extreme value models [101], known as Gumbel–Hougaard or logistic copula. The t–EVC is one other that is used in the context of modelling multivariate financial return data, as mentioned by Demarta and McNeil [52], but there are also applications of this model in environmental modelling, such as, for example, in the study of extreme concentrations of a pollutant at several monitoring stations in a region [122]. Ribatet and Sedki's paper from last year [180] closes this section. Ribatet and Sedki [180] present the copula framework with an emphasis in the link between extreme value copulas and tail dependence, and establish some connections with max–stable processes. According to these two authors, during the last decades, the copula functions have been increasingly used as a convenient tool to model dependence across several random variables. Ribatet and Sedki [180] also made an application of extreme value copulas to the spatial modelling of extreme temperatures in Switzerland.

2.2 Application to rainfall extremes

It seems that the first authors to connect extreme value theory and rainfall values were Gumbel [103] and Potter [174] in 1942 and 1949, respectively. In the following years, other authors, such as Jenkinson [121] in 1955, Sneyers [198, 199] in 1977 and 1979, and Sevruk and Geiger [190] in 1981, considered the Gumbel and Fréchet distributions good fits for maximum rainfall values [211]. Already in 1953, Brooks and Carruthers [16] indicated that the Gumbel distribution tends to underestimate the magnitude of extreme rainfall events, assertion that was also supported many years later, in 2004, by Koutsoyannis [129]. Although the GEV distribution was

recommended for flood frequency analysis in 1975 in the United Kingdom [157], it was only recommended for rainfall frequency in 1995 [224] in the United States of America [146]. Nevertheless, in 1991, Buishand [18] performed a regional estimation of the GEV parameters for annual maximum daily precipitation amounts in Netherlands. In 1985, Buishand [17] investigated the limiting distribution of maxima of sequences of dependent random variables, working also with rainfall data and considering the GEV distribution. The idea behind a regional analysis is that if a region is relatively homogeneous, the extreme observations at different sites can be used to improve the estimation of extreme quantiles at a given distinct site within the same region [124]. According to the paper from 1991 by Buishand [18], the inference about the form of the upper tail of the distribution of rainfall amounts needs to be based on a joint evaluation of several records from a same region.

With the purpose of evaluate the accuracy of a regional approach relative to a single site frequency analysis, Alila [1] proposed in 1999 a regional rainfall frequency approach for estimating design storms, used in hydrological design applications [23]. Alila [1] performed a simulation study using rainfall extreme values from 375 rain gauge stations located in Canada, presenting this rain gauge network an average record length smaller than 25 years, with only a few stations having more than 40 years of records. Also in Canada and in an earlier study from 1980, Watt and Nozdryn-Plotnicki observed that the Gumbel distribution is not always a satisfactory fit model for the annual rainfall extremes. More recently, in 2002, Nguyen et al. [163] also applied a regional frequency analysis to extreme rainfall in that country. In the same year, Crisci et al. [34] made an analysis of extreme rainfall events in Tuscany, Italy, using the GEV distribution and also a regional frequency analysis approach. An emerging topic analysed by Crisci et al. [34] was the changes in extreme precipitation, which was also addressed by Aronica et al. [4] in the same year and in the same country. In 2003, the temporal changes in the occurrence of extreme rainfall events in the United Kingdom were analysed by Fowler and Kilsby [67].

The use of extreme value distributions in the analysis of rainfall extremes is not limited to the regions mentioned above. For instance, some more examples can be found in Belgium (Gellens [80]), Greece (Koutsoyannis and Baloutsos [132]), Hawaiian Islands (Chu et al. [24]), New Zealand (Withers and Nadarajah [225]), and South Korea (Nadarajah and Choi [154]). A case study with data from France, Greece, Italy, United Kingdom and United States of America was performed in 2004 by Koutsoyannis [131], who empirically concluded that the GEV distribution

with positive shape parameter is more adequate for modelling annual maximum rainfall series than the Gumbel distribution, confirming the author's own conclusion of the theoretical investigation conducted in the same year [130]. The results of the studies by Koutsoyannis [130, 131] are in agreement with the ones obtained by Chaouche et al. [22], Coles et al. [27] and Sisson et al. [193], since all excluded a Gumbel or an exponential distribution behaviour in the tail of the distribution of rainfall extremes concerning annual maximum series or series of values over a threshold. In 2002, Chaouche et al. [22] developed an algorithm for threshold selection and applied it to rainfall datasets from Burkina Faso and the French island of Reunion. Supported by an analysis made with annual and daily rainfall data from Venezuela, Coles et al. [27] defended the use of a Bayesian approach over a classical likelihood analysis. The work of these authors was extended by Sisson et al. [193], who also considered classical and Bayesian methods of inference for annual maxima and daily POT models. Besides daily rainfall data from Venezuela, Sisson et al. [193] also analysed daily rainfall records from Puerto Rico and water level data from Nicaragua, advocating the application of more flexible inferential methods to the analysis of environmental extremes in the Caribbean region.

Considering modelling of extreme rainfall in a region as a problem of multivariate nature, Coles and Tawn [25, 29] developed in the nineties methods to deal with spatial extremes based on the spectral representation due to de Haan [41]. Coles, in 1993, treated the problem of model specification and inference within the class of max–stable processes [29], developing a model that consists of a multivariate extreme value distribution that describes the extremes at a subset of rainfall stations [19]. This method was applied in 1996 by Coles and Tawn [29] to calculate quantiles of extreme daily areal rainfall for a region in the south west of England. According to Schlather [184], the max–stable process approach taken by Coles and Tawn, first considered in 1990 by Smith [197], should be applied to model "convective precipitation", which is characterised by an area of high rainfall intensity in opposition to much less or even no rainfall elsewhere. Schlather [184] also advocated a different max–stable approach to simulate "cyclonic precipitation", characterised by variable rainfall all over the affected region. Following the latter approach, the representation of simple max–stable processes presented in de Haan and Ferreira [42] was used in 2008 by de Haan and Zhou [44] to propose a stationary max-stable process as a model of dependency structure. In the same year, that model was applied by Buishand et al. [19] to rainfall extremes in the province of North Holland, in the Netherlands. From the max–stable process, Buishand et

al. [19] simulated extreme rainfall and estimated the 100–year quantile for the areal average rainfall, having obtained a value lower than the average 100–year quantile for the considered stations. In the previous year, extreme rainfall had also been studied by Cooley et al. [32], who used a Bayesian framework for modelling dependence in spatial extremes.

Considering the copula approach, Bacchi et al. [5] applied in the eighties a bivariate exponential distribution to model storm duration and average intensity. The bivariate exponential distribution applied was that introduced in 1960 by Gumbel [108], in a paper where the Gumbel copula mentioned before had its origins. However, according to Favre et al. [64], the use of copulas was scarce in the hydrological domain until the beginning of 2005. Among the few previous studies using copulas, these authors refer only one paper concerning the study of rainfall, namely a work by De Michelle and Salvadori [46] published in 2003 [46]. De Michelle and Salvadori [46] considered an improved intensity–duration model that, introducing generalised Pareto marginals for both variables, describes the dependence between storm duration and the intensity through a suitable bivariate copula. In 2006, Salvadori and De Michelle [181] described the dependence between three variables, namely the average intensity and duration in wet and dry periods, via a trivariate copula, presenting a list of the most relevant approaches to storm modelling since the seventies. Also applying copulas to the study of association between rainfall characteristics, Gargouri–Ellouze and Chebchoub [77], in 2008, studied the dependence between rainfall depth and duration, being the joint distribution of these two variables built using the Gumbel's EVC. Rainfall as a spatial process observed at a finite number of sites was also studied in recent years by a copula approach by some authors, such as, for example, Serinaldi [189] in 2009 and Ghosh [82] in 2010.

Chapter 3

About Madeira Island's climate characteristics, flash flood history and rainfall data

Madeira Island has an area of 737 km^2, is 57 km long and 22 km wide [162]. The island has a near E–W oriented orographic barrier, approximately perpendicular to the prevailing NE wind direction, which induces a remarkable variation of precipitation between the northern and southern slopes [70]. Madeira Island's mountain ridge located along its central part presents Pico Ruivo, the highest peak with 1861 m, Pico do Areeiro with 1818 m in its eastern part, while Paul da Serra massif is located above 1400 m in the western part [33, 176]. The amount of rainfall increases with altitude and the northern slopes are more humid than the southern ones [70, 175, 176, e.g.]. The total annual precipitation is therefore highest at the highest altitudes, like Areeiro and Bica da Cana located in Paul da Serra, while the lowest values correspond to lowlands in the southern slope, like Funchal and Ponta do Sol [175, 176]. Madeira's location, topography and natural vegetation originate a variety of micro–climates, and this Portuguese island has essentially a Mediterranean climate with mild summers and winters [33]. Some exceptions are found at the highest altitudes, where the mean annual air temperature can decrease to 8°C, while in the coastal regions it ranges between 18°C and 19°C [45]. The precipitation regime over the island is not only affected by local circulation, but also by synoptic systems typical of mid–latitudes such as fronts and extra tropical–cyclones. During the summer season, the precipitation regime is also affected by the Azores anticyclone [33].

Madeira Island has in its history a significant number of flash floods [177, 192, e.g.]. Unfortunately, until very recently, the extreme rainfalls causing these flash flood were not measured. According to Silva and Menezes [192], there is a document dated from 1601 mentioning the occurrence of previous events that might have been flash floods. Records referring flash flood type events in 1611 and in 1707 also exist. The first event of this nature described by Silva and Menezes [192] was the event occurred on the 18th of November 1724 which caused the death of 26 people and 80 damaged houses in Machico, and damages in Santa Cruz and Funchal. In the following century, more precisely in October 9 from 1803, Madeira suffered its worst calamity with hundreds of deaths and a high devastation in Funchal. Other southern areas like Machico, Santa Cruz, Campanário, Ribeira Brava and Calheta were also affected by this calamity [177, 192, *e.g*]. In the same month in the years of 1815 and 1842, flash floods occurred in Madeira, Funchal being the most affected area. Six years later, in November of 1848, floods occurred in Santana, a northern region of Madeira, causing the lost of lives and crops, that were dragged to the sea. In Funchal, no greater damage occurred, even tough it seems the rain was heavier than the one from the 24th October 1842 [177]. Heavy rains were reported in the island in the months of January and March of 1856, and in the first day of year 1876 [177, 192]. In the second and third days of October 1895, torrential rains occurred in the western part of the island, namely in the southern locations Calheta and Ribeira Brava and in the northern location São Vicente and the resulting floods caused some deaths and destruction of houses, roads and bridges [177, 192]. In the beginning of following century, in November 1901, floods and landslides occurred in Funchal and also in Machico. These two locations together with Camacha, Santa Cruz, Ribeira Brava and São Vicente experienced a storm of wind and rain during two days in the 25th and 26th February 1920 [177, 192]. In this event two persons died and boats with their crews disappeared. Almost a year later, in March 1921 it rained heavily again in Machico but also in Faial, Santana and São Jorge [177, 192]. In the twenties, two more extreme events occurred in the history of flash floods in Madeira. In December of 1926, a ferocious storm hit Funchal, but the consequences were not comparable with the ones occurred on the 6th of March of 1929 in São Vicente where after consecutive days of rain a flash–flood caused 40 casualties and 11 destroyed houses [70, 177]. Fragoso et al. [70], based on the information of the SRES 2010 technical report [56], identify the 10 main flash–floods events in Madeira between 1800 and 2010, the dates of their occurrence, the affected areas and the resulting casualties and damage. The event of March 1929 ranks second among the most destructive ones after October 1803. The following five events, one in the

thirties, three in the seventies and one in the nineties, are also described in the work of R. Quintal [177], which compiles information about all the previous events and about others in the same century. All these events happened between September and March and mainly affected the following locations: Funchal, Machico, Ribeira Brava and São Vicente. The last event described in [177] occurred in São Vicente on the 5th and 6th of March of 2001 and occupies the eight place in the list presented by Fragoso et al. [70] with 4 casualties and 120 dislodged people. This event is followed in that list by the event occurred on December 22, 2009, that affected the regions of Madalena do Mar and São Vicente and by the one which occurred on February 20, 2010, and affected mainly Funchal and Ribeira Brava. Besides Fragoso et al. [70], other authors such as Baioni [6], Couto et al. [33], Luna et al. [139] and Nguyen et al. [162] also studied the event occurred on the 20th February 2010, the most severe one in the last 211 years.

Relatively to Madeira's rainfall data records, the oldest weather station in Madeira, the one from Funchal, started to operate in January 1865 [192]. Thirty years later, the General Council of the Autonomous District of Funchal had intended to install another weather station in Pico do Areeiro, whose observations combined with the ones from Funchal's station would give a better insight of Madeira Island's climate and would allow its comparison with the ones of other health resort islands. Nevertheless, the newer weather station began to provide rainfall and temperature data only in November 1936 [192]. In order to provide useful information for agriculture, more weather stations were settled on the island, at different altitudes, from 1936 to 1955 [169]. However in 1990, according to Gonçalves and Nunes [91], some stations would no longer be functioning, and others would provide data only concerning to the direction and height of waves and to the prevailing wind direction and intensity. The remaining stations ceased to be maintained by the General Council of the Autonomous District of Funchal [56]. Nowadays Madeira Island is well covered by rain gauge stations maintained by three different organisations, namely the Madeira's Investments and Water Management company, IPMA and LREC [70, 56].

Madeira Civil Engineering Laboratory's Department of Hydraulics and Energy Technologies provided for this study daily rainfall data from 25 rain gauge stations maintained in the past by the General Council of the Autonomous District of Funchal (Set LREC). In Figure 3.1 a circle with a letter from A to Y, according to a decreasing altitude order, marks the location of each station. The 25 rain gauge stations are distributed by four altitude classes termed as Class 1, 2, 3 and 4 and the colour of

the circle in Figure 3.1 varies according to the altitude class of the station. Classes 1 and 4 include the stations located above 900 m and below 300 m, respectively. Class 2 includes the rain gauge stations located at an altitude between 600 m and 900 m, while Class 3 includes the rain gauge stations located at an altitude between 300 m and 600 m.

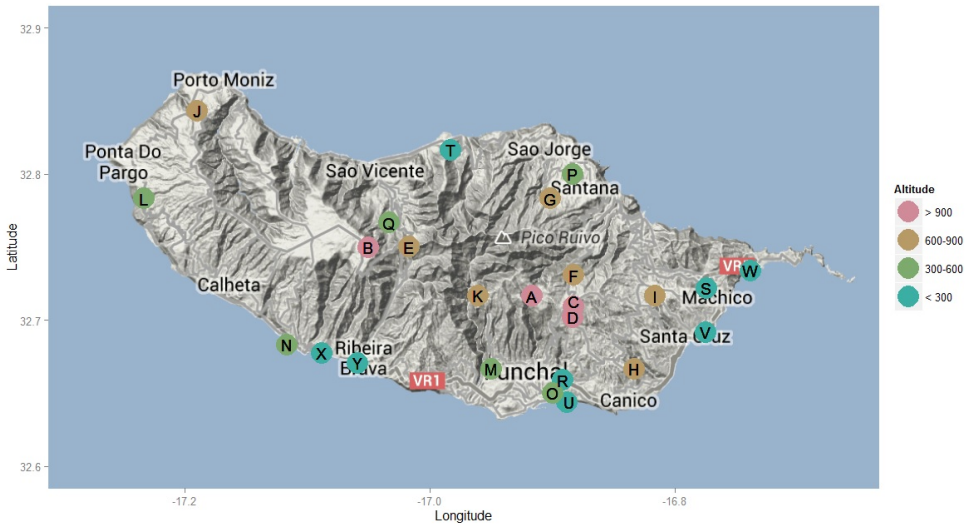

Figure 3.1: Location and altitude range of the rain gauge stations–Set LREC (Map data ©2014 Google).

The letters A, C and D correspond to Areeiro, Poiso and Montado do Pereiro rain gauge stations which are located in the southern slope of the island, while the letter B belongs to the remaining station in Class 1, Bica da Cana, which is located in the northern slope. Class 2 contains the northern stations Encumeada, Queimadas and Porto Moniz with the corresponding letters E, G and J. To the southern stations Ribeiro Frio, Camacha, Santo da Serra and Curral das Freiras were attributed respectively the letters F, H, I and K. The only northern stations located at an altitude between 300 m and 600 m are Santana and Loural with the corresponding letters P and Q while the other stations in Class 3, represented by the letters L, M, N and O, are all located in the southern slope of the island. This group of four stations is formed by Santo António and Sanatório with the corresponding letters M and O, two stations located in Funchal municipality, and by Ponta do Pargo and Ribeira Brava with the letters L and N, being the former the southern rain gauge station located further west. Class 4 includes only one rain gauge station located in the northern slope of the island, namely Ponta Delgada, which is represented by the letter T. This class also includes Machico, Santa Catarina and Caniçal, the three rain gauge stations located further east in the island, corresponding to the letters

S, V and W. The remaining stations belonging to Class 4, Bom Sucesso, Funchal, Lugar de Baixo and Ribeira Brava are represented by the letters R, U, X and Y, being the former two located in Funchal municipality. For an easy identification of the stations, these will usually be referred to by their name and identification letter. When the writing space does not allow it (e.g., in tables), stations will be referred to only by their identification letters.

The map displayed in Figure 3.1 was created by the *ggmap* R language package [178], while the distances between rain gauges stations presented in the following Tables 3.1, 3.2 and 3.3 were obtained by the application of the *SpatialExtremes* R language package [178].

Table 3.1: Distances (m) between rain gauge stations (A to I).

	A	B	C	D	E	F	G	H	I
A	–	13032	3256	3501	10135	3605	7533	9627	9423
B	13032	–	16278	16464	3170	15808	14348	22335	22200
C	3256	16278	–	849	13343	2427	8376	6692	6319
D	3501	16464	849	–	13583	3242	9179	6170	6538
E	10135	3170	13343	13583	–	12733	11352	19554	19139
F	3605	15808	2427	3242	12733	–	6062	8515	6421
G	7533	14348	8376	9179	11352	6062	–	14440	10889
H	9627	22335	6692	6170	19554	8515	14440	–	5761
I	9423	22200	6319	6538	19139	6421	10889	5761	–
J	29213	16721	32357	32687	19208	31336	27764	38733	37683
K	4265	9158	7383	7445	6421	7476	9183	13206	13531
L	30603	17601	33841	33984	20611	33342	31028	39669	39744
M	6457	13206	7912	7367	11205	9505	13677	10945	13679
N	19152	9748	22113	21944	11952	22539	22956	26641	28374
O	7656	17950	6854	6016	15627	9128	14773	6529	10762
P	9832	16611	10086	10914	13685	7677	2615	15514	11158
Q	12329	2725	15479	15772	2452	14646	12436	21787	21053
R	6942	17982	5772	4927	15507	8054	13825	5580	9541
S	13429	26057	10354	10559	22961	10255	13782	8268	4036
T	12813	9783	15198	15815	8041	13391	8494	21787	19161
U	8638	19250	7406	6558	16893	9699	15517	5778	10520
V	13659	26622	10410	10343	23608	11053	15672	6165	4829
W	16886	29290	13889	14138	26174	13577	16301	11624	7600
X	16725	8931	19591	19379	10510	20137	21014	23933	25825
Y	14407	8971	17132	16863	9722	17854	19321	21217	23331

The first four columns of the Table 3.1 contain the distances between the stations belonging to Class 1–Areeiro (A), Bica da Cana (B), Poiso (C) and Montado do Pereiro (D)– and all the stations from Set LREC. The distances between Encumeada (E), Ribeiro Frio (F), Queimadas (G), Camacha (H) and Santo da Serra (I) rain gauge stations and all the ones in Set LREC form the remaining five columns of Table 3.1.

Table 3.2: Distances (m) between rain gauge stations (J to Q).

	J	K	L	M	N	O	P	Q
A	29213	4265	30603	6457	19152	7656	9832	12329
B	16721	9158	17601	13206	9748	17950	16611	2725
C	32357	7383	33841	7912	22113	6854	10086	15479
D	32687	7445	33984	7367	21944	6016	10914	15772
E	19208	6421	20611	11205	11952	15627	13685	2452
F	31336	7476	33342	9505	22539	9128	7677	14646
G	27764	9183	31028	13677	22956	14773	2615	12436
H	38733	13206	39669	10945	26641	6529	15514	21787
I	37683	13531	39744	13679	28374	10762	11158	21053
J	–	25618	7789	29818	19018	34609	29111	16953
K	25618	–	26566	5672	15068	9376	11742	8746
L	7789	26566	–	29547	15577	34575	32840	18833
M	29818	5672	29547	–	15743	5043	16053	13568
N	19018	15068	15577	15743	–	20658	25410	12102
O	34609	9376	34575	5043	20658	–	16708	17991
P	29111	11742	32840	16053	25410	16708	–	14530
Q	16953	8746	18833	13568	12102	17991	14530	–
R	34613	9139	34856	5519	21253	1244	15670	17849
S	41192	17509	43548	17574	32379	14228	13387	24771
T	19576	11267	23712	16930	19362	20067	9549	7260
U	35892	10603	35858	6330	21866	1328	17321	19243
V	42362	17673	44151	16652	32058	12607	15733	25605
W	43999	20952	46699	21195	35902	17780	15428	27871
X	20722	12709	17988	13016	2791	17907	23514	11144
Y	22721	10573	20551	10281	5570	15130	21861	10921

Besides these five stations, Class 2 includes two more stations, Porto Moniz (J) and Curral das Feiras (K). The distances between these two stations and all the other stations form the two first columns of Table 3.2. The remaining columns of this table correspond to the distances between pairs of stations formed by all the considered stations and the six rain gauge stations in Class 3, namely, Ponta do Pargo (L), Santo António (M), Canhas (N), Sanatório (O), Santana (P) and Loural (Q). Table 3.3

presents the distances between Bom Sucesso (R), Machico (S), Ponta Delgada (T), Funchal (U), Santa Catarina (V), Caniçal (W), Lugar de Baixo (X) and Ribeira Brava (Y), and all the rain gauge stations in Set LREC.

Table 3.3: Distances (m) between rain gauge stations (R to Y).

	R	S	T	U	V	W	X	Y
A	6942	13429	12813	8638	13659	16886	16725	14407
B	17982	26057	9783	19250	26622	29290	8931	8971
C	5772	10354	15198	7406	10410	13889	19591	17132
D	4927	10559	15815	6558	10343	14138	19379	16863
E	15507	22961	8041	16893	23608	26174	10510	9722
F	8054	10255	13391	9699	11053	13577	20137	17854
G	13825	13782	8494	15517	15672	16301	21014	19321
H	5580	8268	21787	5778	6165	11624	23933	21217
I	9542	4036	19161	10520	4829	7600	25825	23331
J	34613	41192	19576	35892	42362	43999	20722	22721
K	9139	17509	11267	10603	17673	20952	12709	10573
L	34856	43548	23712	35858	44151	46699	17988	20551
M	5519	17574	16930	6330	16652	21195	13016	10281
N	21253	32379	19362	21866	32058	35902	2791	5570
O	1244	14228	20067	1328	12607	17780	17907	15130
P	15670	13387	9549	17321	15733	15428	23514	21861
Q	17849	24771	7260	19243	25605	27871	11144	10921
R	–	13055	19483	1712	11558	16625	18513	15761
S	13055	–	22218	13750	3358	3622	29822	27319
T	19483	22218	–	21129	23944	24707	18291	17685
U	1712	13750	21129	–	11877	17238	19104	16319
V	11558	3358	23944	11877	–	5803	29402	26770
W	16625	3622	24707	17238	5803	–	33369	30893
X	18513	29822	18291	19104	29402	33369	–	2795
Y	15761	27319	17685	16319	26770	30893	2795	–

For each rain gauge station in Set LREC, the station's name and identification letter, geographical location, altitude and the measurement period considered are presented in Table 3.4. The island slope where each one of the mentioned rain gauge stations is located is also shown in Table 3.4, with 1 denoting the northern slope and 2 the southern one. For a quick identification of all the rain gauge stations within a specific class of altitude, there are three extra horizontal lines in Table 3.4 separating the stations that are included in Classes 1, 2, 3 and 4.

Table 3.4: Information about the rain gauge stations–Set LREC.

Station Name	Latitude	Longitude	Altitude (m)	Period	Slope
Areeiro (A)	32°43'N	16°55'W	1610	1950–1980	2
Bica da Cana (B)	32°45'N	17°03'W	1560	1950–1980	1
Poiso (C)	32°42'N	16°53'W	1360	1959–1980	2
Montado do Pereiro (D)	32°42'N	16°53'W	1260	1950–1980	2
Encumeada (E)	32°45'N	17°01'W	900	1959–1980	1
Ribeiro Frio (F)	32°43'N	16°53'W	874	1950–1980	2
Queimadas (G)	32°46'N	16°54'W	860	1950–1980	1
Camacha (H)	32°40'N	16°50'W	680	1950–1980	2
Santo da Serra (I)	32°43'N	16°49'W	660	1950–1980	2
Porto Moniz (J)	32°50'N	17°11'W	653	1950–1972	1
Curral das Freiras (K)	32°43'N	16°58'W	650	1950–1972	2
Ponta do Pargo (L)	32°47'N	17°14'W	570	1950–1972	2
Santo António (M)	32°40'N	16°57'W	525	1950–1972	2
Canhas (N)	32°41'N	17°07'W	425	1950–1972	2
Sanatório (O)	32°39'N	16°54'W	380	1950–1980	2
Santana (P)	32°48'N	16°53'W	380	1950–1980	1
Loural (Q)	32°46'N	17°02'W	307	1950–1972	1
Bom Sucesso (R)	32°39'N	16°54'W	290	1959–1980	2
Machico (S)	32°43'N	16°47'W	160	1959–1980	2
Ponta Delgada (T)	32°49'N	16°59'W	136	1950–1980	1
Funchal (U)	32°38'N	16°53'W	58	1950–1980	2
Santa Catarina (V)	32°41'N	16°46'W	49	1959–1980	2
Caniçal (W)	32°44'N	16°44'W	40	1959–1980	2
Lugar de Baixo (X)	32°40'N	17°05'W	15	1950–1980	2
Ribeira Brava (Y)	32°40'N	17°04'W	10	1950–1972	2

IPMA provided for this study monthly maxima obtained from the collected daily rainfall data of the seven rain gauge stations (Set IPMA) displayed in Table 3.5. For each rain gauge station in this Set IPMA, which is included in Set LREC, Table 3.5 provides the corresponding identification name and letter, geographical location, altitude and the measurement period considered. The island slope where each one of these seven rain gauge stations is located is also shown in Table 3.5, with 1 denoting the northern slope and 2 the southern one like in Table 3.4.

Table 3.5: Information about the rain gauge stations–Set IPMA.

Station Name	Latitude	Longitude	Altitude (m)	Period	Slope
Areeiro (A)	32°43'N	16°55'W	1610	1961–1992	2
Bica da Cana (B)	32°45'N	17°03'W	1560	1961–2008	1
Santo da Serra (I)	32°43'N	16°49'W	660	1970–2009	2
Santana (P)	32°48'N	16°53'W	380	1942–2007	1
Funchal (U)	32°38'N	16°53'W	58	1949–2009	2
Santa Catarina (V)	32°41'N	16°46'W	49	1961–2009	2
Lugar de Baixo (X)	32°40'N	17°05'W	15	1961–2004	2

Figures 3.2 and 3.3 show the annual maximum of daily precipitation recorded at each station from Set IPMA over the measurement period. With the exception of these rain gauge stations, Figures 3.4 to 3.8 also show the annual maximum of daily precipitation for the rain gauge stations belonging to Set LREC. There is no evidence in each one of these figures that the pattern of variation of the annual maximum of daily precipitation has changed over the observation period, with the possible exception of Areeiro (A) station data. In this case, Figure 3.2 (upper left) shows a slight decrease in the data values over time.

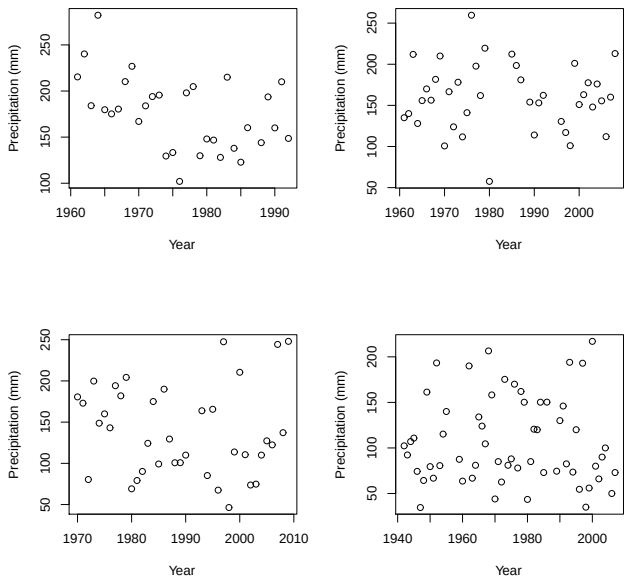

Figure 3.2: Annual maximum of daily precipitation values at Areeiro (A) (up left), Bica da Cana (B) (up right), Santo da Serra (I) (down left), and Santana (P) (down right) stations–Set IPMA.

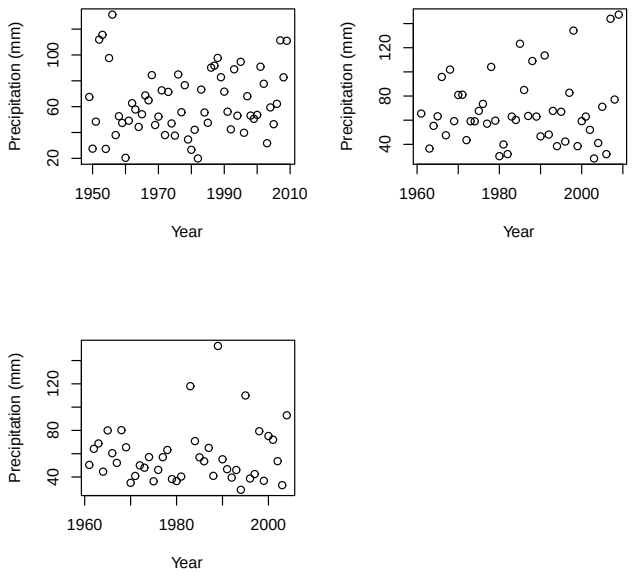

Figure 3.3: Annual maximum of daily precipitation values at Funchal (U) (up left), Santa Catarina (V) (up right), and Lugar de Baixo (X) (down) stations–Set IPMA.

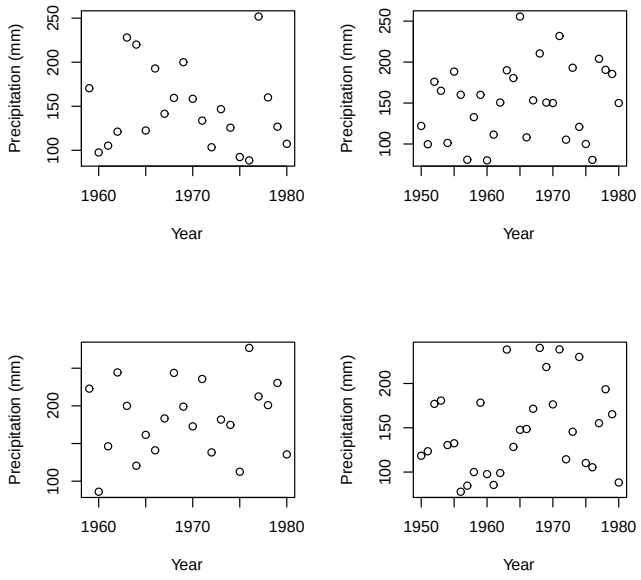

Figure 3.4: Annual maximum of daily precipitation values at Poiso (C) (up left), Montado do Pereiro (D) (up right), Encumeada (E) (down left), and Ribeiro Frio (F) (down right) stations–Set LREC.

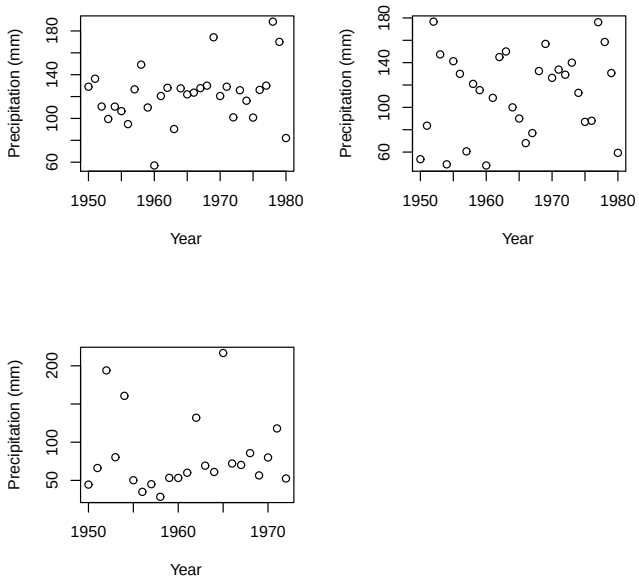

Figure 3.5: Annual maximum of daily precipitation values at Queimadas (G) (up left), Camacha (H) (up right), and Porto Moniz (J) (down) stations–Set LREC.

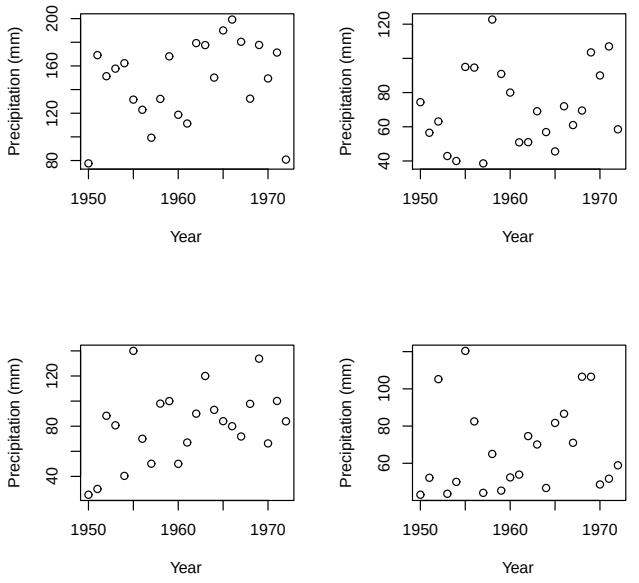

Figure 3.6: Annual maximum of daily precipitation values at Curral das Freiras (K) (up left), Ponta do Pargo (L) (up right), Santo António (M) (down left), and Canhas (N) (down right) stations–Set LREC.

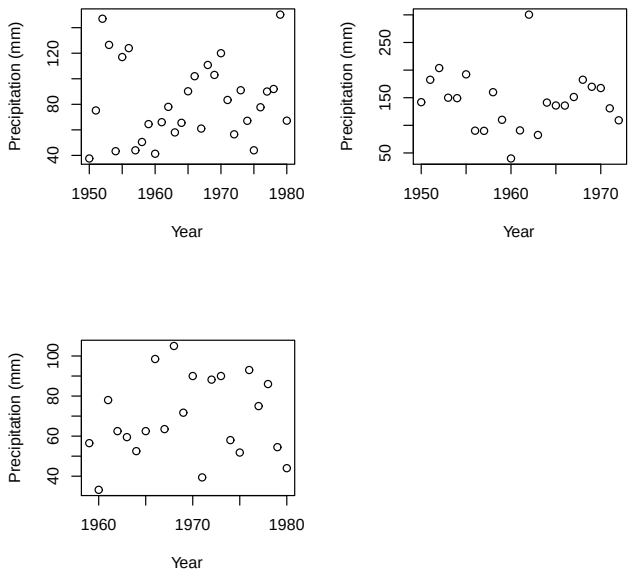

Figure 3.7: Annual maximum of daily precipitation values at Sanatório (O) (up left), Loural (Q) (up right), and Bom Sucesso (R) (down) stations–Set LREC.

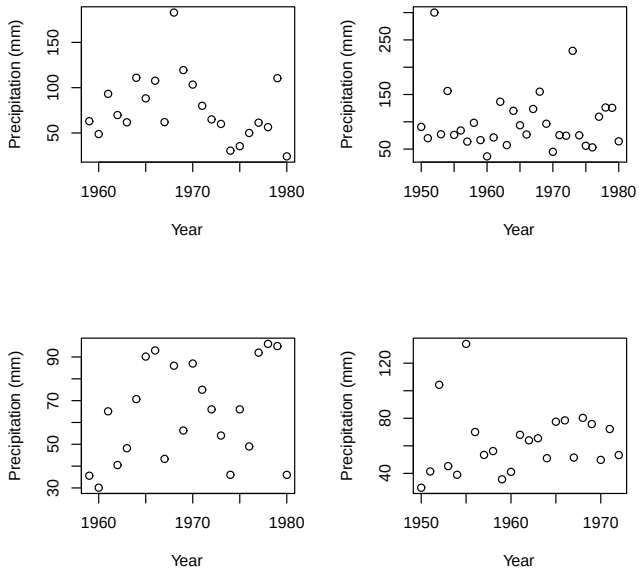

Figure 3.8: Annual maximum of daily precipitation values at Machico (S) (up left), Ponta Delgada (T) (up right), Caniçal (W) (down left), and Ribeira Brava (Y) (down right) stations–Set LREC.

Chapter 4

Methodology

4.1 Gumbel's model approach

The present section is related to the univariate extreme value theory, especially to the so called Gumbel's approach. The opening subsection recalls the generalised and also the standard extreme value distributions, while the second one presents the parameter estimation methods and statistical tests applied in Section 5.1 of Chapter 5. The model checking procedures used in this thesis are presented in subsection 4.1.3. Subsection 4.1.4 concludes the section. In this subsection, the models considered in the trend analysis of Madeira Island's annual rainfall data are presented.

One method of extracting upper extremes from a set of data is called annual maxima, blocks or Gumbel method. In this method, the considered dataset is organised in blocks of equal size – assume that there are n blocks of size m – from which the maximum values are chosen:

$$x_i = \max\{y_{i,1}, ..., y_{i,m}\}, i = 1, ..., n.$$

To implement this model a block size choice is needed, which implies an underlying trade-off between bias and variance. A large block size yields few block maxima and consequently large estimation variance. On the other hand, a small block size can lead to a poor limit model approximation. Addressing this problem, blocks are often chosen to correspond to a time period of one year, being m the number of observations in a year and, therefore, block maxima being annual maxima [26].

Let $X_1, X_2, ..., X_n$ be independent random variables with a common distribution function F. The distribution function of the maximum is given by

$$P\left\{\max_{i\leq n} X_i \leq x\right\} = P\{X_1 \leq x, ..., X_n \leq x\} = F^n(x).$$

It is important to notice that a distribution function of the form F^n may still be an accurate approximation of the actual distribution of the maximum, even when the conditions of independence and homogeneity fail. When the variables X_i are independent but heterogeneous with distribution functions F_i, F^n is replaced by $\prod_{j\leq n} F_j$. The distribution function F^n can still be used instead of $\prod_{j\leq n} F_j$ if the deviations between the different distribution functions are negligible. On the other hand, even if there is a slight dependence in the data, a distribution function of the form F^n may still be considered as a good approximation of the distribution function of the maximum [179].

4.1.1 Extreme value distributions

The distribution of the largest extreme values in hydrology generally appears as a type I extreme value distribution since most hydrologic variables are unbounded on the right. Type I extreme value distribution is also referred to as the Gumbel's extreme value distribution, the Fisher–Tippett type I distribution, and the double exponential distribution. Besides Gumbel's extreme value distribution, there are two other extreme value distributions, the Fisher-Tippett types II and III distributions, also known as the Fréchet and the Weibull distribution functions.

The three standard extreme value distribution functions are defined in the following way, for $x \in \mathbb{R}$:

- Gumbel (EV0): $G_0(x) = \exp(-\exp(-x))$,
- Fréchet (EV1), $\alpha > 0$: $G_{1,\alpha}(x) = \exp\left(-x^{-\alpha}\right)\mathbf{I}_{\mathbb{R}_0^+}(x)$,
- Weibull (EV2), $\alpha < 0$: $G_{2,\alpha}(x) = \exp\left(-\left(-x\right)^{-\alpha}\right)\mathbf{I}_{\mathbb{R}^-}(x) + \mathbf{I}_{\mathbb{R}_0^+}(x)$.

Besides the above terminologies, the Gumbel distribution is also represented in the literature by the Greek letter Λ, while the Fréchet distribution with shape parameter $\alpha > 0$ is represented by Φ_α, and the Weibull distribution function by Ψ_α, where $\alpha < 0$ [179].

A unified model, known as the GEV distribution, is obtained through the von Mises' parametrization [219]. This model, which is also frequently attributed to Jenkinson [121], is defined for $\gamma = \frac{1}{\alpha}$ in the following way:

$$G_\gamma(x) = \begin{cases} \exp(-(1+\gamma x)^{-1/\gamma}), & \text{if } 1+\gamma x > 0,\ \gamma \neq 0; \\ \exp(-\exp(-x)), & \text{if } x \in \mathbb{R},\ \gamma = 0. \end{cases} \tag{4.1}$$

By adding location and scale parameters, μ and $\sigma > 0$, the full GEV family $G_\gamma(\frac{x-\mu}{\sigma})$ follows. This unified model allows a unified expression also for the return levels. For a given small probability p, a return level is a threshold q_p, whose probability of exceedance is p. In the context of annual block maxima, the return level is the value exceeded by the annual maximum in any particular year with probability p. In other words, the return level q_p is the value expected to be exceeded once every $1/p$ years [26].

Return level estimates $\widehat{q_p}$ can be obtained by the estimation of the extreme quantiles of the annual maximum distribution given by

$$q_p = \begin{cases} \mu - \frac{\sigma}{\gamma}[1 - (-\log(1-p))^{-\gamma}], & \text{if } \gamma \neq 0; \\ \mu - \sigma \log\left(-\log(1-p)\right), & \text{if } \gamma = 0, \end{cases} \tag{4.2}$$

where μ, σ and γ are replaced by their respective estimates.

The use of Fréchet, Weibull and Gumbel distribution functions in the modelling of maxima is justified by the works of Fréchet [71], Fisher and Tippet [66], Gnedenko [83] and de Haan [39]. Together, these authors have found these distributions to be the possible non-degenerate limits of sequences $F^n(b_n + a_n x)$, when $n \to +\infty$, for some sequences of constants b_n and $a_n > 0$. The same authors have also found the sufficient and necessary conditions on the distribution function F for the convergence to these limits (see, e.g., J. Galambos [76]). In short, if $F^n(b_n + a_n x)$ has a non-degenerate limiting distribution function as $n \to \infty$ for constants b_n and $a_n > 0$, then

$$\left| F^n(b_n + a_n x) - G\left(\frac{x-\mu}{\sigma}\right) \right| \to 0, \ \ n \to \infty$$

with $G \in \{G_0, G_{1,\alpha}, G_{2,-\alpha}, \text{for some } \alpha \in \mathbb{R}^+\}$ or, equivalently, $G = G_\gamma$, for some $\gamma \in \mathbb{R}$, where μ and $\sigma > 0$ are the location and scale parameters, respectively. It is important to notice that the behaviour of the right tail of the distribution function F determines the limit distribution of the normalised maximum (see, e.g., J. Galambos [76]). Even the right endpoint of the support of F has some influence,

for a finite one excludes as limit distribution the ones from the Fréchet family and an infinite one excludes the distributions from the Weibull family.

4.1.2 Parameter estimation methods and statistical tests

A variety of estimation methods for the extreme value distributions parameters are present in the literature, such as, for example, the method of moments, the ML and the PWM methods (see, e.g. [10, 21, 128]). The ML method is based on maximising the likelihood of the observed sample, while the moments estimators are obtained by comparing moments of the random variable to the corresponding sample moments. The PWM method is a variant of the latter method, which was introduced in 1979 by Greenwood et al. [98]. In the same year, Landwehr et al. [133] proposed the use of this method for extreme value distributions. According to Embrechts et al. [61], the method of moments attracted a lot of interest among the researchers. For example, in 1958, Gumbel [107] preferred this method and argued that the ML method required too much numerical work for routine use. However, in 1982, Lettenmaier and Burges [137] showed that the ML method gave better parameter estimates than the ones given by the method of moments. In fact, Lettenmaier and Burges [137] paper is one among many papers found in the literature devoted to the ML estimation [128]. The big advantage of the ML method is to allow the study of more complex situations as non–stationarity and covariate effects [28], without the need of a lot of changes in the basic methodology of its procedures [61]. On the other hand, the major disadvantage of the ML method is that it can be extremely erratic for small samples, contrary to what happens with the PWM method [124]. The latter method is also a popular one in extreme value investigations, and especially in environmental sciences [128], having in its favour the simplicity of application and a good performance in simulation studies [61]. In 1979, Landwehr et al. [133] addressed the comparability between the PWM method and the two methods applied extensively in hydrology at that time, ML and moments methods, arriving to the conclusion that for the Gumbel distribution the results obtained with the PWM method were favourably compared with those for the two older methods. However, as mentioned by Embrechts et al. [61] in 1997, the PWM method has the disadvantage of not yet being extended to more complex situations. Despite their advantages and disadvantages, both methods can be applied in a complementary way since the PWM method can be used to provide initial values for the iterative numerical procedure that leads to the ML estimates [124].

ML method

The ML estimator $(\widehat{\sigma}, \widehat{\gamma}, \widehat{\mu})$ for (σ, γ, μ) is obtained by maximising the log-likelihood function. Given a sample $X_1, ..., X_n$ of independent and identically distributed random variables with common GEV distribution defined by expression (4.1), this function is given, when $\gamma \neq 0$, by

$$\log L(\sigma, \gamma, \mu) = -n \log \sigma - \left(\frac{1}{\gamma} + 1\right) \sum_{i=1}^{n} \log \left(1 + \gamma \frac{X_i - \mu}{\sigma}\right) - \sum_{i=1}^{n} \left(1 + \gamma \frac{X_i - \mu}{\sigma}\right)^{\frac{1}{\gamma}},$$

provided $1 + \gamma \frac{X_i - \mu}{\sigma} > 0$, $i = 1, ..., n$. In case $\gamma = 0$, the log-likelihood function reduces to

$$\log L(\sigma, 0, \mu) = -n \log \sigma - \sum_{i=1}^{n} \exp\left(\frac{X_i - \mu}{\sigma}\right) - \sum_{i=1}^{n} \left(\frac{X_i - \mu}{\sigma}\right).$$

Confidence intervals concerning the GEV parameters (σ, γ, μ) follow from the asymptotic normality of the ML estimators. For example, for $\alpha \in (0, 1)$ the $(1 - \alpha)100\%$ confidence interval for γ is given by

$$\left(\widehat{\gamma} - z_{1-\frac{\alpha}{2}} \sqrt{\frac{\hat{v}_{2,2}}{n}}, \widehat{\gamma} + z_{1-\frac{\alpha}{2}} \sqrt{\frac{\hat{v}_{2,2}}{n}}\right) \tag{4.3}$$

with $\widehat{\gamma}$ the ML estimate of γ, $z_{1-\frac{\alpha}{2}}$ the $(1 - \frac{\alpha}{2})$–quantile of the normal distribution and $\hat{v}_{2,2}$ the second diagonal element of the inverse of the Fisher information matrix, which is defined by

$$I(\theta) = -E\left(\frac{\partial^2 \log g(X; \theta)}{\partial \theta \partial \theta'}\right),$$

with $\theta = (\sigma, \gamma, \mu)$ and g the GEV density function

$$g(x; \sigma, \gamma, \mu) = \frac{1}{\sigma}\left(1 + \gamma \frac{x - \mu}{\sigma}\right) \exp\left(-\left(1 + \gamma \frac{x - \mu}{\sigma}\right)^{-\frac{1}{\gamma}}\right).$$

The Fisher information matrix has as generic elements

$$
\begin{aligned}
I_{1,1}(\theta) &= \frac{1}{\sigma^2\gamma^2}(1 - 2\Gamma(2+\gamma) + a),\\
I_{1,2}(\theta) &= -\frac{1}{\sigma\gamma^2}\left(1 - \epsilon - b + \frac{1-\Gamma(2+\gamma)}{\gamma} + \frac{a}{\gamma}\right),\\
I_{1,3}(\theta) &= \frac{1}{\sigma^2\gamma}(a - \Gamma(2+\gamma)),\\
I_{2,2}(\theta) &= \frac{1}{\gamma^2}\left[\frac{\pi^2}{6} + \left(1 - \epsilon + \frac{1}{\gamma}\right) - \frac{2b}{\gamma} + \frac{a}{\gamma^2}\right],\\
I_{2,3}(\theta) &= -\frac{1}{\sigma\gamma}\left(b - \frac{a}{\gamma}\right),\\
I_{3,3}(\theta) &= \frac{a}{\sigma^2},
\end{aligned}
$$

where $\epsilon \approx 0.5772157$ is Euler's constant,

$$a = (1+\gamma)^2\Gamma(1+2\gamma),$$

$$b = \Gamma(2+\gamma)\left(\psi(1+\gamma) + \frac{1+\gamma}{\gamma}\right),$$

with $\psi(x) = d\log\Gamma(x)/dx$ [10]. The greek letter Γ stands, as usual, for the gamma function defined by

$$\Gamma(t) = \int_0^{+\infty} \exp(-x)\, x^{t-1} dx, \text{ for } t > 0. \tag{4.4}$$

Nevertheless, it is important to have in mind that inference based on the normal limit results may be misleading as the normal approximation to the true sampled distribution of the corresponding estimator can be poor [10]. In general, better approximations can be obtained by the profile likelihood function as the confidence intervals obtained in this way are not necessarily centred in the corresponding point estimates as the ones resulting from the normality approximation [10, 87]. More explicitly, profile likelihood intervals may present a shift to the right while the ones resulting from the normality approximation are always centred in the corresponding point estimates due the symmetry presented by the normal distribution (see, e.g., [26, 87]).

The profile likelihood function for γ is given by

$$L_p(\gamma) = \max_{(\sigma,\mu)|\gamma} L(\sigma, \gamma, \mu),$$

and the profile likelihood ratio statistic by

$$R = \frac{L_p(\gamma_0)}{L_p(\widehat{\gamma})},$$

which coincides with the classical likelihood ratio statistic for testing the hypothesis $H_0 : \gamma = \gamma_0$ versus $H_1 : \gamma \neq \gamma_0$. Hence, under H_0, when $n \to \infty$,

$$-2 \log R \xrightarrow{d} \chi^2_1,$$

where $\xrightarrow{d}$ stands for "converges in distribution to" and χ^2_1 for the qui–square distribution with one degree of freedom. The null hypothesis H_0 will be rejected at a significance level of α if $-2 \log R > \chi^2_1(1-\alpha)$, where $\chi^2_1(1-\alpha)$ is the $(1-\alpha)$–quantile of the χ^2_1 distribution. Consequently, the profile likelihood-based $(1-\alpha)100\%$ confidence interval for γ is given by

$$CI_\gamma = \left\{ \gamma : -2 \log \frac{L_p(\gamma)}{L_p(\widehat{\gamma})} \leq \chi^2_1(1-\alpha) \right\}$$

or equivalently

$$CI_\gamma = \left\{ \gamma : \log L_p(\gamma) \geq \log L_p(\widehat{\gamma}) - \frac{\chi^2_1(1-\alpha)}{2} \right\}.$$

PWM method

The test of the so–called Gumbel hypothesis ($H_0 : \gamma = 0$), can also be based on the PWM estimate of γ presented by Hosking et al. [119]. Given a random variable X with distribution function F, the PWM of X are defined as

$$M_{m,r,s} = E\left[X^m \{F(X)\}^r \{1 - F(X)\}^s\right],$$

where $m, r, s \in \mathbb{R}$ (cf., e.g., [119]). The PWM generalise the noncentral moments of X, $E(X^m)$, which are obtained when $r = s = 0$ and $m = 1, 2, ...$ When $s \in \mathbb{N}_1$,

$$\{1 - F(x)\}^s = \sum_{j=0}^{s} \binom{s}{j} [-F(x)]^j$$

and

$$M_{m,r,s} = E\left[X^m \{F(X)\}^r \{1 - F(X)\}^s\right] = \sum_{j=0}^{s} \binom{s}{j} (-1)^j M_{m,r+j,0},$$

and though special attention is given to the moments $M_{m,r,0}$ (a similar reasoning can be made for $r \in \mathbb{N}_1$).

Consider X with distribution function given by $G_\gamma\left(\frac{\bullet-\mu}{\sigma}\right)$ where G_γ is the GEV distribution with expression given by (4.1). It is not difficult to prove that

$$M_{1,r,0} = \frac{1}{r+1}\left(\mu - \frac{\sigma}{\gamma}\left(1-(r+1)^\gamma \Gamma(1-\gamma)\right)\right), \tag{4.5}$$

for $\gamma < 1$, taking into account that when F is an injective function,

$$\begin{aligned} M_{m,r,s} &= \int_{\mathbb{R}} x^m \left\{F(x)\right\}^r \left\{1-F(x)\right\}^s dF(x) \\ &= \int_0^1 \left[F^{-1}(y)\right]^m y^r (1-y)^s \, dy, \end{aligned}$$

where $F^{-1}(y) = q_{1-y}$, and q_p is given by expression (4.2). The greek letter Γ stands as before for the gamma function defined by (4.4).

The PWM estimators of γ, σ and μ $(\widehat{\sigma}, \widehat{\gamma}, \widehat{\mu})$ are the solutions of the following system of equations obtained from (4.5) taking $r = 0, 1, 2$, after $M_{1,r,0}$ is replaced by an appropriate estimator:

$$\begin{cases} M_{1,0,0} = \mu - \frac{\sigma}{\gamma}\left(1-\Gamma(1-\gamma)\right), \\ 2M_{1,1,0} - M_{1,0,0} = \frac{\sigma}{\gamma}\Gamma(1-\gamma)(2^\gamma - 1) \\ \dfrac{3M_{1,2,0} - M_{1,0,0}}{2M_{1,1,0} - M_{1,0,0}} = \dfrac{3^\gamma - 1}{2^\gamma - 1} \end{cases}. \tag{4.6}$$

The system above is solved after replacing $M_{1,r,0}$ by, for example, the estimator proposed by Landwehr et al. [133]:

$$\hat{M}_{1,r,0} = \frac{1}{n}\sum_{j=1}^{n}\left(\prod_{l=1}^{r}\frac{(j-l)}{(n-l)}\right) X_{j:n}.$$

The third equation in system (4.6) is solved numerically to obtain $\widehat{\gamma}$ and, using this result, the second equation in system (4.6) is solved for $\widehat{\sigma}$:

$$\widehat{\sigma} = \frac{\widehat{\gamma}(2\hat{M}_{1,1,0} - \hat{M}_{1,0,0})}{\Gamma(1-\widehat{\gamma})(2^{\widehat{\gamma}} - 1)}.$$

Finally, $\widehat{\mu}$ is obtained through the first equation in system (4.6)

$$\widehat{\mu} = \hat{M}_{1,0,0} + \frac{\widehat{\sigma}}{\widehat{\gamma}}(1-\Gamma(1-\widehat{\sigma})).$$

The test based on the PWM estimator of γ proposed by Hosking et al. [119] is performed by comparing the test statistic

$$\widehat{\gamma}\left(\frac{n}{0.5633}\right)^{\frac{1}{2}} \tag{4.7}$$

with the critical values of the standard normal distribution.

4.1.3 Plots and statistical tests for model diagnostics

After having found the estimates for the parameters, the adequacy of a Gumbel or a non-Gumbel model can be checked through probability, quantile and return level plots, which are based on a comparison of model–based and empirical estimates of the distribution function [26]. The GEV distribution defined in (4.1) with μ as the location parameter, σ as the scale parameter and γ as the shape parameter will be from now on denoted by $GEV(\mu, \sigma, \gamma)$, and referred to as Model 1 when $\gamma \neq 0$. The particular case of $\gamma = 0$ in (4.1) will be designated as Model 2 ($GEV(\mu, \sigma, 0)$).

Let $x_{1:n}, ..., x_{n:n}$ be the ordered sample of the block maxima $x_1, ..., x_n$. The empirical distribution function at $x_{i:n}$ is

$$\tilde{G}(x_{i:n}) = \frac{i}{n+1},$$

and

$$\hat{G}(x_{i:n}) = \exp\left\{-\left[1 + \hat{\gamma}\left(\frac{x_{i:n} - \hat{\mu}}{\hat{\sigma}}\right)\right]^{-1/\hat{\gamma}}\right\}, \quad i = 1, \ldots, n,$$

are the GEV model-based estimates, where $\widehat{\gamma}$, $\widehat{\mu}$ and $\widehat{\sigma}$ are estimates for γ, μ and σ, respectively. The probability plot consists of the points

$$\left(\tilde{G}(x_{i:n}), \hat{G}(x_{i:n})\right), \quad i = 1, \ldots, n,$$

which are expected to lie close to the diagonal $\{(x, x), x \in [0, 1]\}$ if Model 1 is adequate. For the highest values of $x_{i:n}$, both $\hat{G}(x_{i:n})$ and $\tilde{G}(x_{i:n})$ are, by definition, close to one, which may be misleading in the interpretation of the region of major interest. Therefore, the analysis of this plot should be complemented with the one resulting from the quantile plot defined by the points

$$\left(\hat{G}^{-1}\left(\frac{i}{n+1}\right), x_{i:n}\right), \quad i = 1, \ldots, n,$$

where by (4.2)

$$\hat{G}^{-1}\left(\frac{i}{n+1}\right) = \widehat{\mu} - \frac{\widehat{\sigma}}{\widehat{\gamma}}\left[1 - \left(-\log\left(\frac{i}{n+1}\right)^{-\widehat{\gamma}}\right)\right].$$

As it happened before with the probability plot, departures from linearity in the quantile plot indicate that Model 1 is not an adequate model. Analogously, probability and quantile plots can be used to check the adequacy of Model 2. Considering again the return levels defined by (4.2), the return level plot consists of the points

$$(\log y_p, \hat{q}_p), \quad 0 < p < 1,$$

where $y_p = -\log(1-p)$. This plot is linear when Model 2 is an adequate choice, being convex or concave for Model 1 particular cases of $\gamma < 0$ and $\gamma > 0$, respectively. Also, when $\gamma < 0$, the graphical representation of the set $\{(\log y_p, q_p)\,,\ p \in (0,1)\}$ has an asymptotic limit, as $p \to 0$, equal to $\mu - \sigma/\gamma$. When $\gamma > 0$, the graph is unbounded when $p \to 0$. The simplicity of the interpretation of these plots turns these particularly important for both model presentation and validation.

To complement the information obtained by the previous analysis, confidence intervals for the return level q_p can be added. These are defined by

$$\left(\hat{q}_p - z_{1-\frac{\alpha}{2}}\sqrt{Var(\hat{q}_p)}, \hat{q}_p + z_{1-\frac{\alpha}{2}}\sqrt{Var(\hat{q}_p)}\right)$$

with $z_{1-\frac{\alpha}{2}}$ the $(1-\alpha)$–quantile of the standard normal distribution and $Var(\hat{q}_p) = \nabla q_p^T V \nabla q_p$, where V is the variance–covariance matrix of $(\widehat{\mu}, \widehat{\sigma}, \widehat{\gamma})$ and

$$\begin{aligned}\nabla q_p^T &= \left[\frac{\partial q_p}{\partial \mu}, \frac{\partial q_p}{\partial \sigma}, \frac{\partial q_p}{\partial \gamma}\right] \\ &= \left[1, -\gamma^{-1}(1-y_p^{-\gamma}), \sigma\gamma^{-2}(1-y_p^{-\gamma}) - \sigma\gamma^{-1}y_p^{-\gamma}\log y_p\right]\end{aligned}$$

evaluated at $(\widehat{\mu}, \widehat{\sigma}, \widehat{\gamma})$ [26]. For example, the values $\hat{q}_p$ can be obtained by substitution of the ML estimates of the GEV parameters into (4.2), being its normality justified by the delta method [10].[1] The analysis of the adequacy of Model 1 and 2 through the probability, quantile and return level plots can also be complemented with a comparison between a histogram of the data and the probability density function of the fitted model. The graphical approach to the analysis of the adequacy of the model should be followed by a goodness of fit test such as the Kolmogorov–Smirnov test. The evaluation of the adequacy of Model 2 can also be made by the application of a goodness of fit test developed by Stephens [200]. This test is based on the empirical distribution function statistic A^2 defined by

[1] The delta method is the term usually attributed to the following theorem [26]: Let $\widehat{\theta_0}$ be the large–sample ML estimator of the d–dimensional parameter θ_0 with approximate variance–covariance matrix V_θ. If $\Phi = g(\theta)$ is a scalar function, then the ML estimator of $\Phi_0 = g(\theta_0)$ satisfies

$$\widehat{\Phi}_0 \approx N(\Phi_0, V_\Phi)$$

where

$$V_\Phi = \nabla\Phi^T V_\theta \nabla\Phi$$

with

$$\nabla\Phi = \left[\frac{\partial\Phi}{\partial\theta_1}, ..., \frac{\partial\Phi}{\partial\theta_d}\right]^T$$

evaluated at $\widehat{\theta_0}$.

$$A^2 = -\frac{1}{n}\sum_{i=1}^{n}(2i-1)\left[\log z_i + \log(1-z_{n+1-i})\right] - n \tag{4.8}$$

where

$$z_i = G(x_{i:n}) = \exp\left[-\exp\left(\frac{x_{i:n}-\hat{\mu}}{\hat{\sigma}}\right)\right]$$

are the Gumbel model-based estimates obtained, for example, by substitution of the parameters μ and σ by the PWM estimates $\widehat{\mu}$ and $\widehat{\sigma}$. For small samples, Stephens [200] recommends the replacement of A^2 by

$$A^{*2} = A^2\left(1+\frac{0.2}{\sqrt{n}}\right). \tag{4.9}$$

The obtained values for A^2 or A^{*2} can then be compared with the corresponding upper tail points [Table 1 in [200]].

4.1.4 A trend analysis

Until now the random variables involved are assumed to be independent and to have identical distributions, and both estimation methods, ML and PWM, were considered. At the presence of non–stationarities, a usual aspect when a time series is involved, the ML estimation method is the one that should be applied, as it allows this aspect to be included in the analysis. According to Engeland et al. [62] the non–stationarity can be accounted by three ways, namely, by a decomposition of the time series into a deterministic seasonal component and a stationary sequence, by a subdivision of the dataset into blocks that can be assumed homogeneous or by the inclusion of parameters in the GEV distribution depending on the time or other covariates. The Kruskal–Wallis test can be used to test the distributional identity of the subsamples mentioned in the second approach (see, e.g., [132]). This approach has the drawback of requiring the construction of the blocks. The third approach is considered more flexible and was applied by a number of authors [26, 62, 154, e.g.]. This approach consists in the introduction of time dependence in the parameters of the GEV distribution. The simplest way is to consider a linear trend although according to Coles [26] there are many applications for which the variations through time do not have the low order polynomial form. Coles [26] also advocates that is usually unrealistic to try to model the shape parameter γ for it is difficult to obtain a precise estimate for this one. Taking this into account, only location and scale parameters are considered in the following trend analysis.

Let Models 3 and 4 be variations of Models 1 and 2 characterised by the inclusion of a linear trend in the location parameter, $\mu(t) = \beta_0 + \beta_1 t$, with $\beta_0,\ \beta_1 \in \mathbb{R}$ ($GEV(\mu(t), \sigma, \gamma)$, with $\gamma \neq 0$, and $GEV(\mu(t), \sigma, 0)$, respectively). Non–stationarity may also be expressed in terms of a transformation of the scale parameter, $\sigma(t) = \exp(\beta_2 + \beta_3 t)$, with $\beta_2,\ \beta_3 \in \mathbb{R}$, and this will define Models 5 ($GEV(\mu, \sigma(t), \gamma)$, $\gamma \neq 0$) and 6 ($GEV(\mu, \sigma(t), 0)$). If the fit to the GEV distribution with a linear trend in both location and scale parameters is considered, then the models will be termed by Models 7 or 8 ($GEV(\mu(t), \sigma(t), \gamma)$, with $\gamma \neq 0$, or $GEV(\mu(t), \sigma(t), 0)$, respectively). All these models are summarised in Table 4.1.

Table 4.1: Models $GEV(\beta_0 + \beta_1 t, \exp(\beta_2 + \beta_3 t), \gamma)$.

	$\beta_1 = 0$		$\beta_1 \neq 0$	
	$\gamma \neq 0$	$\gamma = 0$	$\gamma \neq 0$	$\gamma = 0$
$\beta_3 = 0$	Model 1	Model 2	Model 3	Model 4
$\beta_3 \neq 0$	Model 5	Model 6	Model 7	Model 8

Some of those models are nested in other models and, given a pair of models in this situation, the likelihood ratio test [26] can be used to test the simpler model against the complex one. Consider a random sample $x_1, ..., x_n$ of a random variable with probability density function f depending on a d-dimensional parameter $\theta = (\overline{\theta}_1, \overline{\theta}_2)$, where θ_1 is a k–dimensional component. Let $\widehat{\theta}$ denote the ML estimator of θ, that is the value of θ that maximises the log-likelihood function defined by $l(\theta) = \sum_{i=1}^{n} \log f(x_i, \theta)$. At the significance level α, the submodel of Model M_1 obtained when $\theta_1 = 0$, M_0, is rejected in favour to M_1 if $2[l_1(M_1) - l_0(M_0)]$ is greater than the $(1-\alpha)$–quantile of the χ^2_k distribution, where $l_0(M_0)$ and $l_1(M_1)$ are the maximised values of the log-likelihood for models M_0 and M_1, respectively.

An approximate $(1-\alpha)100\%$–confidence interval for each individual component θ_i of $\theta = (\theta_1, ..., \theta_d)$ is given by $\widehat{\theta}_i \pm z_{\frac{\alpha}{2}} \sqrt{\widetilde{\psi}_{i,i}}$, where $\widetilde{\psi}_{i,i}$ is the i–th diagonal element of the inverse of the observed information matrix. Confidence intervals for θ_i can also be obtained by the use of the maximised log-likelihood with respect to all the other components, that is, in result of the application of the profile log-likelihood for θ_i.

These $(1-\alpha)100\%$–confidence intervals can be defined by $C_\alpha = \{\theta_i \colon 2(l(\widehat{\theta}) - l_p(\theta_i)) \leq c_\alpha\}$ with the profile log-likelihood defined by $l_p(\theta_i) = \max_{\theta_{-i}} l(\theta_i, \theta_{-i})$, where θ_{-i} stands for the $(d-1)$–dimensional vector given by θ without the i–th component and c_α is the $(1-\alpha)$–quantile of the χ^2_1 distribution [26].

4.2 About extreme domains of attraction, number of observations above a random threshold and threshold choices

This section, like the previous one, is related to the univariate extreme value theory and is a preparation for Section 5.2 of Chapter 5. Here, a method for testing extreme value conditions, two statistical procedures for the problem of choice of extreme domains of attraction and some concepts and results related to the POT method are reviewed. The section ends with the review of two graphical methods for threshold selection.

The POT and the PORT approaches result from different classification methods of extreme observations of a random variable [88]. In the latter the attention is focused on a predetermined number of observations above the random threshold $x_{n-k:n}$, while the former deals with a random number k_u of observations that exceed a predetermined threshold u [159].

The PORT approach is a semi-parametric one and requires only that the underlying distribution belongs to the domain of attraction of G_γ as defined by (4.1), for some $\gamma \in \mathbb{R}$ [88]. Let $X_1, ..., X_n$ be independent and identically distributed random variables with common distribution function F. The assumption that F is in the domain of attraction of an extreme value distribution, $F \in \mathcal{D}(G_\gamma)$, for some $\gamma \in \mathbb{R}$, means that there are normalising constants $a_n > 0$ and $b_n \in \mathbb{R}$ such that, for x such that $1 + \gamma x > 0$,

$$\lim_{n\to\infty} P\left(\max_{1\leq i\leq n} \frac{X_i - b_n}{a_n} \leq x\right) = G_\gamma(x) \tag{4.10}$$

with G_γ defined by (4.1) [120, 179, e.g.].

Not all distribution functions belong to a domain of attraction, and for that reason it is important to check the following null-hypothesis

$$H_0 : F \in D(G_\gamma), \text{ for some } \gamma \in \mathbb{R}. \tag{4.11}$$

Hüsler and Li et al. [120] have compared three statistical tests for (4.11) and based on this study the test statistic developed by Dietrich et al. [54] will be here considered. This test statistic is given by:

$$E_n(k) = k \int_0^1 \left(\frac{\log X_{n-[kt]:n} - \log X_{n-k:n}}{\widehat{\gamma}_+} - \frac{t^{-\widehat{\gamma}_-} - 1}{\widehat{\gamma}_-}(1 - \widehat{\gamma}_-) \right)^2 t^\eta dt, \qquad (4.12)$$

where $\eta > 0$ and the estimates $\widehat{\gamma}_+$ and $\widehat{\gamma}_-$ are obtained through the moment estimator of

$$\gamma = \gamma_+ + \gamma_-,$$

with $\gamma_+ = \max\{\gamma, 0\}$ and $\gamma_- = \min\{\gamma, 0\}$. The moment estimator for γ, due to Dekkers et al. [51], is defined by $\widehat{\gamma} = \widehat{\gamma}_+ + \widehat{\gamma}_-$ where

$$\widehat{\gamma}_+ = M_n^{(1)} = \frac{1}{k} \sum_{k=0}^{k-1} (\log X_{n-i:n} - \log X_{n-k:n}) \qquad (4.13)$$

is the Hill estimator [115], and

$$\widehat{\gamma}_- = 1 - \frac{1}{2} \left\{ 1 - \frac{\left(M_n^{(1)}\right)^2}{M_n^{(2)}} \right\}^{-1}, \qquad (4.14)$$

with

$$M_n^{(2)} = \frac{1}{k} \sum_{k=0}^{k-1} (\log X_{n-i:n} - \log X_{n-k:n})^2 .$$

The recommended procedure (see [120, 179]) for application of the test of Dietrich et al. [54] is to estimate the value of the test statistic $E_n(k)$ and, after, use Table 1 in [120] to find the corresponding quantile $Q_{1-\alpha,\widehat{\gamma}}$. If $E_n(k) > Q_{1-\alpha,\widehat{\gamma}}$, then H_0 is rejected with nominal type I error α.

When the null hypothesis (4.11) is not rejected, it may be useful to know which domain of attraction best suits the sampled distribution. Neves and Fraga Alves [159] point out the Hasofer and Wang test [113] as one of the most frequently used statistical tests for testing the null hypothesis $H_0 : F \in \mathcal{D}(G_0)$ against one of the alternative hypotheses: $H_1 : F \in \mathcal{D}(G_\gamma)_{\gamma \neq 0}$, $H_1 : F \in \mathcal{D}(G_\gamma)_{\gamma > 0}$ or $H_1 : F \in \mathcal{D}(G_\gamma)_{\gamma < 0}$. This test statistic is given by

$$W_n(k) = \frac{\left(\sum_{i=1}^n Z_i\right)^2}{k^2 \sum_{i=1}^n Z_i^2 - k \left(\sum_{i=1}^n Z_i\right)^2},$$

where $Z_i = X_{n-i+1:n} - X_{n-k:n}$, with $i = 1, ..., k$. The normalised versions of this test statistic given by

$$W_n^*(k) = \sqrt{k/4}\,(kW_n(k) - 1) \tag{4.15}$$

and of the Greenwood's test statistic [99] given by

$$R_n^*(k) = \sqrt{k/4}\left(\frac{k^{-1}\sum_{i=1}^{k} Z_i^2}{(k^{-1}\sum_{i=1}^{k} Z_i)^2} - 2\right) \tag{4.16}$$

were both proposed by Neves and Fraga Alves [159], who used a simulation study to evaluate their behaviour. Under the null hypothesis of the Gumbel domain of attraction and some additional (second order) conditions (see, e.g., [159]), the test statistics $W_n^*(k)$ and $R_n^*(k)$, where $k = k(n)$ is an intermediate sequence of integers, that is, with $k \to +\infty$ and $k/n \to 0$ as the sample size n tends to infinity, are asymptotically normal, as $n \to \infty$. The critical region for the two-sided test with an approximate size α,

$$H_0 : F \in \mathcal{D}(G_0)\ vs.\ H_1 : F \in \mathcal{D}(G_\gamma)_{\gamma \neq 0},$$

is given by $|W_n^*(k)| > z_{1-\frac{\alpha}{2}}$ and by $|R_n^*(k)| > z_{1-\frac{\alpha}{2}}$, where $z_{1-\frac{\alpha}{2}}$ denotes, as usual, the $(1-\frac{\alpha}{2})$–quantile of the standard normal distribution.

The one-sided testing problem of testing the Gumbel domain against the Weibull domain,

$$H_0 : F \in \mathcal{D}(G_0)\ vs.\ H_1 : F \in \mathcal{D}(G_\gamma)_{\gamma < 0},$$

has the critical region given by $W_n^*(k) > z_{1-\alpha}$ for the Hasofer and Wang's test and by $R_n^*(k) < -z_{1-\alpha}$ for the Greenwood type statistic $R_n^*(k)$. On the other hand, when testing H_0 against the Fréchet domain

$$H_0 : F \in \mathcal{D}(G_0)\ vs.\ H_1 : F \in \mathcal{D}(G_\gamma)_{\gamma > 0},$$

the rejection criterion is, respectively, $W_n^*(k) < -z_{1-\alpha}$ and $R_n^*(k) > z_{1-\alpha}$. Neves and Fraga Alves [159] concluded that on the presence of heavy–tailed distributions, the test based on $R_n^*(k)$ has a better behaviour than the Greenwood type test. On the other hand, for negative values of γ, the test statistic $W_n^*(k)$ is the most powerful, for the Greenwood type test barely detects the small negative values of γ.

The main purpose of the statistical theory of extremes is the prediction of rare events, the adequate estimation of parameters such as high quantiles, return

periods and other parameters related to natural disaster events [89]. Among such parameters, the extreme value index γ is of primary interest in extreme value analysis, being its estimation under a semi-parametric approach based on the k top order statistics of the sample by estimators such as the moment estimator. According to Gomes et al. [88], the semi–parametric estimation of any parameter of extreme events, and in particular of γ, should be done through an adaptive selection of the sample fraction to be used in the estimation under consideration. For the moment estimator, Draisma et al. [58] in 1999 presented an adaptive method based on a double bootstrap to choose the number of order statistics involved in an optimal way, in order to balance the variance and bias components. The double bootstrap procedure was proposed by Hall [111] in 1990 in the selection of the optimal sample fraction for the Hill estimator. In fact, knowing that the selection of the optimal sample fraction by a resampling procedure such as the usual bootstrap underestimated the bias of the Hill estimator, Hall [111] proposed to use resamples whose size was of smaller order than the original sample size [60]. Hall's suggestion was followed by Danielson et al. [35], who developed a two–step subsample bootstrap method which adaptively determines the sample fraction that minimises the asymptotic mean–squared error. The Danielson et al. [35] bootstrap approach and as well the Hall's [111] and the Drees and Kaufmann [60] bootstrap approaches were compared by Gomes and Oliveira [89]. The comparison of alternative choices of the optimal sample fraction made by these authors also included the adaptive estimators suggested by Hall and Welsh [112] and by Beirlant et al. [11, 12]. The bootstrap technique of Danielson et al. [35] was elected by Gomes and Oliveira [89] as the most appealing among all the methodologies considered by these authors for selection of the optimal sample fraction of the Hill estimator, due to the lack of need of an initial estimation of γ in this method. In a different perspective, the value of k can also be selected by the heuristic method proposed by Reiss and Thomas in [179], whose performance evaluation was carried out by Neves and Fraga Alves [158].

Choosing a value for k, the number of top order statistics to be used in parameter estimation, in the PORT approach and choosing a value for the threshold u in the POT approach are parallel problems [87]. The choice of the threshold u is an open and controversial problem, and involves a balance between the size of the bias of the estimators and their variances, where high values of u lead to small bias and large variances and small values of u lead to the opposite effects [87]. Nevertheless, the choice of the threshold u is a key point in the definition of extreme events. Indeed, if

$X_1, X_2, ...$ is a sequence of independent random variables with common distribution F and X denote an arbitrary term in the X_i sequence, an extreme event of X can be set as a value of X that exceeds u. Let F belong to the GEV family $G_\gamma(\frac{\cdot - \mu}{\sigma})$, for some $\gamma,\ \mu \in \mathbb{R}$, $\sigma > 0$. For u sufficiently large, the distribution function of $X - u$, given $X > u$, is approximately given by

$$H(y) = 1 - \left(1 + \frac{\gamma y}{\sigma_u}\right)^{-1/\gamma},$$

where $y > 0$, $1 + \frac{\gamma y}{\sigma_u} > 0$, $\sigma_u = \sigma + \gamma(u - \mu) > 0$ and $\gamma \neq 0$. For $\gamma = 0$ and $y > 0$

$$H(y) = 1 - \exp\left(-\frac{y}{\sigma_u}\right),$$

the exponential distribution function with parameter $1/\sigma_u$ (see [26], e.g.). The function H is the GPD function, and the values σ and γ are the parameters of scale and shape, respectively. The duality between the GPD and GEV distribution functions was established by Pickands [171] and also by Balkema and de Haan [7].

Having a threshold u, the k values exceeding this value, $\{x_i : x_i > u\}$, labelled by $x_{(1)}, ..., x_{(k)}$, are called exceedances and the values $x_{(j)} - u$, with $j = 1, ..., k$ the threshold excesses. If a GPD is valid as a model for the excesses of a threshold u_0 and $\gamma < 1$, then

$$E(X - u_0 | X > u_0) = \frac{\sigma_{u_0}}{1 - \gamma},$$

where σ_{u_0} is the scale parameter concerning to the excesses of the threshold u_0. In this case, the GPD is also the distribution function of the excesses over any threshold $u > u_0$, having in consideration the suited change of the scale parameter. Therefore, for $u > u_0$

$$E(X - u | X > u) = \frac{\sigma_u}{1 - \gamma} = \frac{\sigma_{u_0} + \gamma u}{1 - \gamma},$$

as $\tilde{\sigma} = \sigma + \gamma(u - \mu)$ and $E(X - u | X > u)$ is a linear function of u.

Since $E(X - u | X > u)$ is the mean of the excesses over the threshold u, it follows that the mean residual life plot consisting of the points of the set

$$\left\{ \left(u, \frac{1}{k} \sum_{i=1}^{k} (x_{(i)} - u) \right) : u < x_{n:n} \right\}$$

should be approximately linear in u [26]. This graphical method for choosing the threshold u based on the interpretation of the mean residual life plot was proposed by Davison and Smith [38].

A complementary graphical method for selecting the threshold u follows from adjusting the GPD function for a variety of thresholds. As referred before, if the GPD function is appropriate for the excesses over a threshold u_0, then it is also an appropriate distribution for the excesses over $u > u_0$, where both distributions have identical shape parameters. On the other hand, if σ_u is the value of the scale parameter considering the threshold u, then $\sigma_u = \sigma_{u_0} + \gamma(u - u_0)$ and $\sigma^* = \sigma_u - \gamma u$ is constant relative to u. Therefore, if the GPD is a suitable model for the excesses over u_0, then the estimates of σ^* and γ should be approximately constant for the values greater than u_0 [26].

4.3 An extreme value copula approach

This section aims to present some concepts and results on copula functions, with special attention given to extreme value copulas.

Consider a natural number $n \geq 2$ and $(X_1, \ldots, X_n)$ a random vector with continuous marginal probability distribution functions $F_1, \ldots, F_n$ and common probability distribution function H. Associated to each $n-$vector of real numbers $(x_1, \ldots, x_n)$, consider the $n+1-$vector of numbers of the interval $\mathbb{I} = [0, 1]$ given by

$$\left(F_1\left(x_1\right), \ldots, F_n\left(x_n\right), H\left(x_1, \ldots, x_n\right)\right).$$

The correspondence which assigns the value of the joint probability distribution function $H\left(x_1, \ldots, x_n\right)$ to the vector of the values of the marginal probability distribution functions $\left(F_1\left(x_1\right), \ldots, F_n\left(x_n\right)\right)$ is called the copula function [156]. Sklar's theorem [194] establishes that for every continuous joint distribution function H there is a unique function C, called the copula function, such that

$$H\left(x_1, \ldots, x_n\right) = C\left(F_1\left(x_1\right), \ldots, F_n\left(x_n\right)\right), \; x_1, \ldots, x_n \in \mathbb{R},$$

Conversely, given a copula function $C : \mathbb{I}^n \to \mathbb{I}$ (defined in the next paragraph) and univariate distribution functions F_i, then $C(F_1(x_1), F_2(x_2), \ldots, F_n(x_n))$ defines a joint probability distribution function with margins $F_1(x_1), F_2(x_2), \ldots, F_n(x_n)$. According to Nelsen ([156]) the term "copula" was chosen to emphasise the way in which this function C "couples" a joint distribution function to its univariate

margins. It should be noted that, by changing the margins, each copula can of course define infinitely many different joint probability distributions.

A function $C : \mathbb{I}^n \to \mathbb{I}$ is called a copula when (i) it is such that

$$C(u) = 0$$

if at least one coordinate of $u = (u_1, \ldots, u_n) \in \mathbb{I}^n$ is 0, and

$$C(u) = u_i$$

if all coordinates of $u \in \mathbb{I}^n$ are 1 except u_i; and (ii) C is an n-increasing function, that is given $a = (a_1, \ldots, a_n)$, $b = (b_1, \ldots, b_n) \in \mathbb{I}^n$ with $a_i \leq b_i$, $i = 1, \ldots, n$,

$$\sum_{i_1=1}^{2} \ldots \sum_{i_n=1}^{2} (-1)^{i_1+\ldots+i_n} C\left(x_{1i_1}, \ldots, x_{ni_n}\right) \geq 0,$$

where $x_{j1} = a_j, x_{j2} = b_j$. In other words, a copula function is a multivariate distribution whose univariate margins are all uniform on $(0, 1)$.

Special examples of copula functions are the Fréchet–Hoeffding upper bound copula defined for $u = (u_1, \ldots, u_n) \in \mathbb{I}^n$ by

$$M_n(u) = \min(u_1, \ldots, u_n),$$

and the product copula defined by

$$\Pi_n(u) = u_1 \ldots u_n.$$

Because the variables $X_1, \ldots, X_n$ are independent if and only if the corresponding copula is Π_n [156], this copula is also called the independence copula [182]. The Fréchet–Hoeffding upper bound copula is characterised by the fact that each of the continuous random variables X_i, $i \in \{1, \ldots, n\}$ is almost surely a strictly increasing function of any of the others if an only if the corresponding copula is M_n [156].

According to Nelsen [155], many of the ways to describe and measure dependence between random variables remain unchanged under strictly increasing transformations of these ones. The concordance is one of these scale-invariant dependence forms. On the other hand, it is also known (cf. e.g. [187]) that the copula functions capture the properties of dependence between random variables. In 2002, R. B. Nelsen [155] made a survey about the relationships between concordance of random variables and their copulas, focusing on the relationship

between concordance and measures of association such as Kendall's τ, Spearman's ρ and Gini's coefficient. The two first measures, Kendall's τ and Spearman's ρ play an important role in applications, since the practical fit of a copula to the available data is often carried out via the estimation of these values. In fact, according to Salvadori et al. [182], Kendall's τ and Spearman's ρ are the two most widely known and used scale-invariant measures.

The relation between Kendall's τ measure of association of two random variables (X, Y), $\tau_{X,Y}$, and its copula function, $C_{X,Y}$ is easily deduced. Let (X_1, Y_1) and (X_2, Y_2) be two independent replicas of (X, Y), a random pair with joint distribution function given by $F_{(X,Y)}$. Kendall's τ is a measure of association of the random variables X and Y given by the probability of concordance

$$P\left[(X_1 - X_2)(Y_1 - Y_2) > 0\right]$$

minus de probability of discordance

$$P\left[(X_1 - X_2)(Y_1 - Y_2) < 0\right],$$

i.e.,

$$\tau_{X,Y} = P\left[(X_1 - X_2)(Y_1 - Y_2) > 0\right] - P\left[(X_1 - X_2)(Y_1 - Y_2) < 0\right] \tag{4.17}$$

(see, e.g., [156]). It can be observed that $-1 \leq \tau_{X,Y} \leq 1$ and, since the random variables are continuous, the equation (4.17) can be rewritten in the following way:

$$\tau_{X,Y} = 2P\left[(X_1 - X_2)(Y_1 - Y_2) > 0\right] - 1.$$

Since

$$P\left[(X_1 - X_2)(Y_1 - Y_2) > 0\right] = P\left[X_1 > X_2, Y_1 > Y_2 \text{ or } X_1 < X_2, Y_1 < Y_2\right],$$

taking $(x, y) = \left(F_X^{-1}(u_x), F_Y^{-1}(u_y)\right)$, where $F^{-1}(a) = \inf\{x \in \mathbb{R} : F(x) \geq a\}$ is the generalised inverse distribution function, in the following integral

$$P\left[X_1 < X_2, Y_1 < Y_2\right] = \int_{\mathbb{R}^2} P\left[(X_1, Y_1) < (x, y)\right] dF_{(X,Y)}(x, y)$$

leads to

$$P\left[X_1 < X_2, Y_1 < Y_2\right] = \int_{[0,1]^2} C_{(X,Y)}(u_x, u_y)\, dC_{(X,Y)}(u_x, u_y).$$

In this way, the following expression is obtained

$$\tau_{X,Y} = 4 \int_{[0,1]^2} C_{(X,Y)}(u, v)\, dC_{(X,Y)}(u, v) - 1, \tag{4.18}$$

which shows the relation between the copula function and the measure of association given by Kendall's τ. Alternatively, Nelsen [156] presents a more tractable expression for $\tau_{X,Y}$ that was proved by Li et al. [138]:

$$\begin{aligned}\tau_{X,Y} &= 4\left[\frac{1}{2} - \int_{[0,1]^2} \frac{\partial}{\partial u} C_{(X,Y)}(u,v)\, \frac{\partial}{\partial v} C_{(X,Y)}(u,v)\, dudv\right] - 1 \\ &= 1 - 4\int_{[0,1]^2} \frac{\partial}{\partial u} C_{(X,Y)}(u,v)\, \frac{\partial}{\partial v} C_{(X,Y)}(u,v)\, dudv. \end{aligned} \tag{4.19}$$

Spearman's ρ is, like Kendall's τ, a measure of association between two random variables that is based on concordance and discordance. Spearman's ρ uses three independent replicas of a random vector (X,Y) of continuous random variables, $(X_1,Y_1), (X_2,Y_2)$ and (X_3,Y_3), and is defined in the following way

$$\rho_{X,Y} = 3\left\{P\left[(X_1 - X_2)(Y_1 - Y_3) > 0\right] - P\left[(X_1 - X_2)(Y_1 - Y_3) < 0\right]\right\}.$$

In a similar way it is possible to show the following relation between Speaman's ρ and the copula function $C_{(X,Y)}$:

$$\rho_{X,Y} = 12\int_{[0,1]^2} C_{(X,Y)}(u,v)\, dudv - 3. \tag{4.20}$$

A known statistical test of independence [81] is based on the empirical version of Kendall's τ measure defined by

$$\tau_n = \frac{c-d}{c+d} = \frac{4}{n(n-1)}c - 1, \tag{4.21}$$

where c and d represents the number of concordant and discordant pairs, respectively, in a sample of size n from a vector of continuous random variables (X,Y). As when considering random variables, we say that the pairs of observations (x_i,y_i) and (x_j,y_j) are concordant if $(x_i - x_j)(y_i - y_j) > 0$ and discordant if $(x_i - x_j)(y_i - y_j) < 0$. Since the random variables X and Y are continuous, the probability of the event $(X_i - X_j)(Y_i - Y_j) = 0$ is zero. Under the null hypothesis $H_0 : C = \Pi$ of independence between X and Y, the random variable τ_n has approximately a normal distribution with zero mean and variance $2(2n+5)/9n(n-1)$ [81]. Thus, H_0 would be rejected, for example, at an approximate confidence level of 99% if

$$\sqrt{\frac{9n(n-1)}{2(2n+5)}}|\tau_n| > 2.58.$$

The empirical version of the Kendall's τ can also be obtained in terms of the empirical copula, which is itself a characterisation of the dependence between the random variables of the pair (X, Y) [81]. Empirical copulas were introduced and first studied by Deheuvels [48], who called them empirical dependence functions. The empirical copula C_n is defined by

$$C_n(u, v) = \frac{1}{n} \sum_{k=1}^{n} I\left(\frac{R_k}{n+1} \leq u, \frac{S_k}{n+1} \leq v\right),$$

with $u, v \in [0, 1]$, I denoting the indicator function and R_k, S_k the ranks for the observations X_k e Y_k, respectively $(k = 1, \ldots, n)$ [156]. Since $(X_i - X_j)(Y_i - Y_j) > 0$ if and only if $(R_i - R_j)(S_i - S_j) > 0$, the value of τ_n can also be obtained using ranks and, consequently, in terms of the empirical copula C_n [81]. More precisely, the empirical versions of Kendall's τ and the copula function C_n are connected in the following way:

$$\tau_n = \frac{4}{n-1} \sum_{i=1}^{n} C_n\left(\frac{R_i}{n+1}, \frac{S_i}{n+1}\right) - \frac{n+3}{n-1}. \tag{4.22}$$

Relatively to the Spearman's ρ measure of association, the empirical version is given by

$$\rho_n = \frac{12}{n(n+1)(n-1)} \sum_{i=1}^{n} R_i S_i - 3\frac{n+1}{n-1}, \tag{4.23}$$

that has approximately a normal distribution with zero mean and variance $1/(n-1)$ [81]. In this way, the null hypothesis $H_0 : C = \Pi$ may be rejected, for instance, at an approximate confidence level of 99%, if $\sqrt{n-1}|\rho_n| > 2.58$ [81].

A family of copulas of particular interest when modelling extreme values is the family of extreme value copulas. Given $d \geq 2$ a $d-$copula C^* is an EVC if there exists a copula C such that

$$C^*(u_1, \ldots, u_d) = \lim_{n \to \infty} C^n\left(u_1^{1/n}, \ldots, u_d^{1/n}\right), \tag{4.24}$$

for all $u = (u_1, \ldots, u_d) \in \mathbb{I}^d$. An extreme value d–copula C^*, with $d \geq 2$, can also be defined as a copula satisfying the following equality

$$C^*(u_1^t, \ldots, u_d^t) = (C^*)^t(u_1, \ldots, u_d), \tag{4.25}$$

for all $t > 0$. This alternative definition of an EVC highlights one of its important properties which is known as max-stability. A d–copula C is max–stable if

$$C(u_1, \ldots, u_d) = C^t\left(u_1^{1/t}, \ldots, u_d^{1/t}\right) \tag{4.26}$$

is valid for all $t > 0$ and $u \in \mathbb{I}^d$.

For example, $C = \Pi_d$ given by $\Pi_d(u_1, \ldots, u_d) = u_1 \ldots u_d$ is a extreme value d–copula for $d \geq 2$. In fact,

$$\Pi_d(u_1^t, \ldots, u_d^t) = u_1^t \ldots u_d^t = \Pi_d^t(u_1, \ldots, u_d). \tag{4.27}$$

The Fréchet–Hoeffding upper bound copula is also an EVC since

$$M_d(u_1^t, \ldots, u_d^t) = \min\left\{u_1^t, \ldots, u_d^t\right\} = M_d^t(u_1, \ldots, u_d). \tag{4.28}$$

The weighted geometric means of Π_d and M_d, known as Cuadras–Augé family of copulas, are also extreme value copulas. For $\theta \in \mathbb{I}$, the members of the Cuadras–Augé's family of copulas are given by

$$C_\theta(u) = \Pi_d^{1-\theta}(u) M_d^\theta(u), \tag{4.29}$$

where $u \in \mathbb{I}^d$ and $d \geq 2$. In fact, from (4.27) and (4.28) it follows that

$$C_\theta(u^t) = \Pi_d^{1-\theta}\left(u^t\right) M_d^\theta(u^t) = \left[\Pi_d^{1-\theta}(u)\right]^t \left[M_d^\theta(u)\right]^t = C_\theta^t(u) \tag{4.30}$$

for $u^t = (u_1^t, \ldots, u_d^t)$.

More generally, if A and B are d–EVC then

$$C_{\alpha_1,\ldots,\alpha_d}(u) = A\left(u_1^{\alpha_1}, \ldots, u_d^{\alpha_d}\right) B\left(u_1^{1-\alpha_1}, \ldots, u_d^{1-\alpha_d}\right)$$

defines a family of d–EVC with parameters $\alpha_1, \ldots, \alpha_d \in \mathbb{I}$. Indeed, from (4.26) follows that

$$\begin{aligned} C_{\alpha_1,\ldots,\alpha_d}^t(u_1^{1/t}, \ldots, u_d^{1/t}) &= A^t\left(u_1^{\alpha_1/t}, \ldots, u_d^{\alpha_d/t}\right) B^t\left(u_1^{(1-\alpha_1)/t}, \ldots, u_d^{(1-\alpha_d)/t}\right) \\ &= A\left(u_1^{\alpha_1}, \ldots, u_d^{\alpha_d}\right) B\left(u_1^{1-\alpha_1}, \ldots, u_d^{1-\alpha_d}\right) \\ &= C_{\alpha_1,\ldots,\alpha_d}(u_1, \ldots, u_d). \end{aligned}$$

These facts allow the construction of a more versatile family of extreme value copulas. For example, taking $d = 3$, the three–dimensional Cuadras–Augé copula for A, and Π_3 for B, defined respectively by

$$A(u_1, u_2, u_3) = (u_1 u_2 u_3)^{1-\theta} \left(\min\left(u_1, u_2, u_3\right)\right)^\theta, \ \theta \in \mathbb{I},$$

and

$$B(u_1, u_2, u_3) = u_1 u_2 u_3,$$

it follows that

$$\begin{aligned} C_{\alpha_1,\alpha_2,\alpha_3}(u_1,u_2,u_3) &= A\left(u_1^{\alpha_1},u_2^{\alpha_2},u_3^{\alpha_3}\right) B\left(u_1^{1-\alpha_1},u_2^{1-\alpha_2},u_2^{1-\alpha_3}\right) \\ &= u_1^{\alpha_1(1-\theta)}u_2^{\alpha_2(1-\theta)}u_3^{\alpha_3(1-\theta)} \min\left(u_1^{\theta\alpha_1},u_2^{\theta\alpha_2},u_3^{\theta\alpha_3}\right) u_1^{1-\alpha_1}u_2^{1-\alpha_2}u_3^{1-\alpha_3} \\ &= u_1^{1-\alpha_1\theta}u_2^{1-\alpha_2\theta}u_3^{1-\alpha_3\theta} \min\left(u_1^{\theta\alpha_1},u_2^{\theta\alpha_2},u_3^{\theta\alpha_3}\right) \end{aligned}$$

defines a family of 3-EVC. Letting $\beta_i = \theta\alpha_i \in \mathbb{I}$ this family can be defined in the following way

$$C(u_1,u_2,u_3) = \Pi_{i=1}^3 u_i^{1-\beta_i} \min\left(u_1^{\beta_1},u_2^{\beta_2},u_3^{\beta_3}\right). \tag{4.31}$$

The two-dimensional marginals of C, which are obtained when $u_i \to 1$, for $i = 1, 2$ or 3, are Marshall–Olkin bivariate copulas with parameters (β_i, β_j) for $i \neq j$, with $i, j = 1, 2, 3$. The Marshall–Olkin copula received its name from Ingram Olkin and Albert Marshall who in 1967 [145] characterised a bivariate distribution, assuming that it had an exponential marginal and that the following functional equation hold:

$$\overline{F}_{(X,Y)}(s_1+t, s_2+t) = \overline{F}_{(X,Y)}(s_1,s_2)\,\overline{F}_{(X,Y)}(t,t), \tag{4.32}$$

where X and Y are two random variables, $\overline{F}_{(X,Y)}(s,t) = P(X > s, Y > t)$, with $s_1, s_2, t > 0$.[2] Condition (4.32) together with the conditions that make $F_{(X,Y)}$ a cumulative distribution function lead to the bivariate exponential distribution of two random variables with parameters $\lambda_1, \lambda_2, \lambda_{12} > 0$, which can be denoted by $(X,Y) \frown BE(\lambda_1,\lambda_2,\lambda_{12})$, with joint survival probability function given by

$$\overline{F}_{(X,Y)}(x,y) = P(X > x, Y > y) = \exp\left[-\lambda_1 x - \lambda_2 y - \lambda_{12}\max(x,y)\right], x, y > 0. \tag{4.33}$$

What is known today as the Marshall–Olkin copula (cf. e.g. [182]) should in fact be known as the Marshall–Olkin survival copula. A survival copula of two random variables X and Y is the function $\widehat{C}_{(X,Y)} : [0,1]^2 \to [0,1]$ such that

$$\overline{F}_{(X,Y)}(x,y) = \widehat{C}_{(X,Y)}\left(\overline{F}_X(x), \overline{F}_Y(y)\right), \tag{4.34}$$

[2]This distribution was derived by Marshall and Olkin as the model to the life of a two–component system that survives or dies according to the occurrences of "shocks" to each or both of the components, being the fatal shocks governed by Poisson process $\{N_S(t), t \geq 0\}$ that with rate λ_S, $S \subseteq \{1,2\}$, destroys the components with indexes in S. Equation (4.32) is a natural generalisation of the 1–dimensional exponential distribution property given by

$$\overline{F}_X(s+t) = \overline{F}_X(s)\,\overline{F}_X(t),$$

thus representing a particular type of the lack of memory property.

which is related to the copula C of X and Y in the following way:

$$\widehat{C}_{(X,Y)}(u,v) = u + v - 1 + C_{(X,Y)}(1-u, 1-v) \tag{4.35}$$

(see, e.g., [156], page 33). From the expression (4.33) it follows that

$$\begin{aligned}
\overline{F}_{(X,Y)}(x,y) &= \begin{cases} \exp\left[-(\lambda_1+\lambda_{12})x - \lambda_2 y\right], & x > y \\ \exp\left[-\lambda_1 x - (\lambda_2+\lambda_{12})y\right], & x \leq y \end{cases} \\
&= \begin{cases} \overline{F}_X(x) \exp\left[-\frac{\lambda_2}{\lambda_2+\lambda_{12}}(\lambda_2+\lambda_{12})y\right], & x > y \\ \overline{F}_Y(y) \exp\left[-\frac{\lambda_1}{\lambda_1+\lambda_{12}}(\lambda_1+\lambda_{12})x\right], & x \leq y \end{cases} \\
&= \begin{cases} \overline{F}_X(x)\,\overline{F}_Y(y)^{1-\beta}, & x > y \\ \overline{F}_Y(y)\,\overline{F}_X(x)^{1-\alpha}, & x \leq y \end{cases},
\end{aligned}$$

where $\alpha = \frac{\lambda_{12}}{\lambda_1+\lambda_{12}}$ and $\beta = \frac{\lambda_{12}}{\lambda_2+\lambda_{12}}$. Taking $u = \overline{F}_X(x)$ and $v = \overline{F}_Y(y)$, i.e., $x = -\frac{1}{\lambda_1+\lambda_{12}}\ln u$ and $y = -\frac{1}{\lambda_2+\lambda_{12}}\ln v$, and noting that

$$\begin{aligned}
x > y &\Leftrightarrow -\frac{1}{\lambda_1+\lambda_{12}}\ln u > -\frac{1}{\lambda_2+\lambda_{12}}\ln v \\
&\Leftrightarrow -\alpha \ln u > -\beta \ln v \Leftrightarrow u^\alpha < v^\beta \Leftrightarrow u^{\frac{\alpha}{\beta}} < v,
\end{aligned}$$

the following definition for the bivariate Marshall–Olkin (survival) copula is deduced for the random pair $(X,Y) \frown BE(\lambda_1,\lambda_2,\lambda_{12})$, $\lambda_1,\lambda_2,\lambda_{12} > 0$, for $u,v \in [0,1]$:

$$C_{(X,Y)}(u,v) = \begin{cases} u^{1-\alpha}v, & v \leq u^{\alpha/\beta} \\ uv^{1-\beta}, & v > u^{\alpha/\beta} \end{cases} \tag{4.36}$$

$$= \min(u^{1-\alpha}v, uv^{1-\beta}). \tag{4.37}$$

Replacing the expression (4.36) in the integral defined in (4.19) it follows that

$$\begin{aligned}
\tau_{X,Y} &= \int_{[0,1]^2} \frac{\partial}{\partial u} C_{(X,Y)}(u,v)\, \frac{\partial}{\partial v} C_{(X,Y)}(u,v)\, du dv \\
&= \int_0^1 du \left[\int_{u^{\alpha/\beta}}^1 \frac{\partial}{\partial u} uv^{1-\beta} \frac{\partial}{\partial v} uv^{1-\beta} dv + \int_0^{u^{\alpha/\beta}} \frac{\partial}{\partial u} vu^{1-\alpha} \frac{\partial}{\partial v} vu^{1-\alpha} dv \right] \\
&= \int_0^1 u(1-\beta) \left[\frac{v^{2-2\beta}}{2-2\beta}\right]_{v=u^{\alpha/\beta}}^{v=1} + u^{1-2\alpha}(1-\alpha)\left[\frac{v^2}{2}\right]_{v=0}^{v=u^{\alpha/\beta}} du \\
&= \frac{1}{2}\int_0^1 u - u^{1-2\alpha+2\frac{\alpha}{\beta}} + u^{1-2\alpha+2\frac{\alpha}{\beta}} - \alpha u^{1-2\alpha+2\frac{\alpha}{\beta}} du \\
&= \frac{1}{2}\int_0^1 u - \alpha u^{1-2\alpha+2\frac{\alpha}{\beta}} du = \frac{1}{2}\left[\frac{u^2}{2} - \alpha\frac{u^{2-2\alpha+2\frac{\alpha}{\beta}}}{2-2\alpha+2\frac{\alpha}{\beta}}\right]_{u=0}^1 \\
&= \frac{1}{4}\left[1 - \frac{\beta\alpha}{\beta-\beta\alpha+\alpha}\right],
\end{aligned}$$

i.e.,

$$\tau_{X,Y} = \frac{\alpha\beta}{\alpha - \alpha\beta + \beta}, \tag{4.38}$$

which can be written in the following way

$$\tau = \tau_{X,Y} = \frac{1}{\frac{1}{\alpha} + \frac{1}{\beta} - 1}. \tag{4.39}$$

Inverting this relationship, e.g., for α, it follows that

$$\frac{1}{\tau} = \frac{1}{\alpha} + \frac{1}{\beta} - 1 \Leftrightarrow \alpha = \frac{1}{\frac{1}{\tau} - \frac{1}{\beta} + 1}. \tag{4.40}$$

A similar relation can be written for the Spearman's ρ association measure[3] but considering that (see, e.g., [125]) the convergence of τ_n to normality for increasing sample size is quicker than that of ρ_n from now on only Kendall's τ will be used.

Expressions (4.39) and (4.40) allow the estimation of the parameters β_1, β_2 and β_3 from the extreme value copula C defined in (4.31), using the estimated values of Kendall's τ. Indeed, writing, for simplicity, $\tau_{i,j}$ instead of τ_{X_i,X_j}, for $i, j \in \{1, 2, 3\}$, $i \neq j$, from

$$\frac{1}{\beta_i} = \frac{1}{\tau^{i,j}} - \frac{1}{\beta_j} + 1$$

[3]If (X, Y) is a random pair whose copula function is given by the bivariate Marshall–Olkin survival copula given by (4.36), then

$$\rho = \rho_{X,Y} = \frac{3\alpha\beta}{2\alpha - \alpha\beta + 2\beta}. \tag{4.41}$$

The association measures Kendall's τ and Spearman's ρ for a random pair having as copula the bivariate Marshall–Olkin survival copula family are given by the expression (4.38) and (4.41). Replacing α given by expression (4.40), $\alpha = \frac{1}{\frac{1}{\tau} - \frac{1}{\beta} + 1}$, in the equality given by (4.41) a relationship between the measures is obtained:

$$\rho = \frac{3\alpha\beta}{2\alpha - \alpha\beta + 2\beta} = \frac{3\beta}{2 - \beta + 2\frac{\beta}{\alpha}} = \frac{3\beta}{2 - \beta + \frac{2\beta}{\tau} - \frac{2\beta}{\beta} + 2\beta} = \frac{3}{\frac{2}{\tau} + 1} = \frac{3\tau}{2 + \tau},$$

i.e.,

$$\rho = \frac{3\tau}{2 + \tau},$$

for ρ and τ both in $[0, 1]$.

it follows that, for $k \in \{1,2,3\}\backslash\{i,j\}$,

$$\begin{aligned}\frac{1}{\beta_i} &= \frac{1}{\tau^{i,j}} - \frac{1}{\beta_j} + 1 = \frac{1}{\tau^{i,j}} - (\frac{1}{\tau^{j,k}} - \frac{1}{\beta_k} + 1) + 1 \\ &= \frac{1}{\tau^{i,j}} - \frac{1}{\tau^{j,k}} + \frac{1}{\beta_k} = \frac{1}{\tau^{i,j}} - \frac{1}{\tau^{j,k}} + (\frac{1}{\tau^{i,k}} - \frac{1}{\beta_i} + 1) \\ &= 1 + \frac{1}{\tau^{i,j}} + \frac{1}{\tau^{i,k}} - \frac{1}{\tau^{j,k}} - \frac{1}{\beta_i}\end{aligned}$$

that is equivalent to

$$\frac{2}{\beta_i} = 1 + \frac{1}{\tau^{i,j}} + \frac{1}{\tau^{i,k}} - \frac{1}{\tau^{j,k}}.$$

Therefore,

$$\frac{1}{\beta_i} = \frac{1}{2}\left(1 + \frac{1}{\tau^{i,j}} + \frac{1}{\tau^{i,k}} - \frac{1}{\tau^{j,k}}\right), \tag{4.42}$$

where (i,j,k) is a permutation of $(1,2,3)$.

These relationships allow the estimation of the probability of extremal events. In practice, given a random vector $(X_1,\ldots,X_n)$, an event is defined as extreme if one or more variables exceed some given high values. Of particular practical interest is the event

$$E_n^{x_1,\ldots,x_n} = \{X_1 > x_1, ..., X_n > x_n\}.$$

Taking $n = 3$, assuming that the random vector (X_1, X_2, X_3) has as continuous distribution with copula function C and taking $u_i = P(X_i \leq x_i)$, it follows that

$$\begin{aligned}P(E_3^{x_1,x_2,x_3}) &= P(X_1 > x_1, X_2 > x_2, X_3 > x_3) \\ &= 1 - \sum_{i=1}^{3} P(X_i \leq x_i) + \sum_{\substack{i,j=1 \\ i<j}}^{3} P(X_i \leq x_i, X_j \leq x_j) \\ &\quad -P(X_1 \leq x_1, X_2 \leq x_2, X_3 \leq x_3) \\ &= 1 - u_1 - u_2 - u_3 - C(u_1,u_2,u_3) + C(u_1,u_2,1) \\ &\quad + C(u_1,1,u_3) + C(1,u_2,u_3).\end{aligned} \tag{4.43}$$

Let X_i denote the observation at the i–th rain gauge station and $x_{i,q}$ the $(1-q)$–quantile of X_i for $q \in (0,1)$ and $i \in \{1,2,3\}$, and consider the extremal event

$$E_q = E_3^{x_{1,q},x_{2,q},x_{3,q}} = \{X_1 > x_{1,q}, X_2 > x_{2,q}, X_3 > x_{3,q}\}.$$

The return period r_q of E_q is given by $\frac{1}{p_q}$, with $p_q = P(E_q)$, which is given by

$$\begin{aligned} p_q &= P\left(E_3^{x_{1,q},x_{2,q},x_{3,q}}\right) \\ &= 1 - 3q - C(q,q,q) + C(q,q,1) + C(q,1,q) + C(1,q,q). \end{aligned} \tag{4.44}$$

In this section, the concepts and methodologies necessary to the application of the chosen extreme copula approach were presented and discussed. Kendall's τ association measure and the extreme value copulas involving the Marshall–Olkin family will have a major role in such application, whose results and discussion are presented in Section 5.3.

Chapter 5

Results and discussion

5.1 Annual maxima – Gumbel's model approach

It was Emil Gumbel who in 1958 [107] firstly proposed the block maxima approach in the study of statistics of extremes. Under this approach, also called block maxima model, a sample of size m is divided into n sub–samples of size r. Then, the sample of the maxima of these n sub-samples is fitted by one of the extremal models (Gumbel, Fréchet or Weibull) [88]. Usually, when data results from a record of some quantity along time, the subsamples coincide with the records of the years and n is the number of years sampled. This is why sometimes this model is also referred as the annual maxima approach. Among the extremal models, Gumbel distribution is a commonly used model for hydrological extremes, especially when quantifying risk associated with extreme rainfall [129]. However, there are studies suggesting that the Gumbel distribution may underestimate the largest extreme rainfall amounts [132, 129, 223, e.g.]. To overcome this problem, statistical practioners tend to prefer to fit the GEV distribution to the data [26, 132, 129, e.g.]. According to Hosking et al. [119], the GEV distribution has been widely utilised for modelling extremes of natural phenomena since this use was recommended in a report of the Natural Environment Research Council [157]. In this report, GEV distributions were fitted to 32 samples, with dimension sizes of at least 30, by the application of the ML estimation method. The major disadvantage of this method is that it can be extremely erratic for small samples as mentioned by Katz et al. [124]. The good performance of the PWM method for small samples [119] was a factor that made this method more popular than ML in applications to hydrological extremes. The differences between these two methods have been analysed and some improvements have been proposed by a number of authors [28, 53, e.g.]. In this section, these two methods, ML and

PWM, were used to obtain estimates for the GEV distribution parameters. Also, tests based on the likelihood ratio statistic and on the PWM were used to test the hypothesis of a Gumbel distribution versus a GEV distribution. The 50– and 100–year return level estimates were obtained and, in addition, the existence of trends in the parameters' values was also analysed.

5.1.1 Dataset I

The dataset analysed in this subsection consists of annual maximum precipitation data from seven rain gauge stations in Madeira Island maintained by IPMA whose locations are shown in Figure 5.1. Table 5.1 provides information about each data sample, namely size (n), measurement period and the corresponding station's altitude, identification name and letter.

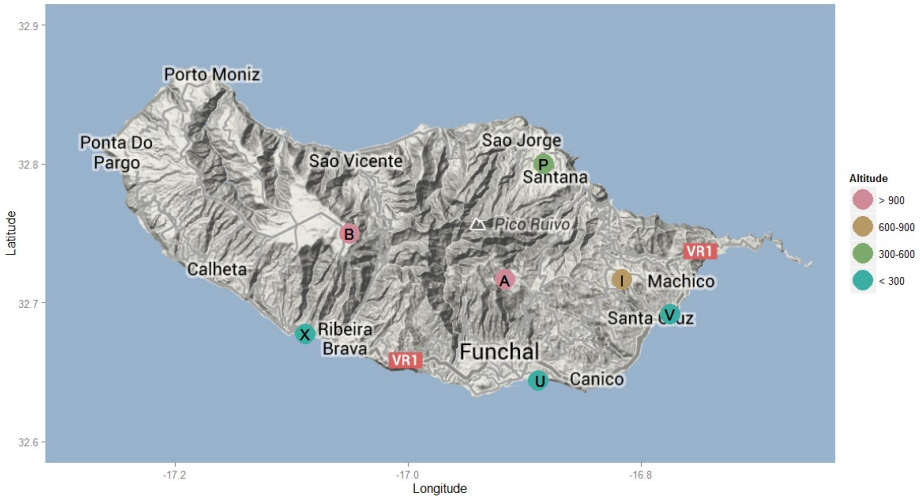

Figure 5.1: Location and altitude range of the rain gauge stations–Dataset I (Map data ©2014 Google).

Table 5.1: Dataset I: annual maximum precipitation (source: IPMA).

Station	Altitude (m)	Period	n
Areeiro (A)	1610	1961–1992	31
Bica da Cana (B)	1560	1961–2008	40
Santo da Serra (I)	660	1970–2009	38
Santana (P)	380	1942–2007	59
Funchal (U)	58	1949–2009	61
Santa Catarina (V)	49	1961–2009	48
Lugar de Baixo (X)	15	1961–2004	43

Hydrological time records may not satisfy the basic requirements of extreme value theory as they can often be autocorrelated and not identically distributed [62]. However, according to Leadbetter and Rootzén [136], under weak dependence restrictions, the general "type" of limiting distribution for the maximum is the same as for an independent and identically distributed sequence. The non-stationarity can be accounted, for example, by subdividing the dataset into blocks that are considered to be homogeneous or by letting the parameters in the GEV distribution depend on time [62]. So, although the full set provided by IPMA contains a series of values for each year, only the annual maxima are considered here. Thus, in this way, intra-year dependencies are avoided and the supposition that the data $x_1, ..., x_n$ are realisations from a sequence $X_1, ..., X_n$ of independent and identically distributed random variables, all with common extreme value distribution may be considered as a valid assumption [61]. Nevertheless, a procedure to detect non-stationarities considered in the work of Koutsoyiannis and Baloutsos [132] was applied to the dataset of each of the seven locations. The procedure consists in dividing each station data record into to four subsets with approximately the same length record and then test the hypothesis that all four subseries have identical distributions by the non parametric Kruskal-Wallis test. The four subsamples record length (n_1, n_2, n_3, n_4), the Kruskal-Wallis statistic test value and the corresponding p–value for each station dataset, obtained by the application of function *kruskal.test* in the *stats* R language package [178], are displayed in Table 5.2.

Table 5.2: Records length, Kruskal-Wallis statistic test value and p–value–Dataset I.

Station	(n_1, n_2, n_3, n_4)	Statistic test value	p–value
Areeiro (A)	$(8, 8, 8, 7)$	6.0318	0.1101
Bica da Cana (B)	$(10, 10, 10, 10)$	0.7098	0.8709
Santo da Serra (I)	$(10, 10, 10, 8)$	5.5432	0.1361
Santana (P)	$(15, 15, 15, 14)$	2.1671	0.5385
Funchal (U)	$(16, 16, 16, 13)$	2.0754	0.5569
Santa Catarina (V)	$(12, 12, 12, 12)$	0.5341	0.9113
Lugar de Baixo (X)	$(11, 11, 11, 10)$	1.6237	0.6540

At a 0.05 significance level, the hypothesis of homogeneity is not rejected for all seven station datasets. As mentioned above, another way to deal with non-stationarities is to let the parameters in the chosen distribution to be time–dependent. So, besides testing the null hypothesis H_0 of a Gumbel distribution (Model 2) against the alternative hypothesis H_1 of another extreme value

distribution (Model 1), the existence of trends in the parameters' values was also analysed through likelihood ratio tests. As outlined in Table 4.1 of Section 4.1 (page 40), Models 3–8 are variations of Models 1 and 2. Models 3 and 4 are characterised by a linear trend in the location parameter, Models 5 and 6 by a linear trend in the scale parameter, and Models 7 and 8 by a linear trend in both of these parameters. Table 5.3 presents all the calculated p–values for the data of each of the seven locations, being each one identified by its identification letter.

Assuming the Gumbel distribution, only in the case of Areeiro (A) data there is evidence to suggest a linear trend in the location parameter with respect to time at a 0.05 significance level, i.e., Model 2 is rejected in favour of Model 4. In this case, $\widehat{\mu}(t) = \widehat{\beta}_0 + \widehat{\beta}_1 t$ with the ML estimates $\widehat{\beta}_0 = 192.719$ and $\widehat{\beta}_1 = -2.121$ for the location parameter and $\widehat{\sigma} = 31.845$ for the scale parameter. The standard errors for $\widehat{\beta}_0$, $\widehat{\beta}_1$ and $\widehat{\sigma}$ are 14.590, 0.831 and 4.233, respectively. On the other hand, when a non–Gumbel extreme value distribution is assumed, i.e., when $\gamma \neq 0$, Model 1 is also rejected in favour of a model presenting a linear trend in the location parameter ($\widehat{\mu}(t) = 196.020 - 2.107t$), Model 3, with the values of $\widehat{\sigma} = 32.903$ and $\widehat{\gamma} = -0.207$ for the other parameters estimates. For this Model 3, the standard errors for $\widehat{\beta}_0$, $\widehat{\beta}_1$, $\widehat{\sigma}$ and $\widehat{\gamma}$ are 13.369, 0.719, 4.642 and 0.127, respectively.

Table 5.3: p–values for the likelihood ratio tests for each station data–Dataset I.

H_0	H_1	A	B	I	P	U	V	X
Model 1	Model 3	0.0072	0.8714	0.4198	0.5751	0.1449	0.3683	0.1111
Model 1	Model 5	1.0000	0.5992	1.0000	1.0000	0.4517	0.0833	1.0000
Model 1	Model 7	1.0000	1.0000	1.0000	1.0000	1.0000	1.0000	0.2347
Model 2	Model 1	0.3157	0.0095	0.4661	0.8645	0.4520	0.3686	0.0419
Model 2	Model 4	0.0143	0.9998	0.9402	0.5866	0.1159	0.5786	0.4265
Model 2	Model 6	0.1404	0.8709	0.5674	0.5554	0.4378	0.0534	0.0646
Model 2	Model 8	0.0483	1.0000	0.5265	1.0000	0.2570	0.1547	0.1470

Prior to considering a model with or without assuming a trend in any parameter, the test of Model 2 versus Model 1 should be analysed. For the distribution functions corresponding to Areeiro (A), Santo da Serra (I), Funchal (U), Santana (P), Santa Catarina (V) stations, we notice that the Gumbel distribution is not rejected in favour of another EV distribution. Naturally, the same conclusion would have been obtained if the 95% confidence intervals for the shape parameter γ were computed: $0 \in [-0.392, 0.103]$ for Areeiro (A), $0 \in [-0.294, 0.127]$ for Funchal (U),

$0 \in [-0.235, 0.278]$ for Santana (P), $0 \in [-0.147, 0.371]$ for Santa Catarina (V), and $0 \in [-0.451, 0.199]$ for Santo da Serra (I). The adequacy of the choice of Model 2 can also be checked by the profile likelihood interval for γ observed in Figures 5.2 and 5.3. The 95% confidence intervals obtained for the profile likelihood are $[-0.347, 0.170]$ for Areeiro (A), $[-0.272, 0.151]$ for Funchal (U), $[-0.225, 0.292]$ for Santana (P), $[-0.118, 0.414]$ for Santa Catarina (V), and $[-0.420, 0.235]$ for Santo da Serra (I).

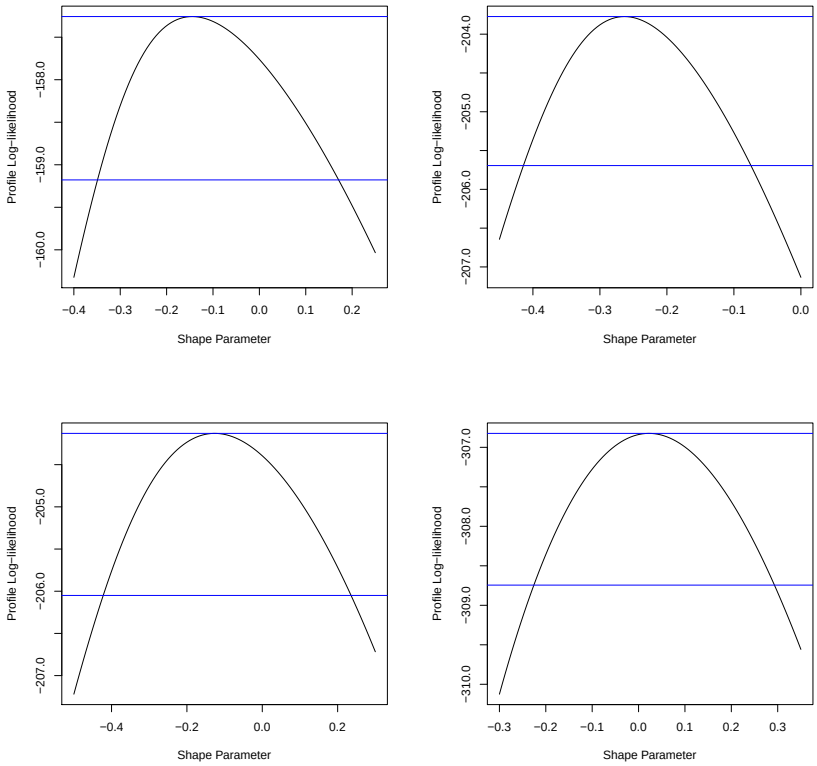

Figure 5.2: Profile log-likelihood for γ in Model 1 for Areeiro (A) (up left), Bica da Cana (B) (up right), Santo da Serra (I) (down left), and Santana (P) (down right) stations.

The opposite happens in the case of Bica da Cana (B) and Lugar de Baixo (X) datasets. For the Bica da Cana (B) station the fitted model is the GEV distribution with parameters' estimates $\widehat{\mu} = 145.47$, $\widehat{\sigma} = 39.46$ and $\widehat{\gamma} = -0.263$. These values allow us to estimate the upper end point of the fitted distribution as $\widehat{z}_0 = \widehat{\mu} - \widehat{\sigma}/\widehat{\gamma} = 295.51$. A positive estimate for the shape parameter, $\widehat{\gamma} = 0.206$, is obtained for the case of Lugar de Baixo (X) station. The 95% confidence intervals for γ are $[-0.423, -0.104]$ and $[-0.032, 0.527]$ for Bica da Cana (B) and Lugar de Baixo (X)

data, respectively. The corresponding 95% confidence profile likelihood intervals are $[-0.414, -0.076]$ and $[0.007, 0.563]$. All choices resulting from the application of the likelihood ratio test, the corresponding model parameters' estimates, and the standard errors obtained by the application of the *ismev* and *extRemes* R language packages [178] for each location are presented in Table 5.4.

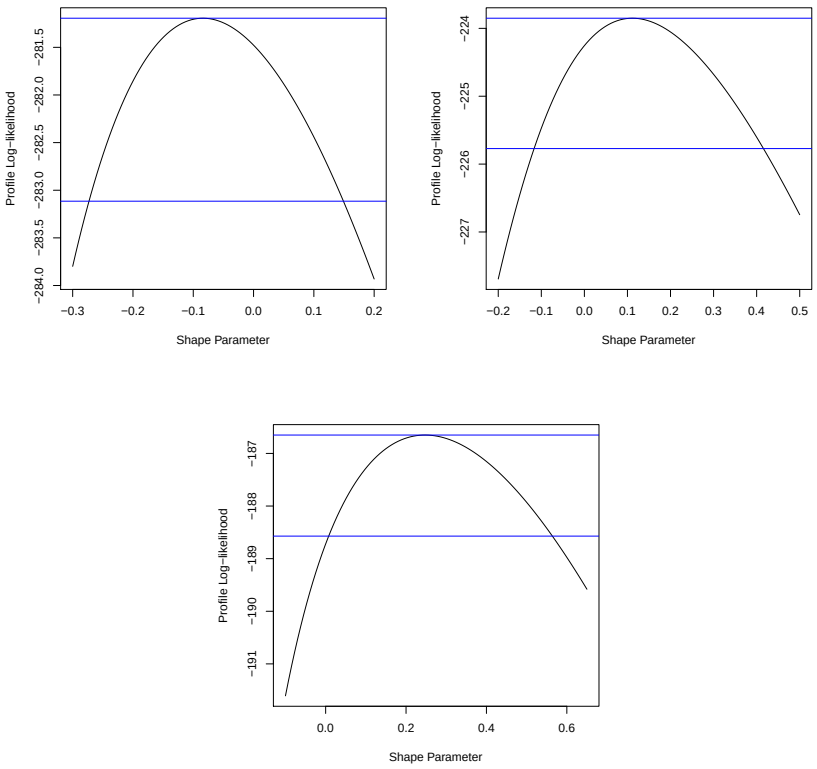

Figure 5.3: Profile log-likelihood for γ in Model 1 for Funchal (U) (up left), Santa Catarina (V) (up right) and Lugar de Baixo (X) (down) stations.

Table 5.4: Resulting models, ML parameter estimates and standard errors – Dataset I.

Station	Model	$\widehat{\mu}$	$\widehat{\sigma}$	$\widehat{\gamma}$
Areeiro (A)	Model 2	156.75 (6.53)	34.41 (4.73)	
Bica da Cana (B)	Model 1	145.47 (6.78)	39.46 (4.62)	−0.263 (0.082)
Santo da Serra (I)	Model 2	113.34 (7.73)	45.16 (5.76)	
Santana (P)	Model 2	85.17 (5.07)	37.00 (3.86)	
Funchal (U)	Model 2	51.34 (2.85)	21.07 (2.10)	
Santa Catarina (V)	Model 2	55.21 (3.25)	21.46 (2.50)	
Lugar de Baixo (X)	Model 1	46.71 (2.43)	13.75 (1.99)	0.247 (0.143)

The adequacy of the model was tested through the Kolmogorov-Smirnov test by the application of the function *gofstat* in the *fitdistrplus* R language package [178]. The test statistic values obtained when Model 2 was tested were 0.1146 for Areeiro (A), 0.0602 for Funchal (U), 0.0955 for Santana (P), 0.0948 Santa Catarina (V), and 0.0953 for Santo da Serra (I). In the two cases where Model 1 was tested, the calculated test statistic values were 0.0708 and 0.0669 for Bica da Cana (B) and Lugar de Baixo (X), respectively. So, each station data do not provide sufficient evidence to conclude that the chosen model is not an appropriate model for modelling the respective annual maxima.

The same models' choices are made when the hypothesis of a Gumbel distribution is analysed by a test based on the PWM estimate of γ presented by Hosking et al. [118]. The value for the test statistic given by (4.7), $Z = \widehat{\gamma}(n/0.5633)^{1/2}$, is not significant in comparison with the critical values of the standard normal distribution for Areeiro (A), Funchal (U), Santana (P), Santa Catarina (V) and Santo da Serra (I) data. As before, the opposite happens with the cases of Bica da Cana (B) and Lugar de Baixo (X). The models' choices resulting from the application of this test are presented in Table 5.5, which also shows the corresponding model parameter estimates obtained by the use of the *fExtremes* R package.

Table 5.5: Resulting models and PWM parameter estimates–Dataset I.

Station	Model	$\widehat{\mu}$	$\widehat{\sigma}$	$\widehat{\gamma}$
Areeiro (A)	Model 2	93.04	143.22	
Bica da Cana (B)	Model 1	145.54	39.52	−0.274
Santo da Serra (I)	Model 2	68.10	122.86	
Santana (P)	Model 2	51.33	96.42	
Funchal (U)	Model 2	30.92	56.07	
Santa Catarina (V)	Model 2	33.13	60.78	
Lugar de Baixo (X)	Model 1	46.74	14.38	0.206

Although for the distributions corresponding to Areeiro (A), Funchal (U), Santana (P), Santa Catarina (V) and Santo da Serra (I) data there is no significant evidence to decide to choose a non-Gumbel EV model in opposition to the Gumbel model, it is observed that the ML estimate for each γ is not zero (see Table 5.6). The same observation can be made when the PWM estimates are considered. Besides the γ estimates, Table 5.6 presents the ML and PWM estimates for the location and scale parameters. The values of estimates are similar for both methods for Model 1 but that is not the case when the Model 2 is chosen. For the Gumbel

distribution the ML parameter estimates are larger than the estimates obtained by the PWM method.

Analysing graphically the adequacy of Models 1 (Figure 5.4) and 2 (Figure 5.5) to the corresponding distribution function for Funchal (U) station when the ML method is applied, a difference in terms of the return level plots can be observed. Figures 5.4 and 5.5 reveal that the confidence intervals are wider for Model 1 than for the Model 2 for long return periods, although the estimated return level curves are similar. The set of plotted points is nearly linear in the probability and quantile plots for both models. Also for both cases, the corresponding estimated density is apparently consistent with the presented data histogram. Also, Model 1 was not rejected for Funchal (U) by the Kolmogorov-Smirnov test whose test statistic value was 0.0756. The result was the same for the other cases as the test statistic values obtained were 0.0949 for Areeiro (A), 0.0909 for Santana (P), 0.1041 Santa Catarina (V), and 0.0817 for Santo da Serra (I). The diagnostic plots for Models 1 and 2 for these stations, and also for Bica da Cana (B) and Lugar de Baixo (X) stations, are displayed in Appendix A.

Table 5.6: GEV parameter estimates by ML and PWM–Dataset I.

Station	Method	$\widehat{\mu}$	$\widehat{\sigma}$	$\widehat{\gamma}$
Areeiro (A)	ML	159.49	35.74	−0.145
Areeiro (A)	PWM	159.55	37.82	−0.175
Bica da Cana (B)	ML	145.47	39.46	−0.263
Bica da Cana (B)	PWM	145.54	39.52	−0.274
Santo da Serra (I)	ML	116.44	47.27	−0.126
Santo da Serra (I)	PWM	115.45	49.69	−0.115
Santana (P)	ML	84.78	36.75	0.021
Santana (P)	PWM	84.73	38.40	0.002
Funchal (U)	ML	52.30	21.63	−0.084
Funchal (U)	PWM	51.89	22.04	−0.065
Santa Catarina (V)	ML	53.95	20.47	0.111
Santa Catarina (V)	PWM	53.93	21.12	0.092
Lugar de Baixo (X)	ML	46.71	13.75	0.247
Lugar de Baixo (X)	PWM	46.74	14.38	0.206

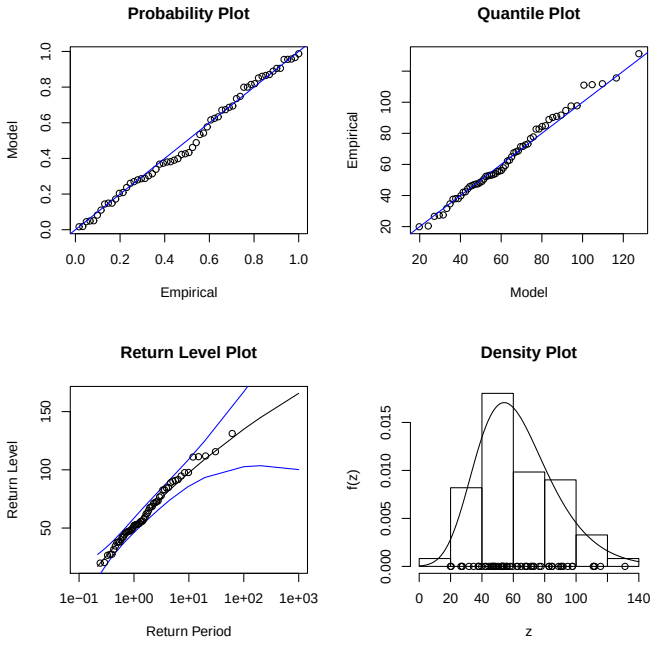

Figure 5.4: Diagnostic plots for non-Gumbel GEV fit to the Funchal (U) station data–Dataset I.

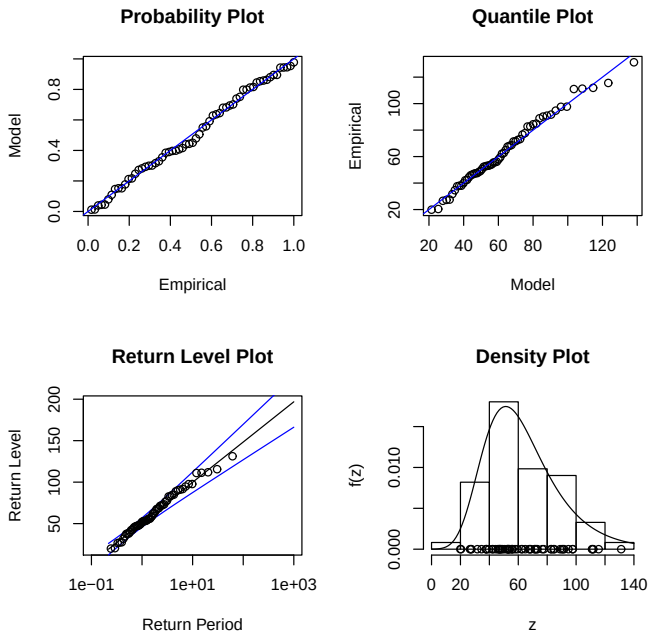

Figure 5.5: Diagnostic plots for Gumbel fit to the Funchal (U) station data–Dataset I.

Following Coles [26], who advocates that the safest option is to accept there is uncertainty about the value of the shape parameter and to prefer the inference

based on the GEV model whether the Gumbel model is adequate or not, here the choice was to deal only with the general GEV distribution. Also, the fact that the samples in this study are of small to medium sizes demanded some care in choosing the estimation method. Diebolt et al. [53] developed an estimation method based on generalised PWM and through a simulation study using GEV distributions compared the proposed method with the ML and PWM methods for $\gamma = -0.2, 0, 0.2$ and 1.2. The study was performed with small and medium random sample sizes of 15, 25, 50 and 100. One of the conclusions was that, for $\gamma = -0.2$, 0 and 0.2, the generalised PWM and the ML methods produce similar results in the estimation of the shape parameter, and that the PWM method presents a smaller interquartile range but a larger bias. The three methods gave also similar results for the estimates of the location and scale parameters, the similarity being improved when the sample dimension increases, as expected. Also, according to these authors, the generalised PWM gives better estimates than the two other methods when $\gamma = 1.2$. The observation made by Hosking et al. [119], that the PWM estimation is superior to the ML estimation in terms of bias and mean-square error, was confirmed by a simulation study made by Coles and Dixon [28]. Nevertheless, these two authors argued that robust measures of estimator performance are more favourable to ML estimator because the distribution of the ML shape parameter has a noticeable positive skew. Coles and Dixon observed also that underestimation is more problematic than overestimation when dealing with return level estimates.

The dataset here analysed revealed estimates for the shape parameter between -0.3 and 0.3. There was, as well, a big similarity for these estimates and also for the location and scale parameters obtained by the two methods (cf. Table 5.6). Because of that, in the particular cases considered, the fitted model by the PWM method will not show a relevant difference in performance in comparison with the ML method. Thus this last mentioned method was the selected one to determine the estimates and confidence intervals for the 50– and 100–year return levels presented in Table 5.7. Funchal (U) station is the one with the lowest estimates for the 50– and 100–year return levels, values that were less than the corresponding values of Santa Catarina (V) and Lugar de Baixo (X). Although, these two stations are in a lower altitude, they present higher estimates values and wider confidence intervals. The highest estimates for the 50– and 100–year return levels belong to the stations located in an altitude above 500 m, namely Areeiro (A), Bica da Cana (B), Santana (P), and Santo da Serra (I) stations.

Table 5.7: Estimates (mm) and confidence intervals (CI) for 50– and 100–year return levels–Dataset I.

	50–year		100–year	
Station	estimate	95% CI	estimate	95% CI
Areeiro (A)	266.0	(225.6, 306.4)	279.5	(228.1, 330.9)
Bica da Cana (B)	241.7	(219.9, 263.5)	250.7	(225.3, 276.0)
Santo da Serra (I)	262.0	(197.0, 327.1)	281.3	(194.3, 368.4)
Santana (P)	234.3	(167.3, 301.4)	262.4	(168.1, 356.7)
Funchal (U)	124.3	(100.0, 148.5)	134.8	(102.6, 167.1)
Santa Catarina (V)	154.0	(101.2, 206.8)	177.0	(100.6, 253.3)
Lugar de Baixo (X)	137.0	(77.3, 196.6)	164.5	(72.8, 256.1)

The assumption of Model 1 for modelling Areeiro (A) station annual maxima resulted into the Areeiro's corresponding values but, recalling the possibility of the existence of a linear trend in the model's parameters, it is important to have in mind that in Areeiro's case, the Model 1 is rejected in favour of Model 3. If this last model is considered for modelling Areeiro's annual maxima, only the estimates for each year for the so called "effective" return levels can be determined because the distribution changes with time. In this case, the largest values found among the ones obtained are 282.0 mm and 291.6 mm for 50– and 100–year return, respectively. Moreover, it can be observed that these last values belong to the confidence intervals of the 50– and 100–year return levels presented in Table 5.7.

5.1.2 Dataset II

Madeira Civil Engineering Laboratory's Department of Hydraulics and Energy Technologies provided for the study presented in this subsection, precipitation data collected daily from 25 rain gauge stations maintained in the past by the General Council of the Autonomous District of Funchal. In Figure 5.6, the location of each station is represented by a circle with the letter of identification and the colour corresponding to the respective altitude class. Like in Chapter 3, Class 1 corresponds to values of altitude above 900 meters. The stations with altitude between 600 and 900 meters belong to Class 2 and the ones with and an altitude between 300 and 600 meters to Class 3. All stations with altitude below 300 meters are represented with a blue circle. Table 5.8 provides information about the obtained samples of annual maximum precipitation, namely size, measurement period and the corresponding station's altitude, identification name and letter.

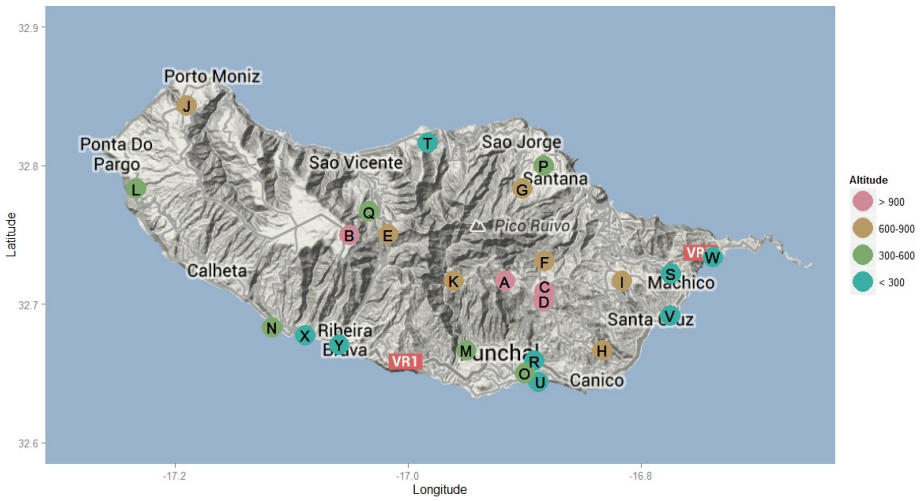

Figure 5.6: Location and altitude range of the rain gauge stations–Dataset II (Map data ©2014 Google).

The procedure to detect non-stationarities [132] that was applied in the Subsection 5.1.1 is also utilised here. So, to analyse the assumption that the data $x_1, ..., x_n$ are realisations from a sequence $X_1, ..., X_n$ of identically distributed random variables, each sample is divided in four subsamples. The last subsample record length, n_4 is 7, 5 and 4 for all the stations with sample size equal to 31, 23 and 22, respectively. Then, by the application of the function *kruskal.test* from *stats* R language package [178], the Kruskal-Wallis statistic test value and the corresponding p–value is determined for each station dataset (Table 5.9).

At a 0.05 significance level, the hypothesis of homogeneity is not rejected for all four station data cases in Class 1. The same happens with the stations in Class 2, with the exception of Porto Moniz (J) and Curral de Freiras (K). Loural (Q) and Machico (S) stations are the only ones in Classes 3 and 4, respectively, that present a p–value lower than 0.05. The existence of trends in the parameters' values is analysed as well through likelihood ratio tests, being the corresponding p–values presented in Appendix B. Figures 5.7 to 5.8 show the annual maximum of daily precipitation recorded at the stations already analysed in Subsection 5.1.1. There is no evidence in these figures that the pattern of variation of the annual maximum of daily precipitation has changed over the shorter observation period considered in this subsection, with the exception of the Areeiro (A) and Bica da Cana (B) stations data. Figure 5.7 (top) shows a slight decrease in the data values over time for Areeiro (A), but a slight increase for Bica da Cana (B). Only in the case of the latter, the rain gauge station located at the highest altitude in the northern

Table 5.8: Dataset II: annual maximum precipitation (source: LREC).

Station	Altitude (m)	Period	n
Areeiro (A)	1610	1950–1980	31
Bica da Cana (B)	1560	1950–1980	31
Poiso (C)	1360	1959–1980	22
Montado do Pereiro (D)	1260	1950–1980	31
Encumeada (E)	900	1959–1980	22
Ribeiro Frio (F)	874	1950–1980	31
Queimadas (G)	860	1950–1980	31
Camacha (H)	680	1950–1980	31
Santo da Serra (I)	660	1950–1980	31
Porto Moniz (J)	653	1950–1972	23
Curral das Freiras (K)	650	1950–1972	23
Ponta do Pargo (L)	570	1950–1972	23
Santo António (M)	525	1950–1972	23
Canhas (N)	425	1950–1972	23
Sanatório (O)	380	1950–1980	31
Santana (P)	380	1950–1980	31
Loural (Q)	307	1950–1972	23
Bom Sucesso (R)	290	1959–1980	22
Machico (S)	160	1959–1980	22
Ponta Delgada (T)	136	1950–1980	31
Funchal (U)	58	1950–1980	31
Santa Catarina (V)	49	1959–1980	22
Caniçal (W)	40	1959–1980	22
Lugar de Baixo (X)	15	1950–1980	31
Ribeira Brava (Y)	10	1950–1972	23

side of the island, there is evidence to suggest a linear trend in both location and scale parameters with respect to time at a 0.05 level of significance. More precisely, there is evidence for a linear trend both in location and scale parameters, with $\widehat{\mu}(t) = 112.35 + 1.36t$ and $\widehat{\sigma}(t) = \exp(2.45 + 0.06t)$, when considering that $\gamma = 0$.

Taking aside for the moment the possible dependence of time of the distribution of the data from stations Areeiro (A) and Bica da Cana (B), the test of Model 2 (Gumbel distribution) versus Model 1 (non–Gumbel, EV distribution) was performed. Table 5.10 compiles the choices that resulted from the application of the

Table 5.9: Kruskal-Wallis statistic test value and p–value–Dataset II.

Station	Statistic test value	p–value
Areeiro (A)	6.5039	0.0895
Bica da Cana (B)	4.8497	0.1831
Poiso (C)	4.9091	0.1786
Montado do Pereiro (D)	1.2319	0.7454
Encumeada (E)	0.4368	0.9325
Ribeiro Frio (F)	5.1632	0.1602
Queimadas (G)	2.2603	0.5202
Camacha (H)	0.5720	0.9028
Santo da Serra (I)	3.4878	0.3224
Porto Moniz (J)	8.3942	0.0385
Curral das Freiras (K)	10.5138	0.0147
Ponta do Pargo (L)	4.3507	0.2260
Santo António (M)	3.3906	0.3352
Canhas (N)	2.0380	0.5646
Sanatório (O)	3.8968	0.2728
Santana (P)	2.3792	0.4975
Loural (Q)	8.1814	0.0424
Bom Sucesso (R)	5.2233	0.1562
Machico (S)	8.1581	0.0429
Ponta Delgada (T)	1.1464	0.7659
Funchal (U)	2.2637	0.5195
Santa Catarina (V)	4.2178	0.2389
Caniçal (W)	7.1528	0.0672
Lugar de Baixo (X)	0.7987	0.8498
Ribeira Brava (Y)	2.2167	0.5287

likelihood ratio test and the corresponding model parameters' estimates, obtained by the application, for each location, of the *ismev* and *extRemes* R language packages [178].

The hypothesis of a Gumbel distribution is only rejected for six locations. In the north of the island, the shape parameter estimate is negative for Queimadas (G), a rain gauge located farther from the sea than Porto Moniz (J) and Ponta Delgada (T) stations, which present positive shape parameter estimates. All the three locations in the southern part of the island, namely Camacha (H), Curral das Freiras (K) and

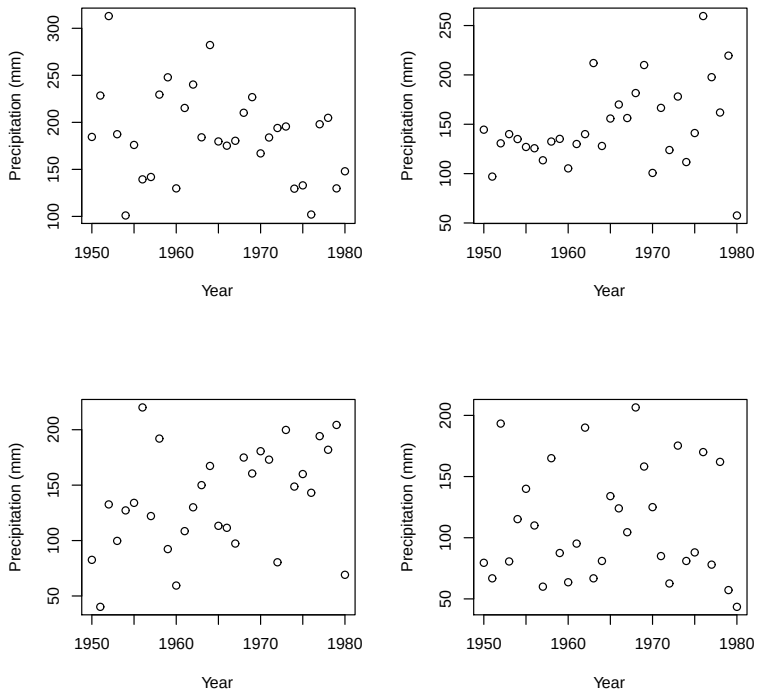

Figure 5.7: Annual maximum of daily precipitation values at Areeiro (A) (up left), Bica da Cana (B) (up right), Santo da Serra (I) (down left), and Santana (P) (down right) stations–Dataset II.

Santo da Serra (I), show negative shape parameter estimates. The highest absolute value of $\widehat{\gamma}$ belongs to Curral das Freiras (K). Also the value of $\widehat{\gamma}$ for Porto Moniz (J) needs extra care, having in mind that the assumption of homogeneity was rejected (cf. Table 5.10). The case of Santo da Serra (I) is another case of particular interest given the rejection of Model 2, in contrast to what happened in the previous section. On the other hand, Model 2 is now not rejected for Bica da Cana (B) and Lugar de Baixo (X) unlike what happened in the previous subsection.

For the stations with 31 annual maxima, the adequacy of the chosen model was tested through the Kolmogorov-Smirnov test by the application of the function *gofstat* in the *fitdistrplus* R language package [178]. For the stations for which Model 2 was selected, the test statistic values obtained were 0.1532 for Areeiro (A), 0.1267 for Bica da Cana (B), 0.0674 for Funchal (U), 0.0688 for Lugar de Baixo (X), 0.1655 for Montado do Pereiro (D), 0.0870 for Ribeiro Frio (F), 0.0893 for Sanatório (O), and 0.1354 for Santana (P). The test statistic values obtained when Model 1 was tested were 0.0961, 0.1132, 0.2027 and 0.0709 for Camacha (H), for Ponta

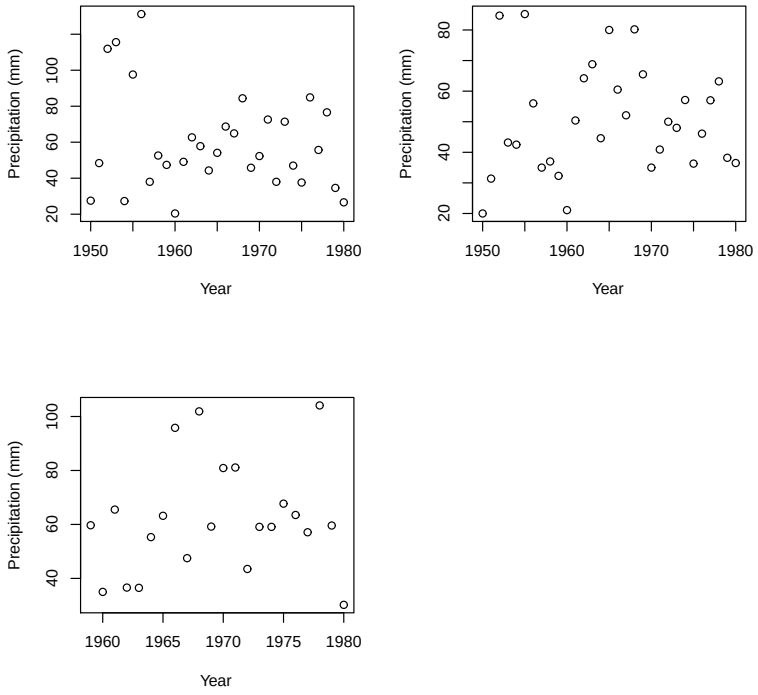

Figure 5.8: Annual maximum of daily precipitation values at Funchal (U) (up left), Santa Catarina (V) (up right), and Lugar de Baixo (X) (down) stations–Dataset II.

Delgada (T), for Queimadas (G) and Santo da Serra (I), respectively. Therefore, for each one rain gauge station, the data do not provide sufficient evidence to conclude that the chosen model is not an appropriate model for modelling the respective annual maxima, at a 0.05 significance level.

For the stations with shorter measurement periods, the adequacy of Model 2 was tested by the application of the A^2 modified statistic test discussed by Stephens [200] and defined by expression (4.9), due to the sample sizes. The obtained values for Poiso (C) and Encumeada (E), the remaining stations of Classes 1 and 2, were 0.267 and 0.351 respectively. The values of the A^2 modified statistic test for the remaining stations that belong to Class 3 is 0.246 for Ponta do Pargo (L), 0.246 for Santo António (M), 0.857 for Canhas (N) and 0.530 for Loural (Q). The values for the stations with altitude below 300 meters are 0.332 for Bom Sucesso (R), 0.322 for Machico (S), 0.525 for Santa Catarina (V), 0.624 for Caniçal (W) and 0.211 for Ribeira Brava (Y). At a 5% significance level, it appears that none of the observed values of the test statistic, with the exception of Canhas (N) station, meets the criteria for rejection, i.e., no value is greater than 0.757 ([200], Table 1). Thus, the

Table 5.10: Resulting models and ML parameter estimates–Dataset II.

Station	Model	$\widehat{\mu}$	$\widehat{\sigma}$	$\widehat{\gamma}$
Areeiro (A)	Model 2	162.49	42.71	
Bica da Cana (B)	Model 2	128.68	36.86	
Poiso (C)	Model 2	127.04	34.69	
Montado do Pereiro (D)	Model 2	129.10	40.00	
Encumeada (E)	Model 2	158.62	45.89	
Ribeiro Frio (F)	Model 2	125.33	39.62	
Queimadas (G)	Model 1	111.70	25.04	−0.209
Camacha (H)	Model 1	102.75	39.49	−0.451
Santo da Serra (I)	Model 1	124.30	47.97	−0.428
Porto Moniz (J)	Model 1	57.43	24.41	0.326
Curral das Freiras (K)	Model 1	140.69	36.50	−0.584
Ponta do Pargo (L)	Model 2	60.21	18.60	
Santo António (M)	Model 2	66.41	27.80	
Canhas (N)	Model 2	57.35	16.66	
Sanatório (O)	Model 2	67.58	24.92	
Santana (P)	Model 2	89.87	35.75	
Loural (Q)	Model 2	119.59	46.02	
Bom Sucesso (R)	Model 2	59.14	17.67	
Machico (S)	Model 2	60.73	27.21	
Ponta Delgada (T)	Model 1	74.43	28.69	0.236
Funchal (U)	Model 2	47.49	20.29	
Santa Catarina (V)	Model 2	52.38	16.89	
Caniçal (W)	Model 2	53.28	19.29	
Lugar de Baixo (X)	Model 2	42.16	14.85	
Ribeira Brava (Y)	Model 2	52.38	17.01	

data do not provide enough evidence to conclude that the Gumbel model is not suitable for modelling annual maxima for these cases.

The same models' choices are made when the hypothesis of a Gumbel distribution is analysed by a test based on the PWM estimate of γ presented by Hosking et al. [119] (cf. Subsection 4.1.2), with the exception of Queimadas (G) and Santo António (M) stations. Table 5.11 shows the corresponding model parameter estimates obtained by the use of the *fExtremes* R package [178]. It can be observed that the parameter estimates are relatively similar in the cases where,

independently of the method used, Model 2 is rejected. This is not the case when Model 2 is chosen since the ML scale parameter estimates are much smaller than the corresponding PWM estimates. The opposite happens with the location parameter estimates, but in a less pronounced way. Although for the distributions corresponding to these cases there is no significant evidence to choose Model 1 in opposition to Model 2, it is important to make the analysis of the situation where only the GEV distribution is considered for the reasons already presented in Subsection 5.1.1. The ML and PWM estimates for the location, scale and shape parameters of the GEV distribution for each station in Classes 1 and 2 are displayed in Table 5.12, while Table 5.13 shows the respective values for the ones that are in Classes 3 and 4.

On the north side of the island, it can be observed that the estimated value of the shape parameter for the GEV distribution is positive for the rain gauge stations located nearest to the sea and it is negative for the three stations located in the interior of the island, namely Bica da Cana (B), Encumeada (E) and Loural (Q). For the rain gauge stations on the south side, there are cases of positive and negative shape parameter estimates both in the interior and near the coast. The negative shape parameter estimate enables the computation of an estimate of the upper end point of the fitted distribution z_0 through the expression $\widehat{z}_0 = \widehat{\mu} - \widehat{\sigma}/\widehat{\gamma}$. For the stations that only appear in this subsection, $\widehat{z}_0$ is equal to 333.71 mm for Montado do Pereiro (D), 308.74 mm for Encumeada (E), 1421.46 mm for Ribeiro Frio (F), 231.51 mm for Queimadas (G), 190.31 mm for Camacha (H), 236.38 mm for Santo da Serra (I), 203.19 mm for Curral das Freiras (K), 557.97 mm for Ponta do Pargo (L), 169.90 mm for Santo António (M), 968.68 mm for Sanatório (O), 510.69 mm for Loural (Q), 123.80 mm for Bom Sucesso (R), and 96.64 mm for Caniçal (W).

If the PWM estimates are used, instead of the ML parameter ones, then the value obtained for $\widehat{z}_0$ is 336.45 mm for Montado do Pereiro (D), 327.85 mm for Encumeada (E), 742.38 mm for Ribeiro Frio (F), 222.64 mm for Queimadas (G), 200.39 mm for Camacha (H), 259.49 mm for Santo da Serra (I), 205.95 mm for Curral das Freiras (K), 397.23 mm for Ponta do Pargo (L), 166.08 mm for Santo António (M), 608.55 mm for Sanatório (O), 419.31 mm for Loural (Q), 153.71 mm for Bom Sucesso (R), and 142.34 mm for Caniçal (W).

Table 5.11: Resulting models and PWM parameter estimates–Dataset II.

Station	Model	$\widehat{\mu}$	$\widehat{\sigma}$	$\widehat{\gamma}$
Areeiro (A)	Model 2	96.86	154.02	
Bica da Cana (B)	Model 2	76.82	123.34	
Poiso (C)	Model 2	75.33	125.75	
Montado do Pereiro (D)	Model 2	77.23	128.24	
Encumeada (E)	Model 2	94.68	152.60	
Ribeiro Frio (F)	Model 2	74.75	127.66	
Queimadas (G)	Model 2	65.07	97.66	
Camacha (H)	Model 1	101.57	41.01	−0.415
Santo da Serra (I)	Model 1	122.05	49.34	−0.359
Porto Moniz (J)	Model 1	56.51	23.88	0.335
Curral das Freiras (K)	Model 1	140.28	38.35	−0.584
Ponta do Pargo (L)	Model 2	35.83	60.98	
Santo António (M)	Model 1	70.87	30.37	−0.319
Canhas (N)	Model 2	34.08	58.51	
Sanatório (O)	Model 2	40.44	72.15	
Santana (P)	Model 2	53.89	99.39	
Loural (Q)	Model 2	72.04	124.34	
Bom Sucesso (R)	Model 2	35.27	58.06	
Machico (S)	Model 2	36.49	69.44	
Ponta Delgada (T)	Model 1	73.14	27.50	0.283
Funchal (U)	Model 2	28.49	53.86	
Santa Catarina (V)	Model 2	31.30	53.04	
Caniçal (W)	Model 2	31.95	55.76	
Lugar de Baixo (X)	Model 2	25.24	43.62	
Ribeira Brava (Y)	Model 2	31.18	54.24	

Although the altitude appears to be a factor influencing the spatial distribution of extreme rainfall, in general it is not possible to conclude that the values of the location parameter estimates increase with altitude. Even though Queimadas (G) rain gauge station presents a higher altitude when compared to Loural (Q), the latter shows a location parameter estimate (of approximately 123 mm) greater than the corresponding value for Queimadas (G). Unlike Loural (Q), Queimadas (G) is not located on the E–W oriented orographic barrier in the interior of the island and therefore, besides altitude, the proximity to the sea seems to be a factor influencing

Table 5.12: GEV parameters estimates by ML and PWM (Classes 1 and 2)

Station	Method	$\widehat{\mu}$	$\widehat{\sigma}$	$\widehat{\gamma}$
Areeiro (A)	ML	166.07	44.22	−0.153
Areeiro (A)	PWM	165.94	45.69	−0.167
Bica da Cana (B)	ML	131.47	37.07	−0.143
Bica da Cana (B)	PWM	129.40	34.15	−0.033
Poiso (C)	ML	124.81	32.74	0.125
Poiso (C)	PWM	125.15	36.50	0.045
Montado do Pereiro (D)	ML	133.85	42.77	−0.214
Montado do Pereiro (D)	PWM	133.45	45.27	−0.223
Encumeada (E)	ML	167.24	49.10	−0.347
Encumeada (E)	PWM	165.69	51.73	−0.319
Ribeiro Frio (F)	ML	125.98	40.16	−0.031
Ribeiro Frio (F)	PWM	126.04	43.76	−0.071
Queimadas (G)	ML	111.70	25.04	−0.209
Queimadas (G)	PWM	111.99	23.68	−0.214
Camacha (H)	ML	102.75	39.49	−0.451
Camacha (H)	PWM	101.57	41.01	−0.415
Santo da Serra (I)	ML	124.30	47.97	−0.428
Santo da Serra (I)	PWM	122.05	49.34	−0.359
Porto Moniz (J)	ML	57.43	24.41	0.326
Porto Moniz (J)	PWM	56.51	23.88	0.335
Curral das Freiras (K)	ML	140.69	36.50	−0.584
Curral das Freiras (K)	PWM	140.28	38.35	−0.584

the spatial distribution of extreme rainfall. Loural (Q) is also near the Encumeada (E) rain gauge station, which presents the highest values for the location and scale parameters estimates. Just below the values observed at Encumeada (E), are the values corresponding to Areeiro (A), the rain gauge station located in the south with the highest altitude in the island. Revealing the natural differences observed on the windward and lee sides of any mountainous island, we have the rainfall data from Sanatório (O) and Santana (P) rain gauge stations. These stations have the same altitude, but Sanatório (O), which is located in the southern part of the island, presents lower values for all the estimated values.

Table 5.13: GEV parameters estimates by ML and PWM (Classes 3 and 4)

Station	Method	$\widehat{\mu}$	$\widehat{\sigma}$	$\widehat{\gamma}$
Ponta do Pargo (L)	ML	60.60	18.90	−0.038
Ponta do Pargo (L)	PWM	60.34	20.55	−0.061
Santo António (M)	ML	70.86	29.02	−0.293
Santo António (M)	PWM	70.87	30.37	−0.319
Canhas (N)	ML	52.64	11.52	0.637
Canhas (N)	PWM	55.66	16.45	0.144
Sanatório (O)	ML	67.96	25.22	−0.028
Sanatório (O)	PWM	67.75	27.04	−0.050
Santana (P)	ML	88.13	34.26	0.093
Santana (P)	PWM	89.08	38.05	0.006
Loural (Q)	ML	122.29	46.22	−0.119
Loural (Q)	PWM	123.23	46.78	−0.158
Bom Sucesso (R)	ML	62.18	19.41	−0.315
Bom Sucesso (R)	PWM	60.86	19.87	−0.214
Machico (S)	ML	60.49	27.06	0.016
Machico (S)	PWM	59.80	27.62	0.030
Ponta Delgada (T)	ML	74.43	28.69	0.236
Ponta Delgada (T)	PWM	73.14	27.50	0.283
Funchal (U)	ML	46.79	19.77	0.066
Funchal (U)	PWM	46.35	20.32	0.070
Santa Catarina (V)	ML	53.24	17.39	−0.094
Santa Catarina (V)	PWM	52.80	17.81	−0.071
Caniçal (W)	ML	62.35	28.32	−0.826
Caniçal (W)	PWM	55.76	23.03	−0.266
Lugar de Baixo (X)	ML	43.33	15.45	−0.145
Lugar de Baixo (X)	PWM	42.68	15.66	−0.091
Ribeira Brava (Y)	ML	51.74	16.55	0.070
Ribeira Brava (Y)	PWM	51.43	17.28	0.060

The differences between the northern and the southern parts of Madeira Island can also be found in terms of return levels. Illustrating these differences, Figures 5.9 and 5.10 present the diagnostic plots (cf. Subsection 4.1.3) for the GEV fit to Ribeira Brava (Y) and Ponta Delgada (T) rain gauge data, respectively. The diagnostic plots for Models 1 and 2 for the stations in Classes 1, 2, 3 and 4 are displayed in

Appendices C, D, E and F, respectively.

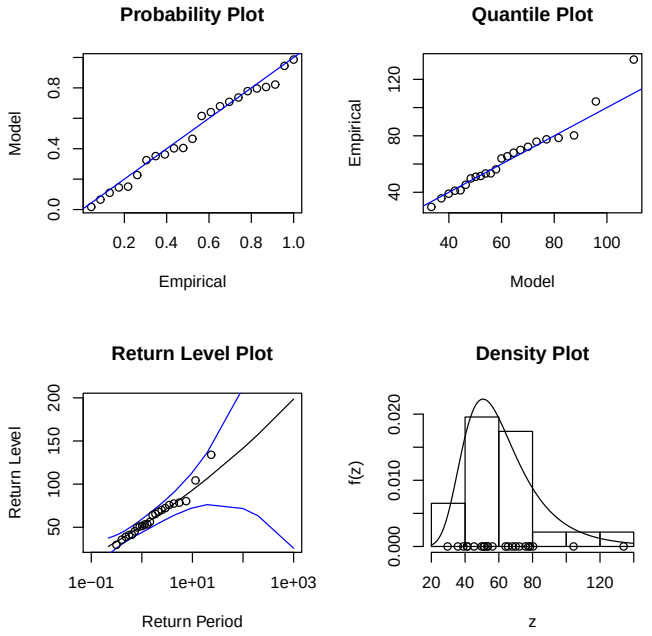

Figure 5.9: Diagnostic plots for GEV fit to the Ribeira Brava (Y) station data– Dataset II.

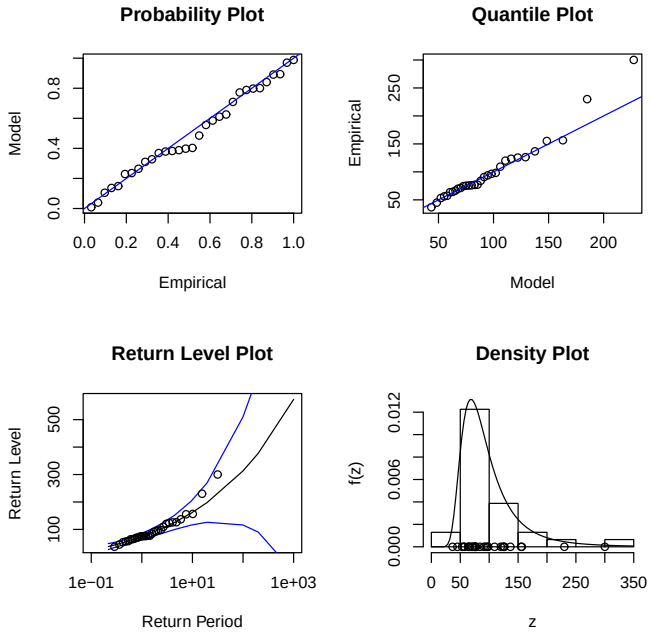

Figure 5.10: Diagnostic plots for GEV fit to the Ponta Delgada (T) station data– Dataset II.

Table 5.14 shows the 50– and 100–year return level estimates ($\widehat{q}_{0.02}$ and $\widehat{q}_{0.01}$) obtained for each location with the Model 1's parameter estimates produced by ML and PWM methods. For Areeiro (A), Ribeiro Frio (F), Porto Moniz (J), Ponta do Pargo (L), Santo António (M) and Ribeira Brava (Y), the 50– and 100–year return values calculated by both methods are approximately similar ($\widehat{q}_{0.02}^{ML} \approx \widehat{q}_{0.02}^{PWM}$ and $\widehat{q}_{0.01}^{ML} \approx \widehat{q}_{0.01}^{PWM}$ respectively). The largest parameter estimates for Poiso (C), Queimadas (G), Canhas (N), Santana (P) and Loural (Q) are obtained by the ML method. For all the rest of rain gauge stations, the higher values for the return levels are found when calculated by the PWM method. In the northern part of Madeira Island, all return level estimates calculated are higher than 240 mm, excluding the values corresponding to Queimadas (G). In turn, on the south side of the island the return values are less than 180 mm for all rain gauge stations with altitudes below 600 m, with the exception of Machico (S). For Areeiro (A), Poiso (C), Montado do Pereiro (D) and Ribeiro Frio (F), the 50– and 100–year return level estimates are greater than 245 mm. The proximity between the return value estimates for Queimadas (G) and Machico (N) rain gauge stations suggests the proximity to the sea as a factor to be taken into account in the study of return levels, in addition to natural factors such as altitude or location in the northern or southern part of the island. These two rain gauge stations have distinct altitudes and are located at different but nearby hillsides. In the southwest, it can be observed another pair of rain gauge stations, Ponta do Pargo (I) and Ribeira Brava (S), with similar return values but closer parameter estimates. Although the distance between rain gauge stations might seem an influential factor, closer rain gauge stations do not necessarily have similar return level estimates, as it is shown by the set of three rain gauge stations located in Funchal municipality, namely Santo António (M), Sanatório (K) and Funchal (P).

Recalling that the values presented in Table 5.14 were obtained using Model 1 for modelling each station annual maxima, it is important to have in mind that for some of the considered stations there is a significant evidence for a linear trend when it is assumed that $\gamma \neq 0$ (cf. Tables B.1 to B.4 in Appendix B). At a 0.05 significance level, Model 1 is rejected in favour of Model 3 when considering Santo António (M), Canhas (N) and Machico (S) stations. More precisely, there was evidence for a linear trend in the location parameter with $\widehat{\mu}(t) = 39.38 + 2.33t$ for Santo António (M), $\widehat{\mu}(t) = 45.43 + 0.33t$ for Canhas (N) and $\widehat{\mu}(t) = 76.11 - 1.44t$ for Machico (S). For these three stations, the values for the scale parameter in Model 3 are $\widehat{\sigma} = 19.07$, $\widehat{\sigma} = 6.90$ and $\widehat{\sigma} = 22.55$, respectively.

Table 5.14: Estimates for 50– and 100–year return levels–Dataset II.

Station	$\widehat{q}_{0.02}^{ML}$	$\widehat{q}_{0.02}^{PWM}$	$\widehat{q}_{0.01}^{ML}$	$\widehat{q}_{0.01}^{PWM}$
Areeiro (A)	296.09	297.05	312.24	312.77
Bica da Cana (B)	242.23	254.33	256.29	275.02
Poiso (C)	289.29	280.82	328.12	311.66
Montado do Pereiro (D)	247.01	251.50	259.05	263.78
Encumeada (E)	272.22	281.18	280.09	290.52
Ribeiro Frio (F)	273.50	275.31	298.05	297.95
Queimadas (G)	178.53	174.60	185.73	181.26
Camacha (H)	175.20	180.86	179.26	185.78
Santo da Serra (I)	215.23	225.56	220.66	233.06
Porto Moniz (J)	249.67	249.71	317.92	318.01
Curral das Freiras (K)	196.81	199.25	198.96	201.50
Ponta do Pargo (L)	129.07	129.07	140.28	140.28
Santo António (M)	138.28	138.66	144.11	144.14
Canhas (N)	251.87	141.71	373.62	162.87
Sanatório (O)	161.09	163.62	176.69	178.89
Santana (P)	249.39	239.26	284.97	266.50
Loural (Q)	266.48	259.36	285.93	276.02
Bom Sucesso (R)	105.78	113.39	109.34	118.97
Machico (S)	169.47	174.08	189.70	195.98
Ponta Delgada (T)	258.24	268.99	312.96	312.96
Funchal (U)	134.70	137.48	152.94	156.56
Santa Catarina (V)	110.05	113.56	118.20	122.77
Caniçal (W)	95.27	111.69	95.87	116.89
Lugar de Baixo (X)	89.38	94.12	95.21	101.55
Ribeira Brava (Y)	125.95	125.93	141.50	141.48

Model 1 is also rejected in favour of Model 5 when considering Queimadas (G) station. In this case, $\widehat{\sigma}(t) = \exp(\widehat{\beta}_2 + \widehat{\beta}_3 t)$ with the ML estimates $\widehat{\beta}_2 = 2.70$ and $\widehat{\beta}_3 = 0.03$ for the scale parameter and $\widehat{\mu} = 111.69$ for the location parameter. In the case of Curral das Freiras (K) and Caniçal (W) stations, Model 1 is rejected in favour of Models 3 and 5 but not in favour of Model 7. That is, although there is evidence for a linear trend both in the location parameter and in the scale parameter (when the other one is considered to be fixed), there is no evidence for a linear trend in both parameters simultaneously (Model 7). On the other hand, for Ribeira Brava (Y)

there is evidence for a linear trend in each one and in both location and scale parameters, i.e., Model 1 is rejected in favour of Models 3, 5 and 7. Finally, for Bica da Cana (B), there is also a significant evidence for a linear trend when it is assumed that $\gamma \neq 0$. More precisely, there is evidence for a linear trend both in location and scale parameters, with $\widehat{\mu}(t) = 115.99 + 1.26t$ and $\widehat{\sigma}(t) = \exp(2.54 + 0.05t)$. The ML estimates for $\widehat{\beta}_1$, $\widehat{\beta}_2$, $\widehat{\beta}_3$ and $\widehat{\beta}_4$ now found are similar with the ones obtained when considering $\gamma = 0$, which were presented above. So, whether γ is null or not, there is a significant evidence for a linear trend both in location and scale parameters in the case of Bica da Cana (B) station when considering the shorter period analysed in this subsection contrary to what is the case when a wider period is considered (cf. Subsection 5.1.1).

5.1.3 Dataset I+II

In this subsection, the analysed dataset results from the union of the datasets of the rain gauge stations that are considered in both previous subsections. So in this way, with the exception of Funchal (U) and Santana (P), a longer measurement period is obtained for each station presented in Table 5.15. Information about each data sample, namely the size (n), the measurement period and also the corresponding station's altitude, identification name and letter, are given in Table 5.15.

Table 5.15: Dataset I+II: annual maximum precipitation (sources: IPMA and LREC).

Station	Altitude (m)	Period	n
Areeiro (A)	1610	1950–1992	42
Bica da Cana (B)	1560	1950–2008	51
Santo da Serra (I)	660	1950–2009	58
Santana (P)	380	1942–2007	59
Funchal (U)	58	1949–2009	61
Santa Catarina (V)	49	1959–2009	50
Lugar de Baixo (X)	15	1950–2004	54

The procedure to detect non–stationarities [132] applied in Subsections 5.1.1 and 5.1.1 is also used here. The sizes of the four subsamples of the augmented samples, (n_1, n_2, n_3, n_4), the Kruskal-Wallis statistic test value and the corresponding p–value, obtained by the application of function *kruskal.test* in the *stats* R language package [178], are displayed in Table 5.16.

Table 5.16: Records length, Kruskal–Wallis statistic test value and p–value–Dataset I+II.

Station	(n_1, n_2, n_3, n_4)	Statistic test value	p–value
Areeiro (A)	$(11, 11, 11, 9)$	6.8257	0.0777
Bica da Cana (B)	$(13, 13, 13, 12)$	10.0429	0.0182
Santo da Serra (I)	$(15, 15, 15, 13)$	5.9010	0.1165
Santa Catarina (V)	$(13, 13, 13, 11)$	1.6774	0.6420
Lugar de Baixo (X)	$(14, 14, 14, 12)$	2.0725	0.5575

At a 0.05 significance level, contrary to what happened before, the hypothesis of homogeneity is rejected for Bica da Cana (B). On the other hand, there is no evidence for the existence of trends in the parameters' values for any of the stations in opposition to what happened in Subsection 5.1.1 with Areeiro (A) station and to what happened in Subsection 5.1.2 with Bica da Cana (B) station. Again a likelihood ratio test was used. Nevertheless, Areeiro (A) augmented sample shows a slight decrease in the annual maxima (Figure 5.11). All p–values for the produced likelihood ratio tests for each station are presented in Appendix B (cf. Table B.5). Figure 5.11 shows the annual maximum of daily precipitation recorded at the stations with augmented samples, with the exception of Santa Catarina (V), which presents only two more values than the graph displayed in Figure 3.3 (up right) in Chapter 3.

As in the two previous subsections, the test of Model 2 (Gumbel distribution) versus Model 1 (non-Gumbel EV distribution) was carried out for each of the augmented samples. The choices resulting from the application of the likelihood ratio test, the model parameters' estimates, and the standard errors for each new station data set, along with those of Funchal (U) and Santana (P) determined in Subsection 5.1.1, are presented in Table 5.17. For the three different measurements periods, it can be observed that for Areeiro (A), Funchal (U), Santana (P) and Santa Catarina (V) there is no sufficient evidence for rejecting Model 2 whatever the period considered. However, that is not the case for Bica da Cana (B), Lugar de Baixo (X) and Santo da Serra (I). Model 2 is rejected for Bica da Cana (B) here and when considering the Dataset I. In the cases of Lugar de Baixo (X) and Santo da Serra (I), Model 2 is only rejected when considering Dataset I or Dataset II, respectively.

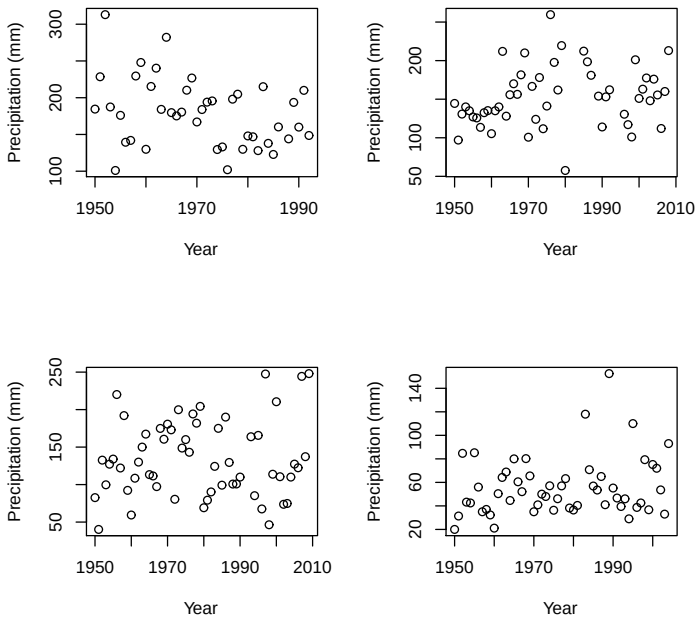

Figure 5.11: Annual maximum daily precipitation values at Areeiro (A) (up left), Bica da Cana (B) (up right), Santo da Serra (I) (down left), and Lugar de Baixo (X) (down right) stations–Dataset I+II.

Table 5.17: Resulting models, ML parameter estimates and standard errors–Dataset I+II.

Station	Model	$\widehat{\mu}$	$\widehat{\sigma}$	$\widehat{\gamma}$
Areeiro (A)	Model 2	157.66 (6.25)	38.35 (4.57)	
Bica da Cana (B)	Model 1	137.57 (5.51)	35.99 (3.77)	−0.190 (0.079)
Santo da Serra (I)	Model 2	110.27 (6.02)	43.38 (4.38)	
Santana (P)	Model 2	85.17 (5.07)	37.00 (3.86)	
Funchal (U)	Model 2	51.34 (2.85)	21.07 (2.10)	
Santa Catarina (V)	Model 2	54.52 (3.14)	21.17 (2.42)	
Lugar de Baixo (X)	Model 2	45.39 (2.43)	17.05 (1.86)	

The Kolmogorov-Smirnov test statistic value obtained, when Model 2 was tested, is 0.1025 for Areeiro (A), 0.0681 for Lugar de Baixo (U), 0.0951 Santa Catarina (V), and 0.0725 for Santo da Serra (I). Therefore, all these stations data do not provide sufficient evidence to conclude that Model 2 is not an appropriate model for modelling the respective annual maxima. The adequacy of the Model 1 was also tested through the Kolmogorov-Smirnov test for Bica da Cana (B)

annual maxima, yielding the value 0.0602 for the test statistic that also results in a non-rejection.

When considering the PWM estimate of γ, the value for the test statistic $Z = \widehat{\gamma}(n/0.5633)^{1/2}$ is not significant in comparison with the critical values of the standard normal distribution for each new station data set. So, Model 2 is not rejected for the stations presented in Table 5.18, which also displays the corresponding model parameter estimates obtained by the use of the *fExtremes* R package.

Table 5.18: Resulting models and PWM parameter estimates–Dataset I+II.

Station	Model	$\widehat{\mu}$	$\widehat{\sigma}$
Areeiro (A)	Model 2	93.75	148.01
Bica da Cana (B)	Model 2	79.96	125.55
Santo da Serra (I)	Model 2	66.37	117.95
Santa Catarina (V)	Model 2	32.71	60.05
Lugar de Baixo (X)	Model 2	27.20	49.50

Unlike what happened in the previous sections, there is one station, Bica da Cana (B), whose chosen model depends on the estimation method of the shape parameter γ. Also, although Model 2 is not rejected, if Model 1 is considered the parameter estimates obtained by the two methods are more similar as it can be observed in Table 5.19. Furthermore, Model 1 is also not rejected for each station's annual maximum since the values for the Kolmogorov-Smirnov test statistic value are 0.0883 for Areeiro (A), 0.0602 for Bica da Cana (B), 0.0520 for Lugar de Baixo (X), 0.1140 Santa Catarina (V), and 0.0638 for Santo da Serra (I).

It is important to notice that the ML shape parameter estimate for Areeiro (A) station approaches zero as the period's sample size increases from Dataset I (cf. Table 5.6 on page 64) to Dataset I+II. The estimates obtained by PWM method are also closer to zero as larger is the sample, but have lower values than ML estimates. The other station that belongs to Class 1, namely Bica da Cana (B), also presents a negative shape parameter estimate, independently of the method used (cf. Tables 5.6 and 5.12 on pages 64 and 76, respectively), being the PWM shape estimate the lower one. For this station, the absolute values of the shape parameter estimates in Table 5.19 are smaller than the absolute values of the ones obtained in Dataset I, but closer to zero than those of the ones observed with the shortest measurement period (cf. Table 5.12 on page 76). Although located

Table 5.19: GEV parameter estimates by ML and PWM–Dataset I+II.

Station	Method	$\widehat{\mu}$	$\widehat{\sigma}$	$\widehat{\gamma}$
Areeiro (A)	ML	159.44	39.32	−0.086
Areeiro (A)	PWM	159.33	40.85	−0.101
Bica da Cana (B)	ML	137.57	35.99	−0.190
Bica da Cana (B)	PWM	136.59	34.99	−0.142
Santo da Serra (I)	ML	113.65	45.20	−0.143
Santo da Serra (I)	PWM	112.60	46.17	−0.116
Santana (P)	ML	84.78	36.75	0.021
Santana (P)	PWM	84.73	38.40	0.002
Funchal (U)	ML	52.30	21.63	−0.084
Funchal (U)	PWM	51.89	22.04	−0.065
Santa Catarina (V)	ML	53.14	20.06	0.124
Santa Catarina (V)	PWM	53.20	20.75	0.097
Lugar de Baixo (X)	ML	44.46	16.37	0.103
Lugar de Baixo (X)	PWM	43.97	16.00	0.140

in a lower altitude but still above the 600 m, Santo da Serra (I) also presents a negative shape parameter estimate for both methods and like in the case of Areeiro (A) station, the absolute values of these estimates increase when compared to the ones obtained for Dataset I, but decrease when compared to the ones obtained for Dataset II. For Santana (P) and Funchal (U) the ML and PWM shape parameter estimates now obtained are approximately equal to the ones estimated for Dataset I. The common point of interest between the stations belonging to Class 1, namely Funchal (U), Santa Catarina (V), Lugar de Baixo (X) is the sign change of the shape parameters estimates from Dataset I to Dataset II (cf. Table 5.13 on page 77). While Santa Catarina (V) and Lugar de Baixo (X) station's shape parameter estimates change from positive to negative ones, the opposite happens to Funchal (U) station's shape parameter estimates. The values in Table 5.19 are back to positive but there is a decrease of the value of Lugar de Baixo (X) station's shape parameter estimates whatever the method used. The shape parameter negative estimate enables the computation of an estimate to the upper endpoint of the fitted distribution ($\widehat{z}_0 = \widehat{\mu} - \widehat{\sigma}/\widehat{\gamma}$). The obtained values for each measurement period and estimation method applied are presented in Table 5.20.

The adequacy of Model 1 to the corresponding distribution function of Areeiro (A), Bica da Cana (B), Lugar de Baixo (U), Santa Catarina (V), and

Table 5.20: Estimate by ML and PWM of the upper endpoint of the fitted distribution.

Station	Method	Dataset I	Dataset II	Dataset I+II
Areeiro (A)	ML	405.97	455.09	616.65
Areeiro (A)	PWM	375.66	439.53	563.79
Bica da Cana (B)	ML	295.51	390.70	326.99
Bica da Cana (B)	PWM	289.77	1164.25	383.00
Santo da Serra (I)	ML	491.60	236.38	429.73
Santo da Serra (I)	PWM	547.54	259.49	510.62
Funchal (U)	ML	309.80	–	309.80
Funchal (U)	PWM	390.97	–	390.97
Santa Catarina (V)	ML	–	238.24	–
Santa Catarina (V)	PWM	–	303.65	–
Lugar de Baixo (X)	ML	–	149.88	–
Lugar de Baixo (X)	PWM	–	214.77	–

Santo da Serra (I) was also analysed graphically by histogram, probability, quantile and return level plots just as in the previous subsections. The diagnostic plots for Models 1 and 2 for all these stations are displayed in Appendix G. Figures 5.12 and 5.13 present the diagnostic plots for the GEV distribution fit to Santo da Serra (I) and Santa Catarina (V) rain gauge data, respectively, and illustrate the differences in return levels, of at least 100 mm, between the stations that belong to Class 4 and the ones located at an altitude higher than 300 meters. The estimates and confidence intervals for the 50– and 100–year return levels for all stations, including the ones obtained in Subsection 5.1.1 for Santana (P) and Funchal (U), are presented in Table 5.21.

The highest estimates for the 50– and 100–year return levels still belong to Areeiro (A) station. These values are also higher than the ones obtained for Dataset I (cf. Table 5.7 on page 67). The estimates below Areeiro (A) station's values are the ones corresponding to Santo da Serra (I). Contrary to what occurred with Areeiro (A) values, the estimates for 50– and 100–year return levels of Santo da Serra (I) station are now lower than those of Subsection 5.1.1 and the confidence intervals obtained there include the new ones. In the two measurement periods, Bica da Cana (B), although located at a higher altitude, presents lower estimates for the 50– and 100–year return levels and less wider confidence intervals than the corresponding estimates and confidence intervals presented by Santo da Serra (I).

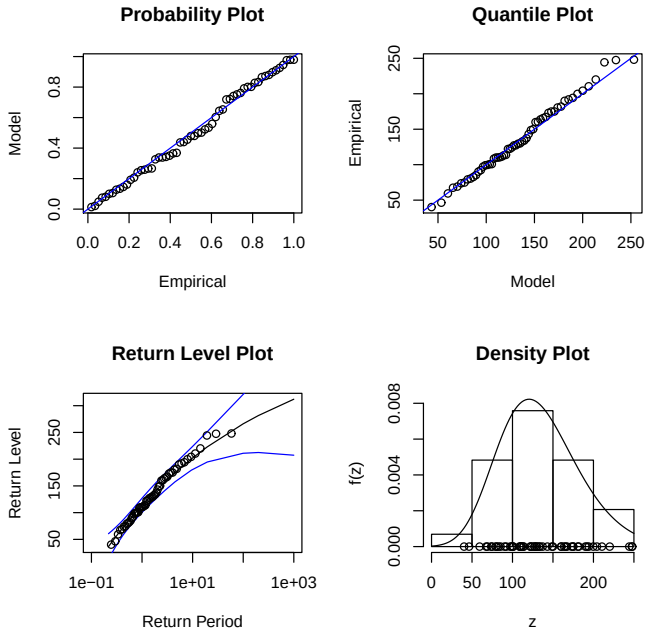

Figure 5.12: Diagnostic plots for GEV distribution fit to the Santo da Serra (I) station data–Dataset I+II.

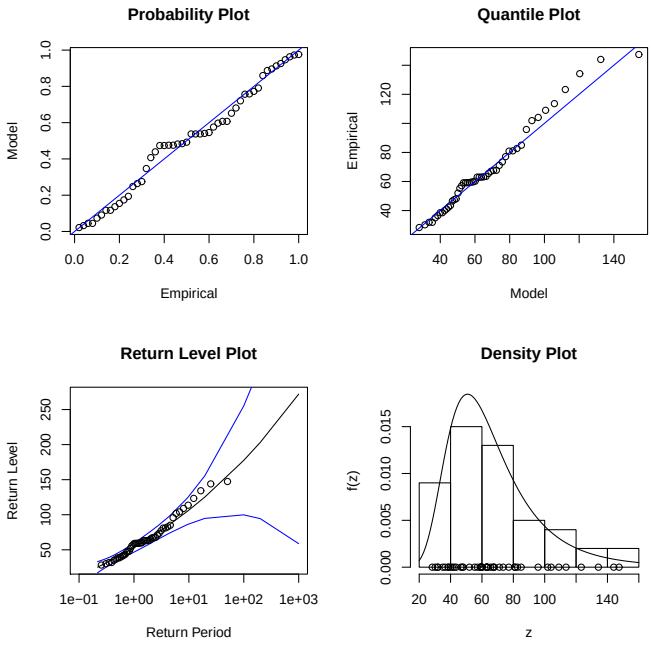

Figure 5.13: Diagnostic plots for GEV ditribution fit to the Santa Catarina (V) station data–Dataset I+II.

Among the stations that belong to Class 4, Santa Catarina (V) is the one that presents higher estimates values and wider confidence intervals. Lugar de Baixo (X)

Table 5.21: Estimates (mm) and confidence intervals (CI) for 50– and 100–year return levels–Dataset I+II.

	50–year		100–year	
Station	estimate	95% CI	estimate	95% CI
Areeiro (A)	289.9	(241.2, 338.5)	308.9	(245.3, 372.5)
Bica da Cana (B)	236.8	(212.3, 261.3)	248.0	(218.2, 277.8)
Santo da Serra (I)	248.9	(206.6, 291.1)	266.1	(211.0, 321.1)
Santana (P)	234.3	(167.3, 301.4)	262.4	(168.1, 356.7)
Funchal (U)	124.3	(100.0, 148.5)	134.8	(102.6, 167.1)
Santa Catarina (V)	153.7	(100.4, 207.0)	177.4	(99.9, 255.0)
Lugar de Baixo (X)	123.2	(88.6, 157.8)	141.0	(92.2, 189.7)

and Funchal (U) are the ones with the lowest estimate for the 50– and 100–year return level, respectively.

The ML method was the one applied to determine the estimates and confidence intervals for the 50– and 100–year return levels presented in Table 5.21. Besides these estimates, Table 5.22 shows the 50– and 100–year return level estimates ($\widehat{q}_{0.02}$ and $\widehat{q}_{0.01}$) obtained for each location with the Model 1's parameter estimates produced by the PWM method. It can be observed that for Areeiro (A) the 50– and 100–year return values calculated by both methods are approximately similar, that the largest parameter estimates for Santana (P) and Santa Catarina (V) are obtained by the ML method and that, for all the remaining rain gauge stations, the higher values for the return levels are found when calculated by the PWM method.

Table 5.22: Estimates for 50– and 100–year return levels–Dataset I+II.

Station	$\widehat{q}_{0.02}^{ML}$	$\widehat{q}_{0.02}^{PWM}$	$\widehat{q}_{0.01}^{ML}$	$\widehat{q}_{0.01}^{PWM}$
Areeiro (A)	289.85	291.14	308.92	309.74
Bica da Cana (B)	236.76	241.46	247.97	254.84
Santo da Serra (I)	248.85	257.44	266.05	277.10
Santana (P)	249.39	235.26	284.97	262.35
Funchal (U)	124.27	127.90	134.84	139.59
Santa Catarina (V)	153.72	151.68	177.42	173.59
Lugar de Baixo (X)	123.19	127.11	140.97	147.41

The same relation between the estimates values obtained through both methods was observed in Subsection 5.1.2 (cf. Table 5.14 on page 80), except in Santa

Catarina (V) station's case. Also for this station, it is important to notice that the return level estimates are now higher compared to the ones obtained for Dataset II. The same happens with another station belonging to Class 4, Lugar de Baixo (X), and the only one here from Class 2, Santo da Serra (I). On the other hand, the estimates for Areeiro (A), Bica da Cana (B) and Funchal (U) datasets have lower values in the longer period of measurement. In the case of Santana (P), for any of the two methods, the estimates for either the 50– or 100–year return levels are very similar between the two periods.

5.2 Monthly and daily precipitation data – PORT and POT approaches

Early works in hydrology [124] usually assumed an exponential distribution for the excess over a high threshold. The option to model excesses over a high threshold relied on the idea that if additional information about the extreme upper tail were used, besides the annual maxima, then more accurate estimates would be obtained. Also, due to Pickands [171] it is well known that, under fairly general conditions, the excesses over a high threshold are generalised Pareto distributed, being the exponential distribution a sub-model of the generalised Pareto family. A milestone publication on the threshold approach was written by Davison and Smith in 1990 [38], where, among other developments, the authors review and extend ideas presented in - using the authors' own words - "cruder form" in the proceedings of the NATO–ASI conference on Statistical Extremes and Application [36, 195]. Besides considering the Pareto distribution the natural distribution for the exceedances over high thresholds, Davison and Smith [38] defended the use of this model in conjunction with regression techniques and extensions to treat the problem of having serially dependent and seasonal data. The handling of seasonal data series was a problem already addressed by Smith in 1984 as well as the problem of the threshold's choice [195]. For solving the latter one, Davison and Smith [38] introduced the application of the mean residual life plot. Nevertheless, in 1994, Davison [36] already remarks that a criterion for the statistical threshold choice should be based on the balance between having maximizing sample information on the extremes and ensuring the adequacy of the model's asymptotic approximation. So, any threshold choice is a bias versus variance trade-off since a value too high for a threshold u results in too few exceedances, and consequently high variance estimators, and a value too small for u results in biased estimators [61].

Similarly to the threshold's choice in a POT approach, the selection of the number k of upper order statistics in the PORT approach is a complex problem. Unlike the parametric methodology, where the fitting of a specific model with location, scale and shape parameters is needed, the only assumption in the semi parametric approach is that the distribution function F is in the domain of attraction of an extreme value distribution. In this last case only a parameter needs to be estimated, the extreme value index γ. The statistical methodologies associated to a semiparametric setup for the PORT approach received a major contribution from the research of Laurens de Haan and collaborators [88].

5.2.1 Statistical choice of extreme domains of attraction

In this subsection, the assumption that the distribution function F belongs to the domain of attraction of an extreme value distribution ($F \in \mathcal{D}(G_\gamma)$, for some $\gamma \in \mathbb{R}$) for monthly maximum precipitation data is tested for the rainy season (October to March). Also, the available data from each station is analysed in order to find the most suitable domain of attraction for the sampled distribution.

The dataset formed by the monthly maximum precipitation data for the rainy season from the seven weather stations maintained by IPMA, whose locations are displayed in Figure 5.14, will be called Dataset III. The altitude, the measurement period considered and the sample size (n) for each station is presented in Table 5.23.

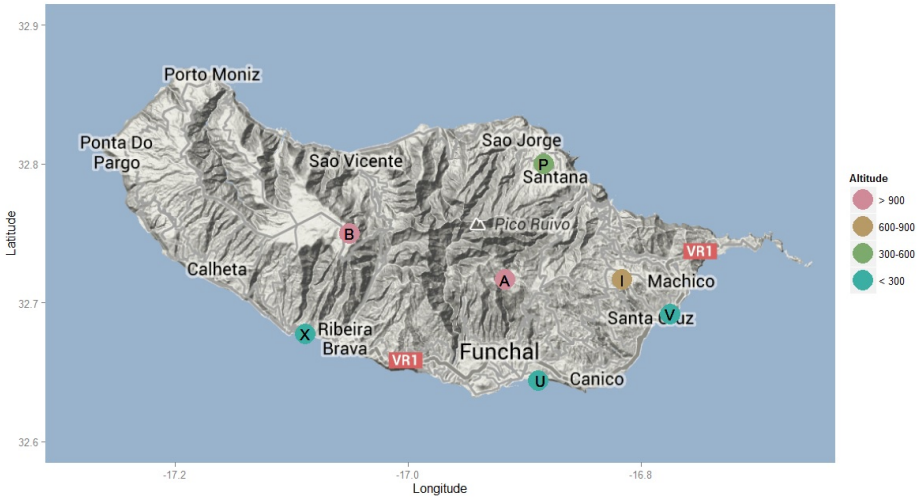

Figure 5.14: Location and altitude range of the rain gauge stations–Dataset III (Map data ©2014 Google).

Table 5.23: Dataset III: monthly maximum precipitation in the rainy season, October to March (source: IPMA).

Station	Altitude (m)	Period	n
Areeiro (A)	1610	1961–1993	196
Bica da Cana (B)	1560	1961–2009	286
Santo da Serra (I)	660	1970–2009	240
Santana (P)	380	1942–2007	382
Funchal (U)	58	1949–2009	366
Santa Catarina (V)	49	1961–2009	293
Lugar de Baixo (X)	15	1961–2004	264

The first step was to check, for each dataset, if the corresponding distribution function F could be considered as belonging to the domain of attraction of an extreme value distribution. To apply the test statistic $E_n(k)$ to the data from each station (cf. expression (4.12) in Section 4.2), the R program code provided by D. Li at www.imsv.unibe.ch/∼deyuan/research.html was used, taking $\eta = 2$, as suggested by Hüsler and Li [120]. The values of the test statistic $E_n(k)$ and its corresponding 0.95 quantile for varying k are shown in Figures 5.15 and 5.16. Table 5.24 shows possible values of k for which $F \in \mathcal{D}(G_\gamma)$, for some $\gamma \in \mathbb{R}$, is not rejected.

Table 5.24: Possible values for k for each location.

Station	Values of k
Areeiro (A)	$28 \leq k \leq 49$; $69 \leq k \leq 145$
Bica da Cana (B)	$12 \leq k \leq 194$
Santo da Serra (I)	$23 \leq k \leq 117$
Santana (P)	$8 \leq k \leq 21$; $23 \leq k \leq 111$; $113 \leq k \leq 179$
Funchal (U)	$22 \leq k \leq 245$
Santa Catarina (V)	$44 \leq k \leq 177$
Lugar de Baixo (X)	$k \leq 137$

This preliminary data analysis assumes that there exists an underlying distribution for the data in the attraction domain of some classical extreme value distribution, either Gumbel, Fréchet, or Weibull. Extreme value distributions arise assuming stability of the limiting distribution of suitably normalised independent and identical random variables. The restriction of the analysis to the six months period of the rainy season minimises the heterogeneity of the data, but does not

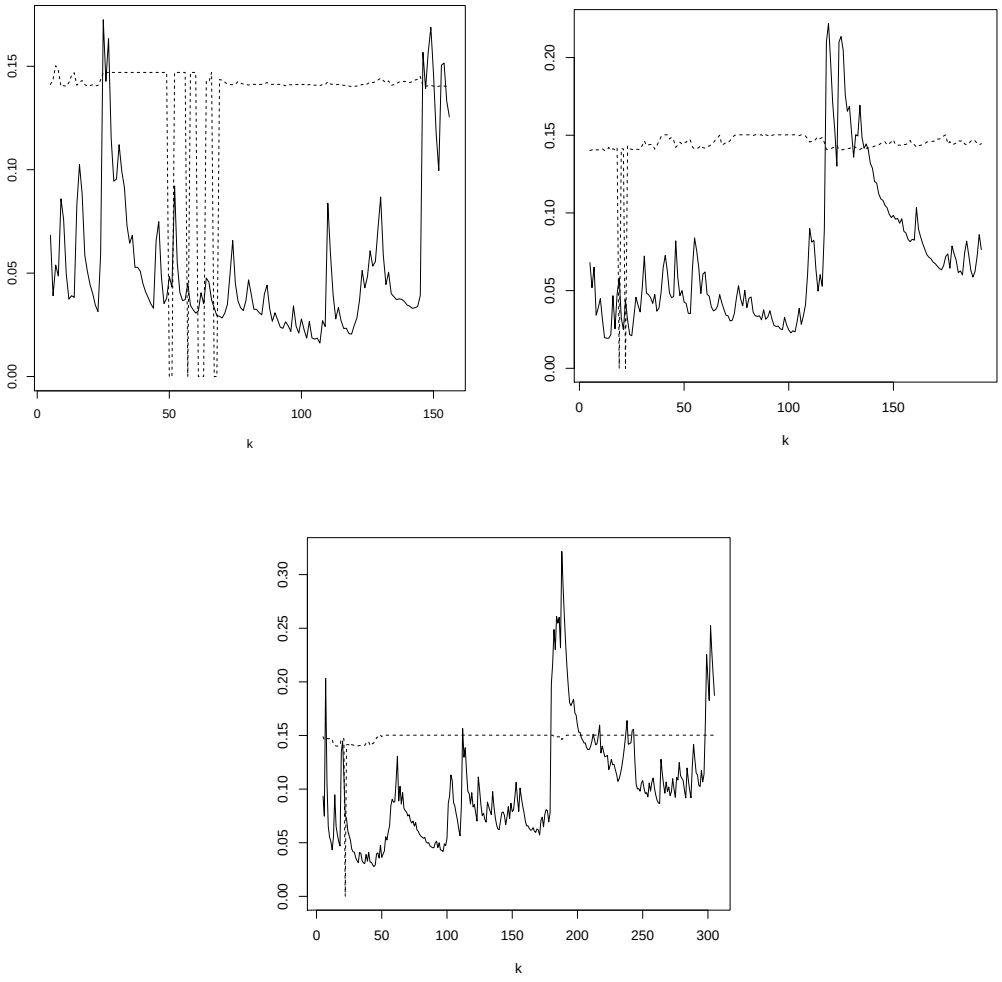

Figure 5.15: Values of the test statistic $E_n(k)$ (solid) and the 0.95 quantile (dotted) applied to the datasets from Areeiro (A) (up left), Santo da Serra (I) (up right) and Santana (P) (down) stations.

guarantee the homogeneity for Santana (P), Santa Catarina (V) and Santo da Serra (I) datasets according to the Anderson-Darling test [186]. The Anderson-Darling's test p–value for each station dataset, obtained by the application of function *adk.test* in the *adk* R language package [178], are displayed in Table 5.25. Table 5.25 also shows the corresponding p–value of the Kruskal-Wallis test, obtained by the application of function *kruskal.test* in the *stats* R language package [178].

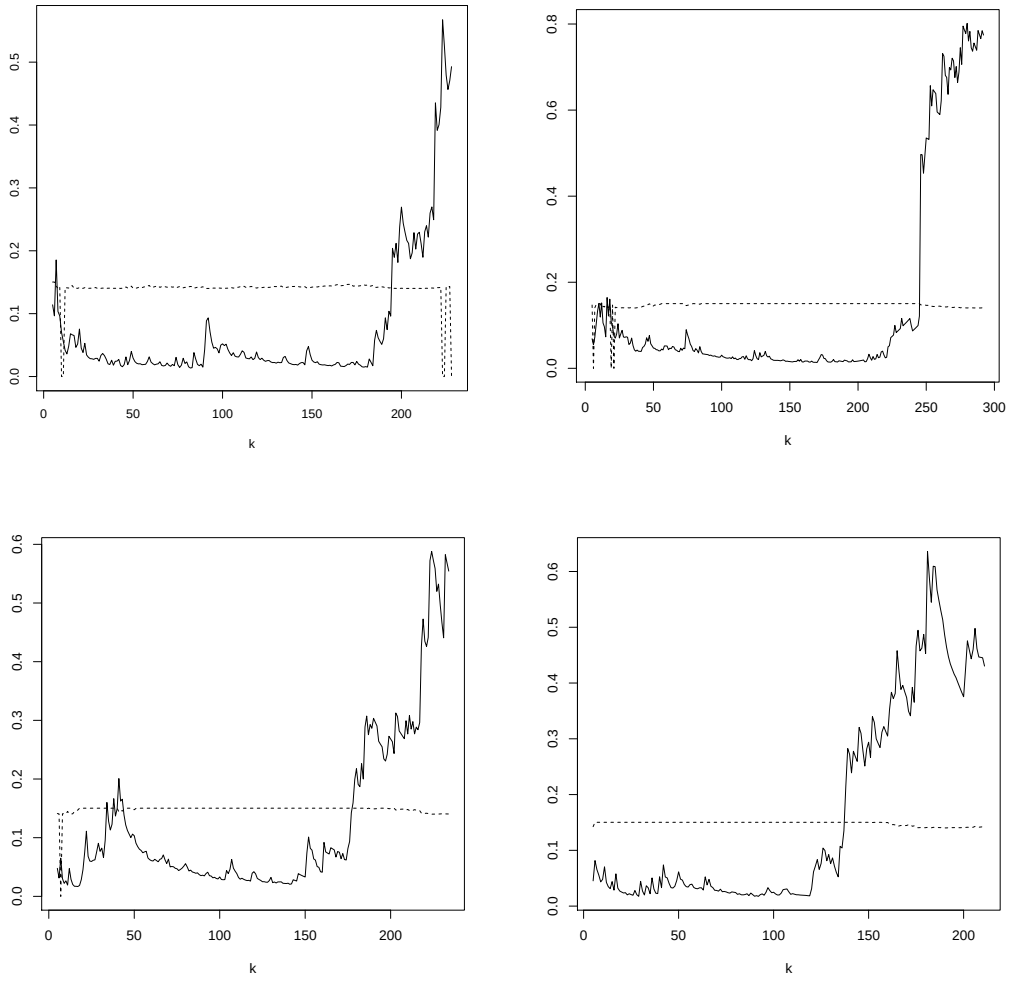

Figure 5.16: Values of the test statistic $E_n(k)$ (solid) and the 0.95 quantile (dotted) applied to the datasets from Bica da Cana (B) (up left), Funchal (U) (up right), Santa Catarina (V) (down left) and Lugar de Baixo (X) (down right) stations.

Although it can be observed that the null hypothesis that all samples come from populations with a common distribution was also rejected, at a 0.05 level of significance, for Santana (P) and Santa Catarina (V) stations when the Kruskal–Wallis test was applied, all datasets were included in the following analysis. Motivations for this procedure are given at the end of the present subsection.

The next step was to find the most suitable domain of attraction for the sampled distribution for each station dataset. The normalised Hasofer and Wang and the Greenwood type test statistics, $W_n^*(k)$ and $R_n^*(k)$, defined by (4.15) and (4.16) in Section 4.2, respectively, were implemented in R. The code of those statistics tests is presented in Appendix M. The application of test statistics $W_n^*(k)$ and $R_n^*(k)$

Table 5.25: Anderson-Darling and Kruskal-Wallis tests p–values.

Station	Anderson-Darling p–value	Kruskal-Wallis p–value
Areeiro (A)	0.1046	0.1341
Bica da Cana (B)	0.3043	0.3807
Santo da Serra (I)	0.0350	0.0514
Santana (P)	0.0005	0.0016
Funchal (U)	0.1636	0.1429
Santa Catarina (V)	0.0327	0.0158
Lugar de Baixo (X)	0.2096	0.2283

to the seven available datasets yielded the plots in Figures 5.17 and 5.18. For the values of k in the Table 5.24 the choice of the domains of attraction suggested by the test statistics $W_n^*(k)$ and $R_n^*(k)$ is presented in Table 5.26 for stations with altitude above 900 meters (Class 1) and between 600 meters and 900 meters (Class 2), and in Table 5.27 for stations with altitude between 300 meters and 600 meters (Class 3) and below 300 meters (Class 4).

Table 5.26: Statistical choice of domain of attraction (Classes 1 and 2).

Test\ Station id. letter	A	B	I
$W_n^*(k)$	Weibull	Weibull (some values of k)	Weibull (some values of k)
$R_n^*(k)$	Weibull	Weibull (some values of k)	Gumbel

Table 5.27: Statistical choice of domain of attraction (Classes 3 and 4).

Test\ Station id. letter	P	U	V	X
$W_n^*(k)$	Weibull (some values of k)	Weibull (some values of k)	Gumbel	Fréchet (some values of k)
$R_n^*(k)$	Gumbel	Gumbel	Gumbel	Gumbel

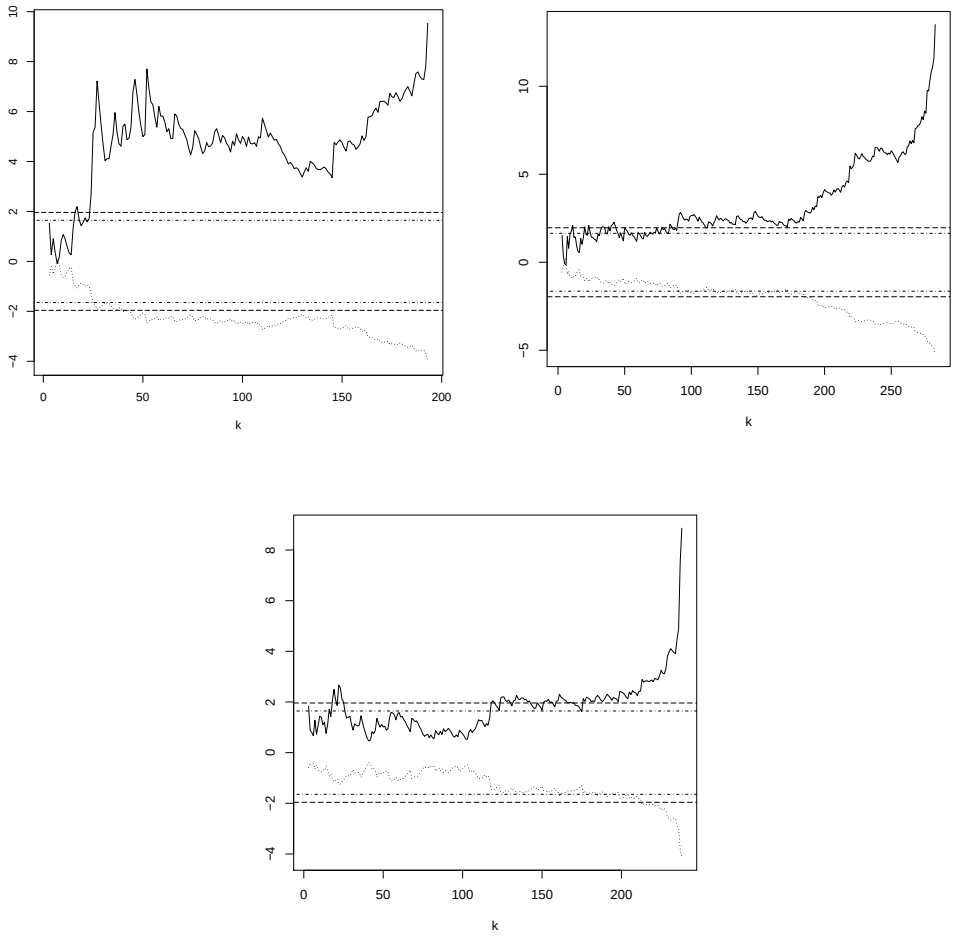

Figure 5.17: Values of the test statistics W_n^* (solid) and R_n^* (dotted) applied to the datasets from Areeiro (A) (up left), Bica da Cana (B) (up right) and Santo da Serra (I) (down) stations.

It can be observed that when the Weibull domain is suggested by the test statistic $W_n^*(k)$, the choice by the test statistic $R_n^*(k)$ can be the Gumbel domain or also the Weibull domain, but for fewer values of k. The difference between the test statistics was pointed out by Neves and Fraga Alves [159], who refer that the Greenwood type test barely detects small negative values of γ, and that the Hasofer and Wang's test is the most powerful test when analysing alternatives in the Weibull domain of attraction. It is important to emphasise again that the extreme value index γ is of primary interest in extreme value analysis and is the only parameter to be estimated when using a semiparametric approach. The estimation of γ is based on the k top order statistics of the sample and this analysis provide information about the region of k values to use for each location. Also it can be observed that for almost all

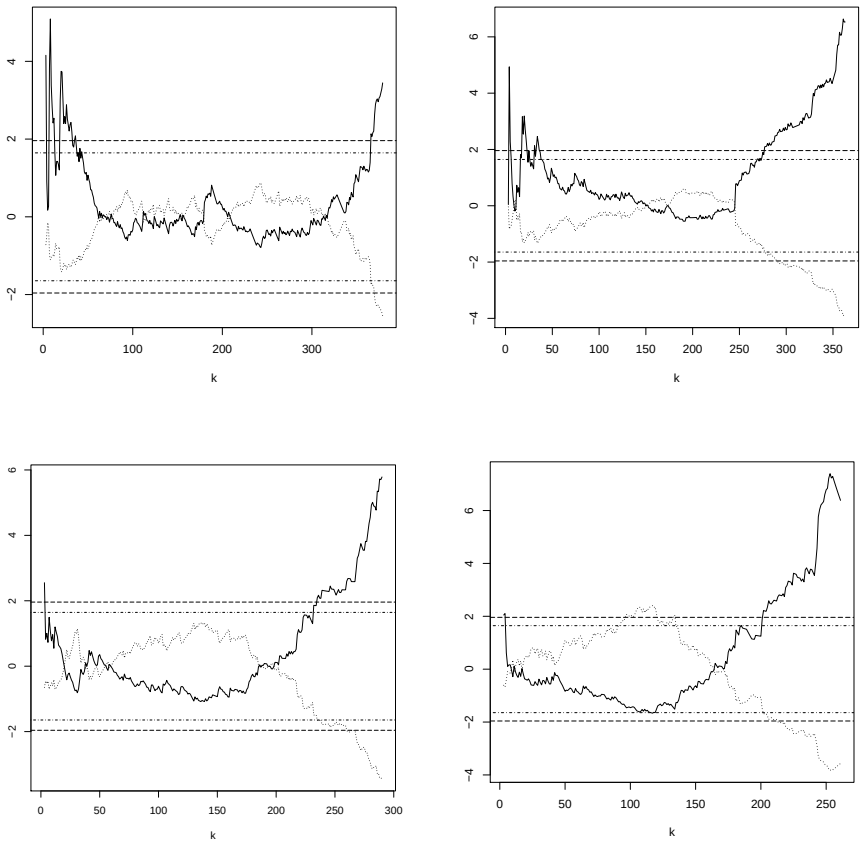

Figure 5.18: Values of the test statistics W_n^* (solid) and R_n^* (dotted) applied to the datasets from Santana (P) (up left), Funchal (U) (up right), Santa Catarina (V) (down left) and Lugar de Baixo (X) (down right) stations.

locations there is an evidence for non-positive values of the shape parameter for some values of k.

Although for three locations the identical distribution hypothesis was rejected, this does not invalidate the present analysis because much progress has been achieved in relaxing the independence and distributional identity assumptions. The distributional identity hypothesis has been relaxed by Mejzler [148, 149, 150, 151, 152] who described a class of limit laws which is the simile in extreme value theory to the Lévy–Khinchine's L class of self-decomposable laws. Observing that any univariate distribution is max-infinite divisible, Graça Martins and Pestana [97, 96] defined classes of distribution functions M_r, $r = 0, 1, \ldots$, M_0 being the class of all distribution functions, M_1 the Mejzler class, M_r, for $r > 1$, the class of the distribution functions F such that $G(x) = G(x + a)\, F_a(x)$, $\forall a > 0$ when $F_a \in M_{r-1}$

and $M_\infty = \bigcap_{r=0}^{\infty} M_r$, where $G = F$ if $\mathbb{R}$ is the support of the distribution function F, or a simple transformation whenever its support is a proper subset of the real line, cf. Galambos [76]. Mejzler's class can be characterised in terms of log-concavity of G. Analogously, Graça Martins and Pestana M_r classes may be characterised in terms of higher order monotonicity (fully described by Pestana and Mendonça [170]) of the corresponding G, and M_∞ in terms of complete monotonicity: $F \in M_\infty$ if and only the corresponding G satisfies $G(x) = \exp[-K(x)]$, with K completely monotone. Hence, M_∞ is a non-trivial extension of both the superclass of stable extreme value distributions for maxima, and a subclass of Mejzler's laws, that can provide a proper framework to analyse maxima of linearly transformed data arising from various parent distributions.

5.2.2 Threshold choice in a POT approach

The dataset analysed in this subsection, called Dataset IV, consists of daily precipitation data provided by the Madeira Civil Engineering Laboratory's Department of Hydraulics and Energy Technologies from the stations whose locations are shown in Figure 5.19.

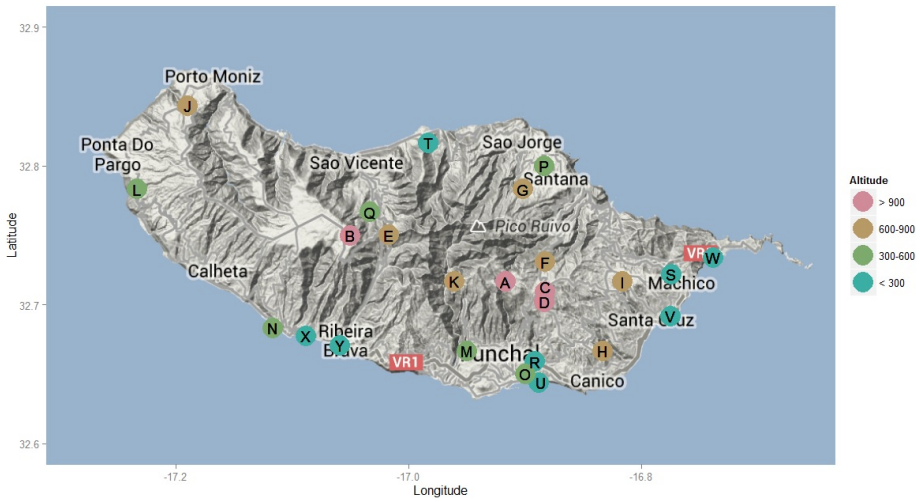

Figure 5.19: Location and altitude range of the rain gauge stations–Dataset IV (Map data ©2014 Google).

In the search for a threshold value for each one of these stations data, the first step taken was to analyse each mean residual life plot. By way of example, Figure 5.20 shows the obtained plots for Areeiro (A), Encumeada (E), Canhas (N) and Funchal (U) stations belonging to the Classes 1, 2, 3 and 4, respectively.

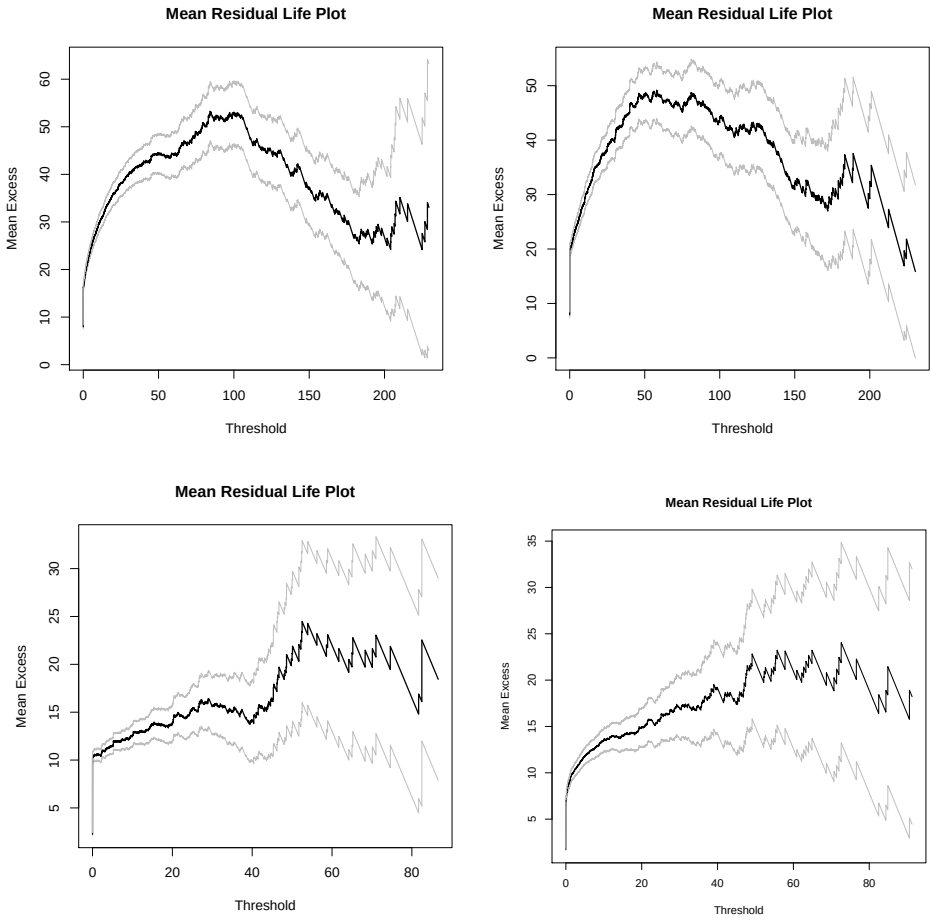

Figure 5.20: Mean residual plot for the Areeiro (A) (up left), Encumeada (E) (up right), Canhas (N) (down left) and Funchal (U) (down right) stations data.

For each one of these stations, the analysis of the mean residual life plot was complemented with the analysis of the corresponding parameter stability plots displayed in Figures 5.21 to 5.24. According to the description of these two graphical methods for choosing the threshold u presented in Subsection 4.2, u is such that the mean residual life plot should be approximately linear in u and the estimates of σ^* and γ should be approximately constant for the values greater than u_0 with $u > u_0$. According to Coles [26], the interpretation of a mean residual plot is not always simple in practice, being the interpretation of the corresponding plot from Areeiro (A) station an example of that. The graph appears to curve from $u = 0$ to $u \approx 50$, presenting beyond it an approximately linearity until $u \approx 80$, an plateau from this point to $u \approx 120$ and approximately linearity again after this value. However, analysing Figure 5.21, it can be observed that the estimates of σ^* and γ are approximately constant close to $u \approx 120$.

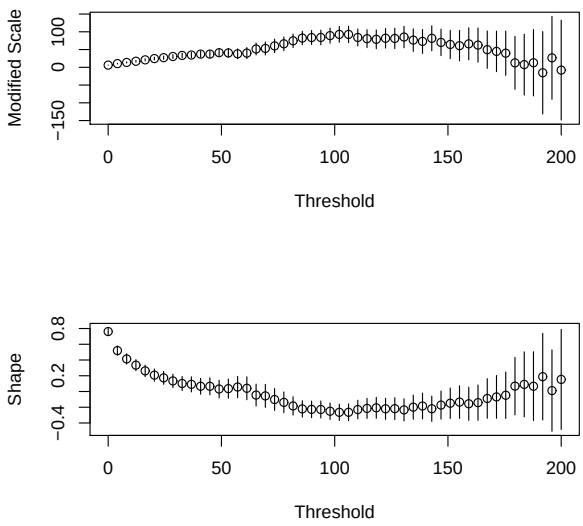

Figure 5.21: Parameter stability plots for the Areeiro (A) station data.

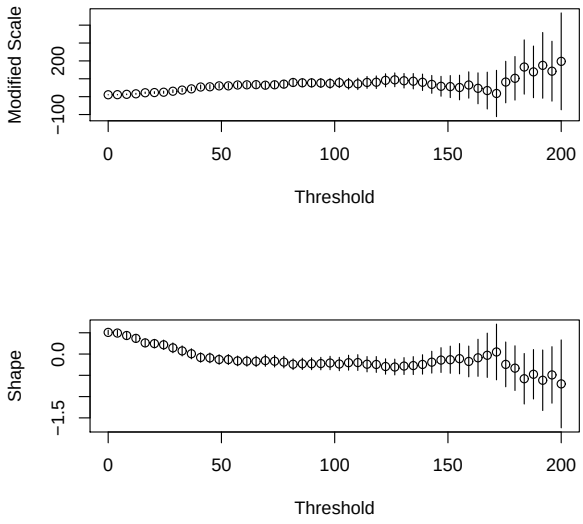

Figure 5.22: Parameter stability plots for the Encumeada (E) station data.

Therefore, ignoring the seasonality and the dependence in the data, an analysis was made to these plots corresponding to Areeiro (A) rain gauge station and, in this way a candidate value for a threshold, u_1, can be chosen. An analogously interpretation of the plots concerning Encumeada (E), Canhas (N) and Funchal (U) stations results in possible corresponding threshold values. Besides these plots, the mean residual plots and the parameter stability plots for all the rest of the stations

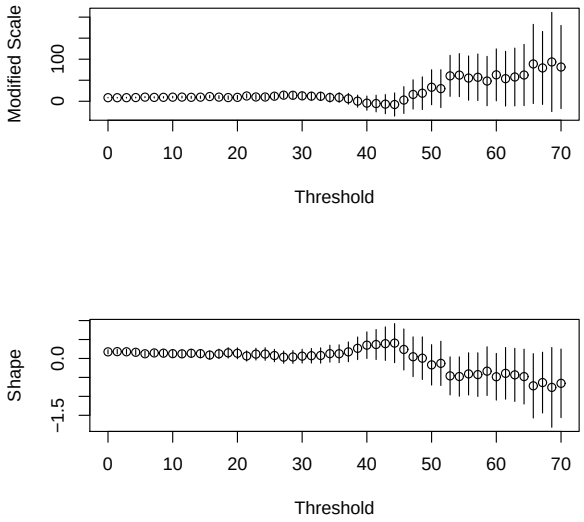

Figure 5.23: Parameter stability plots for the Canhas (N) station data.

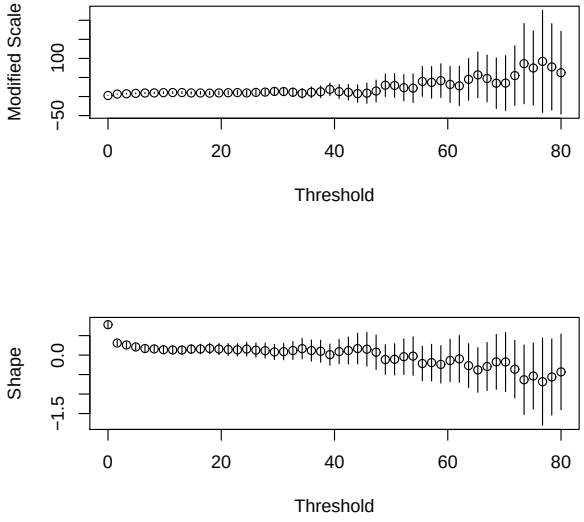

Figure 5.24: Parameter stability plots for the Funchal (U) station data.

in Classes 1, 2, 3 and 4 where also obtained and are displayed in Appendices H, I, J and K, respectively. Table 5.28 shows the resulting values of each station's plots interpretation and also the values for one other commonly used threshold, the smallest annual maximum of each sample, u_1. The values k_1 and k_2 correspond to the number of exceedances for u_1 and u_2, respectively.

Table 5.28: Two possible thresholds and the corresponding exceedance numbers.

Station	u_1	k_1	u_2	k_2
Areeiro (A)	101.0	135	120	107
Bica da Cana (B)	57.6	380	100	109
Poiso (C)	88.6	87	100	57
Montado do Pereiro (D)	80.0	179	110	58
Encumeada (E)	86.0	149	130	61
Ribeiro Frio (F)	77.8	174	100	97
Queimadas (G)	57.0	222	80	111
Camacha (H)	48.0	197	70	92
Santo da Serra (I)	40.2	304	80	87
Porto Moniz (J)	28.5	207	50	60
Curral das Freiras (K)	77.6	129	100	68
Ponta do Pargo (L)	38.6	76	50	42
Santo António (M)	25.4	275	50	72
Canhas (N)	43.0	70	30	123
Sanatório (O)	37.6	143	40	124
Santana (P)	43.5	158	60	91
Loural (Q)	40.0	284	80	94
Bom Sucesso (R)	33.2	107	40	65
Machico (S)	24.2	175	40	72
Ponta Delgada (T)	36.7	176	50	86
Funchal (U)	20.4	257	35	91
Santa Catarina (V)	30.2	81	40	43
Caniçal (W)	30.0	88	20	193
Lugar de Baixo (X)	20.0	233	30	106
Ribeira Brava (Y)	29.6	103	40	40

Notice that only for Canhas (N) and Caniçal (W) $u_1 > u_2$. Another commonly used rule-of-thumb threshold, besides the smallest annual maximum, is the value that, on average, is exceeded between 3 and 4 times in each year [179]. So, in a second step, the mean number of exceedances by year was calculated for the two already chosen threshold for each station data. The two mean values presented in Table 5.29, $\bar{v}_1$ and $\bar{v}_2$, correspond to the mean number of exceedances by year when u_1 and u_2 are chosen, respectively.

Table 5.29: Mean number of selected extremes by year for each threshold.

Station	$\bar{v}_1$	$\bar{v}_2$
Areeiro (A)	4.7	3.8
Bica da Cana (B)	12.7	3.8
Poiso (C)	4.0	3.0
Montado do Pereiro (D)	6.0	2.5
Encumeada (E)	7.1	3.2
Ribeiro Frio (F)	5.8	4.0
Queimadas (G)	7.4	3.7
Camacha (H)	6.6	3.7
Santo da Serra (I)	10.1	3.1
Porto Moniz (J)	9.4	3.2
Curral das Freiras (K)	5.6	3.4
Ponta do Pargo (L)	3.5	2.2
Santo António (M)	12.0	3.8
Canhas (N)	2.4	5.3
Sanatório (O)	4.8	4.1
Santana (P)	5.3	3.3
Loural (Q)	12.9	4.3
Bom Sucesso (R)	5.1	3.2
Machico (S)	8.3	3.8
Ponta Delgada (T)	5.9	3.0
Funchal (U)	8.3	3.5
Santa Catarina (V)	4.1	2.5
Caniçal (W)	4.2	8.8
Lugar de Baixo (X)	7.8	3.7
Ribeira Brava (Y)	4.7	2.0

The mean number of selected extremes by year for Poiso (C), Ponta do Pargo (L), Santa Catarina (V) and Caniçal (W) is around 3 or 4 when the smallest annual maximum is chosen for a threshold value. For the remaining stations, it can be observed that when the threshold is obtained by graphical observation, the mean number of selected extremes by year is around 3 or 4, being equal to 2.0 for Ribeira Brava (Y). It is also important to remark that both u_1 and u_2 could be chosen following the guidelines for using the mean residual and the parameter stability plots. For instance in the Areeiro (A) station's case, the existence of linearity in

the mean residual plot (cf. Figure 5.20 on page 98) might be considered at the right of both $u_1 = 101$ and $u_2 = 120$. Also, at these two values, the shape and the modified scale parameters seem to be in a plateau (cf. Figure 5.21 on page 99) comparing with other lower thresholds which can be considered to show bias–related curvature. Like for Areeiro (A) station, it can be observed what it seems to be an horizontal line for u_1 and a down straight line for u_2 in the mean residual plot of Encumeada (E) station data (cf. Figure 5.20). These somehow similar diagnostic plots for these two stations located in the interior of the island are quite different from the ones corresponding to the two stations located nearest to the sea, Canhas (N) and Funchal (U) (cf. Figure 5.20). For the station that belongs to Class 3, Canhas (N), there are different plateaus in the parameter stability plots for u_1 and u_2, and what it seems to be a down straight line for u_1 and a upper straight line for u_2 in the mean residual plot. For the Funchal (U) station's case, the shape and the modified scale parameters seem to be in the same plateau for both u_1 and u_2, and an approximately upper straight line before both u_1 and u_2 can be observed, but with wider intervals for the latter value. The interpretation of these diagnostic plots is considered a challenge with intrinsic subjectivity [26, 183], that often leads different threshold choices resulting in diverse tail behaviours. Scarrot and MacDonald [183] suggest an informal approach to this problem in which the sensitivity of the parameters and return levels estimates to the different threshold choices are evaluated.

The violation of the independence and distributional equality assumptions may also result into misleading diagnostic plots. The clustering of extreme values is observed in many applications. Sometimes it is sufficient to consider the cluster maxima, but other times the clusters time intervals and sizes of components excesses need to be considered too [36]. Also, according to Engeland et al. [62] the non-stationarity can, for instance, be accounted by subdividing the dataset into blocks that are considered to be homogeneous or, in an alternative approach, by letting the parameters in the GPD depend on time or on other covariates. The present analysis is not complete, but is an important step in the analysis following in what concerns non–stationarity. For the first approach to non–stationarity, the obtained results indicate that caution is needed when dividing each of the stations datasets. Indeed, the exceedances percentage by month for the both chosen thresholds displayed in Appendix L reveal that seasonality might not be the same for all locations. Although for all the stations with the exception of Bom Sucesso (R), the highest percentages belong to the rainy season (October to March), the difference is not so pronounced between some of these percentages and

the ones presented by others months like April or September for a few stations. These sample percentages support the observation made by Lang et al. [134] that the advantages of a seasonal approach may be lost when the division of the year into alleged homogeneous seasons is somehow slightly unreal. The second approach to non–stationarity mentioned by Engeland et al. [62] was applied, for example, in the papers by Smith [196] and Katz et al. [124], but unlike Katz et al. [124], Smith [196] does not assume any specific form of seasonal variation. On the other hand, Katz et al. [124] do not apply an initial declustering process. Indirectly using the POT approach, Katz et al. [124] fit to a time series of daily precipitation the GEV distribution that is fitted to the annual maxima by ML, assuming that these values of daily precipitation amount have a GEV distribution with parameters that can be written through sine waves depending on the day t within a given year. The application of the two mentioned approaches to non-stationarity to the Dataset IV, and the consequent comparison of results in terms of parameters and return levels estimates is postponed for future work.

5.3 Spatial annual maxima – Copula functions

A variety of statistical tools, such as copulas and spatial max-stable processes, have been used in the most recent decades for modelling spatial extreme data. A review of spatial extremes methods based on latent variables, copulas and spatial max-stable processes is presented by Davison et al. [37], who refer that appropriately chosen copula or max-stable models seem to be essential for the modelling of spatial extremes. The importance of max-stable processes and copula approaches for modelling spatial dependence is also emphasised by other authors such as Cooley et al. [31]. Although most of the studies on spatial extremes mentioned in the reviews cited above focus on modelling block maxima data, it is important to mention here that there are other studies (e.g., [185]) where these same methods are also applied to continuous time series of daily aggregated precipitation. The dependence between variables plays a central role in multivariate extremes. The ability to describe and model the dependence between variables, regardless of their marginal distribution functions, is the major advantage of the copula functions approach. In practice, the application of these functions to the data can be considered based on an estimate of a measure of association, for example, the Kendall's τ [156, 182].

In order to quantify this association in the case of Madeira island's extreme rainfall, an estimate for the Kendall's τ value is calculated, using the annual maxima

data from rain gauge stations maintained in the past by the General Council of the Autonomous District of Funchal. Thus, for each pair (X, Y), where X and Y correspond to the maxima annual dataset obtained in the stations identified by the same letters, the independence was analysed through the application of a test based on the empirical version of Kendall's τ association measure [81]. In a second stage of the study, groups of three stations, with the ones for which the independence was rejected at the significance level of $\alpha = 0.01$. Then, the estimated values of Kendall's τ measure of association from each pair were used to determine the coefficients of the extreme value copula C defined by (4.31) in Section 4.3 of the Methodology. Since the regarded stations do not have the same measurement period, the maxima annual datasets were divided into three subsets according to the different periods. The highest values of annual daily precipitation on the island of Madeira, in the period of 1950–1980, that will be termed by Dataset V, come from 12 stations, namely, Areeiro (A), Bica da Cana (B), Montado do Pereiro (D), Ribeiro Frio (F), Queimadas (G), Camacha (H), Santo da Serra (I), Sanatório (O), Santana (P), Ponta Delgada (T), Funchal (U) and Lugar de Baixo (X) stations. Dataset VI corresponds to the shorter period 1950–1972 and includes Porto Moniz (J), Curral das Freiras (K), Ponta do Pargo (L), Santo António (M), Canhas (N), Loural(Q) and Ribeira Brava (Y) stations. Finally, Dataset VII will consist of the 12 stations of the Dataset V and Poiso (C), Encumeada (E), Bom Sucesso (R), Machico (S), Santa Catarina (V) and Caniçal (W) stations. Besides the better coverage of Madeira Island naturally obtained by an increase of the number of rain gauge stations, Datasets VI and VII add information to the study because two regions of the island not considered in the analysis made with Dataset V are included. More precisely, with the data from Porto Moniz (J) and Ponta do Pargo (L) stations the region further west of the island is included in the study performed with Dataset VI, while the region further east is covered when the data coming from Machico (S), Santa Catarina (V) and Caniçal (W) stations included in Dataset VII is considered.

The analysis corresponding to Dataset V led to 17 groups of three pairwise associated stations, while the analysis made to Datasets VI and VII originated 40 and 16 groups, respectively. These differences between the studies of Datasets V, VI and VII visible in terms of number of groups are even more pronounced since there is no group common to these three analysis among the ones formed by three stations with measurement period ranging from 1950 to 1980. For the period 1950–1972, 34 of the groups include one or more rain gauge stations of the seven extra stations considered relatively to the wider period, being the remaining six groups

formed by common stations to both periods. All of these six groups are present in both of these periods, with the exception of the group formed by Sanatório (O), Santana (P) and Funchal (U), that is present exclusively in this period. This group and none of the remaining five groups are observed in the period 1959–1980. On the other hand, in the later period, there are six groups formed entirely by stations that are common to the three periods of measurement which present the particularity of being only observed in this period. Nevertheless, there is as well one common group between the periods 1959–1980 and 1950–1980, which is the one formed by Montado do Pereiro (D), Camacha (H) and Santo da Serra (I) rain gauge stations. For this group and for each of the groups obtained, an adjustment to a family of extreme value copulas involving the Marshall–Olkin family was made by determining the parameters β_i, with $i \in \{1, 2, 3\}$ that define the extreme value copula C. These values and all the remaining results obtained in the analysis of Datasets V, VI and VII are presented, respectively, in the following Subsections 5.3.1, 5.3.2 and 5.3.3.

5.3.1 Dataset V

The dataset used in this subsection corresponds to the highest values of annual daily precipitation on the island of Madeira, in the period of 1950–1980, and is termed as Dataset V. In Figure 5.25, the location of each station considered is represented by a circle with its identification letter and colour corresponding to the respective altitude class. Besides this information, the island slope where the station is located is also indicated in Table 5.30, 1 denoting the northern slope and 2 the southern one.

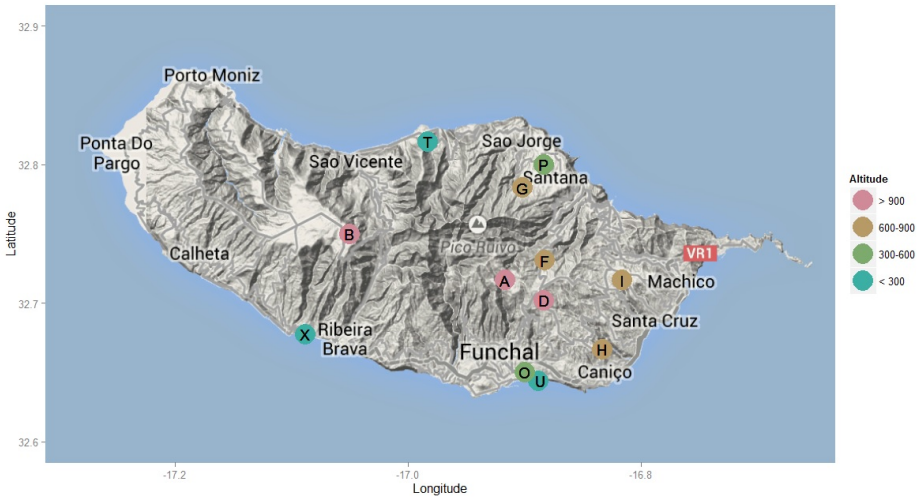

Figure 5.25: Location and altitude range of the rain gauge stations–Dataset V (Map data ©2014 Google).

Table 5.30: Information about the rain gauge stations–Dataset V.

Station	Latitude	Longitude	Altitude (m)	Slope
Areeiro (A)	32°43'N	16°55'W	1610	2
Bica da Cana (B)	32°45'N	17°03'W	1560	1
Montado do Pereiro (D)	32°42'N	16°53'W	1260	2
Ribeiro Frio (F)	32°43'N	16°53'W	874	2
Queimadas (G)	32°46'N	16°54'W	860	1
Camacha (H)	32°40'N	16°50'W	680	2
Santo da Serra (I)	32°43'N	16°49'W	660	2
Sanatório (O)	32°39'N	16°54'W	380	2
Santana (P)	32°48'N	16°53'W	380	1
Ponta Delgada (T)	32°49'N	16°59'W	136	1
Funchal (U)	32°38'N	16°53'W	58	2
Lugar de Baixo (X)	32°40'N	17°05'W	15	2

For all the pairs formed by the 12 stations considered in this subsection, the estimates of Kendall's τ association measure, $\tau_n^{X,Y}$, and their independence tests p–values were determined through the use of the *VineCopula* R language package [178]. The obtained values for each station in Classes 1 and 2 are displayed in Table 5.31, while Table 5.32 shows the respective values for the ones belonging to Classes 3 and 4. The pairs formed by the stations of Classes 1 and 2 with the ones in Classes 3 and 4 are presented in Table 5.33. All tables show the values of $\tau_n^{X,Y}$ above the corresponding p-values in brackets.

Table 5.31: Kendall's τ estimates and p–values in brackets (Classes 1 and 2)–Dataset V.

A	B	D	F	G	H	I
A	0.04	0.25	0.14	0.27	**0.33**	-0.02
	(0.77)	(0.05)	(0.28)	(0.03)	(**0.01**)	(0.91)
	B	0.29	**0.35**	**0.33**	0.25	0.29
		(0.02)	(**0.00**)	(**0.01**)	(0.05)	(0.02)
		D	**0.40**	0.15	**0.49**	**0.35**
			(**0.00**)	0.23	(**0.00**)	(**0.01**)
			F	0.15	**0.32**	0.18
				(0.23)	(**0.01**)	0.16
				G	0.12	0.28
					(0.33)	(0.03)
					H	**0.36**
						(**0.00**)

Table 5.32: Kendall's τ estimates and p–values in brackets (Classes 3 and 4)–Dataset V.

O	P	T	U	X
O	0.25	0.25	**0.51**	**0.39**
	0.05	0.05	(**0.00**)	(**0.00**)
	P	**0.31**	**0.54**	**0.40**
		(**0.01**)	(**0.00**)	(**0.00**)
		T	0.23	**0.33**
			(0.07)	(**0.01**)
			U	**0.42**
				(**0.00**)

Table 5.33: Kendall's τ estimates and p–values in brackets (Classes 1 and 2 with Classes 3 and 4)–Dataset V.

	O	P	T	U	X
A	0.06	0.19	0.29	0.16	0.16
	(0.62)	(0.13)	(0.02)	(0.21)	(0.21)
B	0.16	0.22	0.29	0.27	0.23
	(0.21)	(0.09)	(0.03)	(0.07)	(0.06)
D	**0.37**	0.18	**0.38**	**0.32**	**0.38**
	(**0.00**)	(0.16)	(**0.00**)	(**0.01**)	(**0.00**)
F	0.27	0.14	0.20	0.23	0.26
	(0.03)	(0.28)	(0.12)	(0.07)	(0.04)
G	0.11	0.18	**0.32**	0.06	0.03
	(0.37)	(0.15)	(**0.01**)	(0.62)	(0.83)
H	**0.45**	0.25	0.29	**0.42**	**0.43**
	(**0.00**)	(0.05)	(0.02)	(**0.00**)	(**0.00**)
I	**0.31**	0.29	0.25	0.23	0.20
	(**0.01**)	(0.02)	(0.05)	(0.06)	(0.11)

The station that is at the highest altitude, Areeiro (A), is not associated with any of the two other stations in Class 1, but it forms a pair of associated stations with Camacha (H) station which belongs to Class 2. Likewise, the remaining stations in Class 1, Bica da Cana (B) and Montado do Pereiro (D), are not associated with each other but both are with a station in Class 2, namely Ribeiro Frio (F). Although with a inferior value for τ_n, Bica da Cana (B) is also associated with Queimadas (G), a station that is located in the northern part of Madeira island and a closer distance ($d_{B,F} \approx 15808$ m and $d_{B,G} \approx 14304$ m). It is important to notice that for Ribeiro Frio (F) and Santo da Serra (I) stations the hypothesis

of independence of the corresponding data sets is not rejected at a 0.01 significance level although the proximity between these two stations ($d_{I,F} \approx 6421$ m) is smaller than the one between the associated Santo da Serra (I) and Santana (P) stations ($d_{I,P} \approx 11158$ m). The hypothesis of independence is also not rejected for the even closer stations Santana (P) and Queimadas (G) ($d_{G,P} \approx 2615$ m), that are both located in the northern part of the island. Santana (P) station forms with Funchal (U) station the pair that presents the higher Kendall's τ empirical value. Despite their proximity to the sea, Santana (P) and Funchal (U) are located in different slopes and the distance between them is higher than the one between Santana (P) and Ponta Delgada (T) stations that present a much smaller value of τ_n ($\tau_n^{P,T} = 0.31$). This value is even smaller than the ones presented by the pairs formed by these stations and another station closer to the sea but in the opposite slope, namely Lugar de Baixo (X). Besides this group of three stations, Santana (P) forms with Funchal (U) and Lugar de Baixo (X) another group of pairwise associated stations formed by a station in Class 3 and two others in Class 4. The second highest estimate for Kendall's τ is presented by the pair formed by Sanatório (O) and Funchal (U) stations ($\tau_n^{O,U} = 0.51$), that are located in different altitudes but very close to each other ($d_{O,U} = 1328$ m). These two stations also show a statistically significant concordance with Lugar de Baixo (X) station, forming a group of pairwise associated stations located near the sea. Sanatório (O), Funchal (U) and Lugar de Baixo (X) stations are all in association with Montado do Pereiro (D) and Camacha (H) stations, which belong to different classes of altitude and are located farther way of the sea. These two stations form the pair of associated stations with the third highest value for τ_n observed in Dataset V, being both also associated with Ribeiro Frio (F) and Santo da Serra (I) stations.

In short, Tables 5.34 and 5.35 show all the groups formed by three pairwise associated stations ($s_1 - s_2 - s_3$), the corresponding parameters β_i of the extreme value copula C defined by (4.31) in Section 4.3 of the Methodology, and the distances between stations within each group ($(d_{1,2}, d_{1,3}, d_{2,3})$, where $d_{i,j}$ stands for the distance in m between stations s_i and s_j – cf. Tables 3.1–3.3). Table 5.34 shows all the groups including Montado do Pereiro (D) (set 1), being the remaining groups (set 2) displayed in Table 5.35. All the results presented were obtained using functions that were implemented in R, whose corresponding code is presented in Appendix M.

Table 5.34: Groups in set 1, distances between stations (m) and parameters β_1, β_2 and β_3–Dataset V.

Group	$s_1 - s_2 - s_3$	$(d_{1,2}, d_{1,3}, d_{2,3})$	β_1	β_2	β_3
1	D–F–H	$(3242, 6170, 8515)$	0.8279	0.4363	0.5456
2	D–H–I	$(6170, 6538, 5761)$	0.6410	0.6753	0.4353
3	D–H–O	$(6170, 6016, 6528)$	0.5680	0.7811	0.5149
4	D–H–U	$(6170, 6558, 5778)$	0.5284	0.8708	0.4479
5	D–H–X	$(6170, 19379, 23933)$	0.5976	0.7313	0.5107
6	D–I–O	$(6358, 6016, 10762)$	0.5999	0.4566	0.4912
7	D–O–U	$(6016, 6558, 1326)$	0.4109	0.7879	0.5912
8	D–O–X	$(10762, 19379, 17907)$	0.5305	0.5502	0.5726
9	D–T–X	$(15815, 19379, 18291)$	0.5491	0.7138	0.6411
10	D–U–X	$(6558, 19379, 19104)$	0.4571	0.5162	0.6926

Table 5.35: Groups in set 2, distances between stations (m) and parameters β_1, β_2 and β_3–Dataset V.

Group	(s_1, s_2, s_3)	$(d_{1,2}, d_{1,3}, d_{2,3})$	β_1	β_2	β_3
1	H–I–O	$(5761, 6528, 10762)$	0.7209	0.4183	0.5449
2	H–O–U	$(6528, 5778, 1326)$	0.5491	0.7138	0.6411
3	H–O–X	$(6528, 23933, 17907)$	0.6703	0.5779	0.5453
4	H–U–X	$(5778, 23933, 19104)$	0.6014	0.5820	0.6014
5	O–U–X	$(1326, 17907, 19104)$	0.6361	0.7200	0.5020
6	P–T–X	$(9549, 23514, 18291)$	0.5412	0.4205	0.6052
7	P–U–X	$(17321, 23514, 19104)$	0.6732	0.7318	0.4964

The event $E_q = \{X_1 > x_{1,q}, X_2 > x_{2,q}, X_3 > x_{3,q}\}$, where X_i denote the observation at the i–th rain gauge station and $x_{i,q}$ the $(1-q)$–quantile of X_i, with $q \in (0,1)$ and $i \in \{1,2,3\}$, is an event of practical interest. For $q = 0.98$ and $q = 0.99$, the probability $p_q = P(E_q)$ (cf. (4.44) in Section 4.3 of the Methodology) and the corresponding return period $r_q = 1/p_q$ were calculated for each one of the groups in set 1 (Table 5.36) and in set 2 (Table 5.37).

For the groups in set 1, the lowest and highest return periods were obtained for the stations of Groups 9 and 7, respectively. Group 7 is formed by the three stations that are closer to each other among the ones considered, being all located in the southern part of the island. Group 9 includes two stations in Class 4 that are located near the sea although in different slopes of the island, being distant from

the other station of the group which belongs to Class 1. Besides the Group 9, only the Groups 3, 5 and 8 present values below 100 years for $r_{0.98}$ and 200 years for $r_{0.99}$.

Table 5.36: Return periods in years, $r_{0.98}$ and $r_{0.99}$, and associated probabilities for the groups in set 1–Dataset V.

Group	$s_1 - s_2 - s_3$	$p_{0.98}$	$r_{0.98}$	$p_{0.99}$	$r_{0.99}$
1	D–F–H	0.00880	113.62	0.00438	228.22
2	D–H–I	0.00880	113.60	0.00438	228.46
3	D–H–O	0.01036	96.53	0.00516	193.64
4	D–H–U	0.00903	110.78	0.00500	222.42
5	D–H–X	0.01028	97.25	0.00512	195.16
6	D–I–O	0.00919	108.80	0.00458	218.32
7	**D–O–U**	**0.00831**	**120.33**	**0.00413**	**242.02**
8	D–O–X	0.01066	93.77	0.00532	188.02
9	**D–T–X**	**0.01105**	**90.50**	**0.00551**	**181.57**
10	D–U–X	0.00921	108.62	0.00459	218.02

Table 5.37: Return periods in years, $r_{0.98}$ and $r_{0.99}$, and associated probabilities for groups in set 2–Dataset V.

Group	(s_1, s_2, s_3)	$p_{0.98}$	$r_{0.98}$	$p_{0.99}$	$r_{0.99}$
1	**H–I–O**	**0.00844**	**118.40**	**0.00420**	**237.94**
2	H–O–U	0.01105	90.50	0.00551	181.57
3	H–O–X	0.01096	91.22	0.00547	182.91
4	**H–U–X**	**0.01169**	**85.52**	**0.00583**	**171.44**
5	O–U–X	0.01012	98.84	0.00504	198.44
6	P–T–X	0.00849	117.81	0.00422	236.72
7	P–U–X	0.01001	99.85	0.00499	200.58

For the groups in set 2, it is a group formed by one station in Class 2, one in Class 3 and other in Class 4 that presents the lowest return periods. This group is formed by Lugar de Baixo (X) and two stations that are closer to each other than to this station, but are located at very different altitudes, Camacha (H) and Funchal (U) stations. This group is the only one in set 2 that present values below 90 years for $r_{0.98}$ and 180 years for $r_{0.99}$. It can be observed that Camacha (H) station also belongs to the Group 1, the one that presents the highest return periods among the groups in set 2. This group includes two more southern stations, Santo da Serra (I)

and Sanatório (O), which belong to Class 2 and 3, respectively. Group 6 presents lower but very similar return period values, although being formed by three stations more far apart than the ones in Group 1, being two of them located in the northern part of the island. These two groups are the only ones in set 2 with values above 110 years for $r_{0.98}$ and 230 years for $r_{0.99}$.

5.3.2 Dataset VI

The dataset used in this subsection, termed as Dataset VI, is composed by the highest values of annual daily precipitation on the island of Madeira, in the shorter period of 1950–1972, coming from 19 rain gauge stations. In this period, besides the 12 stations in the previous subsection, seven more stations are considered: two from Class 2 (Porto Moniz (J) and Curral das Freiras (K)), four from Class 3 (Ponta do Pargo (L), Santo António (M), Canhas (N) and Loural (Q)) and one from Class 4 (Ribeira Brava (Y)). In Figure 5.26, the location of each station considered is represented by a circle with its identification letter and colour corresponding to the respective altitude class. For the seven rain gauge stations belonging exclusively to this dataset, Table 5.38 shows their latitude, longitude, altitude and the island slope where they are located, 1 denoting the northern slope and 2 the southern one, as before.

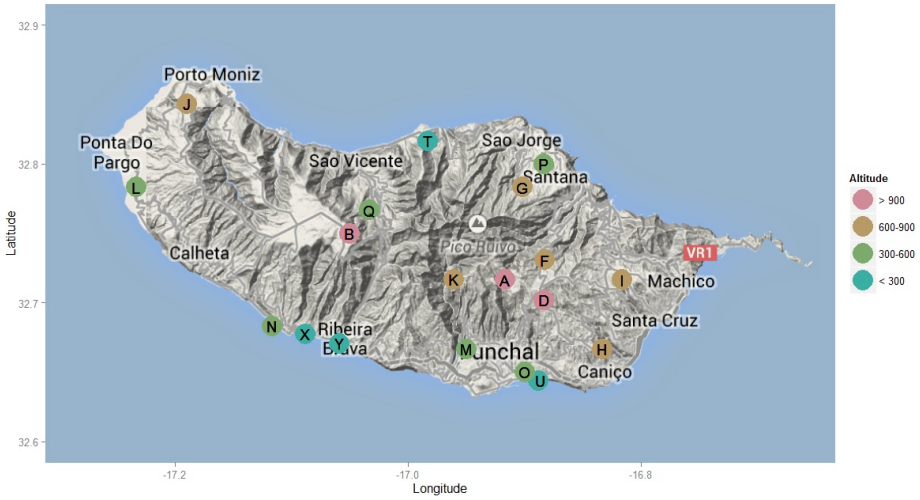

Figure 5.26: Location and altitude range of the rain gauge stations–Dataset VI (Map data ©2014 Google).

Table 5.38: Information about the seven rain gauge stations belonging exclusively to Dataset VI.

Station	Latitude	Longitude	Altitude (m)	Slope
Porto Moniz (J)	32°50'N	17°11'W	653	1
Curral das Freiras (K)	32°43'N	16°58'W	650	2
Ponta do Pargo (L)	32°47'N	17°14'W	570	2
Santo António (M)	32°40'N	16°57'W	525	2
Canhas (N)	32°41'N	17°07'W	425	2
Loural (Q)	32°46'N	17°02'W	307	1
Ribeira Brava (Y)	32°40'N	17°04'W	10	2

As in the previous subsection, for all pairs formed by the stations considered in this subsection, the values of the Kendall's τ association measure, $\tau_n^{X,Y}$, and their independence tests p-values were determined through the use of the *VineCopula* R language package [178]. The obtained values for each station in Classes 1 and 2 are displayed in Table 5.39, while Table 5.40 shows the values for the ones that are in Classes 3 and 4. The pairs formed by the stations of Classes 1 and 2 with the ones in Classes 3 and 4 are presented in Table 5.41. All tables show the values of $\tau_n^{X,Y}$ above the corresponding p-values in brackets.

In the following analysis, the identification of the dataset considered will be added as a subscript when a comparison between obtained values in different datasets shows itself to be relevant. For example, $\tau_{n,VI}^{X,Y}$ will refer to the estimate of the Kendall's τ association between stations X and Y when considering Dataset VI. Despite the high distance between them ($d_{J,K} \approx 25618$ m), Porto Moniz (J) station is only associated with one other station that belongs to the same class of altitude, namely Curral das Freiras (K) station. The latter one is also associated with Bica da Cana (B), a nearest station located in Madeira island's orographic barrier, but at a higher altitude. Like in the period analysed in the previous subsection, there is here also a statistically significant association between Bica da Cana (B) and Ribeiro Frio (F) although with a higher value for the empirical version of the Kendall's τ association measure ($\tau_{n,V}^{B,F} = 0.35$ and $\tau_{n,VI}^{B,F} = 0.48$). Conversely, Montado do Pereiro (D) and Camacha (H) stations form a pair of associated stations that present a lower estimate of τ_n when the shorter period is considered ($\tau_{n,V}^{D,H} = 0.49$ and $\tau_{n,VI}^{D,H} = 0.45$). The stations in this pair are also associated with Sanatório (O) and Funchal (U) stations in Class 4 likewise as in the period 1950–1980, presenting other associations with two stations only considered in this period, namely Santo António (M) and

Loural (Q) stations.

Table 5.39: Kendall's τ estimates and p–values in brackets (Classes 1 and 2)–Dataset VI.

A	B	D	F	G	H	I	J	K
A	0.08	0.17	0.12	0.29	0.31	-0.03	0.04	0.05
	(0.62)	(0.26)	(0.41)	(0.05)	(0.04)	(0.85)	(0.81)	(0.73)
	B	0.34	**0.48**	0.23	0.21	0.12	0.20	**0.44**
		(0.02)	(**0.00**)	(0.12)	(0.16)	(0.41)	(0.18)	(**0.00**)
		D	**0.45**	0.15	**0.45**	0.36	0.26	0.22
			(**0.00**)	(0.98)	(**0.00**)	(0.02)	(0.08)	(0.15)
			F	0.06	0.30	0.15	**0.39**	0.34
				(0.69)	(0.04)	(0.33)	(**0.00**)	(0.02)
				G	-0.07	0.15	0.04	0.13
					(0.65)	(0.33)	(0.81)	(0.38)
					H	0.26	0.12	0.12
						(0.08)	(0.41)	(0.41)
						I	0.05	-0.04
							(0.73)	(0.77)
							J	**0.45**
								(**0.00**)

Santo António (M) and Loural (Q) stations are also in concordance with a station located at a lower altitude and closer to the sea, Ribeira Brava (Y), being the pair Q–Y the one that shows the highest value of Kendall's τ in the present period ($\tau_{n,VI}^{Q,Y} = 0.71$). Ribeira Brava (Y) station also belongs to the pair with the second highest value for τ_n, namely the pair Canhas (N)–Ribeira Brava (Y). The two pairs with the third highest estimate of Kendall's τ are formed by two stations also belonging exclusively to Dataset VI, Canhas (N) and Loural (Q), and by two stations already considered in the previous subsection, Sanatório (O) and Funchal (U), showing here a higher value for τ_n ($\tau_{n,V}^{O,U} = 0.51$ and $\tau_{n,VI}^{O,U} = 0.64$).

Although with a higher estimate for τ_n in the larger period, Santana (P) and Funchal (U) stations are also associated here. Among the pairs of stations that are associated with each other both here and in the previous subsection, there is only one other pair, D–H, that, like the pair P–U, has now a lower estimate for τ_n ($\tau_{n,VI}^{D,H} - \tau_{n,V}^{D,H} = 0.45 - 0.49 = -0.04$ and $\tau_{n,VI}^{P,U} - \tau_{n,V}^{P,U} = 0.37 - 0.54 = -0.17$).

Table 5.40: Kendall's τ estimates and p–values in brackets (Classes 3 and 4)–Dataset VI.

L	M	N	O	P	Q	T	U	X	Y
L	0.32	0.22	0.07	0.22	0.05	-0.07	0.12	0.04	0.14
	(0.03)	(0.15)	(0.65)	(0.15)	(0.73)	(0.65)	(0.41)	(0.81)	(0.36)
	M	**0.38**	0.24	0.26	**0.44**	0.12	0.28	0.16	**0.44**
		(**0.01**)	(0.11)	(0.08)	(**0.00**)	(0.41)	(0.06)	(0.28)	(**0.00**)
		N	**0.39**	**0.48**	**0.64**	0.24	**0.42**	0.23	**0.65**
			(**0.01**)	(**0.00**)	(**0.00**)	(0.11)	(**0.01**)	(0.12)	(**0.00**)
			O	**0.38**	**0.45**	0.17	**0.64**	0.34	**0.47**
				(**0.01**)	(**0.00**)	(0.26)	(**0.00**)	(0.02)	(**0.00**)
				P	**0.47**	**0.49**	**0.37**	**0.50**	**0.42**
					(**0.00**)	(**0.00**)	(**0.01**)	(**0.00**)	(**0.01**)
					Q	0.33	**0.45**	0.21	**0.71**
						(0.03)	(**0.00**)	(0.16)	(**0.00**)
						T	0.21	**0.49**	0.21
							(0.16)	(**0.00**)	(0.16)
							U	0.22	**0.48**
								(0.15)	(**0.00**)
								X	0.19
									(0.21)

Although Canhas (N) and Sanatório (O) belong to the same altitude class and are located in the same slope of the island, at similar distances from the sea, these two stations have a lower estimate for the Kendall's τ association measure ($\tau_n^{N,O} = 0.39$) when compared to the pair of stations Canhas (N)–Santana (P), ($\tau_n^{N,P} = 0.48$) that are located in different slopes of the island and at very different distances from the sea. It can be observed that these four southern stations, Canhas (N), Sanatório (O), Funchal (U) and Ribeira Brava (Y), with two northern stations, Santana (P) and Loural (Q), form 20 groups of three pairwise associated stations. One of these groups is formed by the stations Canhas (N), Loural (Q) and Ribeira Brava (Y) which also show a statistically significant concordance with Santo António (M) a station located farther way. It is important to notice that here, and contrary to what it was observed in the period 1950-1980, for Sanatório (O) and Santana (P) stations the hypothesis of independence of the corresponding data sets is rejected at a 0.01 significance level ($\tau_{n,V}^{O,P} = 0.25$ and $\tau_{n,VI}^{O,P} = 0.38$).

Table 5.41: Kendall's τ estimates and p–values in brackets (Classes 1 and 2 with Classes 3 and 4)–Dataset VI.

	L	M	N	O	P	Q	T	U	X	Y
A	0.03	0.31	0.02	0.04	0.15	0.09	0.23	0.05	0.30	0.04
	(0.85)	(0.04)	(0.89)	(0.77)	(0.32)	(0.54)	(0.13)	(0.73)	(0.05)	(0.81)
B	0.10	**0.37**	0.22	0.08	0.22	0.32	0.28	0.22	0.08	0.23
	(0.51)	(**0.01**)	(0.15)	(0.58)	(0.15)	(0.03)	(0.06)	(0.15)	(0.58)	(0.12)
D	0.19	**0.49**	0.25	**0.38**	0.28	**0.45**	0.22	**0.44**	0.15	0.36
	(0.20)	(**0.00**)	(0.10)	(**0.01**)	(0.06)	(**0.00**)	(0.15)	(**0.00**)	(0.33)	(0.02)
F	0.19	0.35	0.09	0.29	0.20	0.21	0.11	0.26	0.21	0.11
	(0.20)	(0.02)	(0.54)	(0.05)	(0.18)	(0.16)	(0.48)	(0.08)	(0.16)	(0.48)
G	0.09	0.09	0.07	-0.02	0.23	-0.05	0.26	-0.04	**0.38**	0.08
	(0.54)	(0.54)	(0.65)	(0.89)	(0.13)	(0.73)	(0.09)	(0.77)	(**0.01**)	(0.58)
H	0.18	**0.53**	0.31	**0.48**	0.30	**0.45**	0.14	**0.45**	0.27	**0.39**
	(0.23)	(**0.00**)	(0.04)	(**0.00**)	(0.05)	(**0.00**)	(0.36)	(**0.00**)	(0.07)	(**0.01**)
I	0.30	0.34	0.26	0.31	**0.43**	0.28	0.19	0.29	0.12	0.34
	(0.05)	(0.02)	(0.09)	(0.04)	(**0.00**)	0.06	(0.20)	(0.05)	(0.41)	(0.02)
J	-0.27	0.04	0.11	0.30	0.29	0.26	0.26	0.27	0.25	0.13
	(0.07)	(0.77)	(0.44)	(0.05)	(0.05)	(0.08)	(0.09)	(0.07)	(0.10)	(0.38)
K	-0.04	0.20	0.24	0.20	0.23	0.22	0.16	0.21	0.14	0.16
	(0.81)	(0.18)	(0.11)	(0.18)	(0.13)	(0.15)	(0.28)	(0.16)	(0.36)	(0.28)

On the other hand, in both periods, Lugar de Baixo (X) forms a group of pairwise associated stations with Santana (P) and Ponta Delgada (T), having this pair a much higher estimate for τ_n in the shorter period ($\tau_{n,V}^{P,T} = 0.31$ and $\tau_{n,VI}^{P,T} = 0.49$). These stations located on the north of the island present the particularity in the period of 1950-1972 of being also associated with Loural (Q), a northern station that is farther from the sea.

In summary, Tables 5.42, 5.43, 5.44 and 5.45 show all the groups settled by three pairs of associated stations ($s_1 - s_2 - s_3$), the corresponding parameters β_i of the extreme value copula C defined by (4.31) in Section 4.3 of the Methodology, and the distance between stations within each group ($(d_{1,2}, d_{1,3}, d_{2,3})$, where $d_{i,j}$ stands for the distance in m between stations s_i and s_j). Tables 5.42 and 5.43 show all the groups starting with stations belonging to Classes 1 and 2, Montado do Pereiro (D) and Camacha (H), respectively.

Table 5.44 displays the groups that belong exclusively to this period (set 3), while the groups starting with Sanatório (O), Santana (P) and Loural (Q) stations (set 4) are shown in Table 5.45. All the results presented were obtained using functions that were implemented in R, whose corresponding code is presented in Appendix M.

Table 5.42: Groups in set 1, distances between stations (m) and parameters β_1, β_2 and β_3–Dataset VI.

Group	s_1–s_2–s_3	$(d_{1,2}, d_{1,3}, d_{2,3})$	β_1	β_2	β_3
1	D–H–M	(8515, 7367, 10945)	0.5924	0.6518	0.7393
2	D–H–O	(8515, 6016, 6528)	0.5304	0.7479	0.5726
3	D–H–Q	(8515, 15772, 21788)	0.6207	0.6207	0.6207
4	D–H–U	(8515, 6558, 5778)	0.6111	0.6306	0.6111
5	D–M–Q	(7367, 15772, 13568)	0.6688	0.6470	0.5790
6	D–O–Q	(10762, 15772, 17991)	0.5507	0.5507	0.7110
7	D–O–U	(10762, 6558, 1326)	0.4606	0.6846	0.9076
8	D–Q–U	(17991, 6558, 19243)	0.6111	0.6306	0.6111

Table 5.43: Groups in set 2, distances between stations (m) and parameters β_1, β_2 and β_3–Dataset VI.

Group	s_1–s_2–s_3	$(d_{1,2}, d_{1,3}, d_{2,3})$	β_1	β_2	β_3
1	H–M–Q	(10945, 21788, 13568)	0.7051	0.6809	0.5543
2	H–M–Y	(10945, 21217, 10281)	0.6293	0.7706	0.5063
3	H–O–Q	(6528, 13568, 17991)	0.6486	0.6486	0.5950
4	H–O–U	(6528, 5778, 1326)	0.5343	0.8252	0.7404
5	H–O–Y	(6528, 21217, 15130)	0.5682	0.7556	0.5543
6	H–Q–U	(13568, 5778, 19243)	0.6207	0.6207	0.6207
7	H–Q–Y	(13568, 21217, 10921)	0.4568	0.9678	0.7272
8	H–U–Y	(5778, 21217, 16319)	0.5401	0.7295	0.5839

The event $E_q = \{X_1 > x_{1,q}, X_2 > x_{2,q}, X_3 > x_{3,q}\}$, where, as before, X_i denote the observation at the i–th rain gauge station and $x_{i,q}$ the $(1-q)$–quantile of X_i, with $q \in (0,1)$ and $i \in \{1,2,3\}$, was also considered for this shorter period. Tables 5.46 and 5.47 show the obtained values in this subsection for the probability $p_q = P(E_q)$ (cf. (4.44) in Section 4.3 of the Methodology), and the corresponding return period $r_q = 1/p_q$, when $q = 0.98$ and when $q = 0.99$, for each one of the groups in sets 1, 2, 3 and 4. In the following analysis and when relevant, the identification of the dataset considered will be added as a subscript in the return period.

For set 1, the common groups to both periods are D–H–O (Group 3 in Table 5.36 and Group 2 in Table 5.46), D–H–U and D–O–U (Groups 4 and 7 in both Tables 5.36 and 5.46). All these groups present lower return periods in the shorter period than the ones presented in the wider one, the closest values being the ones from the

Table 5.44: Groups in set 3, distances between stations (m) and parameters β_1, β_2 and β_3–Dataset VI.

Group	s_1–s_2–s_3	$(d_{1,2}, d_{1,3}, d_{2,3})$	β_1	β_2	β_3
1	M–N–Q	(21195, 13568, 12102)	0.4606	0.6846	0.9076
2	M–N–Y	(21195, 10281, 5570)	0.4581	0.6903	0.9176
3	M–Q–Y	(13568, 10281, 10921)	0.4834	0.8304	0.8304
4	N–O–P	(20658, 25410, 16708)	0.6632	0.4863	0.6348
5	N–O–Q	(20658, 12102, 17907)	0.6886	0.4735	0.9006
6	N–O–U	(20658, 21866, 1326)	0.4564	0.7284	0.8406
7	N–O–Y	(20658, 5570, 15130)	0.6723	0.4815	0.9515
8	N–P–Q	(25410, 12102, 14530)	0.7942	0.5482	0.7672
9	N–P–U	(25410, 21866, 17321)	0.7242	0.5874	0.5000
10	N–P–Y	(25410, 5570, 21861)	0.8925	0.5095	0.7052
11	N–Q–U	(12102, 21866, 19243)	0.7350	0.8320	0.4950
12	N–Q–Y	(12102, 5570, 10921)	0.7428	0.8222	0.8388
13	N–U–Y	(21866, 5570, 16319)	0.7052	0.5094	0.8925

Table 5.45: Groups in set 4, distances between stations (m) and parameters β_1, β_2 and β_3–Dataset VI.

Group	s_1–s_2–s_3	$(d_{1,2}, d_{1,3}, d_{2,3})$	β_1	β_2	β_3
1	O–P–Q	(16708, 17907, 14530)	0.5367	0.5654	0.7358
2	O–P–U	(16708, 1326, 17321)	0.8028	0.4191	0.7594
3	O–P–Y	(16708, 15130, 21861)	0.5920	0.5148	0.6952
4	O–Q–U	(17907, 1326, 19243)	0.7805	0.5152	0.7805
5	O–Q–Y	(17907, 15130, 10921)	0.5074	0.7990	0.8643
6	O–U–Y	(1326, 15130, 16319)	0.7672	0.7942	0.5482
7	P–Q–U	(14530, 17321, 19243)	0.5543	0.7555	0.5267
8	P–Q–Y	(14530, 21861, 10921)	0.4878	0.9280	0.7514
9	P–T–X	(9549, 23514, 18291)	0.6667	0.6490	0.6667
10	P–U–Y	(17321, 21861, 16319)	0.5000	0.5874	0.7242
11	Q–U–Y	(19243, 10921, 16319)	0.7851	0.5132	0.8812

Group 3 formed by three stations of different classes of altitude, D–H–O ($r_{0.98,V}$ = 96.53, $r_{0.99,V}$ = 193.64, $r_{0.98,VI}$ = 93.75 and $r_{0.99,VI}$ = 188.02). In both periods, Group 7 is the group in set 1 that presents the highest values for the return periods, being the only one group here in set 1 that presents values above 100 years for $r_{0.98}$

and 200 years for $r_{0.99}$. Group 7 includes the three southern stations Montado do Pereiro (D), Sanatório (O) and Funchal (U) stations that are located at very different altitudes. With more similar altitudes, Group 3 formed by the southern stations Montado do Pereiro (D) and Camacha (H) and the northern station Loural (Q) shows the lowest return periods for this set 1 in this period.

Table 5.46: Return periods in years, $r_{0.98}$ and $r_{0.99}$, and associated probabilities for the groups in set 1.

Group	s_1–s_2–s_3	$p_{0.98}$	$r_{0.98}$	$p_{0.99}$	$r_{0.99}$
1	D–H–M	0.01191	83.99	0.00594	168.39
2	D–H–O	0.01067	93.75	0.00532	188.02
3	**D–H–Q**	**0.01246**	**80.24**	**0.00622**	**160.80**
4	D–H–U	0.01227	81.50	0.00612	163.32
5	D–M–Q	0.01164	85.90	0.00581	172.26
6	D–O–Q	0.01106	90.38	0.00552	181.18
7	**D–O–U**	**0.00931**	**107.40**	**0.00463**	**215.95**
8	D–Q–U	0.01227	81.50	0.00612	163.32

Table 5.47: Return periods in years, $r_{0.98}$ and $r_{0.99}$, and associated probabilities for groups in set 2.

Group	s_1–s_2–s_3	$p_{0.98}$	$r_{0.98}$	$p_{0.99}$	$r_{0.99}$
1	H–M–Q	0.01116	89.61	0.00556	179.82
2	H–M–Y	0.01020	98.03	0.00508	196.78
3	H–O–Q	0.01196	83.63	0.00596	167.66
4	H–O–U	0.01078	92.81	0.00537	186.39
5	H–O–Y	0.01114	89.77	0.00556	179.98
6	**H–Q–U**	**0.01246**	**80.24**	**0.00622**	**160.80**
7	**H–Q–Y**	**0.00925**	**108.16**	**0.00460**	**217.62**
8	H–U–Y	0.01086	92.07	0.00542	184.65

Considering the sets 2 for both periods, it can be observed that the only common group is formed by Camacha (H), Sanatório (O) and Funchal (U) stations, being the values for the return periods relatively similar ($r_{0.98,V} = 90.50$, $r_{0.99,V} = 181.57$, $r_{0.98,VI} = 92.81$ and $r_{0.99,VI} = 186.39$). Camacha (H) and Funchal (U) stations form with Loural (Q), the group that presents here in set 2 the lowest return period values. On the other hand, Camacha (H) and Loural (Q) also belong to the group with

the highest return period values. This group (Group 7) includes Ribeira Brava (Y) station, which among the considered stations is the one located at the lowest altitude. Group 7 is the only one in this set 2 that presents values above 100 for $r_{0.98}$ and 200 for $r_{0.99}$.

Table 5.48: Return periods in years, $r_{0.98}$ and $r_{0.99}$, and associated probabilities for groups in set 3.

Group	s_1–s_2–s_3	$p_{0.98}$	$r_{0.98}$	$p_{0.99}$	$r_{0.99}$
1	M–N–Q	0.00931	107.40	0.00463	215.95
2	M–N–Y	0.00926	107.96	0.00461	217.10
3	M–Q–Y	0.00979	102.14	0.00486	205.57
4	N–O–P	0.00981	101.96	0.00488	204.78
5	N–O–Q	0.00957	104.53	0.00476	210.13
6	**N–O–U**	**0.00924**	**108.25**	**0.00459**	**217.80**
7	N–O–Y	0.00972	102.87	0.00484	206.72
8	N–P–Q	0.01105	90.47	0.00550	181.67
9	N–P–U	0.01007	99.32	0.00502	199.32
10	N–P–Y	0.01028	97.28	0.00512	195.42
11	N–Q–U	0.01000	100.01	0.00497	201.02
12	**N–Q–Y**	**0.01490**	**67.10**	**0.00744**	**134.42**
13	N–U–Y	0.01028	97.30	0.00512	195.46

With the exception of Groups 8, 9, 10, 12 and 13, all the groups in set 3 present values above 100 for $r_{0.98}$ and 200 for $r_{0.99}$. The highest return periods were obtained for Canhas (N), Sanatório (O) and Funchal (U) stations that form Group 6, a group located in the southern side of Madeira island. The second highest values are found in Group 2 also formed by southern stations, namely Santo António (M), Canhas (N) and Ribeira Brava (Y). With relatively similar values, Group 1 presents the third highest return periods, belonging each station to the same class of altitude, Class 3, but with a higher distance between the stations that are located at lower altitudes than the corresponding ones in Group 2. Canhas (N), Loural (Q) and Ribeira Brava (Y) form the group with the lowest return periods in this set 3 and in all this subsection.

The second lowest return periods values showed in this subsection belong to another common group to both periods, P–T–X (Group 6 in Table 5.37 and Group 9 in Table 5.49), being the values much lower in the shorter period ($r_{0.98,V} = 117.81$, $r_{0.99,V} = 326.72$, $r_{0.98,VI} = 76.75$ and $r_{0.99,VI} = 153.80$). It is observed for all the

Table 5.49: Return periods in years, $r_{0.98}$ and $r_{0.99}$, and associated probabilities for the groups in set 4.

Group	s_1–s_2–s_3	$p_{0.98}$	$r_{0.98}$	$p_{0.99}$	$r_{0.99}$
1	O–P–Q	0.01079	92.68	0.00538	185.84
2	**O–P–U**	**0.00851**	**117.50**	**0.00422**	**236.80**
3	O–P–Y	0.01036	96.51	0.00516	193.63
4	O–Q–U	0.01041	96.10	0.00518	193.15
5	O–Q–Y	0.01026	97.50	0.00510	196.04
6	O–U–Y	0.01105	90.47	0.00550	181.67
7	P–Q–U	0.01059	94.43	0.00528	189.36
8	P–Q–Y	0.00986	101.41	0.00490	203.91
9	**P–T–X**	**0.01303**	**76.75**	**0.00650**	**153.80**
10	P–U–Y	0.01007	99.32	0.00502	199.32
11	Q–U–Y	0.01037	96.45	0.00516	193.88

remaining groups in set 4, excluding Groups 2 and 8, that $90 \leq r_{0.98} \leq 100$ and $180 \leq r_{0.98} \leq 200$. Group 2, formed by the northern station Santana (P) with the two southern closest stations Sanatório (O) and Funchal (U), presents the higher return periods in this set 4 and in all the measurement period of 1950–1972.

5.3.3 Dataset VII

The dataset used in this subsection, termed as Dataset VII, is composed by the highest values of annual daily precipitation on the island of Madeira, in the period of 1959–1980, coming from 18 rain gauge stations. In this shorter period, besides the 12 stations considered in Subsection 5.3.1, six more stations are considered: one from Class 1 (Poiso (C)), one from Class 2 (Encumeada (E)) and four from Class 4 (Bom Sucesso (R), Machico (S), Santa Catarina (V) and Caniçal (W)). In Figure 5.27, the location of each station considered is represented by a circle with its identification letter and colour corresponding to the respective altitude class. The identification letter, the geographical location, altitude and the island slope where the station is located (1 denoting the northern slope and 2 the southern one, as before) are displayed in Table 5.50 for the six rain gauge stations that belong exclusively to the present dataset.

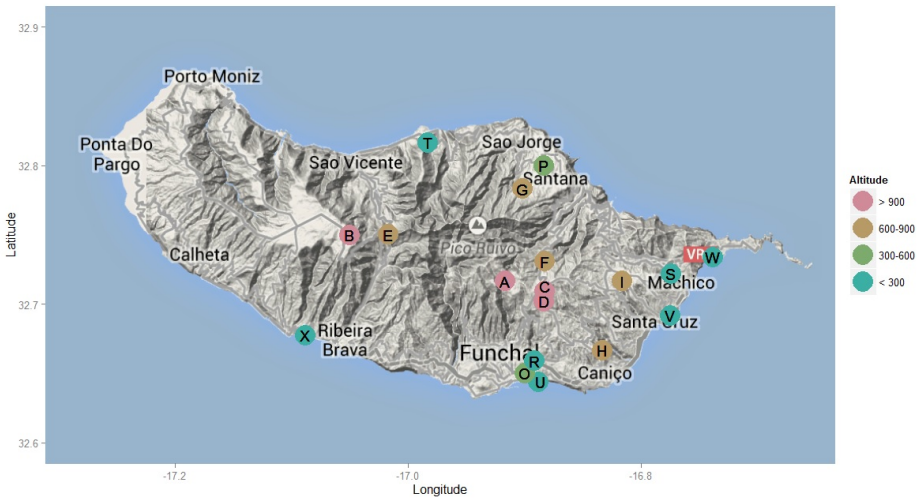

Figure 5.27: Location and altitude range of the rain gauge stations–Dataset VI (Map data ©2014 Google).

Table 5.50: Information about the seven rain gauge stations belonging exclusively to Dataset VII.

Station	Latitude	Longitude	Altitude (m)	Slope
Poiso (C)	32°42'N	16°53'W	1360	2
Encumeada (E)	32°45'N	17°01'W	900	1
Bom Sucesso (R)	32°39'N	16°54'W	290	2
Machico (S)	32°43'N	16°47'W	160	2
Santa Catarina (V)	32°41'N	16°46'W	49	2
Caniçal (W)	32°44'N	16°44'W	40	2

As in the two previous subsections, for all the pairs formed by the stations considered in this subsection, the values of the Kendall's τ association measure, $\tau_n^{X,Y}$, and their independence tests p-values were determined by the application of the *VineCopula* R language package [178]. The obtained values for each station in Classes 1 and 2 are displayed in Table 5.51, while Table 5.52 shows the respective values for the ones that are in Classes 3 and 4. The pairs formed by the stations of Classes 1 and 2 with the ones in Classes 3 and 4 are presented in Table 5.53. All tables show the values of $\tau_n^{X,Y}$ above the corresponding p-values in brackets. In the following analysis and like in the previous subsection, the identification of the dataset considered will be added as a subscript when a comparison between obtained values in different datasets shows itself to be relevant. For example, $\tau_{n,VII}^{X,Y}$ will refer to the estimate of the Kendall's τ association between stations X and Y when considering Dataset VII.

Table 5.51: Kendall's τ estimates and p–values in brackets (Classes 1 and 2)–Dataset VII.

A	B	C	D	E	F	G	H	I
A	0.11	**0.41**	0.28	0.19	0.17	0.15	0.36	0.02
	(0.48)	(**0.01**)	(0.07)	(0.23)	(0.27)	(0.32)	(0.02)	(0.89)
	B	0.27	0.24	**0.47**	0.30	**0.45**	0.28	**0.38**
		(0.08)	(0.12)	(**0.00**)	(0.05)	(**0.00**)	(0.07)	(**0.01**)
		C	**0.43**	0.18	**0.44**	0.30	0.39	0.31
			(**0.01**)	(0.25)	(**0.00**)	(0.05)	(0.03)	(0.05)
			D	0.37	**0.40**	0.35	**0.42**	**0.38**
				(0.02)	(**0.01**)	(0.02)	(**0.01**)	(**0.01**)
				E	**0.38**	**0.43**	**0.45**	0.32
					(**0.01**)	(**0.01**)	(**0.00**)	(0.04)
					F	0.27	0.32	0.32
						(0.08)	(0.03)	(0.04)
						G	**0.39**	**0.51**
							(**0.01**)	(**0.00**)
							H	**0.47**
								(**0.00**)

In this period, Areeiro (A) station is not in concordance with Bica da Cana (B) and Montado do Pereiro (D) stations as in the Subsections 5.3.1 and 5.3.2, but is with another station of Class 1, namely Poiso (C) ($\tau_n^{A,C} = 0,41$). Poiso (C) forms with Montado do Pereiro (D) and Ribeiro Frio (F) a group of pairwise associated stations, with values for the empirical version of the Kendall's τ association measure not less than 0.4. Like in the two previous periods, Montado do Pereiro (D) is associated with Camacha (H), presenting here the lowest estimate for τ_n ($\tau_{n,V}^{D,H} = 0.49$, $\tau_{n,VI}^{D,H} = 0.45$ and $\tau_{n,VII}^{D,H} = 0,42$). These two stations with Santo da Serra (I) station form the only group of pairwise associated stations common to Datasets V and VII. It can be observed that Camacha (H) and Santo da Serra (I), stations that are located at more similar altitudes, present a higher estimate for τ_n than the one presented by nearest stations Poiso (C) and Montado do Pereiro (D) ($d_{H,I} \approx$ 5761 m and $d_{C,D} \approx$ 849 m). The southern stations Montado do Pereiro (D) and Camacha (H) are also associated with a station belonging to Class 4 that is located farther away, namely Ponta Delgada (T) ($d_{D,T} \approx$ 33984 m and $d_{H,T} \approx$ 21787 m). On the other hand, Ponta Delgada (T) station is in concordance with Queimadas (G)

Table 5.52: Kendall's τ estimates and p–values in brackets (Classes 3 and 4)–Dataset VII.

O	P	R	S	T	U	V	W	X
O	0.32	0.34	**0.39**	0.37	0.27	**0.39**	**0.45**	0.26
	(0.04)	(0.03)	(**0.01**)	(0.02)	(0.08)	(**0.01**)	(**0.00**)	(0.09)
	P	**0.45**	0.19	0.31	**0.54**	**0.38**	0.08	0.34
		(**0.00**)	(0.23)	(0.05)	(**0.00**)	(**0.01**)	(0.59)	(0.03)
		R	0.19	0.21	**0.50**	0.32	0.28	0.28
			(0.20)	(0.45)	(**0.00**)	(0.04)	(0.07)	(0.07)
			S	0.27	0.04	0.24	0.32	0.22
				(0.08)	(0.80)	(0.12)	(0.03)	(0.15)
				T	0.28	0.05	0.26	**0.39**
					(0.07)	(0.76)	(0.10)	(**0.01**)
					U	0.37	0.19	0.33
						(0.02)	(0.20)	(0.03)
						V	**0.48**	0.08
							(**0.00**)	(0.59)
							W	0.15
								(0.07)

station with the higher estimate for τ_n in this subsection ($\tau_n^{G,T} = 0.55$), forming these two stations with Camacha (H) station another group of pairwise associated stations, that are located in different slopes. Besides Ponta Delgada (T) station, Queimadas (G) and Camacha (H) stations are in concordance with Encumeada (E) and Santo da Serra (I) stations as well, forming two groups of pairwise associated stations. Although the hypothesis of independence, at a 0.01 significance level, is not rejected for the data sets belonging to Ponta Delgada (T) and Encumeada (E) stations ($d_{E,T} \approx 8041$ m), it can be observed that the latter is associated with Queimadas (G) station ($d_{E,G} \approx 11352$ m). The station located at the second highest altitude, Bica da Cana (B), is associated with Encumeada (E) and Queimadas (G) stations but with slight higher values of τ_n ($\tau_n^{B,E} = 0.47$, $\tau_n^{B,G} = 0.45$ and $\tau_n^{E,G} = 0.43$). It can be observed that each one of these three northern stations are associated with the southern station Funchal (U) that belongs to Class 4. Queimadas (G) station is also in concordance with Sanatório (O) station, being G–O one of the three pairs of stations that shows the third highest estimate for τ_n in Dataset VII ($\tau_n^{G,O} = 0.51$). The other two pairs are formed by Santo da Serra (I) with Queimadas (G)

Table 5.53: Kendall's τ estimates and p–values in brackets (Classes 1 and 2 with Classes 3 and 4)–Dataset VII.

	O	P	R	S	T	U	V	W	X
A	-0.06	0.13	0.02	0.20	0.24	0.16	-0.07	-0.06	0.31
	(0.67)	(0.38)	(0.89)	(0.19)	(0.12)	(0.30)	(0.63)	(0.71)	(0.05)
B	0.31	0.25	0.24	0.16	0.26	**0.41**	0.21	0.26	0.30
	(0.05)	(0.11)	(0.12)	(0.30)	(0.09)	(**0.01**)	(0.17)	(0.09)	(0.05)
C	0.27	0.02	0.12	0.28	0.28	0.17	0.17	0.21	0.25
	(0.08)	(0.89)	(0.17)	(0.07)	(0.07)	(0.27)	(0.63)	(0.17)	(0.11)
D	0.31	0.11	0.01	0.19	**0.45**	0.29	0.13	0.28	0.32
	(0.05)	(0.48)	(0.93)	(0.20)	(**0.00**)	(0.06)	(0.41)	(0.07)	(0.04)
E	0.30	0.31	0.16	0.12	0.31	**0.49**	0.17	0.05	0.26
	(0.05)	(0.05)	(0.30)	(0.45)	(0.05)	(**0.00**)	(0.27)	(0.76)	(0.10)
F	0.28	0.08	0.09	0.22	0.19	0.28	0.29	0.22	0.26
	(0.07)	(0.59)	(0.55)	(0.15)	(0.23)	(0.07)	(0.06)	(0.15)	(0.10)
G	**0.51**	0.36	0.26	0.36	**0.55**	**0.42**	0.29	**0.43**	0.27
	(**0.00**)	(0.02)	(0.09)	(0.02)	(**0.00**)	(**0.01**)	(0.06)	(**0.01**)	(0.08)
H	0.26	0.13	0.18	0.15	**0.34**	0.21	0.05	0.20	0.29
	(0.09)	(0.76)	(0.25)	(0.32)	(**0.01**)	(0.17)	(0.38)	(0.19)	(0.06)
I	**0.46**	0.21	0.13	0.18	0.37	0.24	0.32	**0.51**	0.11
	(**0.00**)	(0.17)	(0.38)	(0.25)	(0.02)	(0.12)	(0.04)	(**0.00**)	(0.48)

($\tau_n^{G,I} = 0.51$) and Caniçal (W) ($\tau_n^{I,W} = 0.51$), stations that belong to Classes 2 and 4, respectively. Furthermore, Queimadas (G), Santo da Serra (I), Sanatório (O) and Caniçal (W) stations form a group of four pairwise associated stations. Although Sanatório (O) station is located farther away from Caniçal (W) than from Santa Catarina (V) ($d_{O,V} \approx 12607$ m and $d_{O,W} \approx 17780$ m), the pair O–W presents a higher estimate of τ_n than the one showed by the pair O–V ($\tau_n^{O,V} = 0.39$ and $\tau_n^{O,W} = 0.45$). Nevertheless, these two values are smaller than the one presented by Santa Catarina (V) and Caniçal (W), stations that are more closely located ($d_{V,W} = 5803$ m).

In summary, Table 5.54 shows all the groups settled by three pairwise associated stations ($s_1 - s_2 - s_3$) with s_1 a station belonging to Class 1 (set 1), being the remaining groups (set 2) displayed in Table 5.55. The corresponding parameters β_i of the extreme value copula C defined by (4.31) in Section 4.3 of the Methodology, and the distance between stations within each group ($(d_{1,2}, d_{1,3}, d_{2,3})$, where $d_{i,j}$ stands for the distance in m between stations s_i and s_j) are also displayed in Tables 5.54 and 5.55. All the results presented were obtained using functions that were implemented in R, whose corresponding code is presented in Appendix M.

Table 5.54: Groups in set 1, distance between stations (m) and parameters β_1, β_2 and β_3–Dataset VII.

Group	s_1-s_2-s_3	$(d_{1,2}, d_{1,3}, d_{2,3})$	β_1	β_2	β_3
1	B–E–G	$(3170, 14348, 11352)$	0.6613	0.6190	0.5848
2	B–E–U	$(3170, 19250, 16893)$	0.5672	0.7327	0.5966
3	B–G–I	$(14348, 22200, 10889)$	0.5137	0.7839	0.5934
4	B–G–U	$(14348, 19250, 15517)$	0.6097	0.6321	0.5559
5	C–D–F	$(849, 2426, 3242)$	0.5802	0.6455	0.5629
6	D–H–I	$(8515, 6538, 5761)$	0.5148	0.6952	0.5920
7	D–H–T	$(8515, 19379, 21787)$	0.7513	0.4878	0.5288

Table 5.55: Groups in set 2, distance between stations (m) and parameters β_1, β_2 and β_3–Dataset VII.

Group	s_1-s_2-s_3	$(d_{1,2}, d_{1,3}, d_{2,3})$	β_1	β_2	β_3
1	E–G–H	$(11352, 19554, 14440)$	0.6703	0.5453	0.5779
2	E–G–U	$(11352, 16893, 15517)$	0.6699	0.5456	0.6460
3	G–H–I	$(14440, 10889, 5761)$	0.5887	0.5361	0.7923
4	G–H–T	$(14440, 8494, 21787)$	0.8193	0.4267	0.6259
5	G–I–O	$(10889, 14774, 10762)$	0.7279	0.6301	0.6301
6	G–I–W	$(10889, 16301, 7600)$	0.6014	0.7704	0.6014
7	G–O–W	$(14774, 16301, 17780)$	0.6527	0.6999	0.5576
8	I–O–W	$(10762, 7600, 17780)$	0.6867	0.5822	0.6647
9	O–V–W	$(12607, 17780, 5803)$	0.5401	0.5839	0.7295

The event $E_q = \{X_1 > x_{1,q}, X_2 > x_{2,q}, X_3 > x_{3,q}\}$, where X_i denote the observation at the i–th rain gauge station and $x_{i,q}$ the $(1-q)$–quantile of X_i, with $q \in (0,1)$ and $i \in \{1,2,3\}$, was also considered for this subsection. For $q = 0.98$ and $q = 0.99$, Tables 5.56 and 5.57 show the obtained values in this subsection of the probability $p_q = P(E_q)$ (cf. (4.44) in Section 4.3 of the Methodology), and the corresponding return period $r_q = 1/p_q$ for each one of the groups in sets 1 and 2, respectively.

In set 1, the lowest return period values obtained correspond to Group 1 ($r_{0.98} = 85.10$ and $r_{0.99} = 170.60$), a group formed by the three northern stations Bica da Cana (B), Encumeada (E) and Queimadas (G). The first two stations also belong to the group that presents the second lowest return period ($r_{0.98} = 87.73$ and $r_{0.99} = 175.88$), being the third station, Funchal (U), located in the southern side of the

island, at a much lower altitude and nearer to the sea. Like this group, Group 7 includes a station in each of the Classes 1, 2 and 4 but in this group the stations that are located at higher altitude belong to the southern side of the island.

Table 5.56: Return periods in years, $r_{0.98}$ and $r_{0.99}$, and associated probabilities for the groups in set 1.

Group	s_1-s_2-s_3	$p_{0.98}$	$r_{0.98}$	$p_{0.99}$	$r_{0.99}$
1	**B–E–G**	**0.01175**	**85.10**	**0.00586**	**170.60**
2	B–E–U	0.01139	87.73	0.00569	175.88
3	B–G–I	0.01034	96.71	0.00515	194.04
4	B–G–U	0.01118	89.46	0.00558	179.41
5	C–D–F	0.01131	88.41	0.00564	177.24
6	D–H–I	0.01036	96.51	0.00516	193.63
7	**D–H–T**	**0.00982**	**101.88**	**0.00489**	**204.38**

Presenting the higher return period values for the groups in set 1 ($r_{0.98} = 101.88$ and $r_{0.99} = 204.38$), Group 7 is formed by Montado do Pereiro (D), Camacha (H) and Ponta Delgada (T) stations. All the remaining groups show return period values ranging from 88 to 97 for $r_{0.98}$ and from 177 to 195 for $r_{0.98}$, including the Group 6 (D-H-I) that is also present in the wider period (Group 2 in Table 5.36). For this group, the return periods observed in the wider period are higher than the ones obtained here ($r_{0.98,V} = 113.60$, $r_{0.99,V} = 228.46$, $r_{0.98,VII} = 96.51$ and $r_{0.99,VII} = 193.63$).

Table 5.57: Return periods in years, $r_{0.98}$ and $r_{0.99}$, and associated probabilities for groups in set 2.

Group	s_1-s_2-s_3	$p_{0.98}$	$r_{0.98}$	$p_{0.99}$	$r_{0.99}$
1	E–G–H	0.01096	91.22	0.00547	182.91
2	E–G–U	0.01098	91.07	0.00547	182.71
3	G–H–I	0.01078	92.74	0.00538	186.01
4	**G–H–T**	**0.00863**	**115.88**	**0.00429**	**233.06**
5	**G–I–O**	**0.01265**	**79.05**	**0.00631**	**158.41**
6	G–I–W	0.01208	82.80	0.00603	165.94
7	G–O–W	0.01122	89.13	0.00559	178.81
8	I–O–W	0.01171	85.42	0.00584	171.30
9	O–V–W	0.01086	92.07	0.00542	184.65

In set 2, the highest and the lowest return period values obtained correspond to the Groups 4 and 5, respectively, being Queimadas (G) a common station to the two groups. Besides Queimadas (G) station, Group 4 includes Camacha (H), a southern station that belongs to the same class of altitude, and Ponta Delgada (T) a station that is located in the northern side of the island and nearest the sea. The southern station Santo da Serra (I) belongs to Class 2 like Queimadas (G), but the third station of Group 5, Sanatório (O), is included in Class 4 and is located in the southern side. The return periods for Group 4 ($r_{0.98} = 115.88$ and $r_{0.99} = 233.06$) show the highest values observed in set 2 and in all the period 1959–1980. The lowest values for the same period are shown by Group 5 of set 2: $r_{0.98} = 79.05$ and $r_{0.99} = 158.41$. All the remaining groups present return period values ranging from 82 to 93 for $r_{0.98}$ and from 165 to 187 for $r_{0.99}$.

Chapter 6

Conclusion

Early work in hydrology usually assumed a Gumbel distribution for the block maxima or equivalently an exponential distribution for the excesses over a high threshold [124]. However, since the earlier years of the extreme value theory there was the notion that the Gumbel distribution tends to underestimate the magnitude of extreme rainfall events and the use of the GEV distribution has been recommended for rainfall frequency since 1995 [224]. On the other hand, the GPD has been suggested for the excess distribution function since a long time ago, being the definition of the GPD traceable back to the work of Pickands [171] in 1975. Statistics of extremes for independent and identical random variables were applied following a parametric approach, but a semi–parametric one has gained its space in the most recent times. Under the PORT semi-parametric approach, and also under the classical Gumbel's and POT approaches, an analysis of rainfall values collected in Madeira Island over different periods of time was done in this thesis. Also, a study about the dependence of annual maximum rainfall in Madeira Island by means of the Kendall's τ association measure was carried out, and the multivariate extremes were addressed through an EVC approach.

Using Gumbel's approach, GEV parameters estimates for annual maxima of daily rainfall in Madeira Island are provided by ML and PWM methods. For the annual maxima data drawn from the seven rain gauge stations maintained in the island by IPMA, the hyphotesis of Gumbel distribution was tested by the likelihood ratio test and a test presented by Hosking et al. [119], both methods leading to the same conclusions. For the distributions corresponding to Areeiro (A), Santo da Serra (I), Santana (P), Funchal (U) and Santa Catarina (V), there is not significant evidence to choose the GEV model, with $\gamma \neq 0$, instead of the Gumbel model. Nevertheless, it can be observed that the ML estimate for the shape parameter γ for each of

these stations is not equal to zero and that the GEV location and scale parameters estimates are similar for both methods, but that is not the case when the Gumbel distribution is chosen. Therefore, in these particular cases, the option taken was to determine the estimates for the 50– and 100–year return levels using the ML method and considering the GEV distribution.

The estimates for the shape parameter range from -0.3 to 0.3, being greater than 0.09 for the two stations located at the lowest altitudes and nearest the sea, namely, Santa Catarina (V) and Lugar de Baixo (X) stations. The estimate for γ is also positive for the Santana (P) station but it is closer to zero. Data from Areeiro (A), Bica da Cana (B), Santo da Serra (I) and Funchal (U) rain gauge stations revealed negative estimates for the shape parameter, being the lowest values presented by Bica da Cana (B) station. Exploring the possibility of the existence of trends, a significant evidence for a linear trend in the location parameter was only found for the Areeiro (A) station data. Without considering this trend, this rain gauge station is the one that shows the higher estimates for the location parameter, with values approximately equal to 159 mm, for both methods considered. Bica da Cana (B) presents lower values for the location parameter estimates than the ones from Areeiro (A), but that is not the case for the values of the scale parameter estimates. However, it is Santo da Serra (I) station the one that presents the highest scale parameter estimates, having values approximately equal to 116 mm for the location parameter estimates. Although, Santana (P) presents values for location parameter estimates that are nearly half of the ones presented by Areeiro (A), the values for the scale parameter estimates are still slightly higher than the ones from this station. The stations below 300 m present lower location and scale estimates with values below 55 mm and 25 mm, respectively. The lower values correspond to the rain gauge station located at the lowest altitude, namely Lugar de Baixo (X). It turns out this is the station that presents the second lowest estimate values for the 50– and 100–year return level, being the lowest ones showed by Funchal (U) station. On the other hand, the highest estimates for the 50– and 100–year return levels are showed by Areeiro (A) station. Although Santo da Serra (I) station is located in a lower altitude than Bica da Cana (B), it presents higher estimates for the 50– and 100–year return levels than this station.

Also in this thesis, tests based on the likelihood ratio statistic and the PWM were used to test the hypothesis of a Gumbel distribution for the annual 1-day maximum rainfall data, from 25 rain gauge stations, maintained in the past by the General Council of the Autonomous District of Funchal. From the rainfall

records drawn from these rain gauge stations located in the northern and southern hillsides of the island, annual maxima datasets with 22 to 31 years of extension were obtained. Although most of the rain gauge stations considered are deactivated, and consequently the rainfall time series are relatively short, it is important to analyse all the available data, given the number of major flash flood events reported so far in Madeira Island. The most significant one among the most recent events of this nature occurred on the 20th of February 2010, with 146.9 mm observed in Funchal and 333.8 mm in Areeiro [70]. Given the GEV estimates obtained in this work by ML, these values correspond to return periods of approximately 79 years and 292 years, respectively, or 70 years and 297 years when GEV estimates by PWM are used. Although for almost all rainfall data series there was no significant evidence to choose the GEV distribution, non Gumbel, in opposition to the Gumbel distribution, GEV parameters estimates by ML and PWM methods were provided in this work given that the corresponding shape parameters estimates are not equal to zero and that location and scale GEV estimates are relatively similar for both methods. The hypothesis of a Gumbel distribution was tested by the likelihood ratio test and by the test presented by Hosking et al. [119], and the same conclusions were obtained for both methods, with the exception of the data from Queimadas (G) and Santo António (M) rain gauge stations. For the latter two stations and also for Bica da Cana (B), Curral das Freiras (K), Canhas (N), Machico (S), Caniçal (W) and Ribeira Brava (Y) stations, there was evidence of a linear trend in one or two parameters when modelling the corresponding annual maxima by the GEV distribution. For Bica da Cana (B) and Ribeira Brava (Y) stations, a significant evidence for a linear trend in location and scale parameters was found in the data independently of the model chosen. Estimates for the 50– and 100–year return levels were also determined for all rain gauge stations data using the GEV parameter estimates obtained from both methods.

The parameters and return level estimates, regardless of the method used to obtain them, suggest a complex characterization of the spatial distribution of extreme rainfall in Madeira Island. It seems that there is a simultaneous influence of factors such as altitude, proximity to the sea, distance, and location in nearby hillsides or in the northern or the southern part of the island. Besides, there are differences in the return levels estimates according to the method applied, except for Areeiro (A), Ribeiro Frio (F), Porto Moniz (J), Ponta do Pargo (L), Santo António (M) and Ribeira Brava (Y) rain gauge stations for which the estimates are approximately similar. Nevertheless, it can be observed that the 50– and

100–year return levels estimates are greater than 242 and 255 mm, respectively, for the seven rain gauge stations located farther from the sea Areeiro (A), Bica da Cana (B), Poiso (C), Montado do Pereiro (D), Encumeada (E), Ribeiro Frio (F) and Loural (Q). The same can be observed for three more stations, Porto Moniz (J), Santana (P) and Ponta Delgada (T), that are closer to the sea but located in the northern part of the island. Santo da Serra (I) and Curral das Freiras (K), rain gauge stations, that are located at similar altitudes, present lower estimates than those presented by the three previous stations. Between these two, Curral das Freiras (K), which is located farther from the sea, presents lower 50– and 100–year return levels estimates, being these values around 198 mm and 200 mm, respectively. There is proximity between the estimates values for the northern stations Queimadas (G) and Camacha (H), and between these and the ones presented by the southern station Machico (S). Queimadas (G) and Camacha (H) stations are located in a nearby hillside to the one where Machico (S) is located, as Ponta do Pargo (L) and Ribeira Brava (Y) that are located in the south west and also present similar return value estimates. For all the rest of the rain gauge stations located in the southern part of the island the 50– and 100–year return levels estimates are smaller than 164 mm and 179 mm, respectively. The rain gauge stations that present the highest (without considering the 100–return level ML estimate) and the smallest return level estimates, Areeiro (A) and Lugar de Baixo (X), are both located in the south side of Madeira Island.

With the exception of Santana (P) and Funchal (U), it was possible to obtain an augmented sample for the common stations to the two datasets previously analysed. Contrary to what happened with shorter measurements periods, no evidence was found for the existence of trends in the parameters's values for Areeiro (A) and Bica da Cana (B) stations when the wider period was considered. For the remaining stations, Santo da Serra (I), Santa Catarina (V) and Lugar de Baixo (X), there was again no evidence for the existence of the mentioned trends. Concerning the test of Model 2 versus Model 1, the same conclusions are drawn for Areeiro (A), Santana (P), Funchal (U) and Santa Catarina (V), regardless of the measurement period considered. The particular case of a rejection of the hypothesis of a Gumbel's distribution when considering a shorter period, in spite of its non rejection when considering the wider one, was observed for Santo da Serra (I) and Lugar de Baixo (X) stations. For Bica da Cana (B), Model 2 (Gumbel's distribution) was not rejected only in the shorter period. Nevertheless for all the rain gauge stations cases and measurement periods considered, the inference based

on the GEV distribution was preferred, due to the inherent uncertainty of the shape parameter. In fact, although the sign of this parameter estimate remains unchanged through the different measurement periods for Areeiro (A), Bica da Cana (B), Santo da Serra (I) and Santana (P), this does not happen with the three stations belonging to Class 4 (which are located below 300 m). A negative shape parameter estimate in the shorter period becomes a positive one in the wider periods for Santa Catarina (V) and Lugar de Baixo (X), while the opposite happens with Funchal (U) rain gauge station's. In terms of 50– and 100–year return levels estimates, Bica da Cana (B) presents similar values between both periods, while Areeiro (A), Santana (P) and Funchal (U) present lower values when the larger period is considered. In the opposite way, lower values for the 50– and 100–year return levels estimates are obtained for Santo da Serra (I), Santa Catarina (V) and Lugar de Baixo (X) when the shorter period is considered.

The extreme value index γ is of primary interest in extreme value analysis and it is the only parameter estimated under a semi-parametric approach. The estimation of γ is based on the k top order statistics in the sample and the analysis made in this thesis following a PORT approach provided information about the region of the k values to use for each location. It was observed that for almost all locations there is an evidence for non-positive values of the shape parameter for some values of k. However, the estimates of γ obtained with ML and with PWM estimators were all non-negative. For three locations the identical distribution hypothesis was rejected. Nevertheless, this fact does not invalidate the analysis since much progress has been achieved when the assumptions of independence and of homogeneity are relaxed. In this thesis, a search for thresholds was also performed for daily precipitation values, as if they were independent and identically distributed. Despite the values found through this POT approach being the result of the weakening of the assumptions of independence and homogeneity, they already suggest that the characterization of the extreme rainfall on Madeira Island should take into account factors such as the slope and altitude in which the stations are located and also their proximity to the sea.

The spatial distribution of precipitation in Madeira Island is strongly affected by its highly rugged topography and an aim in this study was to analyse spatial extremes of Madeira's annual maxima precipitation through a copula function [182], using annual maximum daily precipitation data from 25 rain gauge stations spread throughout the island. First, a study was made on the dependence between extreme rainfall values from different stations based on Kendall's τ measure, for three groups

of stations according three different measurement periods. The Kendall's τ estimates were obtained and the independence for pairs of stations was tested by a test based on the empirical version of this association measure. The results obtained here suggest that special attention should be given to different factors, including the altitude, the distance between stations, the slope where they are located, and the proximity to the sea. In some cases, the altitude and the distance to the sea may have a higher influence in the association between stations than the distance factor. For instance, in the period 1959–1980, Camacha (H) and Santo da Serra (I) show a higher Kendall's τ estimate value than the pair formed by Poiso (C) and Montado do Pereiro (D). The latter stations are 849 m far from each other, being the distance from Camacha (H) and Santo da Serra (I) of approximately 5761 m. The justification for the higher value for the pair H–I, when compared to the corresponding value for the pair C–D may be related to the fact that the association between rainfall and altitude tends to be more pronounced at the stations less exposed than those that are facing the sea (see e.g. [114]). Furthermore, greater exposure and proximity to the sea (or other large bodies of water) are more related with intense rainfall events (see e.g. [127]), which may also contribute to the observed extreme rainfall at stations H and I to be less discrepant from each other than the annual maxima rainfall data recorded in stations C and D. This may also be an important factor for the existence of the association observed within both Datasets V and VI between Santana (P) station and each one of the pair Funchal (U) and Lugar de Baixo (X) stations, which are also located near the sea but in the opposite slope. However, the dependence on extreme rainfall does not appear to be characterised only by the mentioned factors, given the existence of associated stations which are distant from each other, located in opposite slopes and altitudes, presenting also different distances from the sea. For example, in the period ranging from 1950 to 1980, the independence is rejected for the pair of stations formed by Montado do Pereiro (D) and Ponta Delgada (T) stations, that are approximately 15815 m apart. While the northern station Ponta Delgada (T) is located near the sea at an altitude of 136 m, the southern Montado do Pereiro (D) station is located at the central mountainous region of Madeira Island at an altitude of 1260 m.

In a second stage of the analysis, groups of three pairwise associated stations were formed within each measurement period with the pairs for which the independence was rejected. For each one of the obtained groups, the parameters β_i, with $i \in \{1, 2, 3\}$, that define the extreme value copula C defined in Chapter 4, were obtained and an adjustment was made to a family of extreme value copulas involving the

Marshall–Olkin family. The analysis corresponding to Datasets V, VI and VII led to 17, 40 and 16 groups of three pairwise associated stations, respectively. Five of these groups are present in the analysis of both Datasets V and VI, while only one is common to the analysis of both Datasets V and VI. An event of practical interest is the one defined by $E_q = \{X_1 > x_{1,q}, X_2 > x_{2,q}, X_3 > x_{3,q}\}$, where X_i denotes the observation at the i–th rain gauge station and $x_{i,q}$ the $(1-q)$–quantile of X_i, with $q \in (0,1)$ and $i \in \{1,2,3\}$. For $q = 0.98$ and $q = 0.99$, the probability p_q and the corresponding return period r_q were calculated for each one of the obtained groups. In Subsection 5.3.1 (Dataset V), the three lowest return period values belong to the groups formed by Camacha (H), Sanatório (O), Funchal (U) and Lugar de Baixo (X), are all located in the southern slope. Among these, the group H–U–X is the one that presents the lowest return periods, although formed with stations that are located more farther away than, for example, the ones in the group H–O–U or even in the group D–H–O, which has the fifth lowest values. The groups H–O–U and D–H–O appeared also in the analysis made in Subsection 5.3.2 (Dataset VI) but here they do not even belong to the six groups with the lowest values for $r_{0.98}$ and $r_{0.99}$. In this subsection, the group with the lowest return periods is the one formed by the rain gauge stations Canhas (N), Loural (Q) and Ribeira Brava (Y), being each one these stations only considered in Dataset VII. Following, there is the group formed by Santana (P), Ponta Delgada (T) and Lugar de Baixo (X), which presents the particularity of also being the group with the third highest values for $r_{0.98}$ and $r_{0.99}$ in the analysis made in Subsection 5.3.1. Contrary to what happens in Subsection 5.3.2, the stations belonging to the group that shows the lowest return periods in Subsection 5.3.3 (Dataset VII) are also included in the other analyses, although that is not the case with the group itself. The stations are Queimadas (G), Santo da Serra (I) and Sanatório (O), forming the former two with Caniçal (W) rain gauge station the group with the second lowest return periods.

The famous sentences *Il est impossible que l' improbable n'arrive jamais* and *Il y aura toujours une valeur qui dépassera toutes les autres* attributed in [87] to Emil Gumbel enhance the importance of the study of extremes, while highlighting its intrinsic uncertainty. According to Embrechts et al. [61], referring to the act of predicting rare events more extreme than the already observed, Richard Smith said: *There is always going to be an element of doubt, as one is extrapolating into areas one doesn't know about. But what extreme value theory is doing is making the best use of whatever data you have about extreme phenomena.* Having in mind that the mentioned theory is the natural one to apply to the study of extreme events,

the main goal of this thesis was to apply this theory in the study of extreme rainfall in Madeira Island. From among the diversity of methodologies inherent to this theory, four of them were applied to the available rainfall data. The application of the two classical and the two more recent approaches gave rise to information concerning annual, monthly and daily rainfall extremes. The results obtained here are relevant to the knowledge about rainfall extreme value events in Madeira Island since, according to Embrechts et al. [61], every piece of knowledge acquired about topics such as the distribution of the annual extremes, the mean excess over a given threshold or the return period of some rare event helps to predict extremal events.

Bibliography

[1] Y. Alila. A hierarchical approach for the regionalization of precipitation annual maxima in Canada. *Journal of Geophysical Research*, 104(D24):31645–31655, 1999.

[2] P. Araújo Santos, M. I. Fraga Alves, and M. I. Gomes. Peaks over random threshold methodology for tail index and quantile estimation. *REVSTAT*, 4(3):227–247, 2006.

[3] B. C. Arnold. Parameter estimation for a multivariate exponential distribution. *Journal of the American Statistical Association*, 63(323):848–852, 1968.

[4] G. Aronica, M. Cannarozo, and L. Noto. Investigating the changes in extreme rainfall series recorded in an urbanised area. *Water Science and Technology*, 45(2):49–54, 2002.

[5] B. Bacchi, R. Rosso, and P. La Barbera. Storm characterization by Poisson models of temporal rainfall. In *22nd Congress of the International Association of Hydraulic Research*, pages 35–40, 1987.

[6] D. Baioni. Human activity and damaging landslides and floods on Madeira Island. *Natural Hazards and Earth System Sciences*, 11(11):3035–3046, 2011.

[7] A. A. Balkema and L. de Haan. Residual life time at great age. *The Annals of Probability*, 2(5):792–804, 1974.

[8] A. A. Balkema and S. I. Resnick. Max-infinite divisibility. *Journal of Applied Probability*, 14(2):309–319, 1977.

[9] W. E. Bardsley. A test for distinguishing between extreme value distributions. *Journal of Hydrology*, 34(3-4):377–381, 1977.

[10] J. Beirlant, Y. Goegebeur, J. Segers, and J. Teugels. *Statistics of Extremes: Theory and Applications*. Wiley, 2004.

[11] J. Beirlant, P. Vynckier, and J. L. Teugels. Excess function and estimation of the extreme–value index. *Bernoulli*, 2(4):293–318, 1996.

[12] J. Beirlant, P. Vynckier, and J. L. Teugels. Excess function, Pareto quantile plots, and regression diagnostics. *Journal of the American Statistical Association*, 91(436):1659–1667, 1996.

[13] S. M. Berman. Convergence to bivariate extreme value distributions. *Annals of the Institute of Statistical Mathematics*, 13(1):217–223, 1961.

[14] N. Bernoulli. *The use of the art of conjecturing in law.* PhD thesis, University of Basel, 1709.

[15] M. F. Brilhante. Exponentiality versus generalized Pareto - a resistant and robust test. *REVSTAT*, 2(1):1–13, 2004.

[16] C. E. P. Brooks and N. Carruthers. *Handbook of Statistical Methods in Meteorology.* Her Majesty's Stationery Office, 1953.

[17] T. A. Buishand. The effect of seasonal variation and serial correlation on the extreme value distribution of rainfall data. *Journal of Climate and Applied Meteorology*, 24(2):154–160, 1985.

[18] T. A. Buishand. Extreme rainfall estimation by combining data from several sites. *Hydrological Sciences Journal*, 36(4):345–365, 1991.

[19] T. A. Buishand, L. De Haan, and C. Zhou. On spatial extremes: with application to a rainfall problem. *The Annals of Applied Statistics*, 2(2):624–642, 2008.

[20] E. Castillo, J. Galambos, and J. M. Sarabia. *Extreme Value Theory*, volume 51 of *Lecture Notes in Statistics*, chapter The selection of the domain of attraction of an extreme value distribution from a set of data. Springer, 1989.

[21] E. Castillo, A. S. Hadi, N. Balakrishnan, and J. M. Sarabia. *Extreme Value and Related Models with Applications in Engineering and Science.* Wiley, 2004.

[22] K. Chaouche, P. Hubert, and G. Lang. Graphical characterization of probability distribution tails. *Stochastic Environmental Research and Risk Assessment*, 16(5):342–357, 2002.

[23] V. T. Chow, D. R. Maidment, and L. W. Mays. *Applied Hydrology.* McGraw–Hill, Singapore, 1988.

[24] P.-S. Chu, X. Zhao, Y. Ruan, and M. Grubbs. Extreme rainfall events in the Hawaiian Islands. *Journal of Applied Meteorology and Climatology*, 48(3):502–516, 2009.

[25] S. Coles. Regional modelling of extreme storms via max-stable processes. *Journal of the Royal Statistical Society: Series B*, 55(4):797–816, 1993.

[26] S. Coles. *An Introduction to Statistical Modeling of Extreme Values*. Springer, London, 2001.

[27] S. Coles, L. R. Pericchi, and S. Sisson. A fully probabilistic approach to extreme rainfall modeling. *Journal of Hydrology*, 273(1–4):35–50, 2003.

[28] S. G. Coles and M. J. Dixon. Likelihood-based inference for extreme value models. *Extremes*, 2(1):5–23, 1999.

[29] S. G. Coles and J. A. Tawn. Modelling extremes of the areal rainfall process. *Journal of the Royal Statistical Society: Series B*, 58(2):329–347, 1996.

[30] S. G. Coles, J. A. Tawn, and R. L. Smith. A seasonal Markov model for extremely low temperatures. *Environmetrics*, 5(3):221–239, 1994.

[31] D. Cooley, J. Cisewski, R. J. Erhardt, S. Jeon, E. Mannshardt, B. O. Omolo, and Y. Sun. A survey of spatial extremes: Measuring spatial dependence and modeling spatial effects. *REVSTAT*, 10(1):135–165, 2012.

[32] D. Cooley, D. Nychka, and P. Naveau. Bayesian spatial modeling of extreme precipitation return levels. *Journal of American Statistical Association*, 102(479):824–840, 2007.

[33] F. T. Couto, R. Salgado, and M. J. Costa. Analysis of intense rainfall events on Madeira Island during the 2009/2010 winter. *Natural Hazards and Earth System Sciences*, 12(7):2225–2240, 2012.

[34] A. Crisci, B. Gozzini, F. Meneguzzo, S. Pagliara, and G. Maracchi. Extreme rainfall in a changing climate: regional analysis and hydrological implications in Tuscany. *Hydrological Processes*, 16(6):1261–1274, 2002.

[35] J. Danielsson, L. de Haan, L. Peng, and C. G. de Vries. Using a bootstrap method to choose the sample fraction in tail index estimation. *Journal of Multivariate Analysis*, 76(2):226–248, 2001.

[36] A. C. Davison. Modelling excesses over high thresholds, with an application. In Tiago de Oliveira, editor, *Statistical Extremes and Applications*, pages 461–482. D. Reidel, 1984.

[37] A. C. Davison, S. A. Padoan, and M. Ribatet. Statistical modeling of spatial extremes. *Statistical Science*, 27(2):161–186, 2012.

[38] A. C. Davison and R. L. Smith. Models for exceedances over high thresholds (with discussion). *Journal of the Royal Statistical Society. Series B*, 52(3):393–442, 1990.

[39] L. de Haan. *On Regular Variation and Its Application to the Weak Convergence of Sample Extremes*, volume 32 of *Mathematical Centre Tracts*. Mathematisch Centrum, Amsterdam, 1970.

[40] L. de Haan. A form of regular variation and its application to the domain of attraction of the double exponential distribution. *Zeitschrift für Wahrscheinlichkeitstheorie und Verwandte Gebiete*, 17(3):241–258, 1971.

[41] L. de Haan. A spectral representation for max-stable processes. *The Annals of Probability*, 12(4):1194–1204, 1984.

[42] L. de Haan and A. Ferreira. *Extreme Value Theory: An Introduction*. Springer, 2006.

[43] L. de Haan and S. I. Resnick. Limit theory for multivariate sample extremes. *Zeitschrift für Wahrscheinlichkeitstheorie und Verwandte Gebiete*, 40(4):317–337, 1977.

[44] L. de Haan and C. Zhou. On extreme value analysis of a spatial process. *REVSTAT*, 6(1):71–81, 2008.

[45] M. I. P. de Lima and J. L. M. P. de Lima. Investigating the multifractality of point precipitation in the Madeira archipelago. *Nonlinear Processes in Geophysics*, 16(2):299–311, 2009.

[46] C. de Michele and G. Salvadori. A generalized Pareto intensity–duration model of storm rainfall exploiting 2–Copulas. *Journal of Geophysical Research*, 108, 2003.

[47] P. Deheuvels. Caractérisation complète des lois extrêmes multivariées et de la convergence des types extrêmes. *Publications de l'Institut de Statistique de l'Université de Paris*, 23(3-4):1–36, 1978.

[48] P. Deheuvels. La fonction de dépendence empirique et ses propriétés, un test non paramétrique d'indépendence. *Académie Royale de Belgique–Bulletin de la Classe des Sciences*, 65(5):274–292, 1979.

[49] P. Deheuvels. The decomposition of infinite order and extreme multivariate distributions. In I. M. Chakravarti, editor, *Asymptotic theory of statistical tests and estimation: In Honor of Wassily Hoeffding*, pages 259–286. Academic Press, 1980.

[50] P. Deheuvels. Probabilistic aspects of multivariate extremes. In Tiago de Oliveira, editor, *Statistical Extremes and Applications*, pages 117–130. D. Reidel, 1984.

[51] A. L. M. Dekkers, J. H. J. Einmahl, and L. de Haan. A moment estimator for the index of an extreme–value distribution. *The Annals of Statistics*, 17(4):1833–1855, 1989.

[52] S. Demarta and A. J. McNeil. The t copula and related copulas. *International Statistical Review*, 73(1):111–129, 2005.

[53] J. Diebolt, A. Guillou, P. Naveau, and P. Ribereau. Improving probability-weighted moment methods for the generalized extreme value distribution. *REVSTAT*, 6(1):33–50, 2008.

[54] D. Dietrich, L. de Haan, and J. Hüsler. Testing extreme value conditions. *Extremes*, 5(1):71–85, 2002.

[55] M. J. Dixon and J. A. Tawn. Extreme sea levels: modelling interactions between tide and surge. In V. Barnett and K. F. Turkman, editors, *Statistics for the Environment II*, pages 221–232. Wiley, 1994.

[56] Secretaria Regional do Equipamento Social da Região Autónoma da Madeira. *Estudo de Avaliação do Risco de Aluviões da Ilha da Madeira–Relatório Síntese*. Instituto Superior Técnico and Universidade da Madeira and Laboratório Regional de Engenharia Civil, Funchal, 2010.

[57] E. L. Dodd. The greatest and least variate under general laws of error. *Transactions of the American Mathematical Society*, 25(4):525–539, 1923.

[58] G. Draisma, L. de Haan, L. Peng, and T. T. Pereira. A bootstrap-based method to achieve optimality in estimating the extreme-value index. *Extremes*, 2(4):367–404, 1999.

[59] H. Drees, L. de Haan, and D. Li. Approximations to the tail empirical distribution function with application to testing extreme value conditions. *Journal of Statistical Planning and Inference*, 136(10):3498–3538, 2006.

[60] H. Drees and E. Kaufmann. Selecting the optimal sample fraction in univariate extreme value distribution. *Stochastic Processes and their Applications*, 75(2):149–172, 1998.

[61] P. Embrechts, C. Klüppelberg, and T. Mikosch. *Modelling extremal events for Insurance and Finance*. Springer, Berlin, 1997.

[62] K. Engeland, H. Hisdal, and A. Frigessi. Practical extreme value modelling of hydrological floods and droughts: A case study. *Extremes*, 7(1):5–30, 2004.

[63] M. Falk. On testing the extreme value index via the POT–method. *The Annals of Statistics*, 23(6):2013–2035, 1995.

[64] A.-C. Favre, S. El Adlouni, L. Perreault, N. Thiémonge, and B. Bobée. Multivariate hydrological frequency analysis using copulas. *Water Resources Research*, 40(1), 2004.

[65] B. V. Finkelstein. On the limiting distributions of the extreme terms of a variational series of a two–dimensional random quantity (in Russian). *Doklady Akademii Nauk SSSR (N.S.)*, 91:209–211, 1953.

[66] R. A. Fisher and L. H. C. Tippett. Limiting forms of the frequency distribution of the largest or smallest member of a sample. *Mathematical Proceedings of the Cambridge Philosophical Society*, 24(2):180–190, 1928.

[67] H. J. Fowler and C. G. Kilsby. A regional frequency analysis of United Kingdom extreme rainfall from 1961 to 2000. *International Journal of Climatology*, 23(11):1313–1334, 2003.

[68] M. I. Fraga Alves. Asymptotic distribution of Gumbel statistic in a semi–parametric approach. *Portugaliae Mathematica*, 56(3):282–298, 1999.

[69] M. I. Fraga Alves and M. I. Gomes. Statistical choice of extreme value domains of attraction – a comparative analysis. *Communications in Statistics – Theory and Methods*, 25(4):789–811, 1996.

[70] M. Fragoso, R. M. Trigo, J. G. Pinto, S. Lopes, A. Lopes, S. Ulbrich, and C. Magro. The 20 February 2010 Madeira flash-floods: synoptic analysis

and extreme rainfall assessment. *Natural Hazards and Earth System Sciences*, 12(3):715–730, 2012.

[71] M. Fréchet. Sur la loi de probabilité de l'écart maximum. *Annales de la Société Polonaise de Mathématique*, 6:93–116, 1927.

[72] M. Fréchet. Sur les tableaux de corrélation dont les marges sont données. *Annales de l'Université de Lyon. Section A: Sciences mathématiques et astronomie*, 9:53–77, 1951.

[73] W. E. Fuller. Flood flows. *Transactions of the American Society of Civil Engineers*, 77(1293):564–694, 1914.

[74] J. Galambos. Order statistics of samples from multivariate distributions. *Journal of the American Statistical Association*, 70(351a):674–680, 1975.

[75] J. Galambos. A statistical test for extreme value distributions. In B. V. Gnedenko, M. L. Puri, and I. Vineze, editors, *Nonparametric Statistical Inference*, pages 221–230, 1982.

[76] J. Galambos. *The Asymptotic Theory of Extreme Order Statistics*. Krieger, Florida, 2nd edition, 1987.

[77] E. Gargouri–Ellouze and A. Chebchoub. Modelling the dependence structure of rainfall depth and duration by Gumbel's copula. *Hydrological Sciences Journal*, 53(4):802–817, 2008.

[78] J. Geffroy. Contribution à la théorie des valeurs extrêmes (Première partie). *Publications de l'Institut de Statistique de l'Université de Paris*, 7(3-4):37–121, 1958.

[79] J. Geffroy. Contribution à la théorie des valeurs extrêmes (Deuxième partie). *Publications de l'Institut de Statistique de l'Université de Paris*, 8(1):3–65, 1959.

[80] D. Gellens. Combining regional approach and data extension procedure for assessing GEV distribution of extreme precipitation in Belgium. *Journal of Hydrology*, 268(1–4):113–126, 2002.

[81] C. Genest and A.-C. Favre. Everything you always wanted to know about copula modeling but were afraid to ask. *Journal of Hydrologic Engineering*, 12(4):347–368, 2007.

[82] S. Ghosh. Modelling bivariate rainfall distribution and generating bivariate correlated rainfall data in neighbouring meteorological subdivisions using copula. *Hydrological Processes*, 24(24):3558–3567, 2010.

[83] B. Gnedenko. Sur la distribution limite du terme maximum d'une série aléatoire. *Annals of Mathematics*, 44(3):423–453, 1943.

[84] M. I. Gomes. A note on statistical choice of extremal models. In *Actas de las IX Jornadas Matemáticas Hispano-Lusas: Salamanca 12-16 abril 1982, Vol. 1*, pages 653–655, Salamanca, 1982. Ediciones Universidad de Salamanca.

[85] M. I. Gomes. Robustness of Gumbel statistic for distribution functions in the domain of attraction of a type I distribution of largest values. In T. Havranek, Z. Sidak, and M. Novak, editors, *COMPSTAT 1984–Proceedings in Computational Statistics*, pages 61–66, 1984.

[86] M. I. Gomes. Extreme value theory – statistical choice. In P. Révész, K. Sarkadi, and P. K. Sen, editors, *Goodness–of–fit (Colloquia mathematica Societatis János Bolyai 45)*, pages 195–209. North–Holland Pub. Co., 1987.

[87] M. I. Gomes, M. I. Fraga Alves, and C. Neves. *Análise de Valores Extremos: Uma introdução*. Sociedade Portuguesa de Estatística, Lisboa, 2013.

[88] M. I. Gomes, L. Canto e Castro, M. I. Fraga Alves, and D. Pestana. Statistics of extremes for IID data and breakthroughs in the estimation of the extreme value index: Laurens de Haan leading contributions. *Extremes*, 11(1):3–34, 2008.

[89] M. I. Gomes and O. Oliveira. The bootstrap methodology in statistics of extremes - choice of the optimal sample fraction. *Extremes*, 4(4):331–358, 2001.

[90] M.I. Gomes and M. A. J. van Montfort. Exponentiality versus generalized Pareto-quick tests. In K. Cehak, editor, *Third International Conference on Statistical Climatology*, pages 185–195, Vienna, 1987.

[91] A. B. Gonçalves and R. S. Nunes. *Ilhas de Zargo (Adenda)*. Câmara Municipal do Funchal, 1990.

[92] D. Gouveia, L. Guerreiro Lopes, and S. Mendonça. Application of the theory of extremes to the study of precipitation in Madeira Island: Statistical choice of extreme domains of attraction. In A. Pacheco, R. Santos, M. R.

Oliveira, and C. D. Paulino, editors, *New Advances in Statistical Modeling and Applications*, Studies in Theoretical and Applied Statistics Societies, pages 187–195. Springer, 2014.

[93] D. Gouveia–Reis, L. Guerreiro Lopes, and S. Mendonça. Modelling annual maxima of daily rainfall in Madeira Island. In J. Jensen, editor, *Proceedings of the 1st International Short Conference on Advances in Extreme Value Analysis and Application to Natural Hazards*, pages 136–143. Institute of Advances Studies, University of Siegen, 2013.

[94] D. Gouveia–Reis, L. Guerreiro Lopes, and S. Mendonça. A spatial extremes characterization of the annual maxima precipitation in Madeira Island. In *Workshop EVT2013 - Extremes in Vimeiro Today*. Notas e Comunicações do CEAUL 19/13, Universidade de Lisboa, 2013.

[95] D. Gouveia–Reis, L. Guerreiro Lopes, and S. Mendonça. Um estudo da dependência entre extremos de precipitação na Ilha da Madeira. In M. Maia, P. Campos, and P. D. Silva, editors, *Estatística: Novos Desenvolvimentos e Inspirações - Actas do XX Congresso da Sociedade Portuguesa de Estatística*, pages 167–174. Sociedade Portuguesa de Estatística, 2013.

[96] M. E. Graça Martins and D. D. Pestana. Nonstable limit laws in extreme value theory. In M. L. Puri, J. P. Vilaplana, and W. Wertz, editors, *New Perspectives in Theoretical and Applied Statistics*, pages 449–457. Wiley, 1987.

[97] M. E. Graça Martins and D. D. Pestana. The extremal limit theorem — extensions. In W. Grossman, J. Mogyoródi, I. Vincze, and W. Wertz, editors, *Probability Theory and Mathematical Statistics with Applications*, pages 143–153. D. Reidel, 1988.

[98] J. A. Greenwood, J. M. Landwehr, N. C. Matalas, and J.R. Wallis. Probability weighted moments: definition and relation to parameters of several distributions expressable in inverse form. *Water Resources Research*, 15(5):1049–1054, 1979.

[99] M. Greenwood. The statistical study of infectious diseases. *Journal of the Royal Statistical Society*, 109(2):85–109, 1946.

[100] A. A. Griffith. The phenomena of rupture and flow in solids. *Philosophical Transactions of the Royal Society A*, 221(582-593):163–198, 1921.

[101] G. Gudendorf and J. Segers. Lecture notes in statistics. In P. Jaworski, F. Durante, W. K. Härdle, and T. Rychlik, editors, *Copula Theory and Its Applications*, chapter Extreme–Value Copulas, pages 127–145. Springer, 2010.

[102] E. J. Gumbel. The return period of flood flows. *The Annals of Mathematical Statistics*, 12(2):163–190, 1941.

[103] E. J. Gumbel. On the frequency distribution of extreme values in meteorological data. *Bulletin of the American Meteorological Society*, 23(3):95–104, 1942.

[104] E. J. Gumbel. On the plotting of flood discharges. *Transactions, American Geophysical Union*, 24(2):699–719, 1944.

[105] E. J. Gumbel. Floods estimated by probability methods. *Engineering News Record*, 134:97–101, 1945.

[106] E. J. Gumbel. *Statistical Theory of Extreme Values and Some Practical Applications*, volume 33 of *Applied Mathematical Series*. U. S. Department of Commerce, National Bureau of Standards, 1st edition, 1954.

[107] E. J. Gumbel. *Statistics of Extremes*. Columbia Univ. Press, 1958.

[108] E. J. Gumbel. Bivariate exponential distributions. *Journal of the American Statistical Association*, 55(292):698–707, 1960.

[109] E. J. Gumbel. Bivariate logistic distributions. *Journal of the American Statistical Association*, 56(294):335–349, 1961.

[110] E. J. Gumbel and N. Goldstein. Analysis of empirical bivariate extremal distributions. *Journal of the American Statistical Association*, 59(307):794–816, 1964.

[111] P. Hall. Using the bootstrap to estimate means squared error and select smoothing parameter in nonparametric problems. *Journal of Multivariate Analysis*, 32(2):177–203, 1990.

[112] P. Hall and A. H. Welsh. Adaptive estimates of parameters of regular variation. *The Annals of Statistics*, 13(1):331–341, 1985.

[113] A. M. Hasofer and Z. Wang. A test for extreme value domain of attraction. *Journal of the American Statistical Association*, 87(417):171–177, 1992.

[114] D. Hayward and R. T. Clarke. Relationship between rainfall, altitude and distance from the sea in the Freetown Peninsula, Sierra Leone. *Hydrological Sciences Journal*, 41(3):377–384, 1996.

[115] B. M. Hill. A simple general approach to inference about the tail of a distribution. *Annals of Statistics*, 3(5):1163–1174, 1975.

[116] W. Hoeffding. Scale–invariant correlation measures for discontinuous distributions. In N. L. Fisher and P. K. Sen, editors, *The Collected Works of Wassily Hoeffding*, pages 109–133. Springer, 1994.

[117] W. Hoeffding. Scale–invariant correlation theory. In N. L. Fisher and P. K. Sen, editors, *The Collected Works of Wassily Hoeffding*, pages 57–107. Springer, 1994.

[118] J. R. M. Hosking. Testing whether the shape parameter is zero in the generalized extreme-value distribution. *Biometrika*, 71(2):367–374, 1984.

[119] J. R. M. Hosking, J. R. Wallis, and E. F. Wood. Estimation of the generalized extreme-value distribution by the method of probability-weighted moments. *Technometrics*, 27(3):251–261, 1985.

[120] J. Hüsler and D. Li. On testing extreme value conditions. *Extremes*, 9(1):69–86, 2006.

[121] A. F. Jenkinson. The frequency distribution of annual maximum (or minimum) values of meteorological elements. *Quarterly Journal of the Royal Meteorological Society*, 81(348):158–171, 1955.

[122] H. Joe. Multivariate extreme value distributions with applications to environmental data. *Canadian Journal of Statistics*, 22(1):47–64, 1994.

[123] M. L. Juncosa. The asymptotic behavior of the minimum in a sequence of random variables. *Duke Mathematical Journal*, 16(4):609–618, 1949.

[124] R. W. Katz, M. B. Parlange, and P. Naveau. Statistics of extremes in hydrology. *Advances in Water Resources*, 25(8-12):1287–1304, 2002.

[125] M. G. Kendall. A new measure of rank correlation. *Biometrika*, 30(1/2):81–93, 1938.

[126] G. Kimeldorf and A. Sampson. Uniform representations of bivariate distributions. *Communications in Statistics*, 4(7):617–627, 1975.

[127] C. E. Konrad II. Relationships between precipitation event types and topography in the southern Blue Ridge Mountains of the southeastern USA. *International Journal of Climatology*, 16(1):49–62, 1996.

[128] S. Kotz and S. Nadarajah. *Extreme Value Distributions, Theory and Applications*. Imperial College Press, 2000.

[129] D. Koutsoyiannis. On the appropriateness of the Gumbel distribution for modelling extreme rainfall. In A. Brath, A. Montanari, and E. Toth, editors, *Hydrological Risk: recent advances in peak river flow modelling, prediction and real-time forecasting. Assessment of the impacts of land–use and climate changes*, pages 303–319, Castrolibero, Italy, 2004.

[130] D. Koutsoyiannis. Statistics of extremes and estimation of extreme rainfall: I. Theoretical Investigation. *Hydrological Sciences Journal*, 49(4):575–590, 2004.

[131] D. Koutsoyiannis. Statistics of extremes and estimation of extreme rainfall: II. Empirical investigation of long rainfall records. *Hydrological Sciences Journal*, 49(4):591–610, 2004.

[132] D. Koutsoyiannis and G. Baloutsos. Analysis of a long record of annual maximum rainfall in Athens, Greece, and design rainfall inferences. *Natural Hazards*, 22(1):29–48, 2000.

[133] J. M. Landwehr, N. C. Matalas, and J. R. Wallis. Probability weighted moments compared with some traditional techniques in estimating Gumbel parameters and quantiles. *Water Resources Research*, 15(5):1055–1064, 1979.

[134] M. Lang, T. B. M. J. Ouarda, and B. Bobée. Towards operational guidelines for over-threshold modeling. *Journal of Hydrology*, 225(3–4):103–117, 1999.

[135] M. R. Leadbetter. On a basis for 'peaks over threshold' modeling. *Statistics & Probability Letters*, 12(4):357–362, 1991.

[136] M. R. Leadbetter and H. Rootzén. Extremal theory for stochastic processes. *The Annals of Probability*, 16(2):431–478, 1988.

[137] D. P. Lettenmaier and S. J. Burges. Gumbel's extreme value I distribution: a new look. *Journal of the Hydraulics Division*, 108(4):502–514, 1982.

[138] X. Li, P. Mikusiński, and M. D. Taylor. Some integration by parts formulas involving 2-copulas. In C. M. Cuadras, J. Fortiana, and J. A. Rodríguez-Lallena, editors, *Distributions With Given Marginals and Statistical Modelling*, pages 153–159, Dordrecht, 2002. Kluwer.

[139] T. Luna, A. Rocha, A. C. Carvalho, J. A. Ferreira, and J. Sousa. Modelling the extreme precipitation event over Madeira Island on 20 February 2010. *Natural Hazards and Earth System Sciences*, 11(9):2437–2452, 2011.

[140] M. B. Marcus and M. Pinsky. On the domain of attraction of $e^{-e^{-x}}$. *Journal of Mathematical Analysis and Applications*, 28(2):440–449, 1969.

[141] F. Marohn. On testing the exponential and Gumbel distribution. In J. Galambos, J. Lechner, and E. Simiu, editors, *Extreme Value Theory and Applications*, pages 159–174. Kluwer, 1994.

[142] F. Marohn. An adaptive efficient test for Gumbel domain of attraction. *Scandinavian Journal of Statistics*, 25(2):311–324, 1998.

[143] F. Marohn. Testing the Gumbel hypothesis via the POT-method. *Extremes*, 1(2):191–213, 1998.

[144] F. Marohn. Testing extreme value models. *Extremes*, 3(4):363–384, 2000.

[145] A. W. Marshall and I. Olkin. A multivariate exponential distribution. *Journal of the American Statistical Association*, 62(317):30–44, 1967.

[146] E. S. Martins and J. R. Stedinger. Generalized maximum-likelihood generalized extreme-value quantile estimators for hydrologic data. *Water Resources Research*, 36(3):737–744, 2000.

[147] D. Mejzler. On a theorem of B. V. Gnedenko (in Russian). *Sb. Trudov Inst. Mat. Akad. Nauk. Ukrain.*, 12:31–35, 1949.

[148] D. Mejzler. On the problem of the limit distributions for the maximal term of a variational series (in Russian). *L'vov. Politechn. Inst. Naučn. Zap., Ser. Fiz.-Mat.*, 38:90–109, 1956.

[149] D. Mejzler. On a certain class of limit distributions and their domain of attraction. *Transactions of the American Mathematical Society*, 117:205–236, 1965.

[150] D. Mejzler. Limit distributions for the extreme order statistics. *Canadian Mathematical Bulletin*, 21(4):447–459, 1978.

[151] D. Mejzler. Asymptotic behaviour of the extreme order statistics in the non identically distributed case. In J. Tiago de Oliveira, editor, *Statistical Extremes and Applications*, pages 535–547. Springer Netherlands, 1984.

[152] D. Mejzler. Extreme value limit laws in the nonidentically distributed case. *Israel Journal of Mathematics*, 57(1):1–27, 1987.

[153] V. G. Mikhailov. Asymptotic independence of vector components of multivariate extreme order statistics. *Teor. Veroyatnost. i Primenen.*, 19:849–853, 1974. (Translation: Theory of Probability & Its Applications, 19(4):817-821, 1975).

[154] S. Nadarajah and D. Choi. Maximum daily rainfall in South Korea. *Journal of Earth System Science*, 116(4):311–320, 2007.

[155] R. B. Nelsen. Concordance and copulas: A survey. In C. M. Cuadras, J. Fortiana, and J. A. Rodríguez-Lallena, editors, *Distributions with given marginals and statistical modelling*, pages 169–177. Kluwer, 2002.

[156] R. B. Nelsen. *An Introduction to Copulas*. Springer, 2nd edition, 2006.

[157] NERC. Flood studies report. Technical report, Natural Environment Research Council, Wallingford, UK, 1975.

[158] C. Neves and M. I. Fraga Alves. Reiss and Thomas' automatic selection of the number of extremes. *Computational Statistics & Data Analysis*, 47(4):689–704, 2004.

[159] C. Neves and M. I. Fraga Alves. Semi-parametric approach to the Hasofer-Wang and Greenwood statistics in extremes. *TEST*, 16(2):297–313, 2007.

[160] C. Neves and M. I. Fraga Alves. Testing extreme value conditions – an overview and recent approaches. *REVSTAT*, 6(1):83–100, 2008.

[161] C. Neves, J. Picek, and M. I. Fraga Alves. The contribution of the maximum to the sum of excesses for testing max-domains of attraction. *Journal of Statistical Planning and Inference*, 136(4):1281–1301, 2006.

[162] H. T. Nguyen, T. Wiatr, T. M. Fernández-Steeger, K. Reicherter, D. M. M. Rodrigues, and R. Azzam. Landslide hazard and cascading effects following the extreme rainfall event on Madeira Island (February 2010). *Natural Hazards*, 65(1):635–652, 2013.

[163] V. T. V. Nguyen, T. D. Nguyen, and F. Ashkar. Regional frequency analysis of extreme rainfalls. *Water Science and Technology*, 45(2):75–81, 2002.

[164] J. M. Nordquist. Theory of largest values, applied to earthquake magnitudes. *Transactions, American Geophysical Union*, 26(1):29–31, 1945.

[165] A. Obrenetov. On the dependence function of Sibuya in multivariate extreme value theory. *Journal of Multivariate Analysis*, 36(1):35–43, 1991.

[166] A. Otten and M. A. J. van Montfort. The power of two tests on the type of distributions of extremes. *Journal of Hydrology*, 37(1-2):195–199, 1978.

[167] B. Peirce. Criterion for the rejection of doubtful observations. *Astronomical Journal*, 2(45):161–163, 1852.

[168] F. T. Peirce. 32–X.–Tensile tests for cotton yarns V.–"The Weakest Link" theorems on the strength of long and of composite specimens. *Journal of the Textile Institute Transactions*, 17(7):355–368, 1926.

[169] E. C. N. Pereira. *Ilhas de Zargo*, volume I. Câmara Municipal do Funchal, 4th edition, 1989.

[170] D. D. Pestana and S. Mendonça. Higher-order monotone functions and probability theory. In N. Hadjisavvas, J. Martínez-Legaz, and J.-P. Penot, editors, *Generalized Convexity and Generalized Monotonicity*, pages 317–331. Springer Berlin Heidelberg, 2001.

[171] J. Pickands III. Statistical inference using extreme order statistics. *The Annals of Statistics*, 3(1):119–131, 1975.

[172] J. Pickands III. Multivariate extreme value distributions. Technical report, University of Pennsylvania, 1976.

[173] J. Pickands III. Multivariate extreme value distributions. In *Proceedings of the 43rd Session of the International Statistical Institute*, pages 859–878. International Statistical Institute, 1981.

[174] W. D. Potter. Effect of rainfall on magnitude and frequency of peak rates of surface runnoff. *Transactions, American Geophysical Union*, 30(5):735–751, 1949.

[175] S. Prada. *Geologia e Recursos Hídricos Subterrâneos da Ilha da Madeira*. PhD thesis, Universidade da Madeira, 2000.

[176] S. Prada, M. M. Sequeira, C. Figueira, and M. O. da Silva. Fog precipitation and rainfall interception in the natural forests of Madeira Island (Portugal). *Agricultural and Forest Meteorology*, 149(6–7):1179–1187, 2009.

[177] R. Quintal. Aluviões da Madeira; Séculos XIX e XX. *Territorium*, 6:31–48, 1999.

[178] R Development Core Team. *R: A Language and Environment for Statistical Computing*. R Foundation for Statistical Computing, Vienna, Austria, 2011.

[179] R.-D. Reiss and M. Thomas. *Statistical Analysis of Extreme Values with Applications to Insurance, Finance, Hydrology and Other Fields*. Birkhäuser, 3rd edition, 2007.

[180] M. Ribatet and M. Sedki. Extreme value copulas and max–stable processes. *Journal de la Société Française de Statistique*, 154(1):138–150, 2013.

[181] G. Salvadori and C. De Michele. Statistical characterization of temporal structure of storms. *Advances in Water Resources*, 29(6):827–842, 2006.

[182] G. Salvadori, C. De Michele, N. T. Kottegoda, and R. Rosso. *Extremes in Nature: An Approach Using Copulas*. Springer, 2007.

[183] C. Scarrott and A. MacDonald. A review of extreme value threshold estimation and uncertainty quantification. *REVSTAT*, 10(1):33–60, 2012.

[184] M. Schlather. Models for stationary max–stable random fields. *Extremes*, 5(1):33–44, 2002.

[185] M. Schlather and J. Tawn. A dependence measure for multivariate and spatial extreme values: Properties and inference. *Biometrika*, 90(1):139–156, 2003.

[186] F. W. Scholz and M. A. Stephens. K-sample Anderson-Darling tests. *Journal of the American Statistical Association*, 82(399):918–924, 1987.

[187] B. Schweizer and E. F. Wolf. On nonparametric measures of dependence for random variables. *The Annals of Statistics*, 9(4):879–885, 1981.

[188] J. Segers and J. Teugels. Testing the Gumbel hypothesis by Galton's ratio. *Extremes*, 3(3):291–303, 2000.

[189] F. Serinaldi. Copula-based mixed models for bivariate rainfall data: an empirical study in regression perspective. *Stochastic Environmental Research and Risk Assessment*, 23(5):677–693, 2009.

[190] B. Sevruk and H. Geiger. Selection of distribution types for extremes of precipitation. Operational hydrology report. *World Meteorological Organization Series*, 560, 1981.

[191] M. Sibuya. Bivariate extreme statistics, I. *Annals of the Institute of Statistical Mathematics*, 11(2):195–210, 1959.

[192] F. A. S. Silva and C. A. Menezes. *Elucidário Madeirense*, volume I/III. DRAC, Funchal, 1945.

[193] S. A. Sisson, L. R. Pericchi, and S. G. Coles. A case for a reassessment of the risks of extreme hydrological hazards in the Caribbean. *Stochastic Environmental Research and Risk Assessment*, 20(4):296–306, 2006.

[194] A. Sklar. Fonctions de répartition à n dimensions et leurs marges. *Publications de l' Institut de Statistique de l' Université de Paris*, 8:229–231, 1959.

[195] R. L. Smith. Threshold methods for sample extremes. In Tiago de Oliveira, editor, *Statistical Extremes and Applications*, pages 621–638. D. Reidel, 1984.

[196] R. L. Smith. Extreme value analysis of environmental time series: An application to trend detection in ground-level ozone. *Statistical Science*, 4(4):367–377, 1989.

[197] R. L. Smith. Max–stable processes and spatial extremes. Unpublished manuscript. http://www.stat.unc.edu/postscript/rs/spatex.pdf, 1990.

[198] R. Sneyers. *L'intensité maximale des précipitations en Belgique*. Institut Royal Météorologique de Belgique, 1977.

[199] R. Sneyers. *L'intensité et la durée maximales des précipitations en Belgique*. Institut Royal Météorologique de Belgique, 1979.

[200] M. A. Stephens. Goodness of fit for the extreme value distribution. *Biometrika*, 64(3):583–588, 1977.

[201] J. Tawn. Applications of multivariate extremes. In J. Galambos, J. Lechner, and E. Simiu, editors, *Extreme Value Theory and Applications*, pages 249–268. Kluwer, 1994.

[202] J. Tiago de Oliveira. Extremal distributions. *Revista da Faculdade de Ciências de Lisboa A*, 7:215–227, 1958.

[203] J. Tiago de Oliveira. La représentation des distributions extrêmales bivariées. In *Bulletin de l'Institut International de Statistique, Actes de la 33e Session*, pages 477–480, 1962.

[204] J. Tiago de Oliveira. Structure theory of bivariate extremes: extensions. *Estudos de Matemática, Estatística e Econometria*, 7:165–195, 1962/63.

[205] J. Tiago de Oliveira. Biextremal distributions: statistical decision. *Trabajos de Estadística y de Investigación Operativa*, 21:107–117, 1970.

[206] J. Tiago de Oliveira. A new model of bivariate extremes: Statistical decision. In *Studi di Probabilità Statistica e Ricerca Operativa in Onore di Giuseppe Pompili*, pages 1–13, Oderisi, Gubbio, 1971.

[207] J. Tiago de Oliveira. Regression in the nondifferentiable bivariate extreme models. *Journal of the American Statistical Association*, 69:816–818, 1974.

[208] J. Tiago de Oliveira. Statistical choice of univariate extreme models. In C. Taillie, G. P. Patil, and B. A. Baldessari, editors, *Statistical Distributions in Scientific Work, Volume 6 – Applications in Physical, Social, and Life Sciences*, pages 367–387, Dordrecht, 1981. D. Reidel.

[209] J. Tiago de Oliveira. *Statistical Extremes and Applications*, volume 131 of *NATO Advanced Science Institutes Series C: Mathematical and Physical Sciences*. D. Reidel, 1984.

[210] J. Tiago de Oliveira. Univariate extremes; statistical choice. In Tiago de Oliveira, editor, *Statistical Extremes and Applications*, pages 91–107. D. Reidel, 1984.

[211] J. Tiago de Oliveira. Extreme values and meteorology. *Journal of Theoretical and Applied Climatology*, 37(4):184–193, 1986.

[212] J. Tiago de Oliveira. *Statistical Analysis of Extremes*. Pendor, Évora, Portugal, 1997.

[213] J. Tiago de Oliveira and M. I. Gomes. Two tests statistics for choice of univariate extreme models. In J. Tiago de Oliveira, editor, *Statistical Extremes and Applications*, pages 651–668. D. Reidel, 1984.

[214] M. A. J. van Montfort. On testing that the distribution of extremes is of type I when type II is the alternative. *Journal of Hydrology*, 11(4):421–427, 1970.

[215] M. A. J. van Montfort. An asymmetric test on the type of the distribution of extremes. *Mededelingen Landbouwhogeschool*, 73(18):1–15, 1973.

[216] M. A. J. van Montfort and J. V. Witter. Testing exponentiality against generalised Pareto distribution. *Journal of Hydrology*, 78(3-4):305–315, 1985.

[217] C. J. Velz. Factors influencing self-purification and their relation to pollution abatement. *Sewage Works Journal*, 19(4):629–644, 1947.

[218] L. von Bortkiewicz. Variationsbreite und mittlerer fehler. *Sitzungsberichte der Berliner Mathematische Gesellschaft*, 21:3–11, 1922.

[219] R. von Mises. La distribution de la plus grande de n valeurs. *Revue Mathématique de l'Union Interbalkanique*, 1:141–160, 1936.

[220] R. von Mises. La distribution de la plus grande de n valeurs. In *Selected Papers II*, pages 271–294. American Mathematical Society, 1954. (Reprint).

[221] W. Weibull. The phenomenon of rupture in solids. *Ingeniörs Vetenskaps Akademien-Handlingar*, 153, 1939.

[222] W. Weibull. A statistical theory of the strength of materials. *Ingeniörs Vetenskaps Akademien-Handlingar*, 151, 1939.

[223] D. S. Wilks. Comparison of three–parameter probability distributions for representing annual extreme and partial duration precipitation series. *Water Resources Research*, 29(10):3543–3549, 1993.

[224] G. E. Willeke, J. R. M. Hosking, J. R. Wallis, and N. B. Guttman. *The national drought atlas (draft)*. Institute for Water Resources Report 94–NSD–4, U. S. Army Corps of Engineers, 1995.

[225] C. S. Withers and S. Nadarajah. Evidence of trend in return levels for daily rainfall in New Zealand. *Journal of Hidrology (New Zealand)*, 39:155–166, 2000.

Appendix

Appendix A

Diagnostic plots for annual maxima – Dataset I

Diagnostic plots for the Gumbel and GEV fits

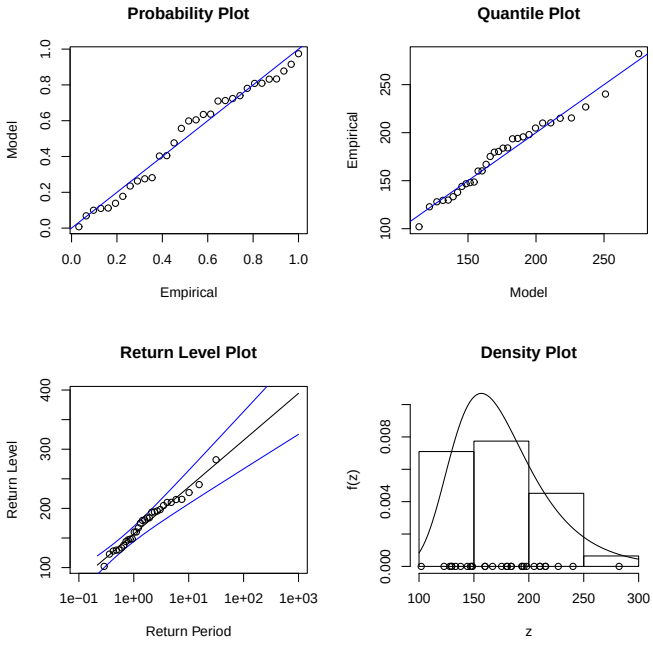

Figure A.1: Diagnostic plots for Gumbel fit to the Areeiro (A) station data–Dataset I.

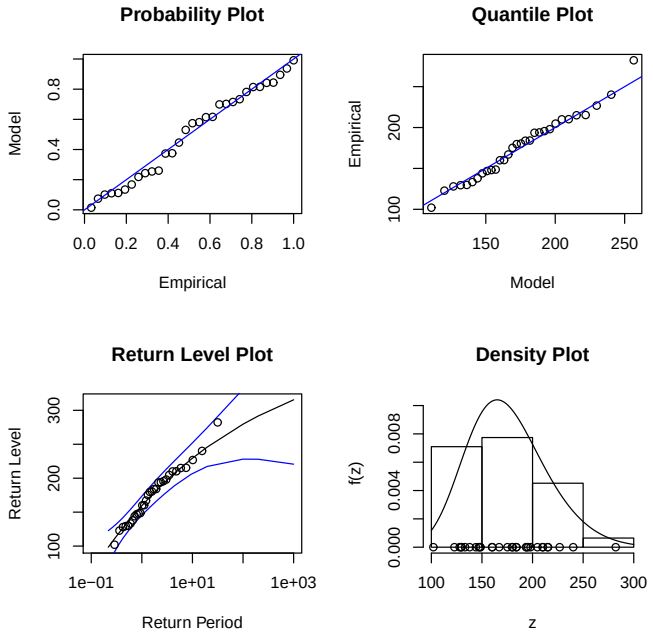

Figure A.2: Diagnostic plots for GEV fit to the Areeiro (A) station data–Dataset I.

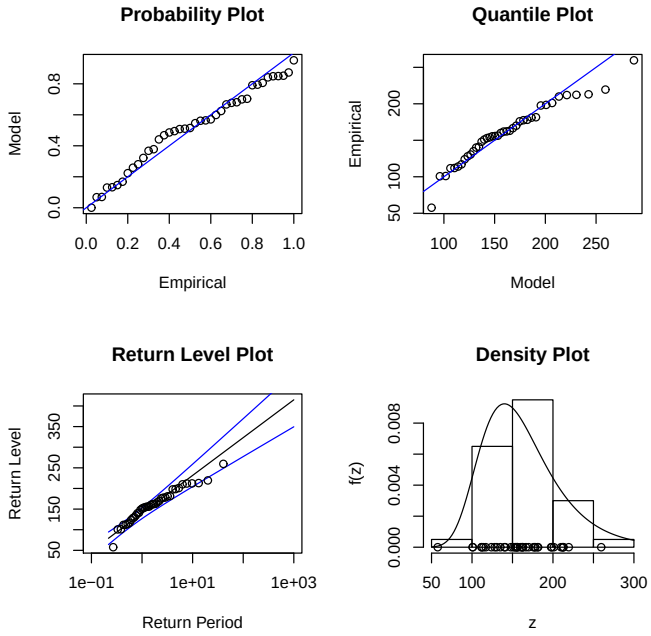

Figure A.3: Diagnostic plots for Gumbel fit to the Bica da Cana (B) station data–Dataset I.

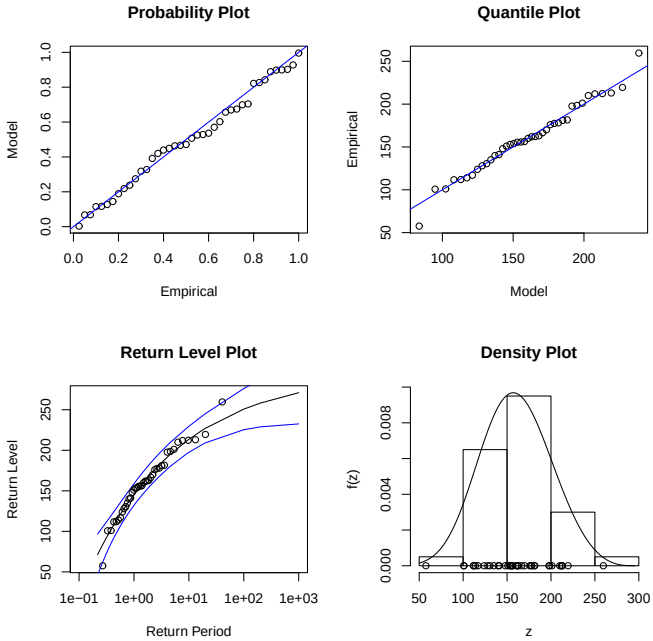

Figure A.4: Diagnostic plots for GEV fit to the Bica da Cana (B) station data–Dataset I.

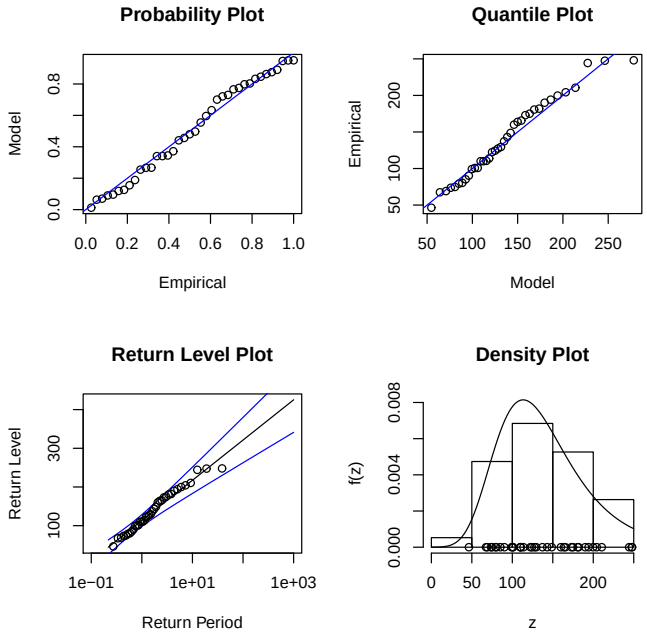

Figure A.5: Diagnostic plots for Gumbel fit to the Santo da Serra (I) station data– Dataset I.

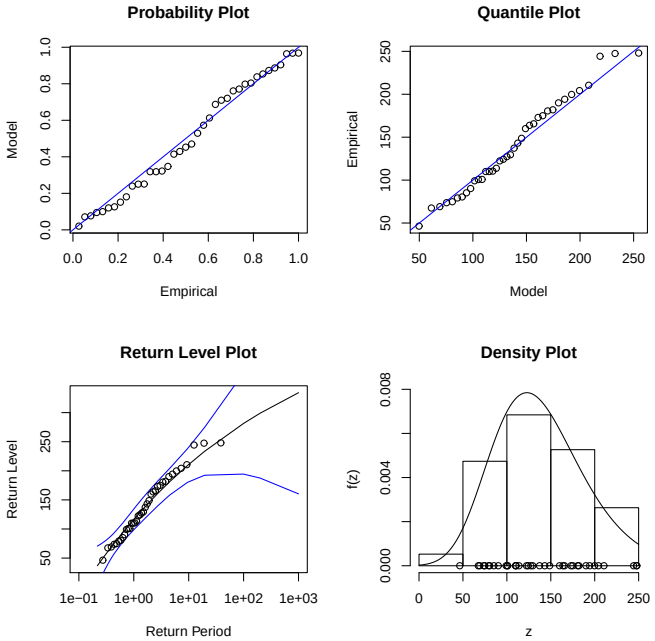

Figure A.6: Diagnostic plots for GEV fit to the Santo da Serra (I) station data– Dataset I.

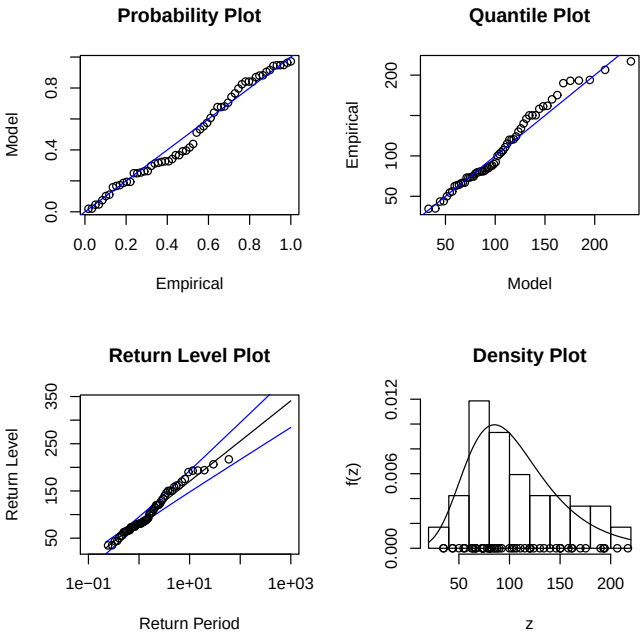

Figure A.7: Diagnostic plots for Gumbel fit to the Santana (P) station data–Dataset I.

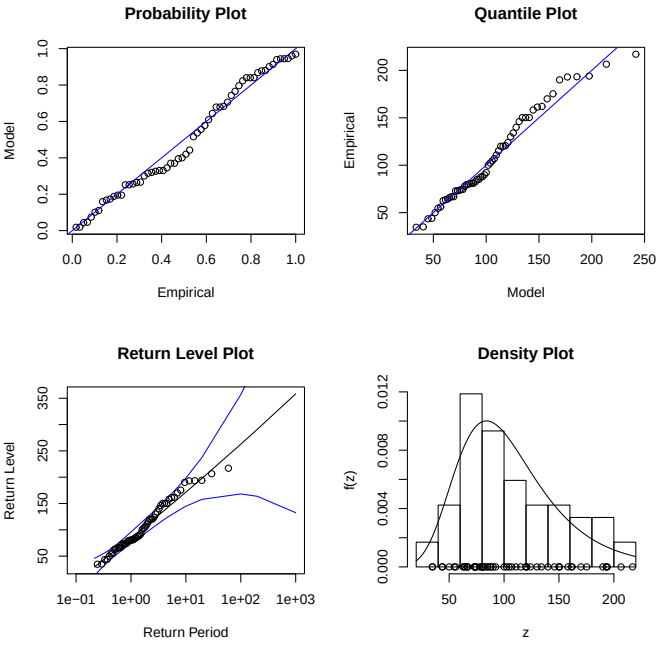

Figure A.8: Diagnostic plots for GEV fit to the Santana (P) station data–Dataset I.

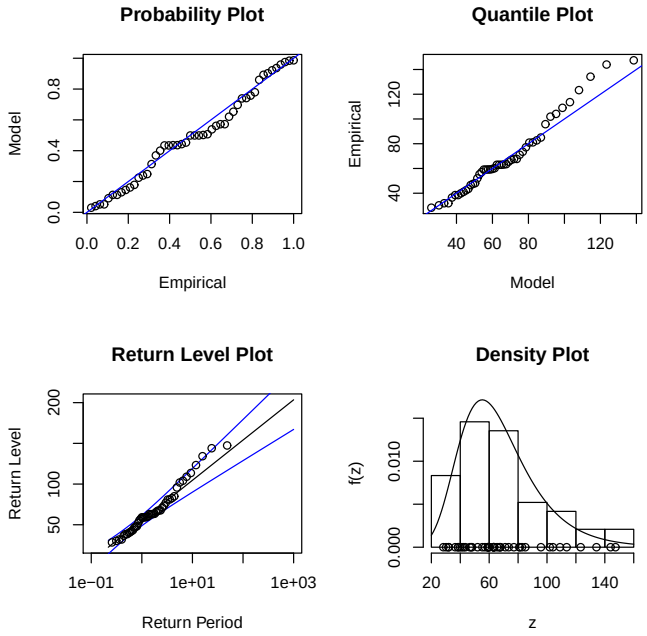

Figure A.9: Diagnostic plots for Gumbel fit to the Santa Catarina (V) station data– Dataset I.

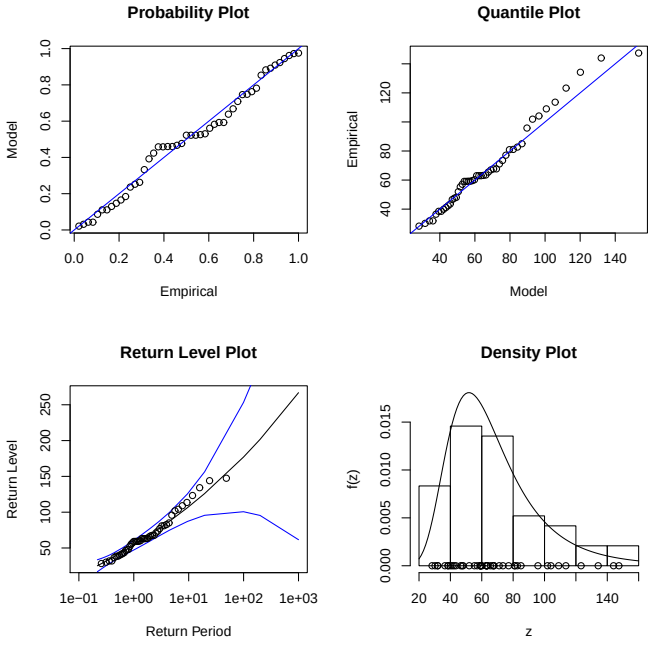

Figure A.10: Diagnostic plots for GEV fit to the Santa Catarina (V) station data– Dataset I.

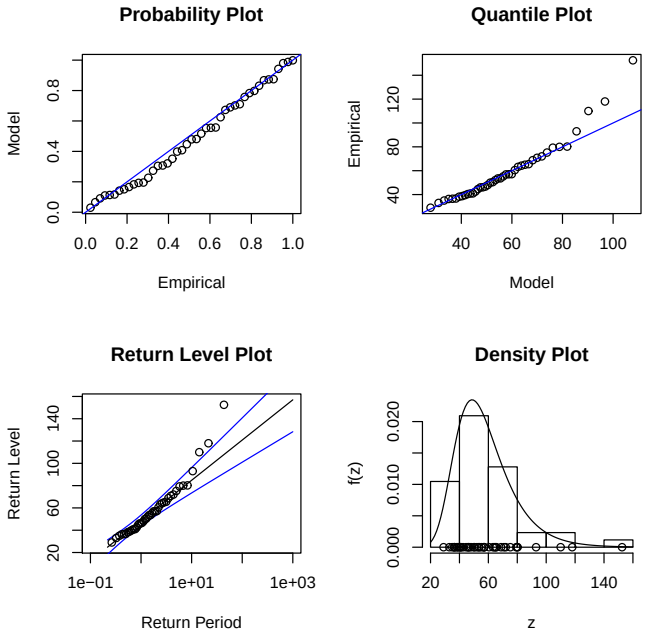

Figure A.11: Diagnostic plots for Gumbel fit to the Lugar de Baixo (X) station data–Dataset I.

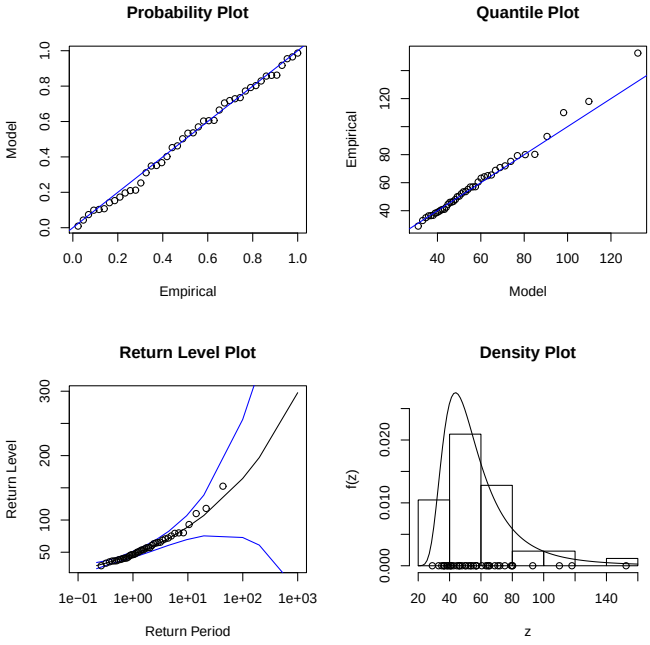

Figure A.12: Diagnostic plots for GEV fit to the Lugar de Baixo (X) station data–Dataset I.

Appendix B

Likelihood ratio tests's p–values – Datasets II and I+II

Table B.1: p–values for the likelihood ratio tests for A to G stations data–Dataset II.

H_0	H_1	A	B	C	D	E	F	G
Model 1	Model 3	0.1750	0.2515	0.5284	0.3195	0.3409	0.3084	0.1720
Model 1	Model 5	1.0000	0.0003	1.0000	1.0000	1.0000	1.0000	0.0273
Model 1	Model 7	0.5525	0.0002	1.0000	0.6581	1.0000	1.0000	0.0698
Model 2	Model 1	0.2670	0.1969	0.6069	0.2165	0.0726	0.8865	0.0409
Model 2	Model 4	0.3764	0.6499	0.5231	0.4599	0.2314	0.3302	0.4447
Model 2	Model 6	0.4661	0.0005	1.0000	0.6145	0.3887	0.6037	0.7080
Model 2	Model 8	0.2269	0.0003	0.9423	0.9024	0.4718	1.0000	0.0630

Table B.2: p–values for the likelihood ratio tests for H to N stations data–Dataset II.

H_0	H_1	H	I	J	K	L	M	N
Model 1	Model 3	0.5915	0.0826	0.0824	0.0101	0.1757	0.0046	0.0276
Model 1	Model 5	1.0000	1.0000	1.0000	0.0089	0.7318	0.0556	0.1667
Model 1	Model 7	0.6384	1.0000	1.0000	1.0000	1.0000	1.0000	1.0000
Model 2	Model 1	0.0132	0.0127	0.0335	0.0021	0.8723	0.0802	0.0534
Model 2	Model 4	0.1806	0.0583	0.3414	0.5389	0.1839	0.0010	0.2849
Model 2	Model 6	0.4158	0.7084	0.2323	0.8836	0.7050	0.0095	0.6276
Model 2	Model 8	0.5871	0.1021	0.3759	0.5649	0.3952	0.0027	0.5644

Table B.3: p–values for the likelihood ratio tests for O to U stations data–Dataset II.

H_0	H_1	O	P	Q	R	S	T	U
Model 1	Model 3	0.1263	0.3268	0.9096	0.5679	0.0389	0.8988	0.8150
Model 1	Model 5	0.2059	1.0000	1.0000	1.0000	1.0000	0.9233	1.0000
Model 1	Model 7	1.0000	1.0000	1.0000	0.8267	1.0000	1.0000	1.0000
Model 2	Model 1	0.8853	0.6648	0.3196	0.1828	0.9181	0.0495	0.6665
Model 2	Model 4	0.1502	0.4992	0.9613	0.5304	0.0589	0.8757	0.9430
Model 2	Model 6	0.2039	0.3607	0.4109	0.7551	0.1891	0.6081	0.1363
Model 2	Model 8	1.0000	0.6518	0.5858	0.8093	0.1679	0.8660	0.1955

Table B.4: p–values for the likelihood ratio tests for V to Y stations data–Dataset II.

H_0	H_1	V	W	X	Y
Model 1	Model 3	0.5402	0.0005	0.2161	0.0083
Model 1	Model 5	0.7259	0.0000	0.0288	0.0240
Model 1	Model 7	0.5710	0.5394	0.2261	0.0259
Model 2	Model 1	0.6210	0.0937	0.3635	0.6593
Model 2	Model 4	0.6247	0.2713	0.1249	0.0381
Model 2	Model 6	0.7254	0.9255	0.0211	0.0245
Model 2	Model 8	0.5404	0.2356	0.0690	0.0402

Table B.5: p–values for the likelihood ratio tests for each station data–Dataset I+II.

H_0	H_1	A	B	I	P	U	V	X
Model 1	Model 3	0.1171	0.1381	0.6048	0.5751	0.1449	0.5922	0.0739
Model 1	Model 5	1.0000	1.0000	1.0000	1.0000	0.4517	0.1089	0.2794
Model 1	Model 7	0.2119	0.4993	1.0000	1.0000	1.0000	0.3368	0.2986
Model 2	Model 1	0.4829	0.0347	0.2232	0.8645	0.4520	0.3125	0.2592
Model 2	Model 4	0.3037	0.3369	0.7167	0.5866	0.1159	0.8393	0.1246
Model 2	Model 6	0.0557	0.0980	0.8155	0.5554	0.4378	0.0620	0.8364
Model 2	Model 8	0.1509	0.0916	0.8332	1.0000	0.2570	0.1486	0.2459

Appendix C

Diagnostic plots for annual maxima – Dataset II (Class 1)

Diagnostic plots for the Gumbel and GEV fits for the stations with altitude above 900 m

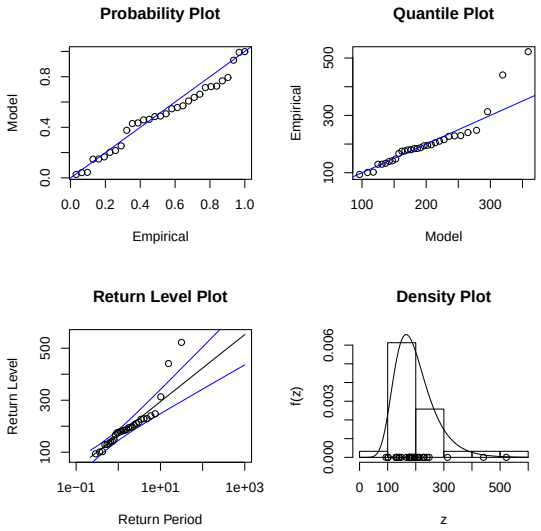

Figure C.1: Diagnostic plots for Gumbel fit to the Areeiro (A) station data–Dataset II.

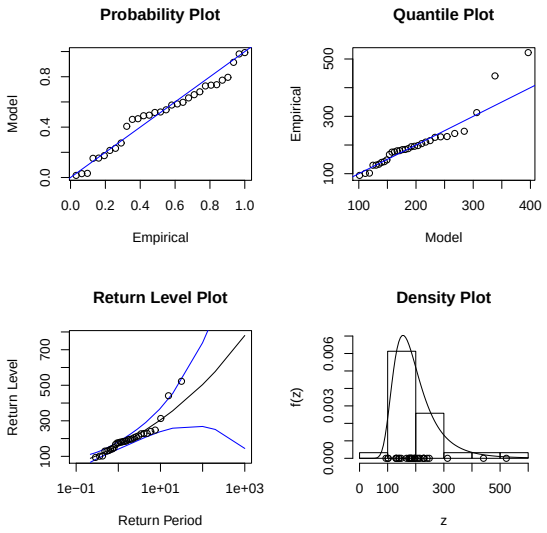

Figure C.2: Diagnostic plots for GEV fit to the Areeiro (A) station data–Dataset II.

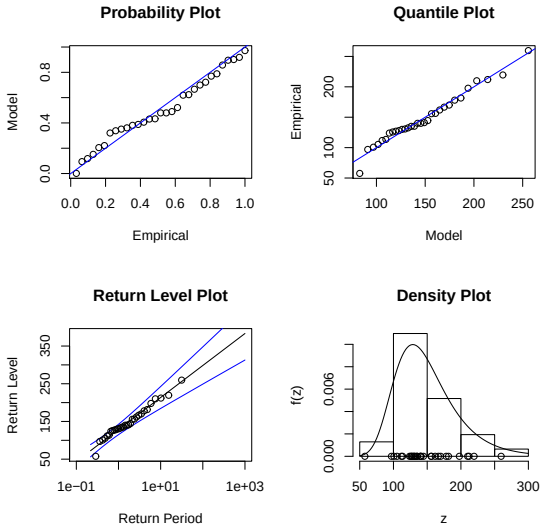

Figure C.3: Diagnostic plots for Gumbel fit to the Bica da Cana (B) station data–Dataset II.

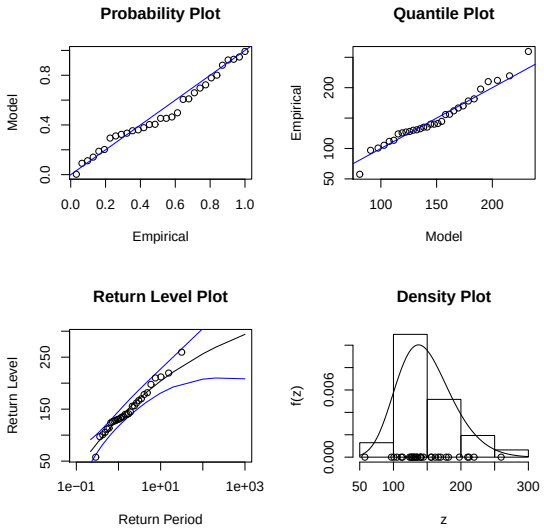

Figure C.4: Diagnostic plots for GEV fit to the Bica da Cana (B) station data–Dataset II.

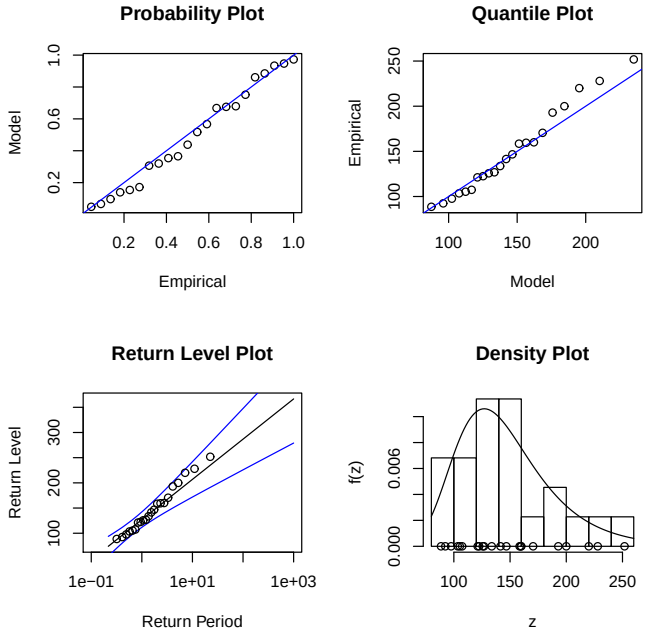

Figure C.5: Diagnostic plots for Gumbel fit to the Poiso (C) station data–Dataset II.

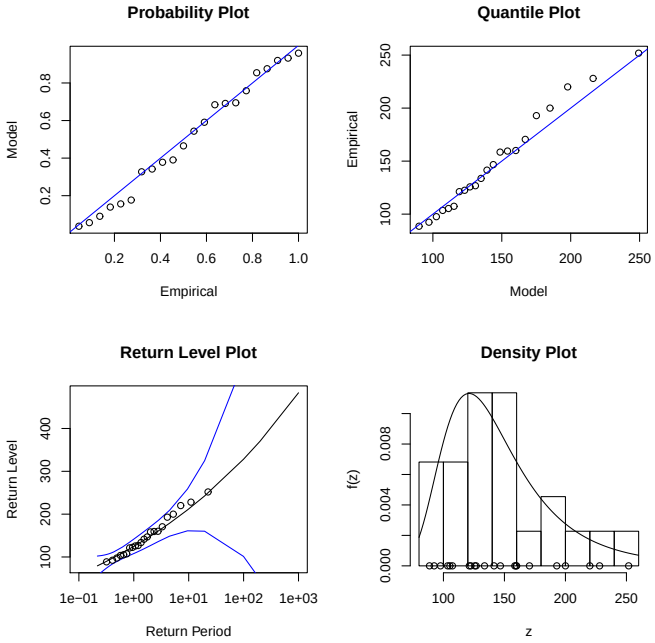

Figure C.6: Diagnostic plots for GEV fit to the Poiso (C) station data–Dataset II.

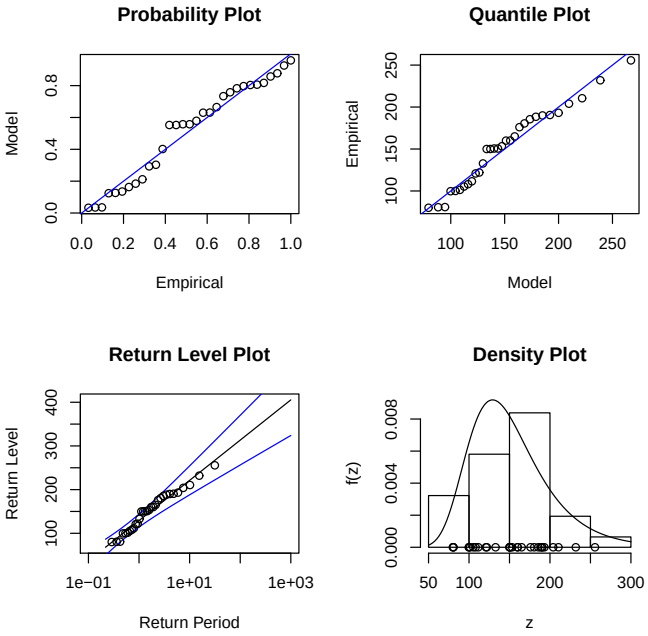

Figure C.7: Diagnostic plots for Gumbel fit to the Montado do Pereiro (D) station data–Dataset II.

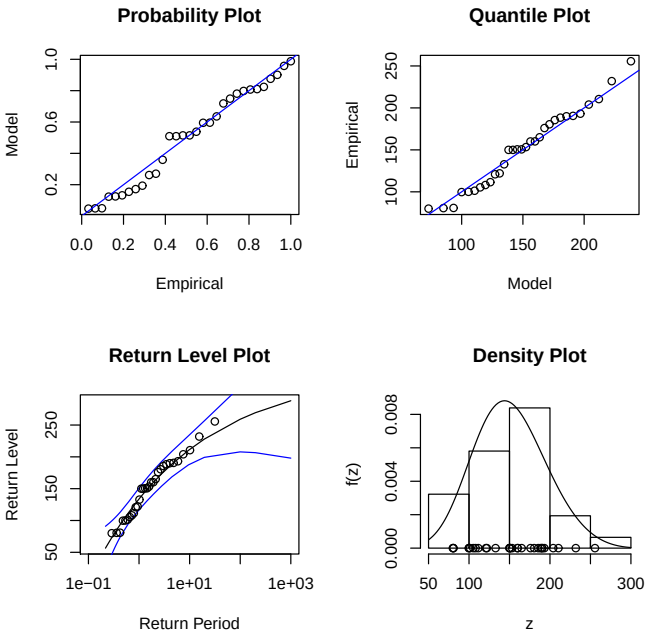

Figure C.8: Diagnostic plots for GEV fit to the Montado do Pereiro (D) station data–Dataset II.

Appendix D

Diagnostic plots for annual maxima – Dataset II (Class 2)

Diagnostic plots for the Gumbel and GEV fits for the stations with altitude between 600 and 900 m

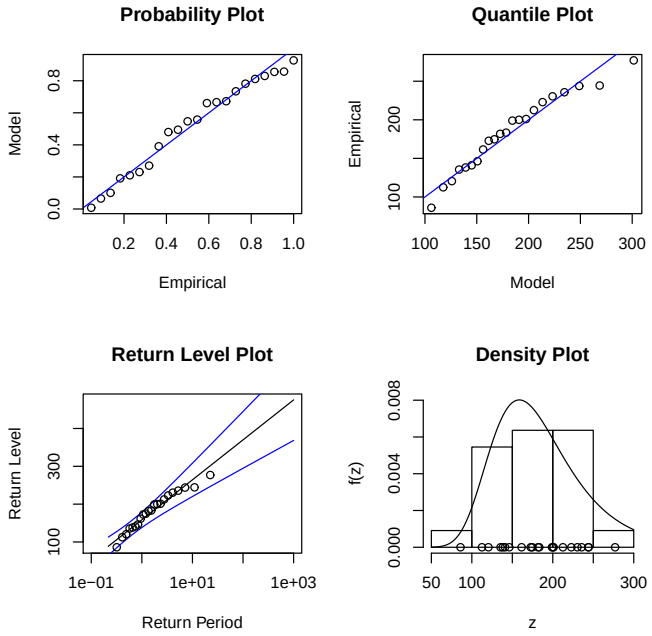

Figure D.1: Diagnostic plots for Gumbel fit to the Encumeada (E) station data– Dataset II.

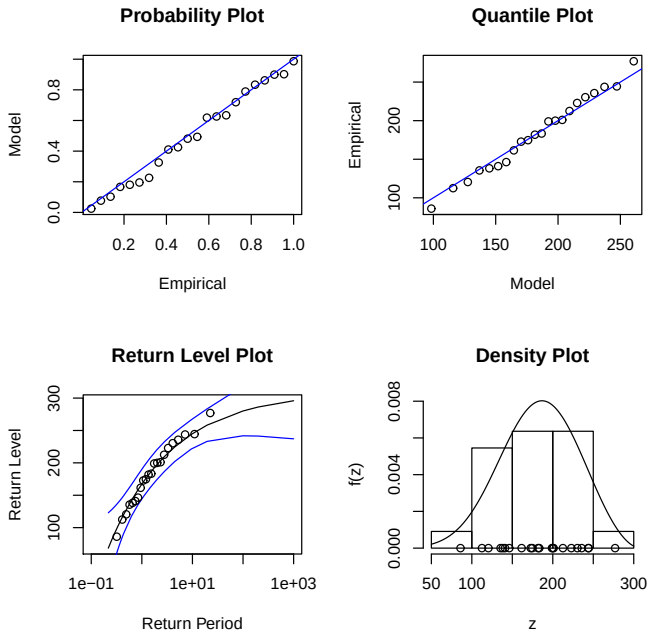

Figure D.2: Diagnostic plots for GEV fit to the Encumeada (E) station data– Dataset II.

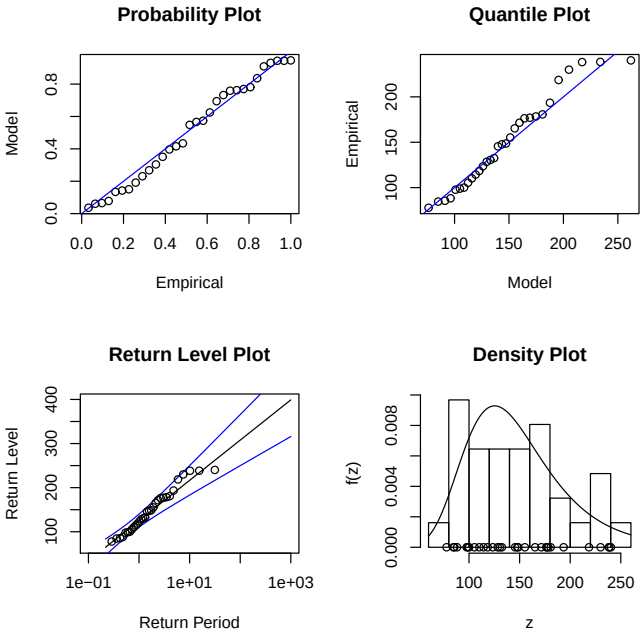

Figure D.3: Diagnostic plots for Gumbel fit to the Ribeiro Frio (F) station data–Dataset II.

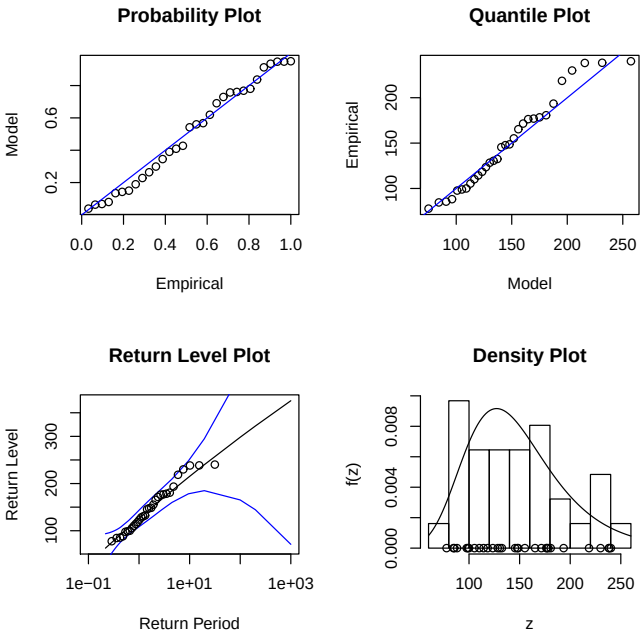

Figure D.4: Diagnostic plots for GEV fit to the Ribeiro Frio (F) station data–Dataset II.

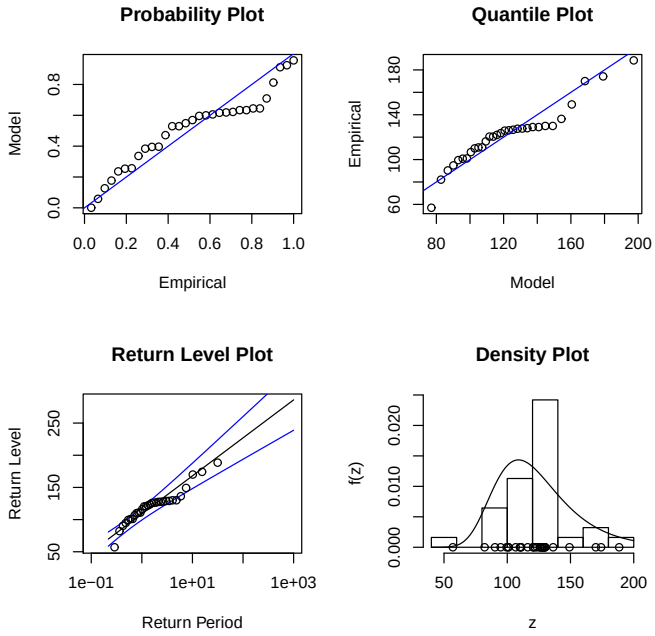

Figure D.5: Diagnostic plots for Gumbel fit to the Queimadas (G) station data– Dataset II.

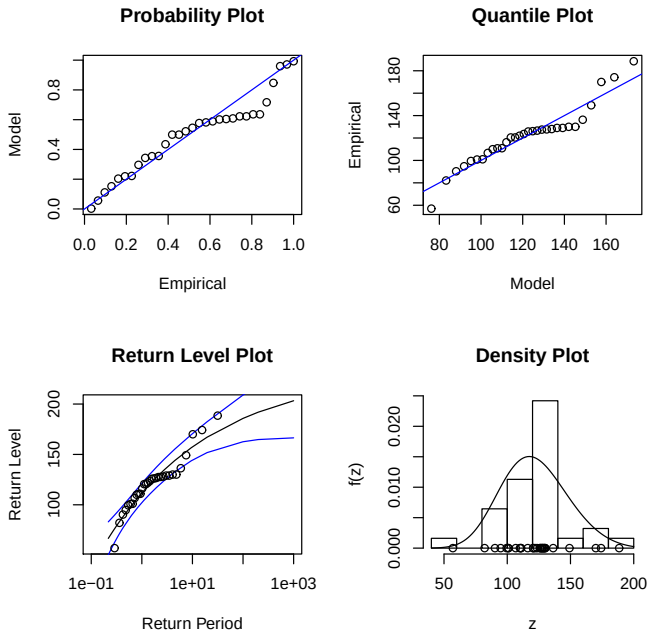

Figure D.6: Diagnostic plots for GEV fit to the Queimadas (G) station data– Dataset II.

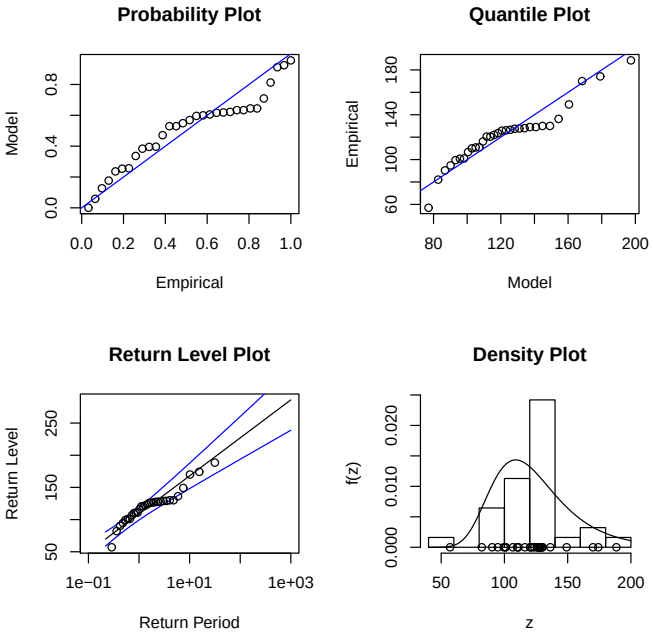

Figure D.7: Diagnostic plots for Gumbel fit to the Camacha (H) station data–Dataset II.

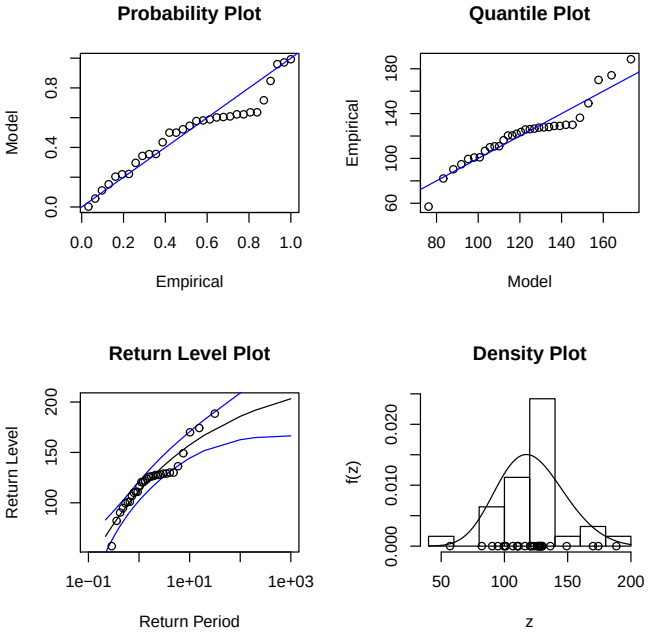

Figure D.8: Diagnostic plots for GEV fit to the Camacha (H) station data–Dataset II.

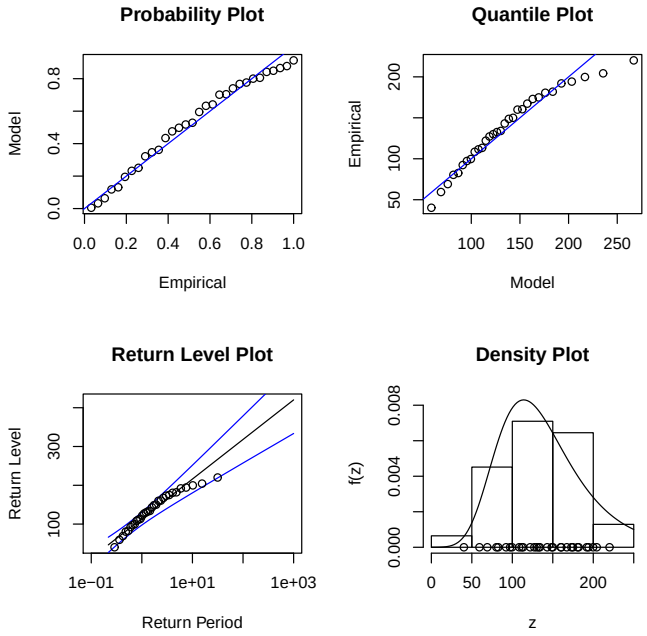

Figure D.9: Diagnostic plots for Gumbel fit to the Santo da Serra (I) station data– Dataset II.

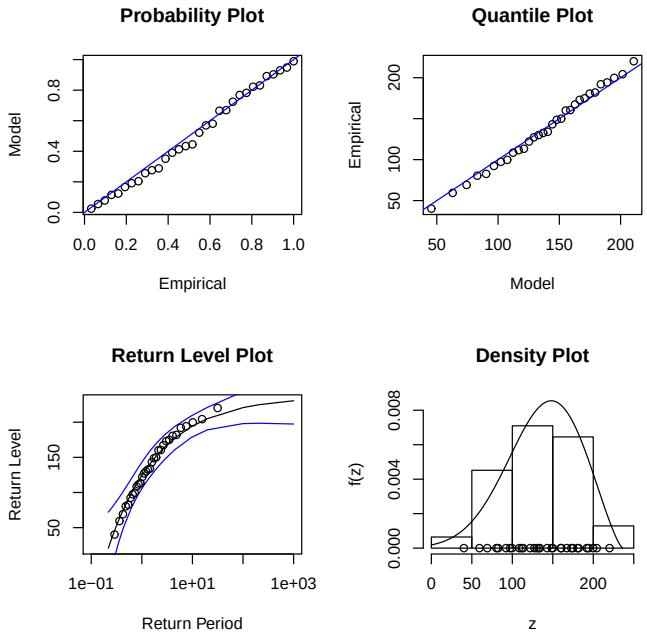

Figure D.10: Diagnostic plots for GEV fit to the Santo da Serra (I) station data– Dataset II.

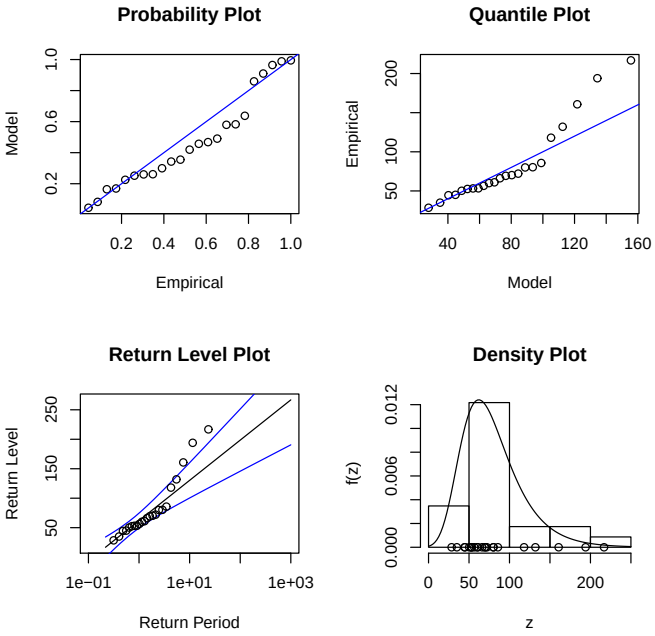

Figure D.11: Diagnostic plots for Gumbel fit to the Porto Moniz (J) station data–Dataset II.

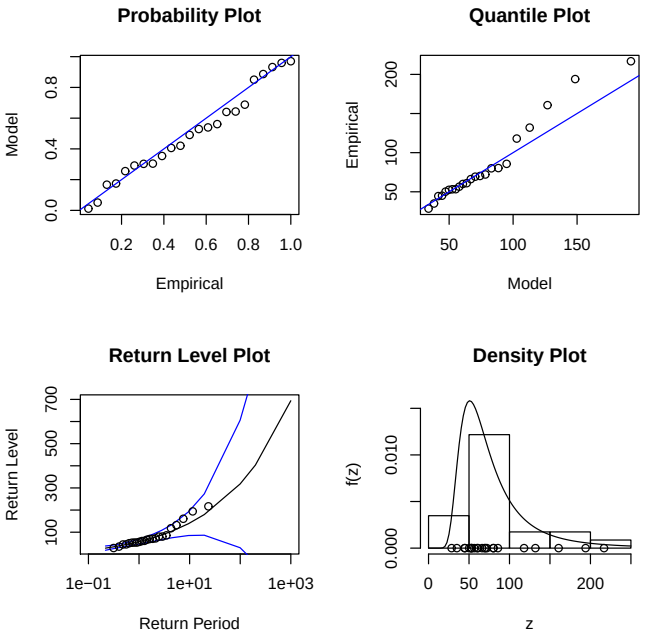

Figure D.12: Diagnostic plots for GEV fit to the Porto Moniz (J) station data–Dataset II.

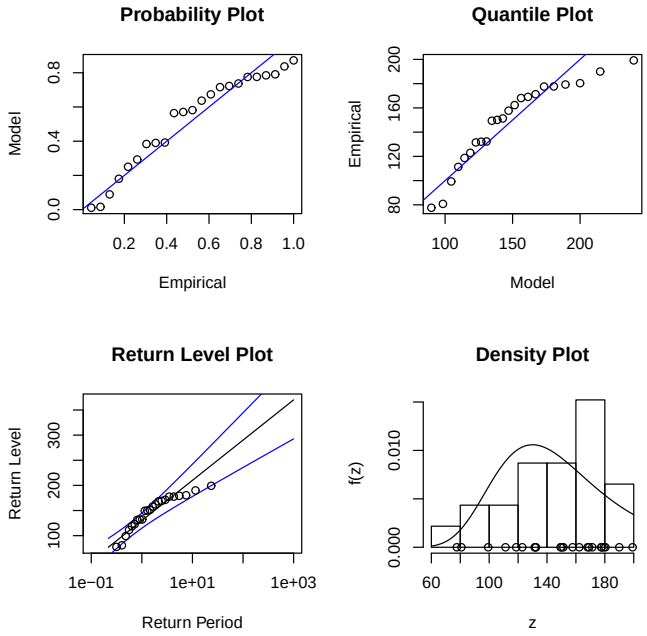

Figure D.13: Diagnostic plots for Gumbel fit to the Curral das Freiras (K) station data–Dataset II.

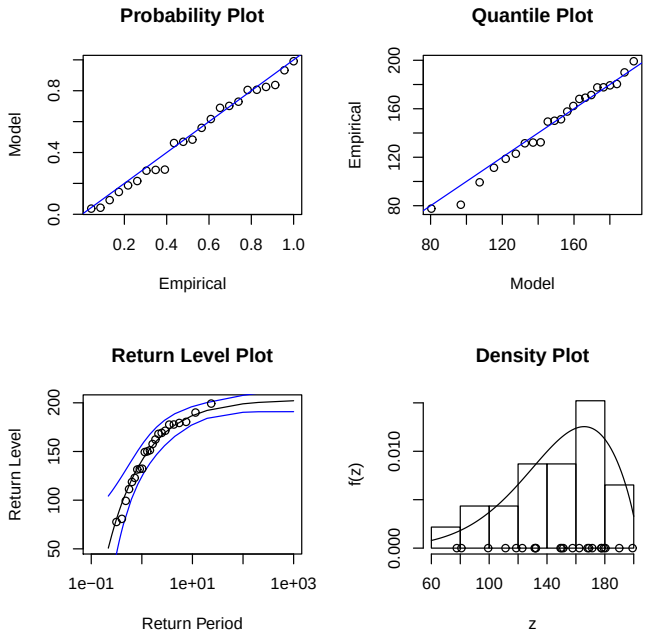

Figure D.14: Diagnostic plots for GEV fit to the Curral das Freiras (K) station data–Dataset II.

Appendix E

Diagnostic plots for annual maxima – Dataset II (Class 3)

Diagnostic plots for the Gumbel and GEV fits for the stations with altitude between 300 and 600 m

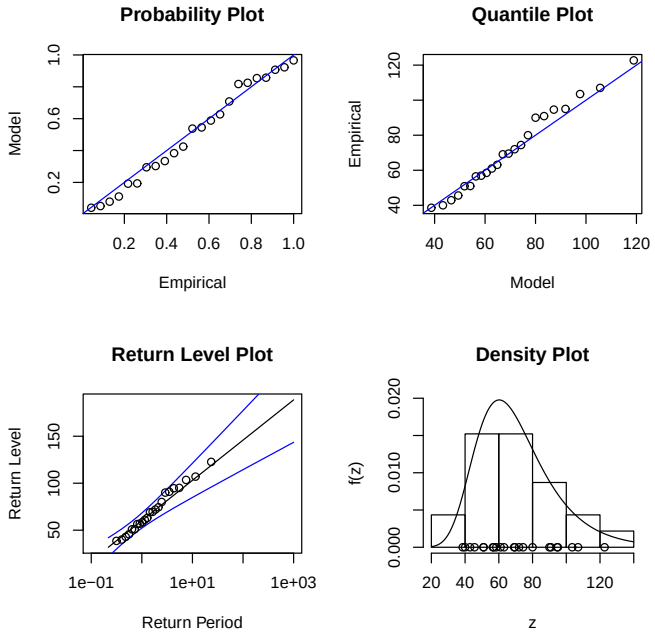

Figure E.1: Diagnostic plots for Gumbel fit to the Ponta do Pargo (L) station data– Dataset II.

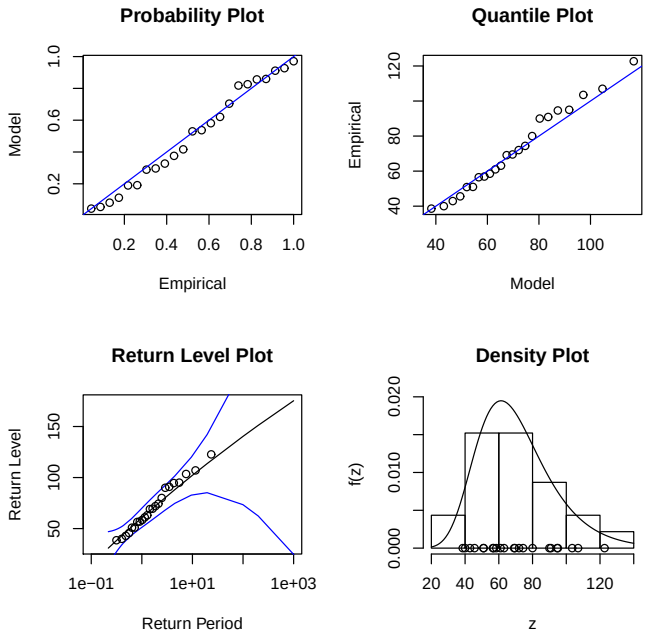

Figure E.2: Diagnostic plots for GEV fit to the Ponta do Pargo (L) station data– Dataset II.

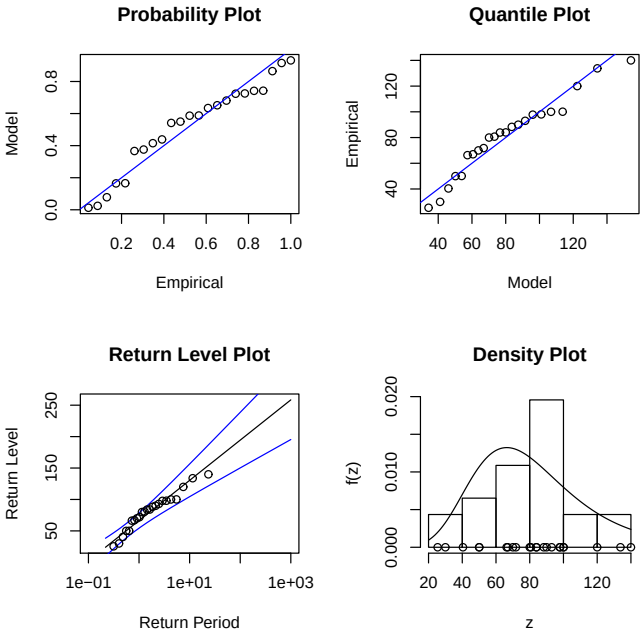

Figure E.3: Diagnostic plots for Gumbel fit to the Santo António (M) station data– Dataset II.

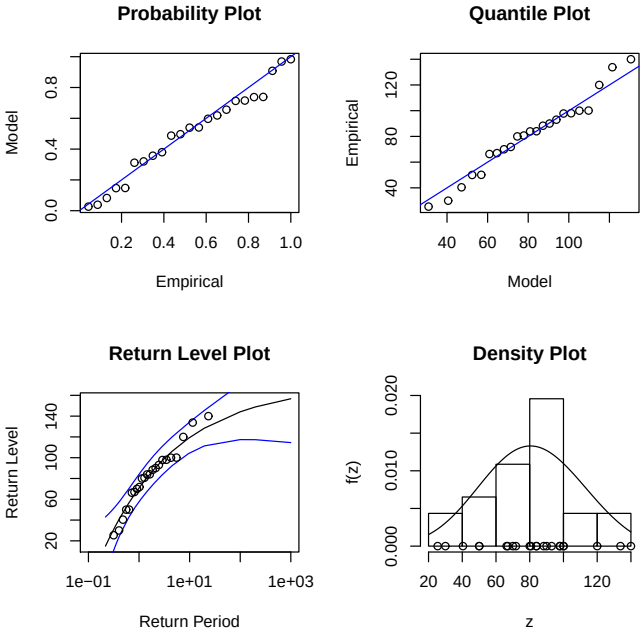

Figure E.4: Diagnostic plots for GEV fit to the Santo António (M) station data– Dataset II.

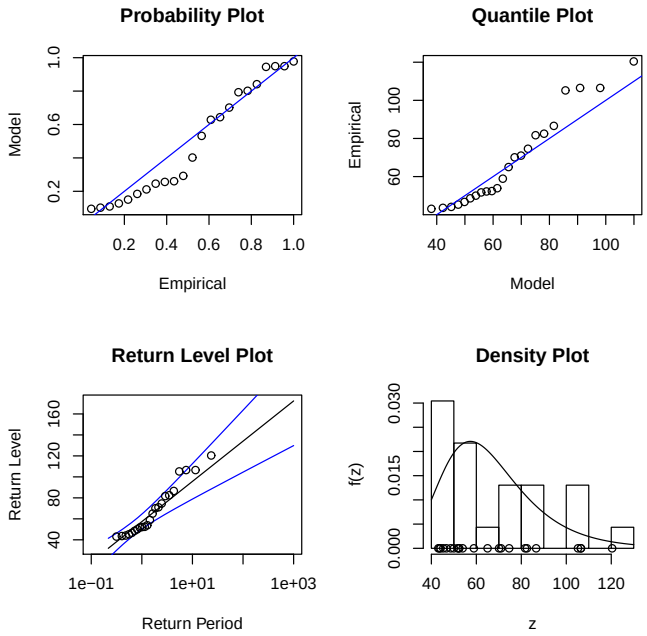

Figure E.5: Diagnostic plots for Gumbel fit to the Canhas (N) station data–Dataset II.

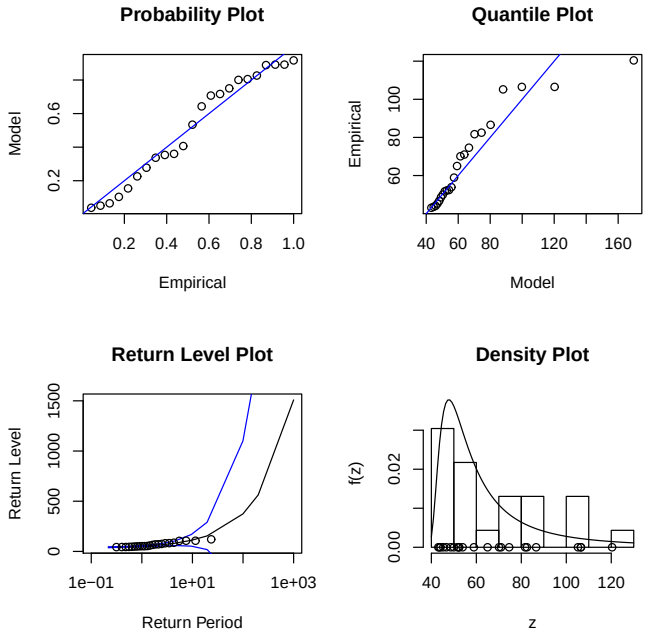

Figure E.6: Diagnostic plots for GEV fit to the Canhas (N) station data–Dataset II.

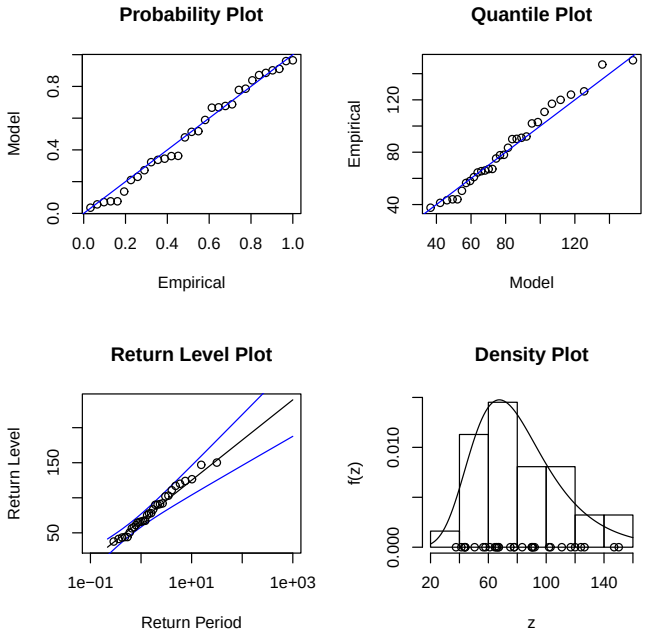

Figure E.7: Diagnostic plots for Gumbel fit to the Sanatório (O) station data– Dataset II.

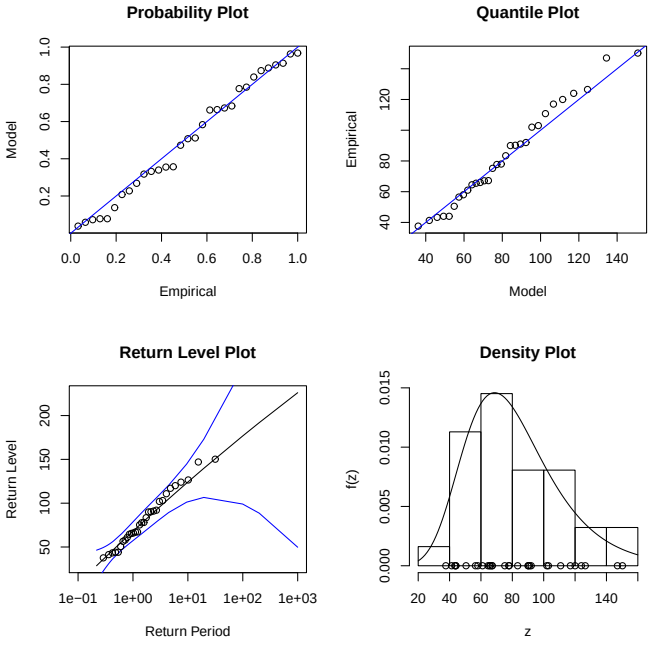

Figure E.8: Diagnostic plots for GEV fit to the Sanatório (O) station data– Dataset II.

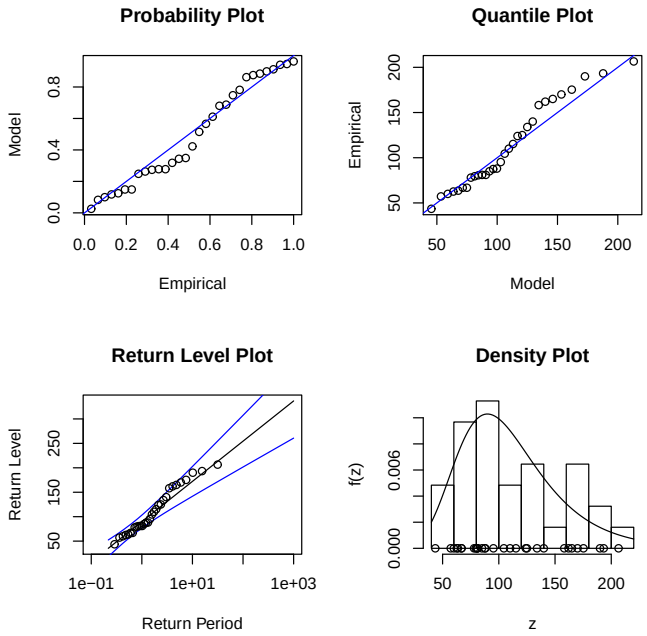

Figure E.9: Diagnostic plots for Gumbel fit to the Santana (P) station data–Dataset II.

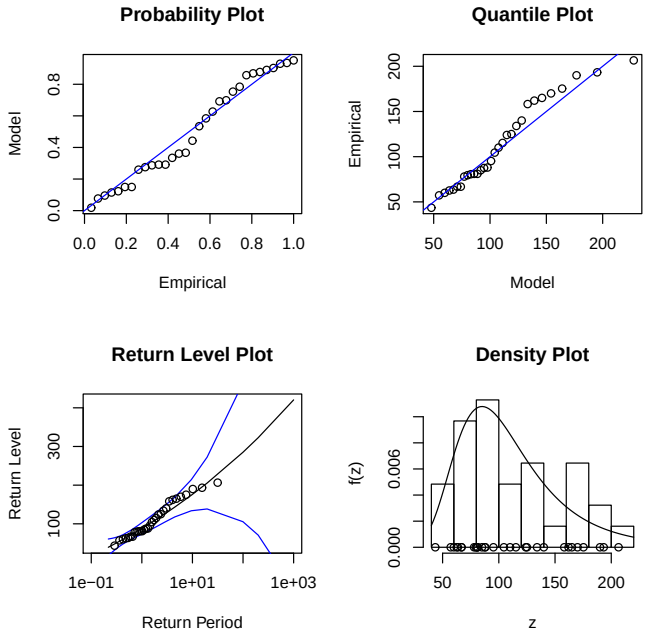

Figure E.10: Diagnostic plots for GEV fit to the Santana (P) station data–Dataset II.

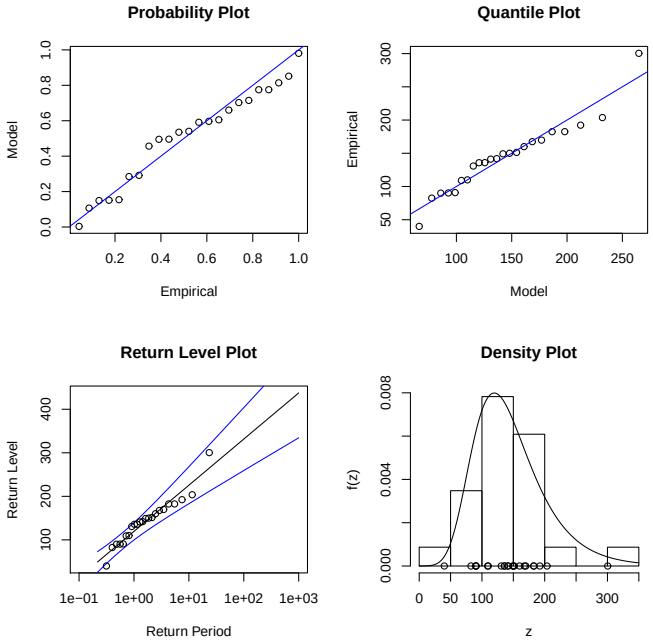

Figure E.11: Diagnostic plots for Gumbel fit to the Loural (Q) station data–Dataset II.

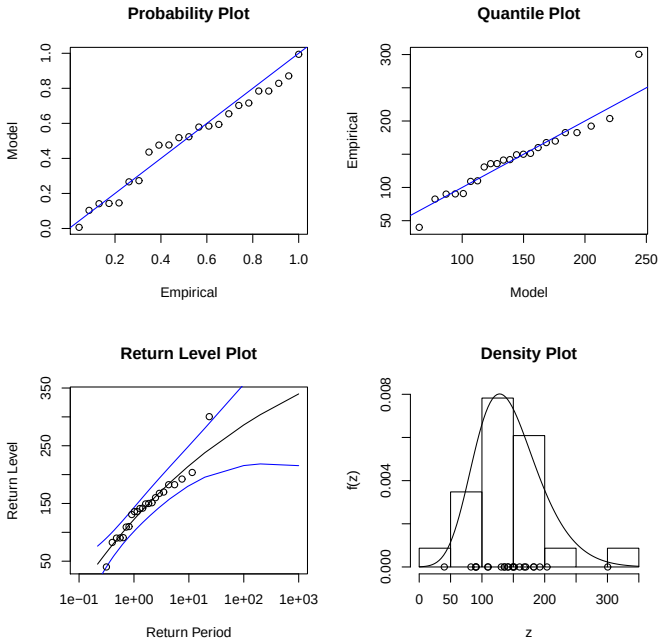

Figure E.12: Diagnostic plots for GEV fit to the Loural (Q) station data–Dataset II.

Appendix F

Diagnostic plots for annual maxima – Dataset II (Class 4)

Diagnostic plots for the Gumbel and GEV fits for the stations with altitude below 300 m

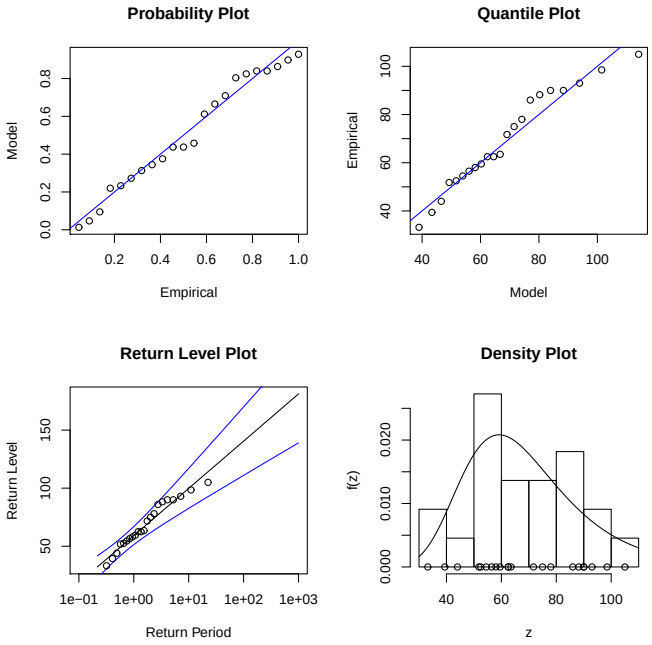

Figure F.1: Diagnostic plots for Gumbel fit to the Bom Sucesso (R) station data– Dataset II.

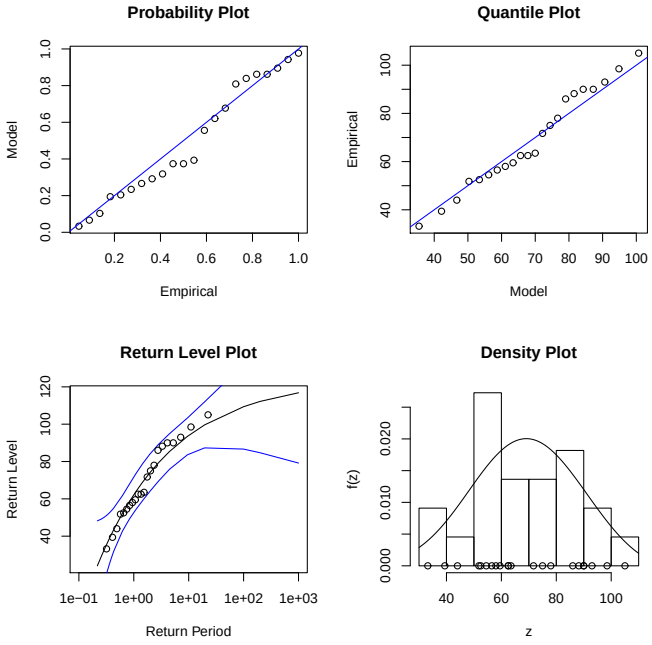

Figure F.2: Diagnostic plots for GEV fit to the Bom Sucesso (R) station data– Dataset II.

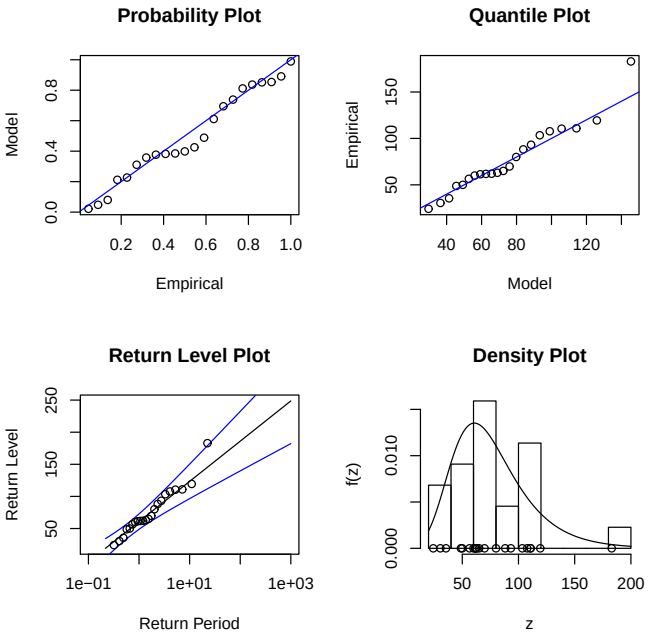

Figure F.3: Diagnostic plots for Gumbel fit to the Machico (S) station data–Dataset II.

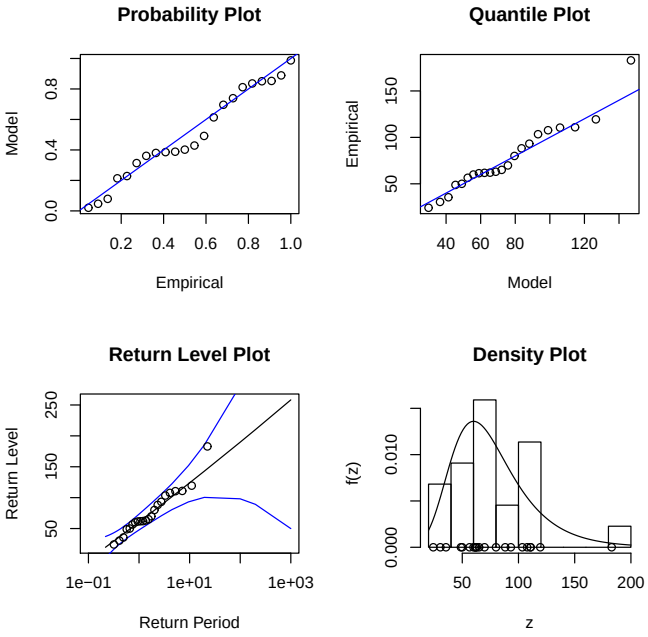

Figure F.4: Diagnostic plots for GEV fit to the Machico (S) station data–Dataset II.

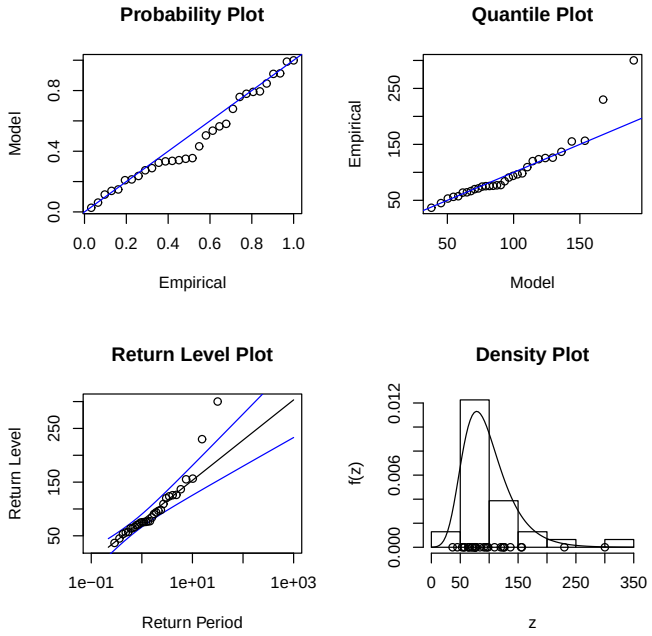

Figure F.5: Diagnostic plots for Gumbel fit to the Ponta Delgada (T) station data– Dataset II.

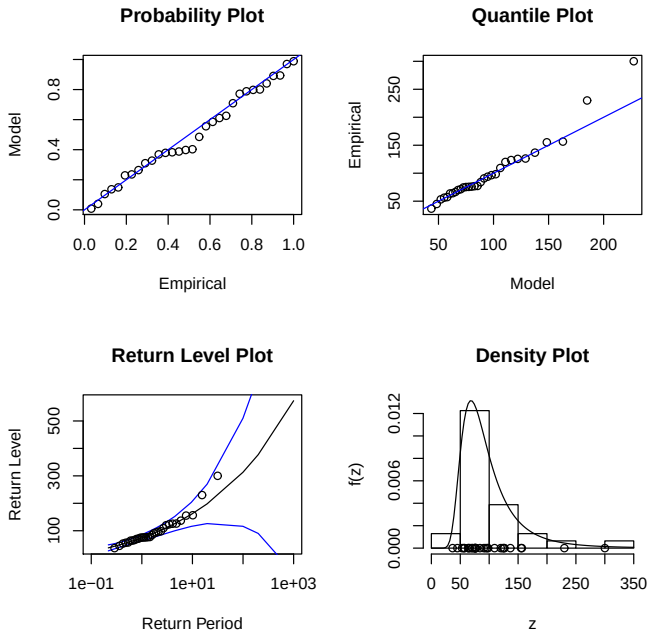

Figure F.6: Diagnostic plots for GEV fit to the Ponta Delgada (T) station data– Dataset II.

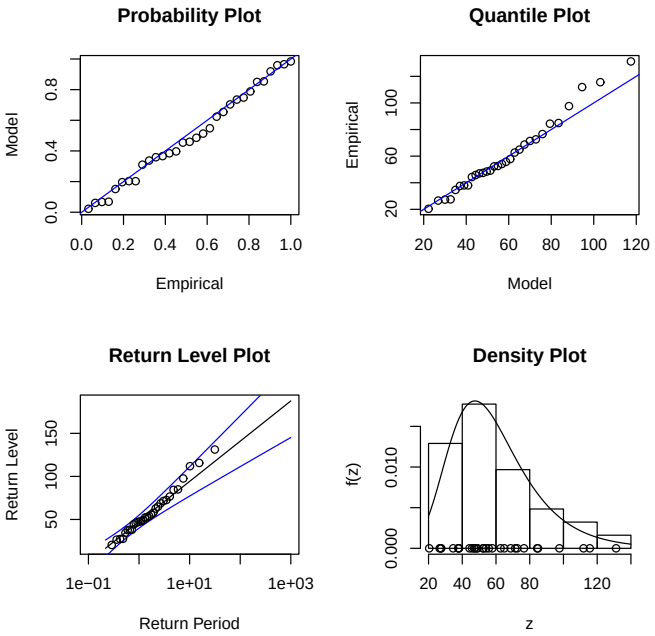

Figure F.7: Diagnostic plots for Gumbel fit to the Funchal (U) station data–Dataset II.

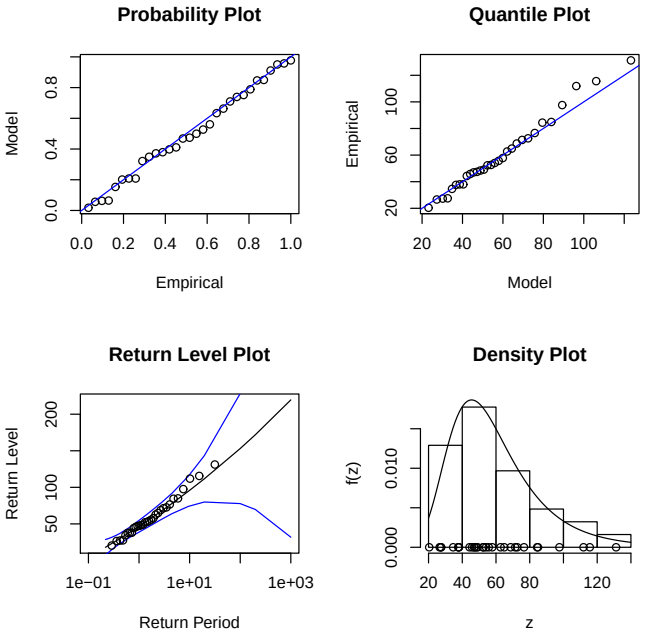

Figure F.8: Diagnostic plots for GEV fit to the Funchal (U) station data–Dataset II.

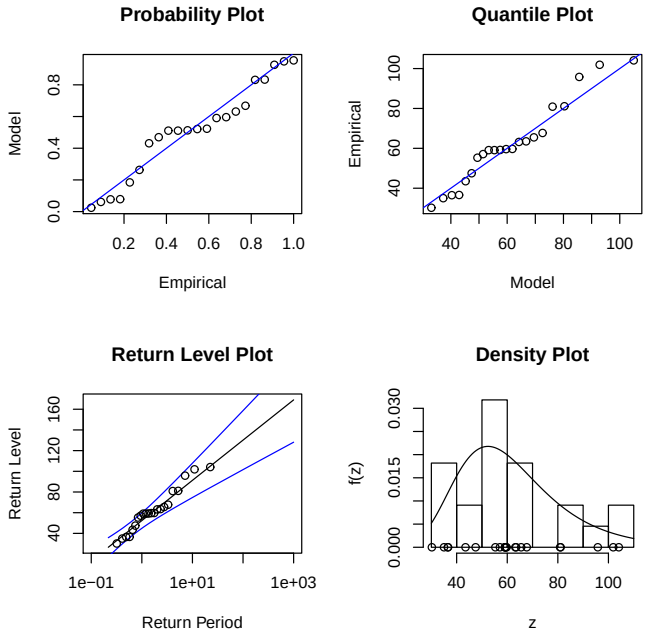

Figure F.9: Diagnostic plots for Gumbel fit to the Santa Catarina (V) station data– Dataset II.

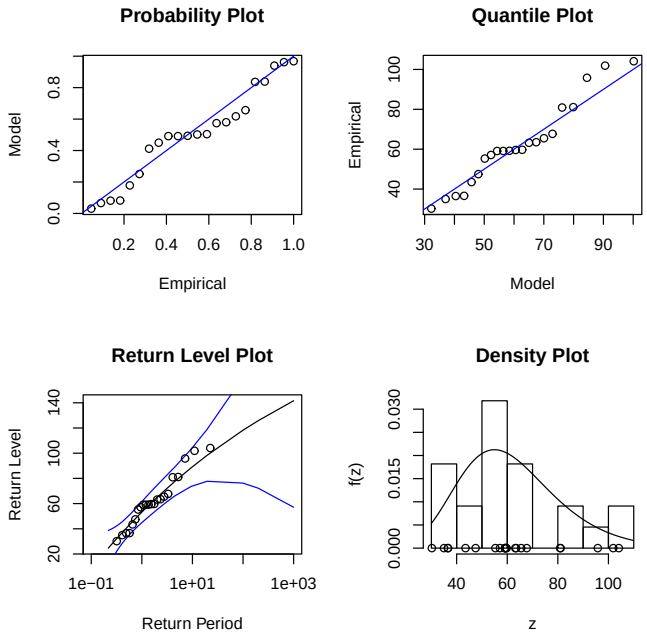

Figure F.10: Diagnostic plots for GEV fit to the Santa Catarina (V) station data– Dataset II.

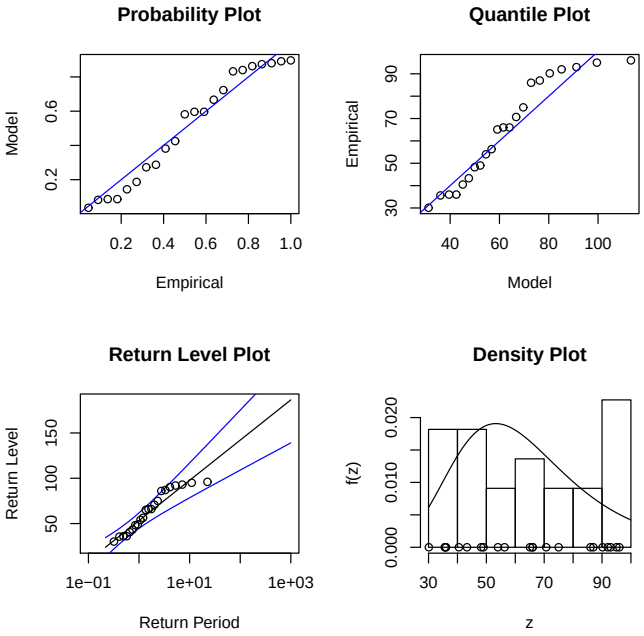

Figure F.11: Diagnostic plots for Gumbel fit to the Caniçal (W) station data– Dataset II.

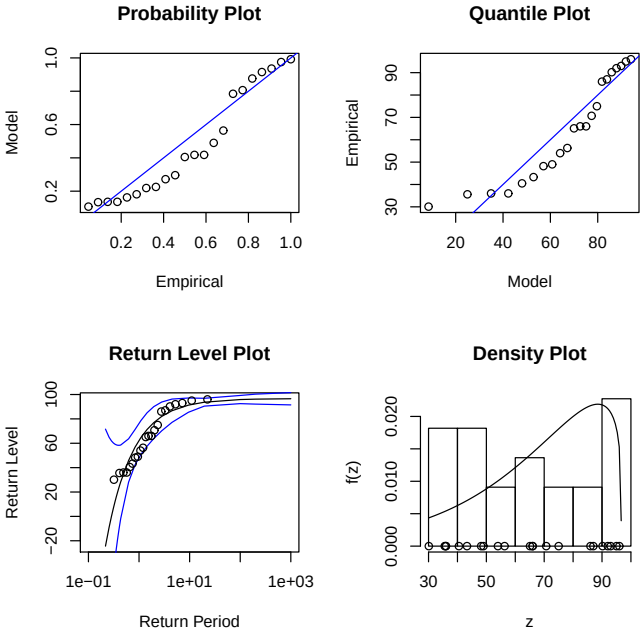

Figure F.12: Diagnostic plots for GEV fit to the Caniçal (W) station data– Dataset II.

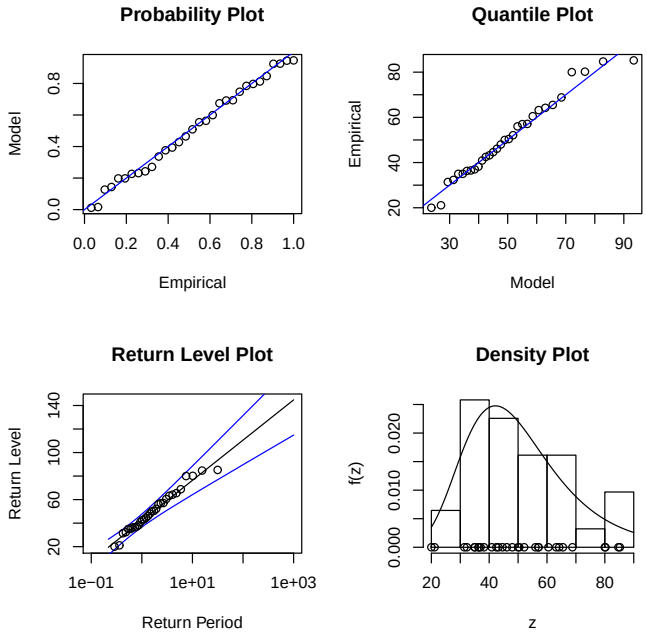

Figure F.13: Diagnostic plots for Gumbel fit to the Lugar de Baixo (X) station data–Dataset II.

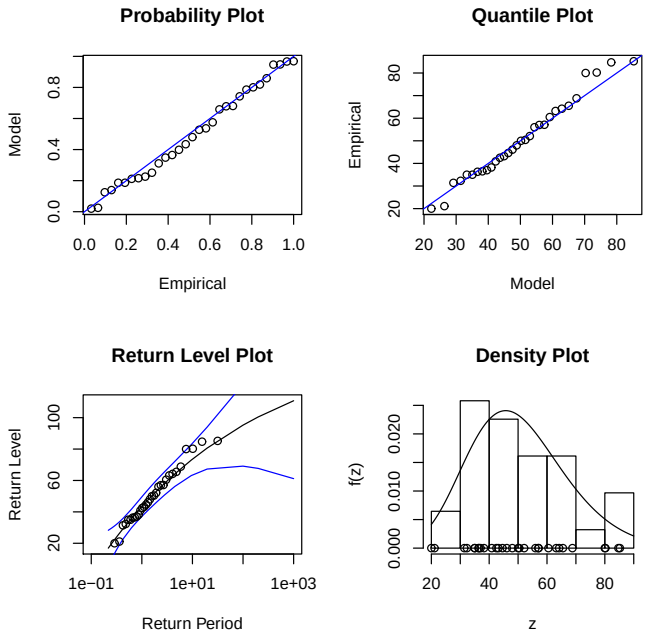

Figure F.14: Diagnostic plots for GEV fit to the Lugar de Baixo (X) station data–Dataset II.

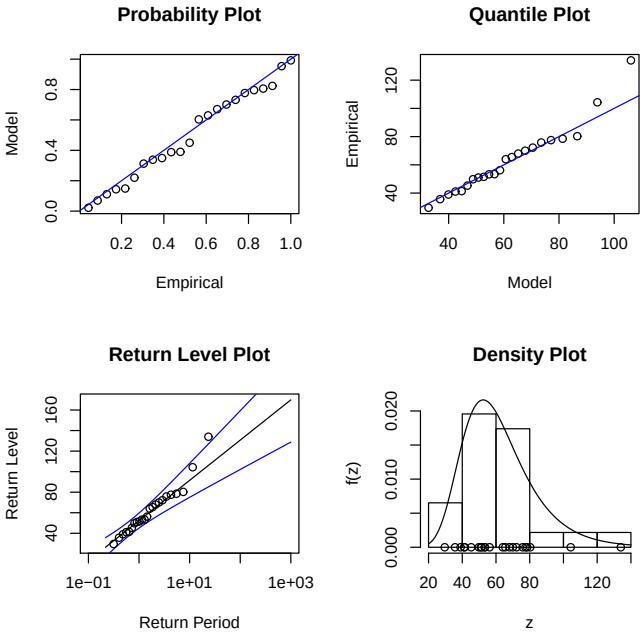

Figure F.15: Diagnostic plots for Gumbel fit to the Ribeira Brava (Y) station data–Dataset II.

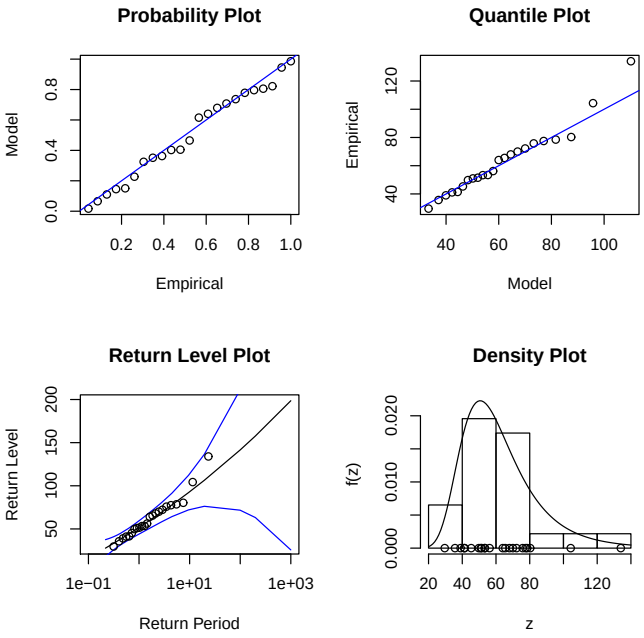

Figure F.16: Diagnostic plots for GEV fit to the Ribeira Brava (Y) station data–Dataset II.

Appendix G

Diagnostic plots for annual maxima – Dataset I+II

Diagnostic plots for the Gumbel and GEV fits

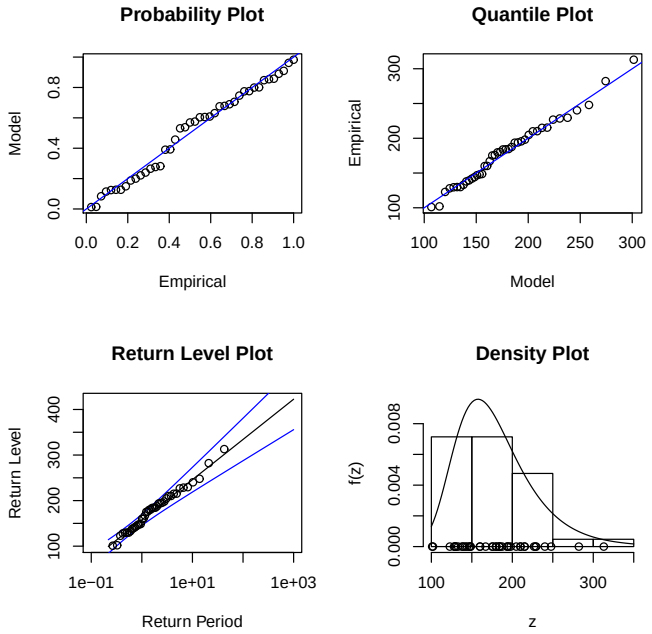

Figure G.1: Diagnostic plots for Gumbel fit to the Areeiro (A) station data– Dataset I+II.

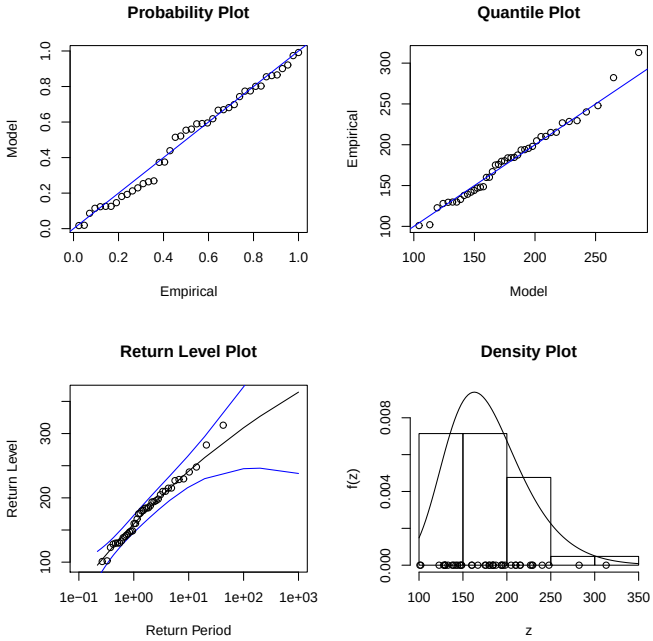

Figure G.2: Diagnostic plots for GEV fit to the Areeiro (A) station data– Dataset I+II.

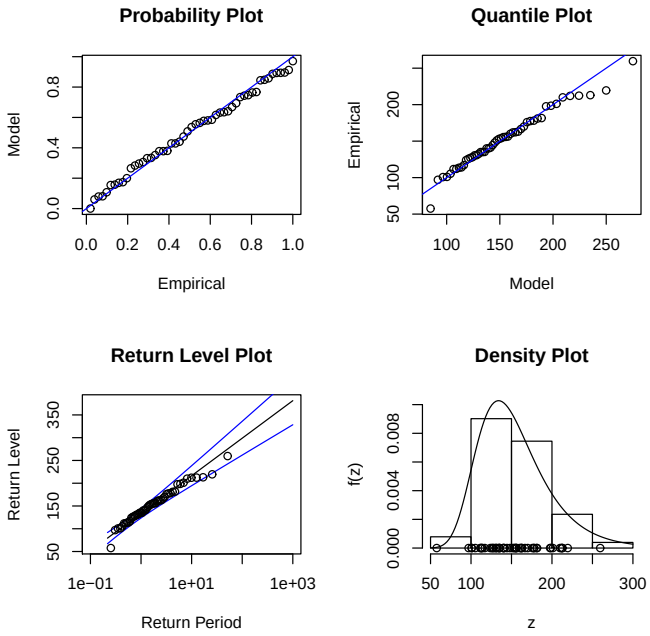

Figure G.3: Diagnostic plots for Gumbel fit to the Bica da Cana (B) station data–Dataset I+II.

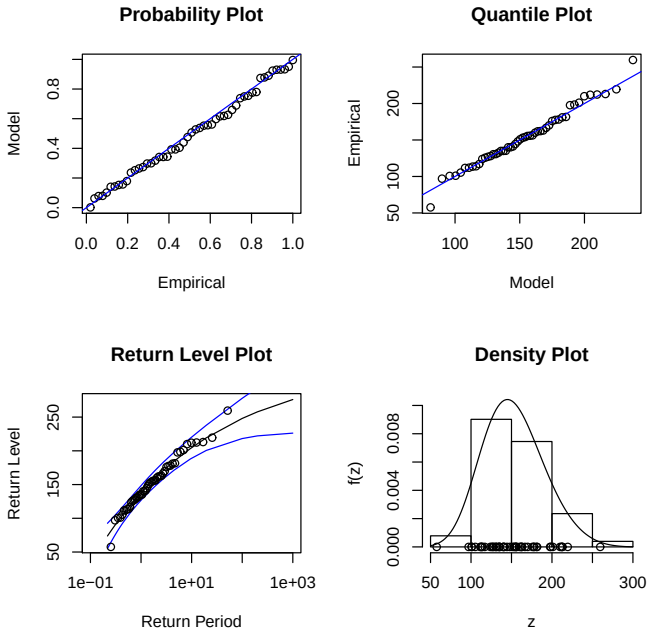

Figure G.4: Diagnostic plots for GEV fit to the Bica da Cana (B) station data–Dataset I+II.

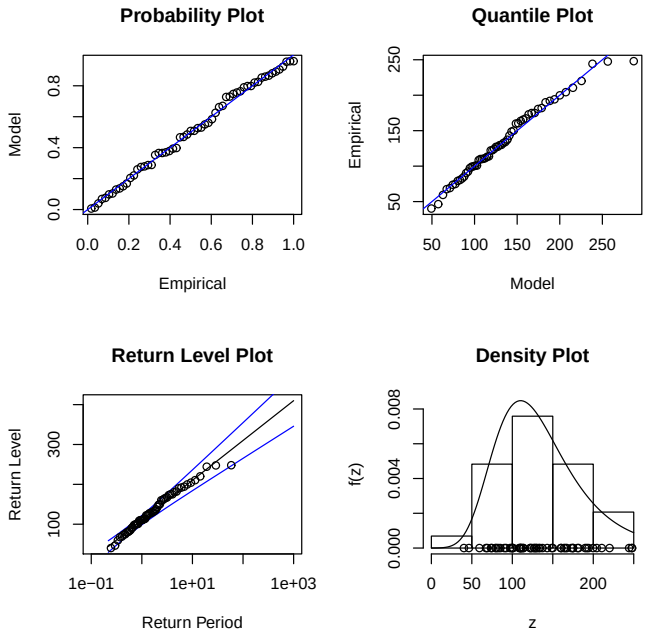

Figure G.5: Diagnostic plots for Gumbel fit to the Santo da Serra (I) station data– Dataset I+II.

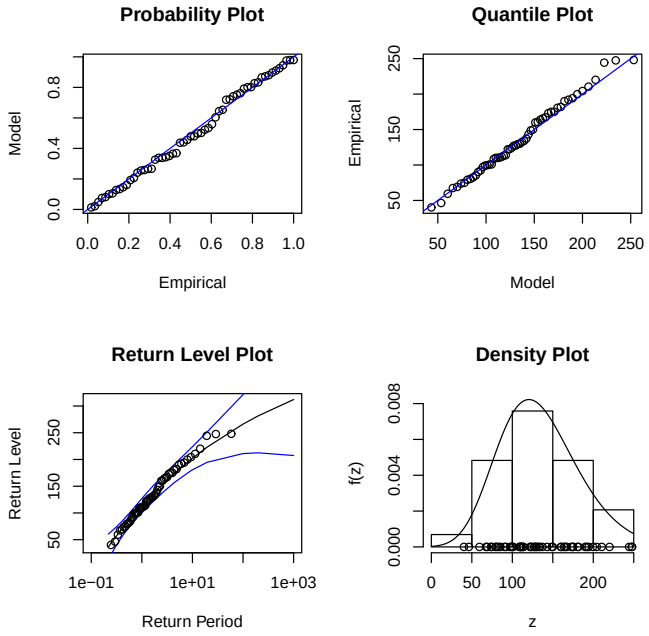

Figure G.6: Diagnostic plots for GEV fit to the Santo da Serra (I) station data– Dataset I+II.

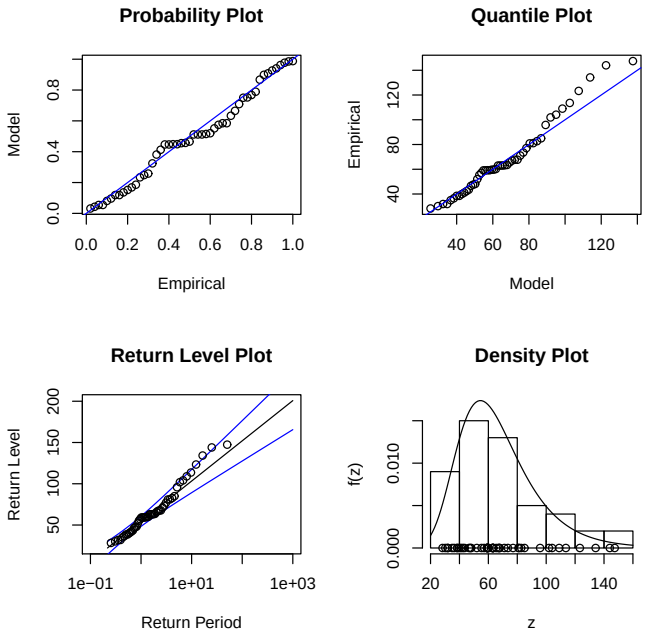

Figure G.7: Diagnostic plots for Gumbel fit to the Santa Catarina (V) station data–Dataset I+II.

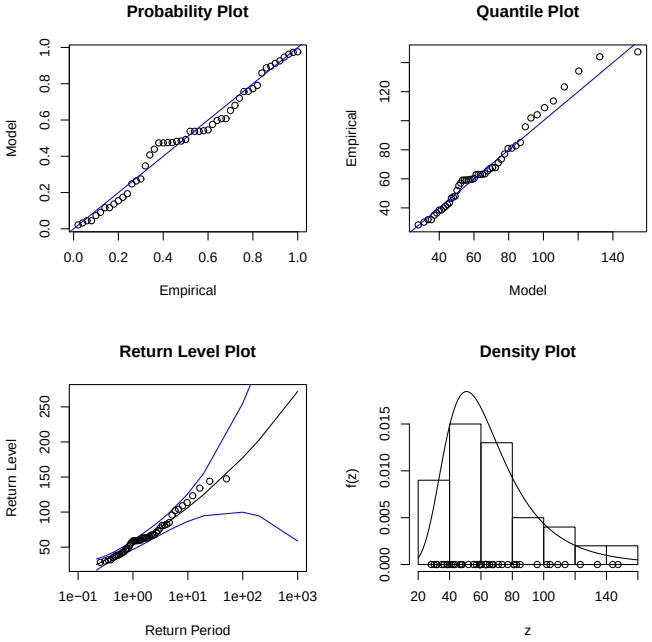

Figure G.8: Diagnostic plots for GEV fit to the Santa Catarina (V) station data–Dataset I+II.

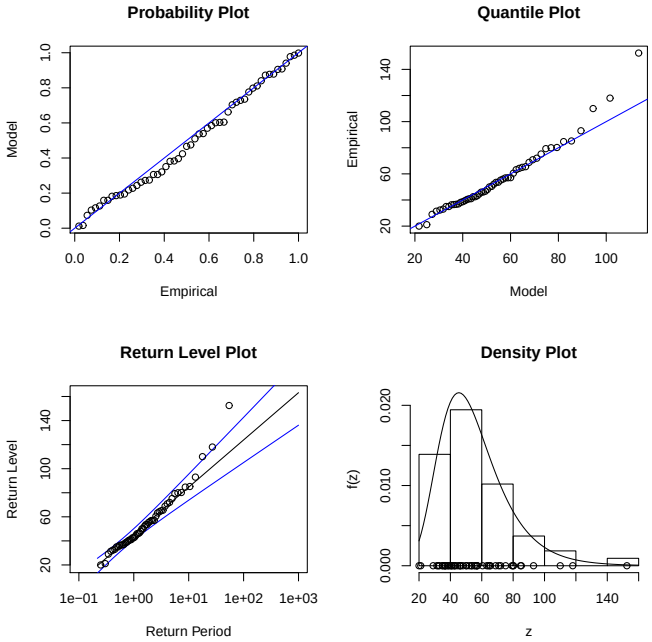

Figure G.9: Diagnostic plots for Gumbel fit to the Lugar de Baixo (X) station data–Dataset I+II.

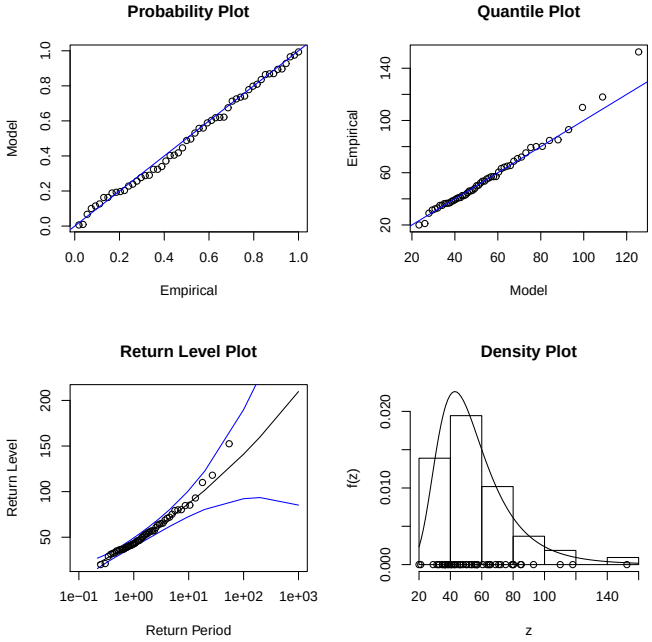

Figure G.10: Diagnostic plots for GEV fit to the Lugar de Baixo (X) station data–Dataset I+II.

Appendix H

Threshold choice plots – Dataset IV (Class 1)

Mean residual and parameter stability plots for the stations with altitude above 900 m

Figure H.1: Mean residual plot for the Bica da Cana (B) station data.

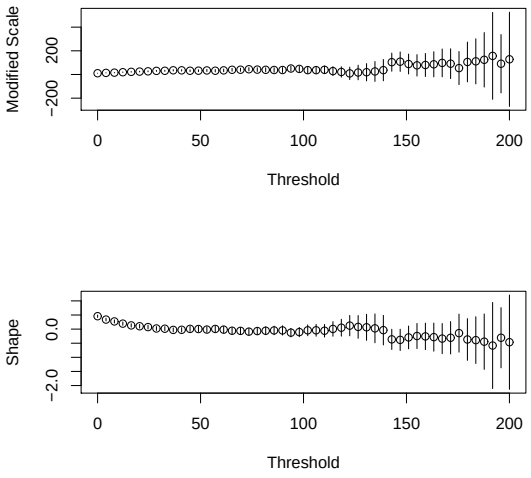

Figure H.2: Parameter stability plots for the Bica da Cana (B) station data.

Figure H.3: Mean residual plot for the Poiso (C) station data.

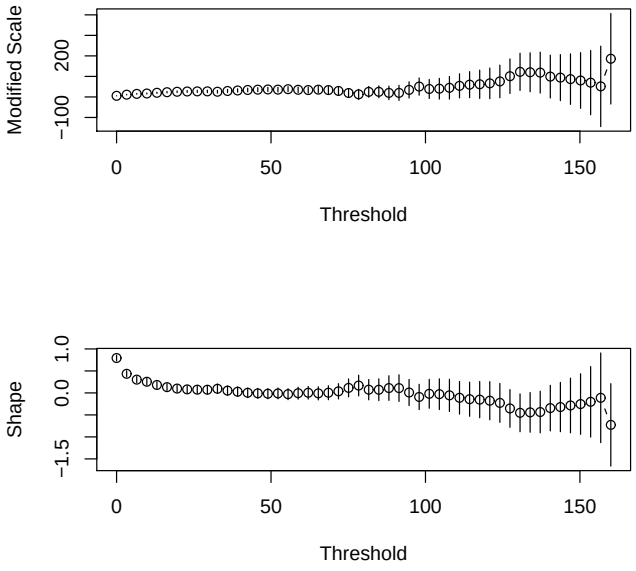

Figure H.4: Parameter stability plots for the Poiso (C) station data.

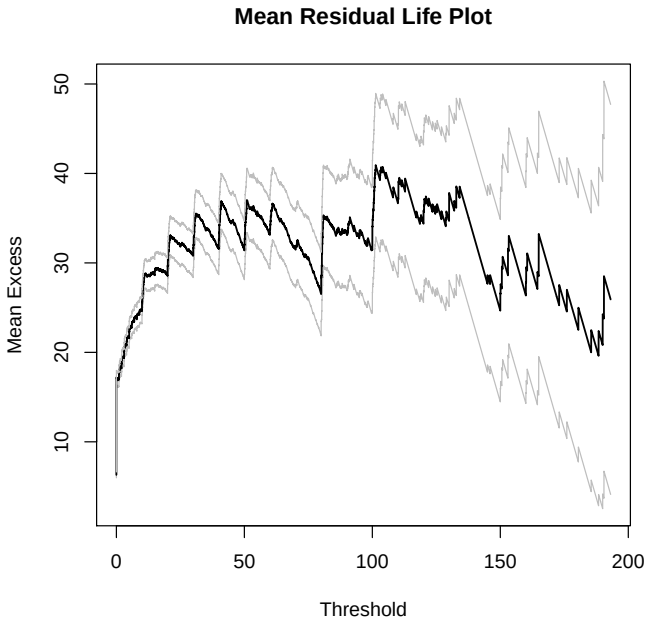

Figure H.5: Mean residual plot for the Montado do Pereiro (D) station data.

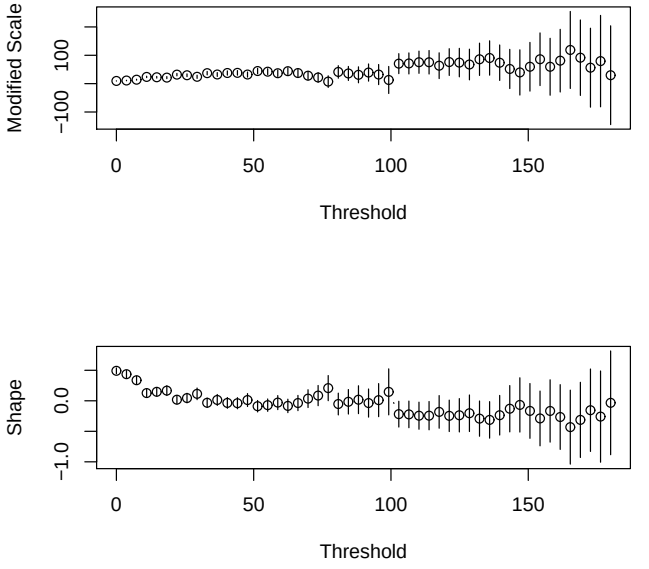

Figure H.6: Parameter stability plots for the Montado do Pereiro (D) station data.

Appendix I

Threshold choice plots – Dataset IV (Class 2)

Mean residual and parameter stability plots for the stations with altitude between 600 and 900 m

Figure I.1: Mean residual plot for the Ribeiro Frio (F) station data.

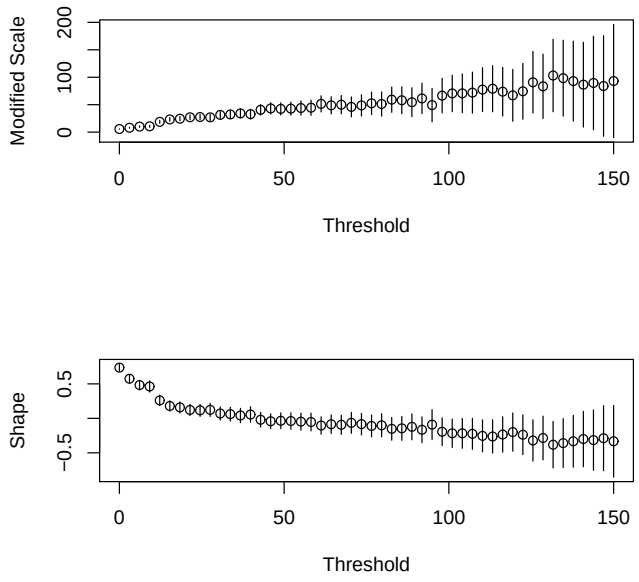

Figure I.2: Parameter stability plots for the Ribeiro Frio (F) station data.

Figure I.3: Mean residual plot for the Queimadas (G) station data.

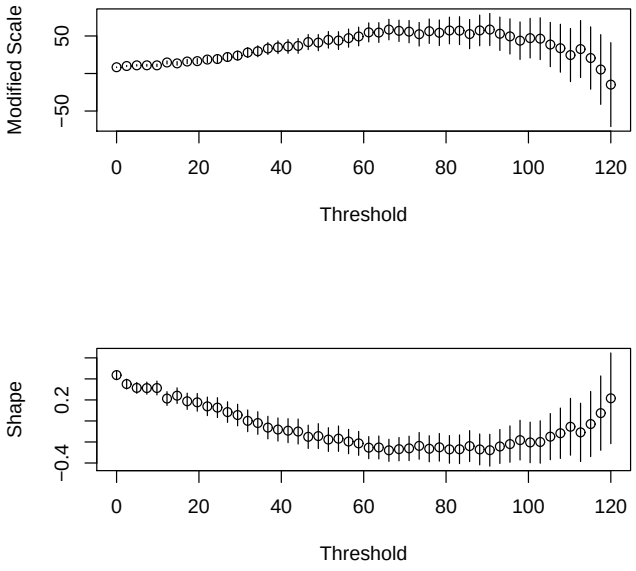

Figure I.4: Parameter stability plots for the Queimadas (G) station data.

Figure I.5: Mean residual plot for the Camacha (H) station data.

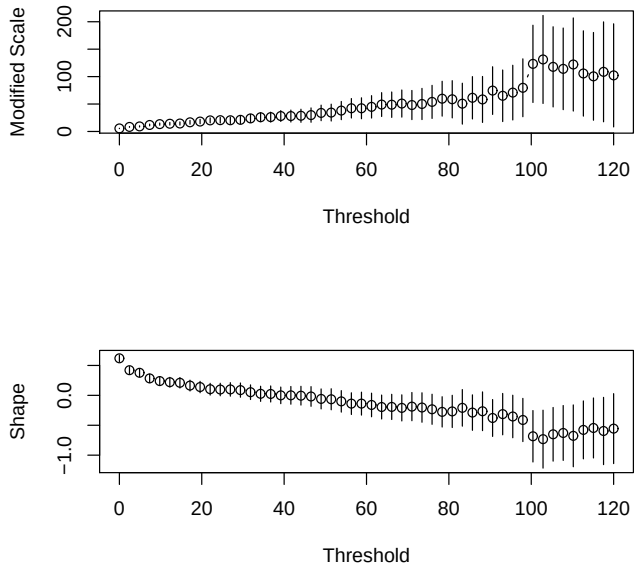

Figure I.6: Parameter stability plots for the Camacha (H) station data.

Figure I.7: Mean residual plot for the Santo da Serra (I) station data.

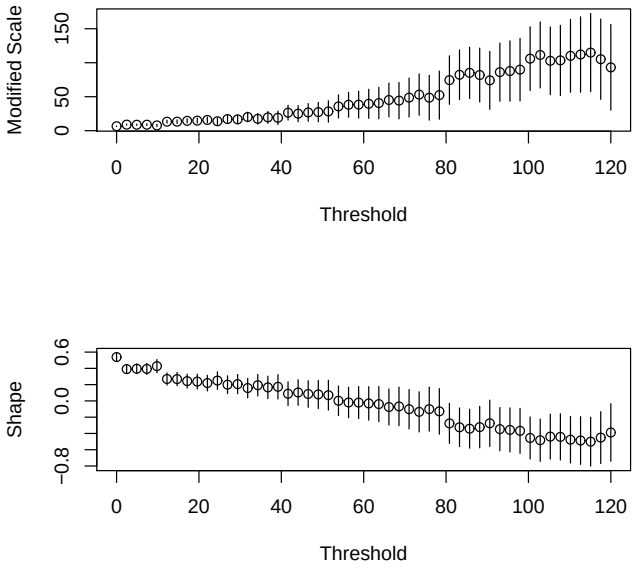

Figure I.8: Parameter stability plots for the Santo da Serra (I) station data.

Figure I.9: Mean residual plot for the Porto Moniz (J) station data.

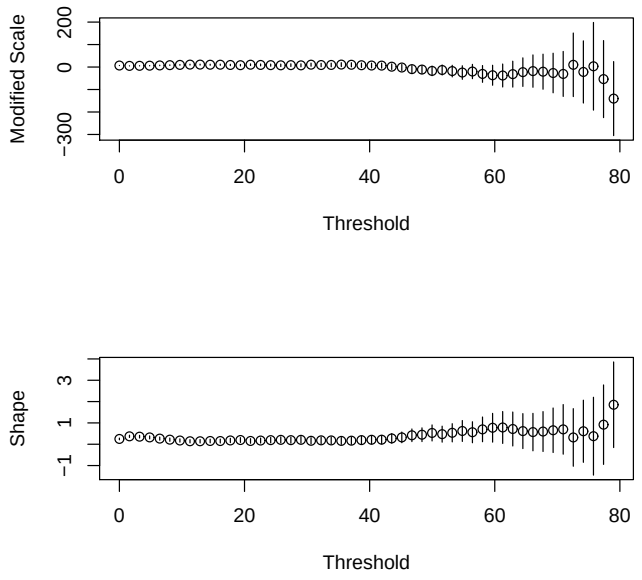

Figure I.10: Parameter stability plots for the Porto Moniz (J) station data.

Figure I.11: Mean residual plot for the Curral das Freiras (K) station data.

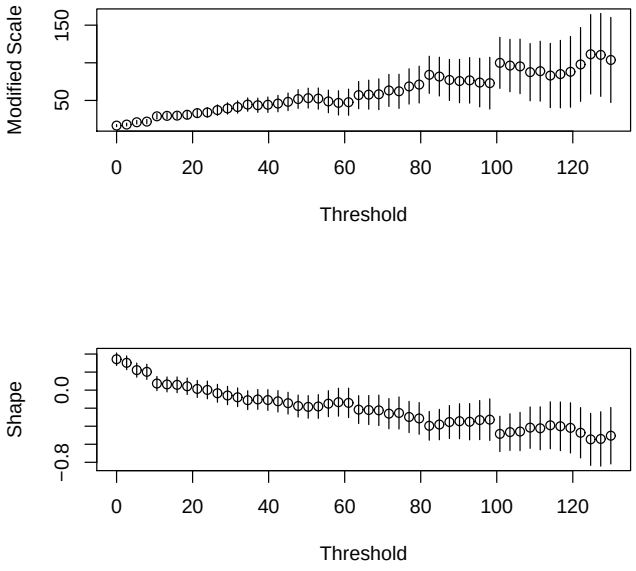

Figure I.12: Parameter stability plots for the Curral das Freiras (K) station data.

Appendix J

Threshold choice plots – Dataset IV (Class 3)

Mean residual and parameter stability plots for the stations with altitude between 300 and 600 m

Figure J.1: Mean residual plot for the Ponta do Pargo (L) station data.

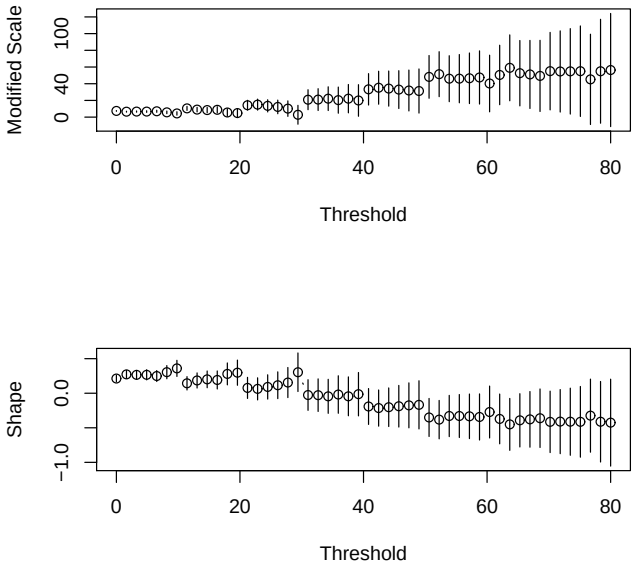

Figure J.2: Parameter stability plots for the Ponta do Pargo (L) station data.

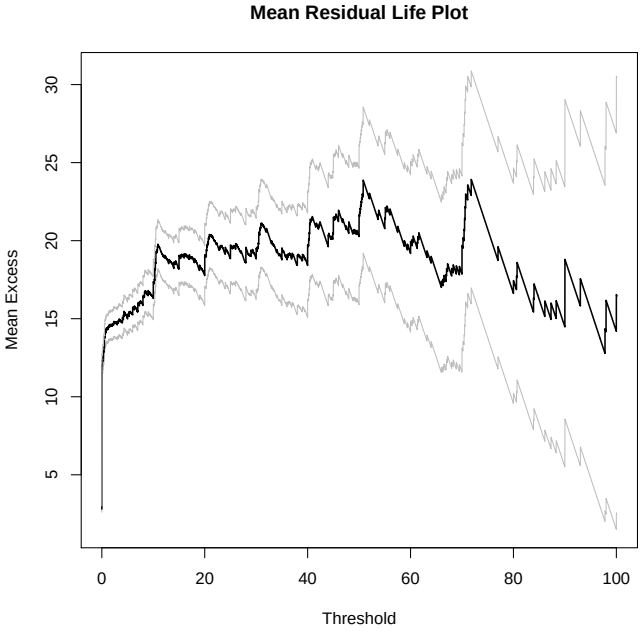

Figure J.3: Mean residual plot for the Santo António (M) station data.

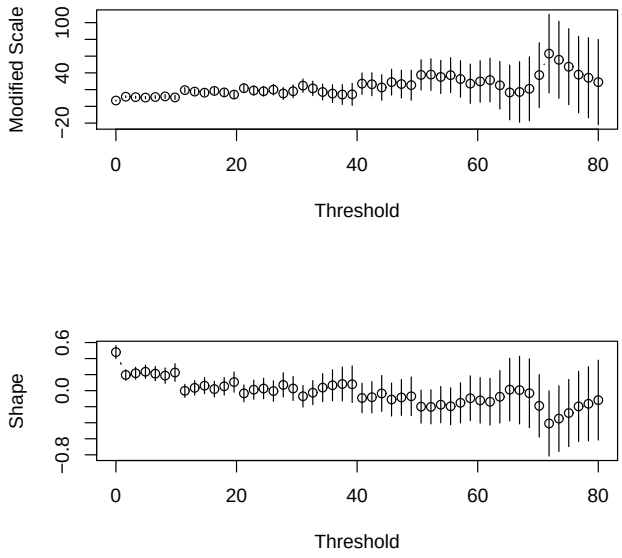

Figure J.4: Parameter stability plots for the Santo António (M) station data.

Figure J.5: Mean residual plot for to the Sanatório (O) station data.

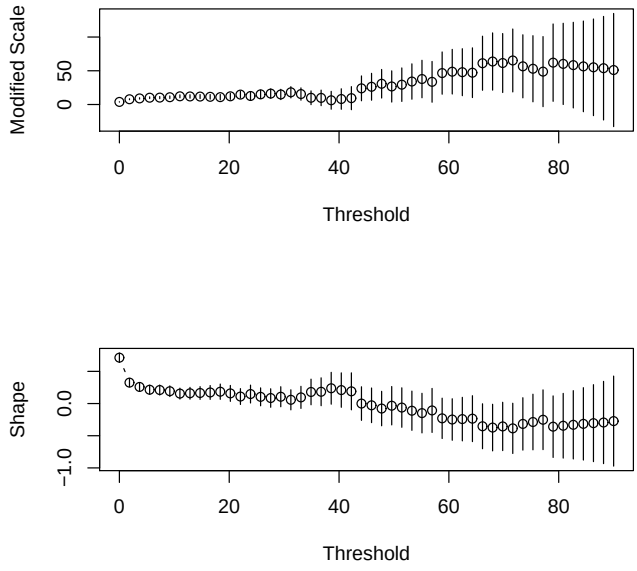

Figure J.6: Parameter stability plots for the Sanatório (O) station data.

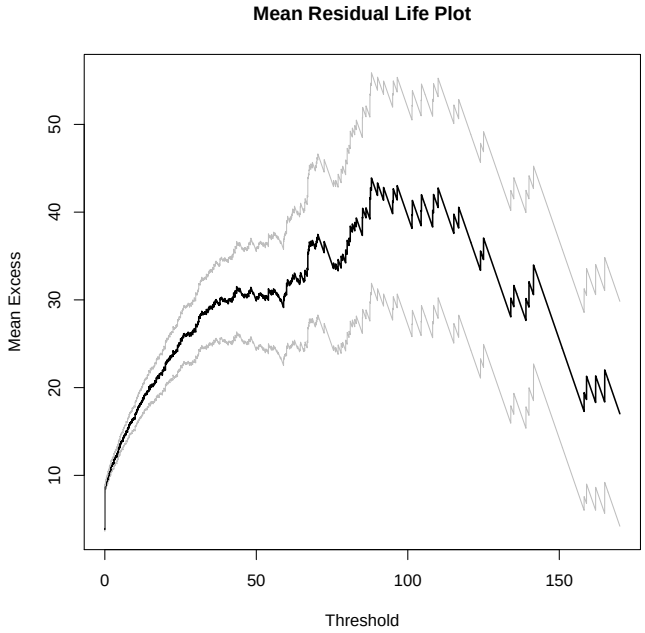

Figure J.7: Mean residual plot for the Santana (P) station data.

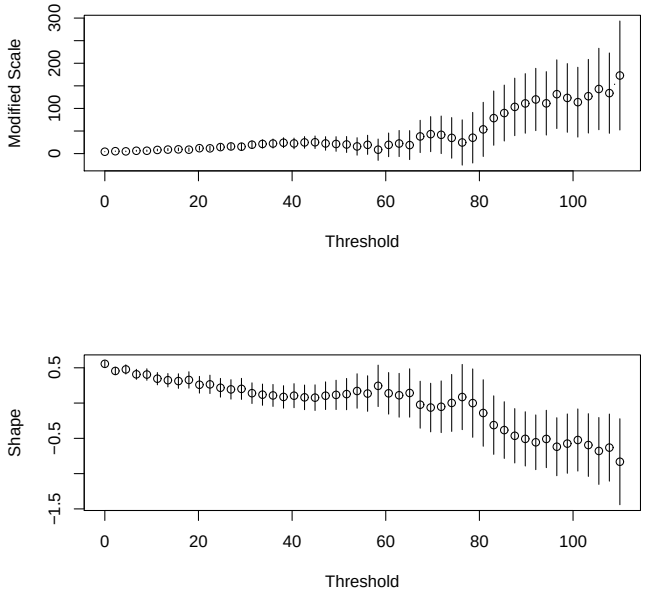

Figure J.8: Parameter stability plots for the Santana (P) station data.

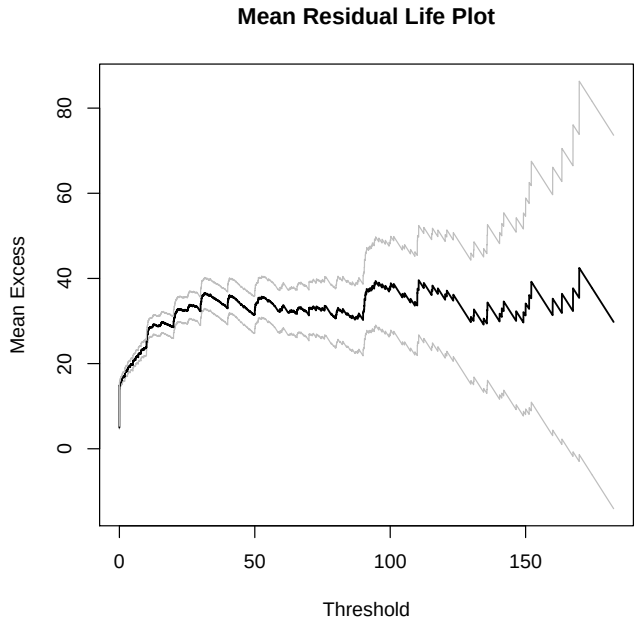

Figure J.9: Mean residual plot for the Loural (Q) station data.

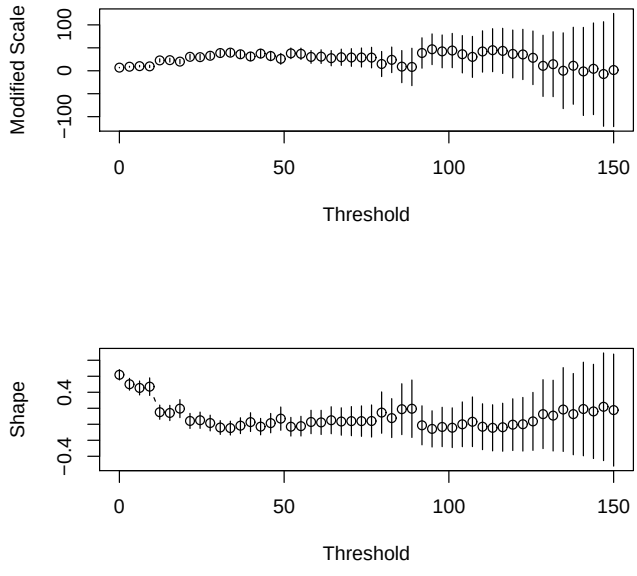

Figure J.10: Parameter stability plots for the Loural (Q) station data.

Appendix K

Threshold choice plots – Dataset IV (Class 4)

Mean residual and parameter stability plots for the stations with altitude below 300 m

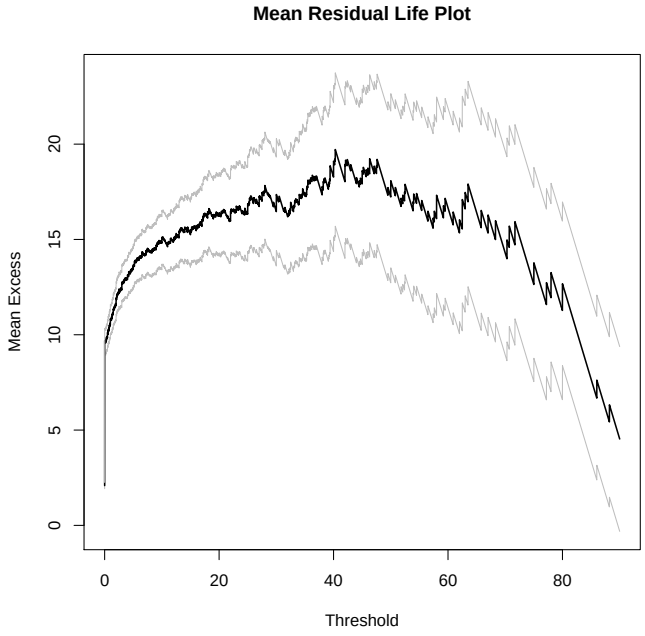

Figure K.1: Mean residual plot for the Bom Sucesso (R) station data.

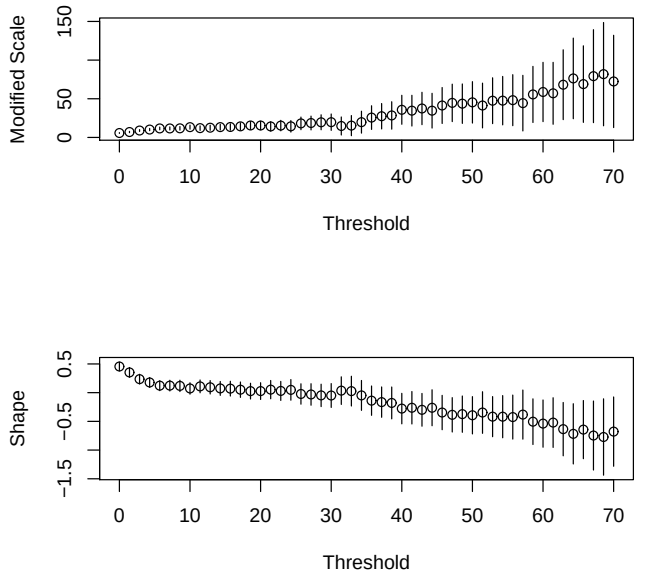

Figure K.2: Parameter stability plots for the Bom Sucesso (R) station data.

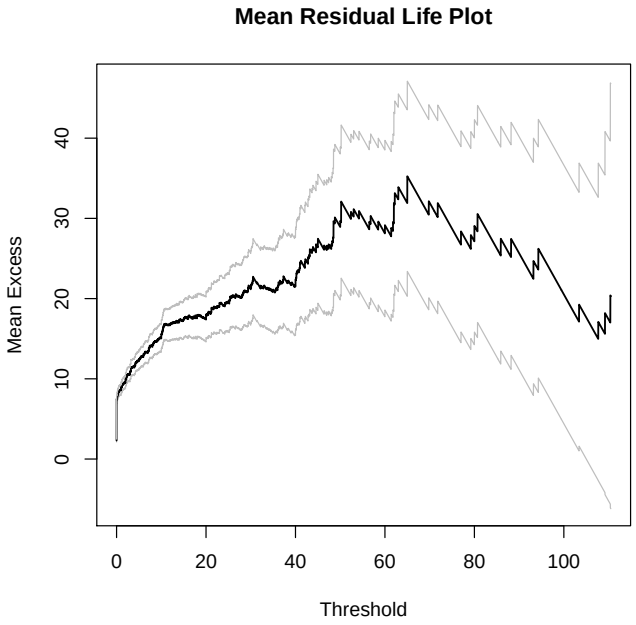

Figure K.3: Mean residual plot for the Machico (S) station data.

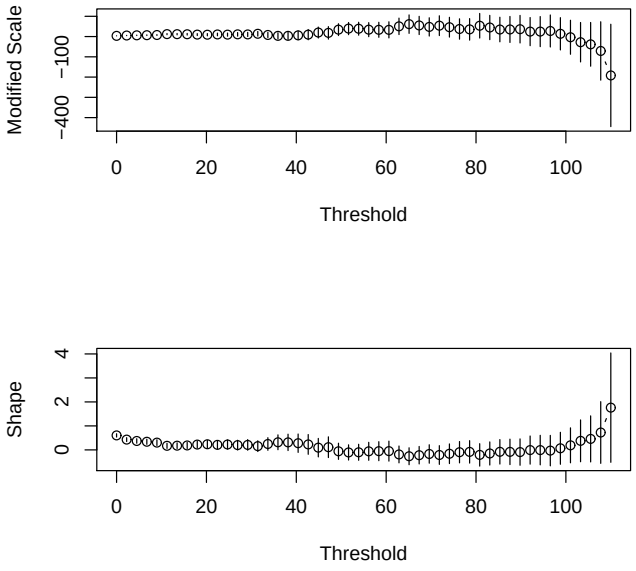

Figure K.4: Parameter stability plots for the Machico (S) station data.

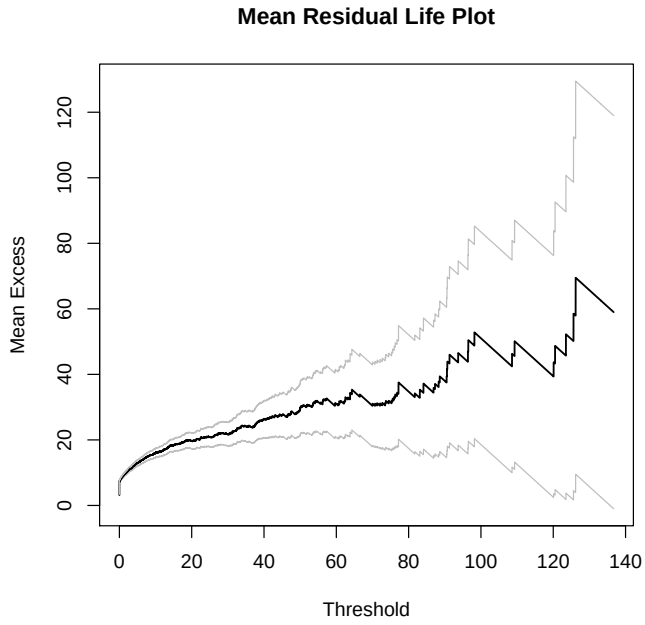

Figure K.5: Mean residual plot for the Ponta Delgada (T) station data.

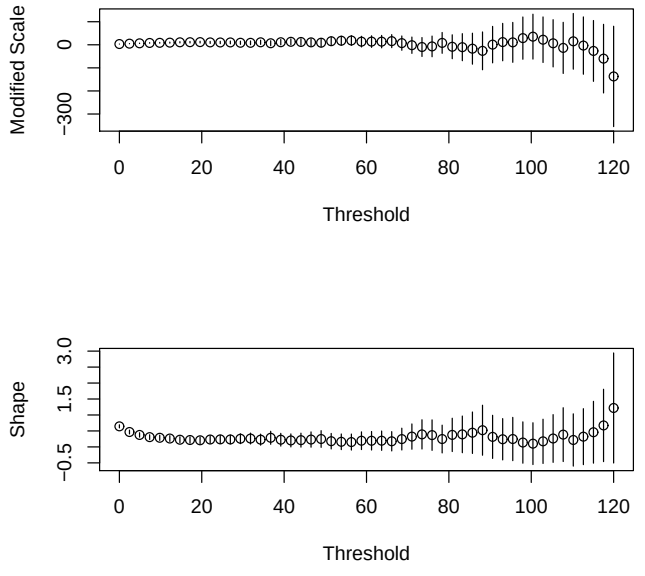

Figure K.6: Parameter stability plots for the Ponta Delgada (T) station data.

Figure K.7: Mean residual plot for the Santa Catarina (V) station data.

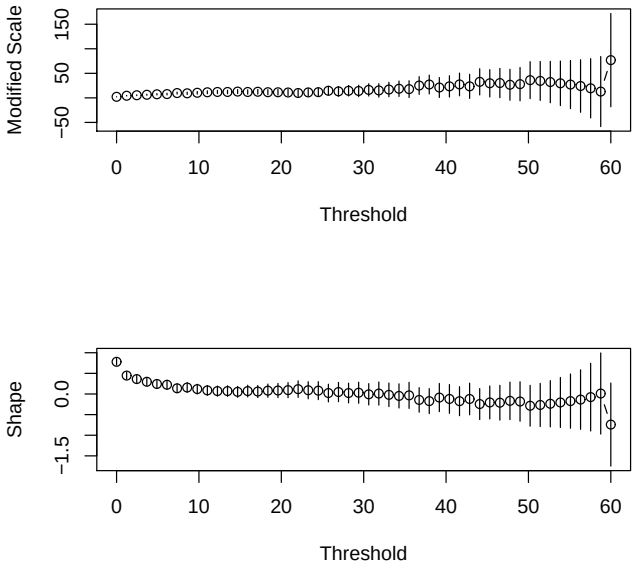

Figure K.8: Parameter stability plots for the Santa Catarina (V) station data.

Figure K.9: Mean residual plot for the Caniçal (W) station data.

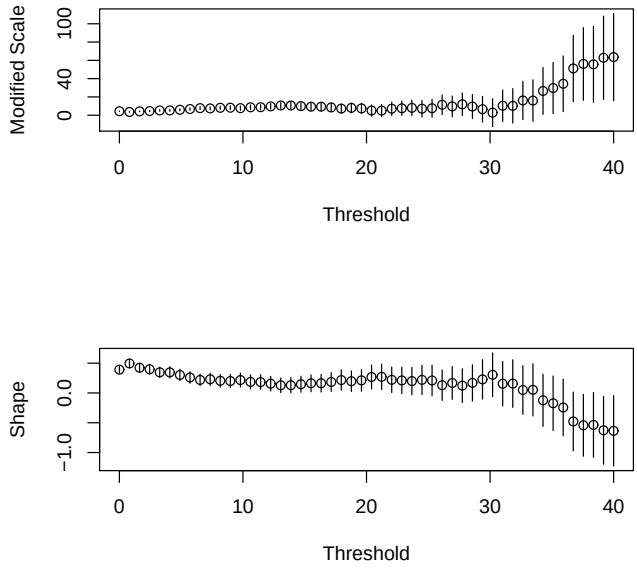

Figure K.10: Parameter stability plots for the Caniçal (W) station data.

Figure K.11: Mean residual plot for the Lugar de Baixo (X) station data.

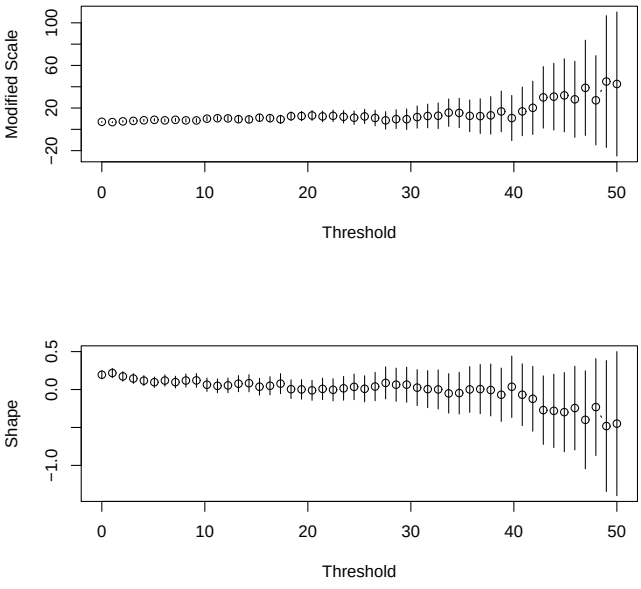

Figure K.12: Parameter stability plots for the Lugar de Baixo (X) station data.

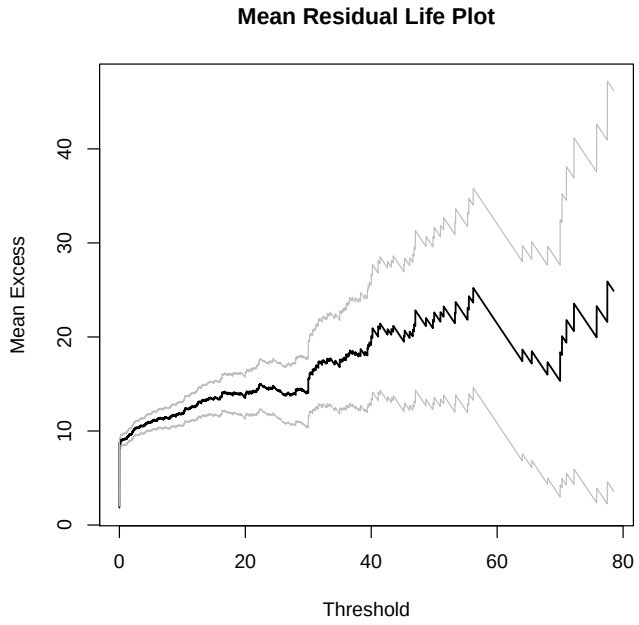

Figure K.13: Mean residual plot for the Ribeira Brava (Y) station data.

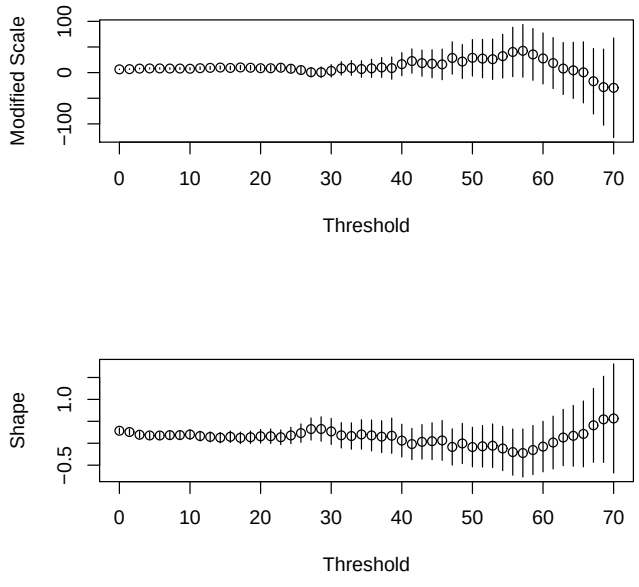

Figure K.14: Parameter stability plots for the Ribeira Brava (Y) station data.

Appendix L

Exceedances percentage by month – Dataset IV

Table L.1: Exceedances percentage by month for u_1.

Station	J	F	M	A	M	J	J	A	S	O	N	D
Areeiro (A)	23	14	10	3	3	1	0	0	3	10	17	15
Bica da Cana (B)	22	13	12	5	2	2	0	0	2	13	15	14
Poiso (C)	18	18	9	2	3	3	0	0	3	7	22	13
Montado do Pereiro (D)	18	17	12	4	4	1	0	0	3	9	18	13
Encumeada (E)	26	15	11	4	2	2	0	0	3	8	13	16
Ribeiro Frio (F)	18	17	9	5	3	1	0	1	5	10	17	15
Queimadas (G)	20	12	9	5	2	1	1	1	5	15	16	12
Camacha (H)	21	16	10	6	3	2	1	0	3	5	20	15
Santo da Serra (I)	21	12	10	5	2	2	1	1	3	13	17	13
Porto Moniz (J)	18	14	8	2	2	2	1	2	5	14	22	11
Curral das Freiras (K)	21	9	16	6	2	2	0	0	4	9	18	14
Ponta do Pargo (L)	26	9	16	4	1	1	0	0	3	7	25	8
Santo António (M)	19	17	12	5	1	1	0	0	2	10	16	16
Canhas (N)	19	11	11	5	2	3	1	2	2	20	11	16
Sanatório (O)	16	15	10	5	1	1	0	1	3	8	23	17
Santana (P)	19	11	6	4	3	1	1	2	5	16	16	15
Loural (Q)	18	19	11	6	2	2	0	0	2	11	18	12
Bom Sucesso (R)	15	18	6	8	1	2	0	0	5	12	21	13
Machico (S)	12	19	11	5	1	2	1	1	3	14	19	12
Ponta Delgada (T)	20	14	10	5	2	1	0	2	2	19	17	8
Funchal (U)	18	14	8	6	1	2	0	0	3	12	19	16
Santa Catarina (V)	22	17	7	5	2	1	0	0	4	12	16	12
Caniçal (W)	16	15	12	6	2	2	1	0	3	15	17	14
Lugar de Baixo (X)	23	13	9	3	2	1	0	0	3	15	16	15
Ribeira Brava (Y)	24	12	11	3	1	3	0	0	4	14	14	16

Table L.2: Exceedances percentage by month for u_2.

Station	J	F	M	A	M	J	J	A	S	O	N	D
Areeiro (A)	24	15	11	4	3	1	0	0	4	9	16	13
Bica da Cana (B)	22	13	11	6	2	2	0	0	1	13	12	18
Poiso (C)	21	18	12	2	2	4	0	0	5	7	16	14
Montado do Pereiro (D)	16	21	12	7	2	3	0	0	5	7	16	12
Encumeada (E)	23	23	10	3	2	0	0	0	3	7	11	18
Ribeiro Frio (F)	16	21	9	3	3	1	0	1	4	10	16	14
Queimadas (G)	28	12	11	4	2	1	0	1	4	15	13	11
Camacha (H)	24	17	9	5	1	2	0	0	3	7	16	15
Santo da Serra (I)	31	14	7	5	1	2	0	0	3	11	14	11
Porto Moniz (J)	23	8	10	2	5	3	2	2	5	15	18	7
Curral das Freiras (K)	22	7	13	6	1	3	0	0	4	9	16	18
Ponta do Pargo (L)	29	7	17	5	2	2	0	0	5	7	21	5
Santo António (M)	21	19	12	4	3	1	0	0	4	8	22	14
Canhas (N)	15	15	17	2	0	4	0	0	4	12	19	12
Sanatório (O)	17	15	10	5	2	1	0	1	3	9	23	16
Santana (P)	27	14	5	5	3	1	1	1	3	16	13	10
Loural (Q)	23	16	9	3	0	3	0	0	3	14	18	11
Bom Sucesso (R)	22	18	5	8	2	3	0	0	3	12	15	12
Machico (S)	15	21	7	4	0	3	1	1	4	13	22	8
Ponta Delgada (T)	30	13	10	5	1	1	0	0	1	21	10	7
Funchal (U)	21	13	5	7	2	2	0	0	3	10	20	16
Santa Catarina (V)	19	26	5	2	2	2	0	0	2	12	19	12
Caniçal (W)	19	17	10	6	1	2	1	0	5	18	9	13
Lugar de Baixo (X)	26	10	7	1	3	3	0	1	2	16	18	13
Ribeira Brava (Y)	33	10	13	3	0	5	0	0	5	15	13	5

Appendix M

Code of the functions implemented in R

Code of the functions applied in Section 5.2

Code for the normalized Hasofer and Wang test statistic, $W_n^*(k)$, defined by (4.15):

$esttesteHWNA < -function(x, k)\{n < -length(x)$
$q < -(1/k)$
$ordx < -sort(x)$
$j < -n - k$
$i < -j + 1$
$threshold < -ordx[j]$
$u < -ordx[i : n]$
$z < -u - threshold$
$v < -z\hat{}2$
$soma1 < -sum(z)$
$soma2 < -sum(v)$
$prod1 < -q * soma1$
$prod2 < -q * soma2$
$quad < -(prod1)\hat{}2$
$w < -q * (quad/(prod2 - quad))$
$return(w)\}$

$arauxHW1 < -function(m)\{vectorf < -dataset\$variable$
$k < -m$
$fvalorHW < -esttesteHWNA(vectorf, k)$
$vobser < -sqrt(k/4) * (k * fvalorHW - 1)$
$return(vobser)\}$

Code for the Greenwood type test statistics, $R_n^*(k)$, defined by (4.16):

$esttesteGt < -function(x, k)\{n < -length(x)$
$q < -(1/k)$
$ordx < -sort(x)$
$j < -n - k$
$i < -j + 1$
$threshold < -ordx[j]$
$u < -ordx[i : n]$
$z < -u - threshold$
$v < -z\hat{}2$
$soma1 < -sum(z)$
$soma2 < -sum(v)$
$prod1 < -q * soma1$
$prod2 < -q * soma2$
$quad < -(prod1)\hat{}2$
$Gt < -prod2/quad$
$return(Gt)\}$

$arauxGt1 < -function(i)\{vectorg < -dataset\$variable$
$k < -i$
$fvalorGt < -esttesteGt(vectorg, k)$
$vobserGt < -sqrt(k/4) * (fvalorGt - 2)$
$return(vobserGt)\}$

Code of the functions applied in Section 5.3

Code for the parameters β_i (4.42), with $i \in \{1, 2, 3\}$ from the copula function:

$$
\begin{array}{l}
betaic < -function(u, v, w)\{ \\
valorbeta < -1/((1/2) * (1 + ((1/u) + (1/v) - (1/w)))) \\
return(valorbeta)\}
\end{array}
$$

Code for the copula function C defined by (4.31):

$$
\begin{array}{l}
copexperiencia < -function(a, b, c, d, e, f)\{ \\
valorcopula < -(a\hat{}(1-d)) * (b\hat{}(1-e)) * (c\hat{}(1-f)) * min((a\hat{}d), (b\hat{}e), (c\hat{}f)) \\
return(valorcopula)\}
\end{array}
$$

Code for the function used to compute probability $p_q = P(E_q)$ defined by (4.43):

$$
\begin{array}{l}
funcaop < -function(a, b, c, d, e, f)\{parcela1 < -(1-a-b-c) \\
parcela2 < -copexperiencia(a, b, c, d, e, f) \\
parcela3 < -copexperiencia(a, b, 1, d, e, f) \\
parcela4 < -copexperiencia(a, 1, c, d, e, f) \\
parcela5 < -copexperiencia(1, b, c, d, e, f) \\
valorp < -parcela1 - parcela2 + parcela3 + parcela4 + parcela5 \\
return(valorp)\}
\end{array}
$$